UNIVERSITÀ DEGLI STUDI DI MILANO
FACOLTÀ DI SCIENZE MATEMATICHE, FISICHE E NATURALI

Doctorate School of Chemical Sciences and Technologies

Department of Chemistry

Doctorate Course of Chemical Sciences - XXV Cycle

SYNTHESIS, STRUCTURAL INVESTIGATION AND BIOLOGICAL EVALUATION OF CONFORMATIONALLY CONSTRAINED PEPTIDOMIMETICS

CHIM/06 Organic Chemistry

Francesco AIRAGHI
Matr. R08767

Tutor: Prof. Giordano LESMA
CoTutor: Dott.ssa Alessandra SILVANI

Coordinator: Prof.ssa Emanuela LICANDRO

Academic Year 2011/2012

To my 少林功夫
brothers and sisters

ABSTRACT

This Ph.D. thesis is located in the medicinal chemistry research field. Peptides are among the most studied entities as potential drug candidates, due to their natural abundance and biological implications. However, as drugs they possess several disadvantages because of low bioavailability and short half-life. Peptidomimetics try to overcome such drawbacks, maintaining meanwhile the biological activity. These mimics can also be useful to define bioactive forms of natural peptides, for instance through insertion of conformational constrictions able to reduce the peptide inherent flexibility.

Thus, I explored the synthesis and the evaluation of some conformationally constrained peptidomimetics which potentially could be employed into different scientific fields and pharmaceutical contexts. Once prepared these scaffolds, I evaluated their secondary structure by means of spectroscopic methods including NMR and IR techniques. After insertion into more complex structures, strictly related to biologically active compounds, I verified their therapeutic potential. In some cases I could achieve very interesting biological results, in the range of activity of the natural corresponding peptides or of the reference lead compounds. I also tried to rationalize the biological activity outcomes, by joining them with molecular mechanics and docking-based structural investigation.

INDEX

LIST OF ABBREVIATIONS

AA	Amino Acid
Aba	Amino benzazepinone
Ac	Acetyl
AD	Alzheimer Disease
Ala	Alanine
aq.	Aqueous
BBB	Blood-Brain Barrier
Boc	tert-Butyloxycarbonyl
BOP	Benzotriazol-1-yloxytris(dimethylamino)phosphonium hexafluorophosphate
Bt	Benzotriazole
BzR	Benzodiazepine Receptor site
CADD	Computer Aided Drug Design
calcd.	Calculated
Cbz	Carbobenzyloxy
conc.	Concentrated
Cys	Cysteine
CSA	Camphorsulfonic acid
DBU	Diazabicyclo[5,4,0]-undec-7-ene
DCM	Dichloromethane
DIPEA	*N,N*-Diisopropylethylamine
DKP	DiKetoPiperazine
DOR	δ-Opioid Receptor
DMF	Dimethylformamide
DMSO	Dimethylsulfoxide
Dmt	Dimethyltyrosine
EM-1	Endomorphin-1
EM-2	Endomorphin-2
equiv	Equivalent
ESI	Electron spray ionization
Fmoc	9-Fluorenylmethoxycarbonyl
GDP	Guanosine diphosphate
Gly	Glycine
GPCRs	G-protein coupled receptors
GTP	Guanosine triphosphate

HATU	2-(1H-7-Azabenzotriazole-1-yl)-1,1,3,3-tetramethylaminium hexafluorophosphate
HBTU	2-(1H-Benzotriazole-1-yl)-1,1,3,3-tetramethylaminium hexafluorophosphate
Hex	Hexane
HOAt	1-Hydroxy-7-azabenzotriazole
HOBt	1-Hydroxybenzotriazole
HPLC	High performance liquid chromatography
IBCF	isobutyl chloroformate
Ile	Isoleucine
IMDA	IntraMolecular Diels-Alder
IP3	Inositol triphosphate
IR	Infrared
KOR	κ-Opioid Receptor
LC	Liquid Chromatography
Leu	Leucine
Lys	Lysine
Me	Methyl
MC/MM	Monte Carlo/multiple minimum
MOR	μ-Opioid Receptor
MS	Mass Spectrometry
NMR	Nuclear Magnetic Resonance
NOESY	Nuclear Overhauser Enhanced Spectroscopy
Ph	Phenyl
Phe	Phenylalanine
Phthal	Phthalimide
POP	Prolyl Oligopeptidase
ppm	Parts per million
Pro	Proline
PS	Pictet-Spengler
PyBOP	Benzotriazol-1-yloxytrispyrrolidinophosphonium hexafluorophosphate
QSAR	Quantitative Structure-Activity Relationship
RDS	Rate Determining Step
RP	Reverse Phase
Rf	Retention factor
rt	Room temperature
SAR	Structure-Activity Relationship

ss	Saturated Solution
SEM	Standard error of the mean
Ser	Serine
Tbac	2,3,4,5-tetrahydro-1H-benzo[c]azepine-4-carboxylic acid
TBTU	O-(Benzotriazol-1-yl)-*N,N,N',N'*-tetramethyluronium tetrafluoroborate
tBu	*tert*-Butyl
TEA	Triethylamine
TfOH	Trifluoromethanesulfonic acid
TFA	Trifluoroacetic acid
TFAA	Trifluoroacetic anhydride
THBC	Tetrahydro-β-carboline
THF	Tetrahydrofuran
Tic	1,2,3,4-Tetrahydroisoquinoline-3-carboxylic acid
Thr	Threonine
TLC	Thin layer chromatography
Trp	Tryptophan
Tyr	Tyrosine
UV	Ultraviolet
Val	Valine
VT-NMR	Variable Temperature - NMR
v/v	Volume per unit volume
Xaa	Unspecified amino acid

CHAPTER I: INTRODUCTION

1.1 *Proteins*

The most abundant biomolecules in living organisms are proteins, long polymers of amino acids, representing more than 50% of the dry weight of animals and bacteria. Some proteins act like a catalyst, functioning as enzymes, other as signal receptors or transporters, which carry specific substances within or outside cells. Proteins are mainly a combination of the twenty different α-amino acids types present in nature and differ in number, composition and sequence. However, the main properties of a protein largely depend on the three-dimensional structure. While denatured proteins (not bent) have similar characteristics between them, the native (which are in their functional conformation), own unique properties and characteristics.
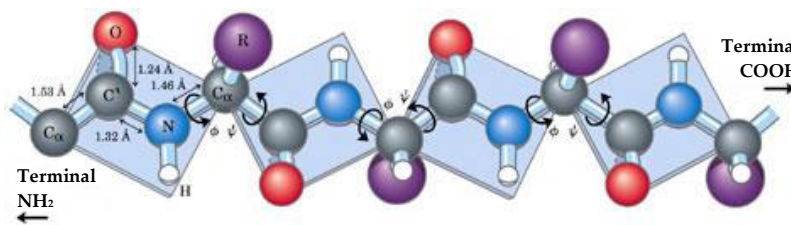

Figure 1. *Trans* conformation of a polypeptidic chain.

Therefore, four different levels in the organization of the structure of a protein can be distinguished.

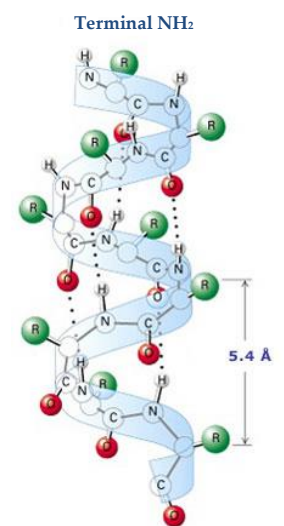The primary structure is the specific sequence of amino acids. The nature of the covalent binding of the polypeptidic chain imposes restrictions to the structure. The peptide bond assumes a partial double bond character, with the six atoms of the peptidic group in a rigid coplanar configuration. Peptide groups show, with few exceptions, a *trans* conformation, i.e. with the side chains outside from the plane containing the amide linkages (**Figure 1**). It's so possible specify the conformation of the polypeptides backbone according to the torsion angles around the Cα-N bond (φ) and the Cα-C bond (ψ) of each of its amino acid residues.

The secondary structure is referred to local spatial conformation of some parts of a polypeptide. The types of stable secondary structure and universally distributed among the proteins are relatively few. The most relevant conformations are α-helices (**Figure 2**), β-sheets (**Figure 3**) and foldings or loops. In the secondary structure two key factors minimize the potential energy of the molecule: the minimization of the steric hindrance between side chains and the optimization of the formation of intrachain hydrogen bonds. The secondary structure of a polypeptidic segment is described by values of bond angles φ and ψ of each residue in that segment.

Figure 2.
An α-helix

Figure 3. A β-sheet structure.

The tertiary structure of a protein defines the disposition of all its atoms in the three-dimensional space. While the secondary structure of a polypeptidic chain is related to a particular spatial order of amino-acidic residues which are adjacent in the primary structure, the tertiary structure considers the long-range connections existing in the amino-acidic sequence (Van der Waals forces). It is possible to distinguish two general classes of proteins based on their tertiary structure: fibrous, which perform numerous structural functions and are constituted by the repetition of a simple element of the secondary structure, and globular, with a more complex tertiary structure, in which there are different types of secondary structure in the same polypeptidic chain. In general, tertiary structure derives from interactions between the hydrophobic groups of polypeptide brought by the side chains of the amino acids of which it is made.
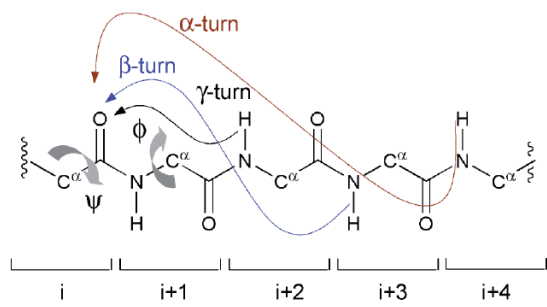
Lastly, the quaternary structure is determined by interactions between the multi-subunit proteins subunits (multimerics) or by the proteins folding of large size. In general, the combination of two or more polypeptides occur through weak bonds, such as disulfide bridges, in a very specific way. Finally, some proteins contain also a non-polypeptidic part called prosthetic group, which gives to the protein a particular reactivity (such as EME hemoglobin group).

As previously stated, proteins play an important role in many biological events. Interactions between receptors/enzymes and relatively small peptidic molecules occur at different level. Amino acid side chains are important for hydrogen bonding with basic or acid groups, lipophilic interactions or π-π stacking. Moreover, the amino acidic sequence may interact with its secondary structure, usually a turn motif is commonly recognized by most of the mammalian receptors (i.e. GPCRs).

A correct classification of turns is important to identify structural similarities between different proteins and make structural predictions about amino acid sequences.[1]

---

[1] Koch O., Klebe G. "Turns revisited: A uniform and comprehensive classification of normal, open, and reverse turn families minimizing unassigned random chain portions" *Proteins*, **2009**, *74*, 353–367

A reverse-turn in a protein structure is defined as a site where a polypeptide chain reverses its overall direction. According to the number of amino acids involved in the turn, there are different denominations: α-turn (*i, i+4*), β-turn (*i, i+3*), γ-turn (*i, i+2*) forming rings respectively to 7, 10 and 13 atoms closed by an hydrogen bond. This classification, however, is complicated by the irregular structure of the turns. In fact, the reverse-turn backbone (**Figure 4**), unlike the α-helices and β-sheets, has a variable conformation. Parameters usually evaluated are mainly geometric and allow to identify eleven different types of *β*-turns.

α-turn: 13-membered ring H-bonding; NH (i+4) → CO (i)
β-turn: 10-membered ring H-bonding; NH (i+3) → CO (i)
γ-turn: 7-membered ring H-bonding; NH (i+2) → CO (i)

Figure 4. Reverse-turn classification.

A peptidic turn can be displayed and easily understood from **Figure 5** where the intramolecular hydrogen bonds are summarized and explained for all the possible turn structures.
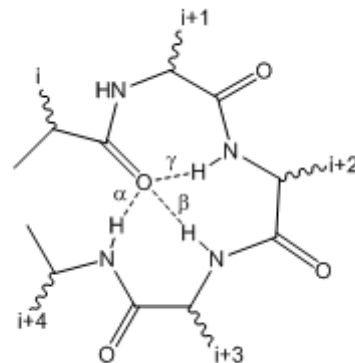

Figure 5. Visual distinction between α, β and γ turn.

Reverse turns play an important role in globular proteins from both a structural and functional point of view.[2] Among the reverse turns, β-turn, usually featuring a 10-membered ring intramolecular hydrogen-bonded network, has been extensively investigated in the past. Recent studies suggest that even α-turns, although less frequently observed in proteins compared to β-turns, play key roles in certain biological functions.[3] For instance, the role of α-turn motifs in molecular recognition processes

[2] Chou K.C. "Prediction of tight turns and their types in proteins" *Anal. Biochem.* **2000**, *286*, 1–16

[3] Prabakaran P., Gan J., Wu Y.O., Zhang M.Y., Dimitrov D.S., Ji X. "Structural mimicry of CD4 by a cross-reactive HIV-1 neutralizing antibody with CDR-H2 and H3 containing unique motifs" *J. Mol. Biol.* **2006**, *357*, 82–99

involving HIV-neutralization has just begun to unfold.[4] It is known that the recognition of a turn conformation normally involves only interactions between residues of the side chains of the ligand with the receptor. Based on this general behavior, our approach to the synthesis of peptidic turns can therefore be regarded as a synthesis of scaffolds with the amino acid component which potentially can be conformationally constrained or completely replaced by non-peptide alternative rigid scaffolds, designed to support fragments mimicking the side peptidic chains in the correct orientation with the binding site.

---

[4] Bell C.H., Pantophlet R., Schiefner A., Cavacini L.A., Stanfield R.L., Burton D.R., Wilson I.A. "Structure of antibody F425-B4e8 in complex with a V3 peptide reveals a new binding mode for HIV-1 neutralization" *J. Mol. Biol.* **2008**, *375*, 969–978

1.2 *Peptidomimetics*

Proteins are vital for basically every known organism. Therefore the investigation of their structure, the development of a deeper understanding of protein–protein interactions and the design of novel peptides, which selectively interact with proteins, are fields of active research. Small peptides consisting of the 20 natural amino acids typically show high conformational flexibility and a low in-vivo stability which hampers their application as tools in medicinal diagnostics or molecular biology. One very versatile strategy to overcome such drawbacks is the use of peptidomimetics.

Peptidomimetics[5] are small protein-like molecules designed to mimic natural peptides or proteins. These mimetics should have the ability to bind to their natural targets in the same way as the natural peptide sequences do and hence should produce the same biological effects. It is possible to design these molecules in such a way that they show the same biological effects as their peptide role models but with enhanced properties like a higher proteolytic stability, higher bioavailability and also often with improved selectivity or potency. This makes them interesting targets for the discovery of new drug candidates.[6] For the development of potent peptidomimetics it is necessary to understand the forces that lead to protein–protein interactions in the nanomolar range or even with higher affinities. These strong interactions between peptides and their corresponding proteins are mainly based on side chain interactions, indicating that the peptide backbone itself is not an absolute requirement for high affinities. This allows chemists to design peptidomimetics basically from any scaffold known in chemistry by replacing the amide backbone partially or completely by other structures. Most important is that the backbone is able to place the amino acid side chains in a defined 3D-position to allow interactions with the target protein. Therefore it is necessary to develop an idea of the required structure of the peptidomimetic to show a high activity against its biological target.

A common strategy to achieve these results is the manipulation of the amino acids' side chains or the peptide structure itself. Conformationally restricted and metabolically more stable peptidomimetics are obtained using unnatural amino acids. In general, two different starting points exist for the modification of peptides at the amino acid level. One is the peptide backbone which can be replaced by bioisosteres (e.g. triazoles,

[5] Wu Y.D., Gellman S. "Peptidomimetics" A*cc. Chem. Res.*, **2008**, *41*, 1231-1232

[6] (a) Hirschmann R. "Medicinal Chemistry in the Golden Age of Biology: Lessons from Steroid and Peptide Research" *Angew. Chem. Int. Ed. Engl.* **1991**, *30*, 1278-1301. (b) Hruby V.J., Al-Obeidi F., Kazmierski W. "Emerging approaches in the molecular design of receptor-selective peptide ligands: conformational, topographical and dynamic considerations." *Biochem. J.* **1990**, *268*, 249-262. (c) Rizo J., Gierasch L.M. "Constrained Peptides: Models of Bioactive Peptides and Protein Substructures" *Annu. Rev. Biochem.* **1992**, *61*, 387-418

thioamides or alkenes). On the other hand, the amino acid side chain can be modified by mean of a different substitution, for instance a quaternary amino acid or a natural amino acid coming from the D-series. Structural rigidifications, for example by the use of cyclization strategies, is a widely used synthetic approach. There several methods which can be summarized as:

- Head-to-Tail
- Side chain-to-side chain
- Backbone-to-side chain
- Same side chain

Although new ways were developed for the head-to-tail cyclization of peptides, most of them are still formed by the cyclization of activated precursors in solution phase, which means in most cases the use of standard peptide coupling conditions using HOBt/HBTU or HOAt/HATU as activating reagents. One interesting example for the head-to-tail cyclization of natural products is the Cyclosporine O.[7] In the same field, the RGD (Arg-Gly-Asp) sequence is the starting point for numerous cyclic peptidomimetics. In some examples RGD is flanked by other amino acids to form a ring system. These compounds offer the possibility to present the side chains of the RGD sequence in a specific conformation. DKP is the smallest head-to-tail cyclized peptidomimetic and has also been applied as a scaffold in the RGD sequence.[8]

The most common methods to lock peptide chains into defined structures like α-helices by the formation of cyclic analogues are the disulfide linkage via the oxidation of two Cys residues and the formation of amide bonds between the side chain residues of the amino acids Lys and Asp/Glu.

A further way to introduce global constraints into peptides is the formation of backbone to side chain cyclizations. One example for such a molecule is the cyclic derivative (Tyr-c[-δ-Orn-2-Nal-δ-Pro-*N*Me-Ala]) of the natural occurring β-casomorphin-5.

Side chain cyclization is one of the most obvious strategy for the synthesis of constrained peptidomimetics and has been applied on both aromatic and non aromatic amino acids. Regarding aromatic amino acids, it will be fully explained during next chapters, whereas for non aromatic amino acids there are several examples in the field

[7] Li P., Xu J.C. "Total Synthesis of Cyclosporin O Both in Solution and in the Solid Phase Using Novel Thiazolium-, Immonium-, and Pyridinium-Type Coupling Reagents: BEMT, BDMP, and BEP1" *J. Org. Chem.* **2000**, *65*, 2951–2958

[8] Marchini M., Mingozzi M., Colombo R., Guzzetti I., Belvisi L., Vasile F., Potenza D., Piarulli U., Arosio D., Gennari C. "Cyclic RGD peptidomimetics containing bifunctional diketopiperazine scaffolds as new potent integrin ligands" *Chemistry*, **2012**, *18*, 6195-6207

of proline analogues. In the same topic, ring-closing metathesis is a precious tool for organic chemists and it has been exploited for the synthesis of new cyclic amino acid.[9]
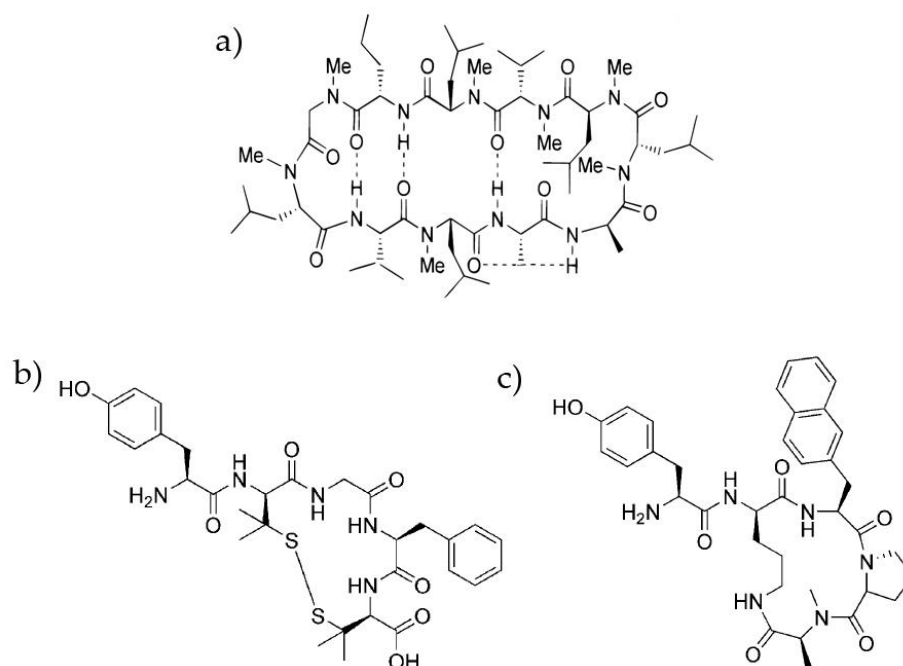

Figure 6. Examples of a) head-to-tail b) side chain-to side chain c) backbone-to-side chain cyclization.

N-methylation is a very common modification, but also occurs in the sequences of natural peptides. *N*-Methylated analogues of biologically relevant peptides have been intensively examined to derive more information about the structural effects of *N*-alkylation. They normally show increased proteolytic stability, increased membrane permeability (lipophilicity) and altered conformational preferences of the amide bond properties.[10] These effects result from the different property changes in the peptide going along with the introduction of *N*-methylation. Firstly, there are steric constraints introduced by the *N*-alkyl group, which have an effect not only on the conformational freedom of the peptide backbone but also on the side chain of the neighbouring amino acid. Secondly, the number of inter- and intramolecular hydrogen bonds decreases due to the removal of the backbone NH groups. And thirdly, the attached carbonyl group shows an increased basicity and decreased polarity.

In this context, and more specifically related to this work, another common strategy involves β-amino acids as building blocks. β-peptides have particular appeal for extending our understanding of protein structure and stabilization into the realm of

[9] Harris P.W.R., Brimble M.A., Gluckman P.D. "Synthesis of Cyclic Proline-Containing Peptides via Ring-Closing Metathesis" *Org. Lett.* **2003**, *11*, 1847-1850

[10] Fairlie D.P., Abbenante G., March D.R. "Macrocyclic peptidomimetics - forcing peptides into bioactive conformations" *Curr. Med. Chem.* **1995**, *2*, 654–686

folded, non biological polymers, because β-amino acids represent the smallest step away from α-amino acids in the "backbone space". Like α-peptides (i.e. peptides composed of α-amino acids), β-peptides contain amide bonds capable of stabilizing intramolecular hydrogen bonds. A large body of structural and synthetic work has laid a solid groundwork for current investigations into β-peptides.[11] That's why we chose β-amino acid containing peptidomimetic as a suitable starting point for the synthesis of interesting and pharmaceutical valuable drug candidates. An extensive dissertation on β-peptides features is reported in the next section.

[11] Cheng R.P., Gellman S., DeGrado W.F. "β–Peptides: From Structure to Function" *Chem. Rev.*, **2001**, *101*, 3219-3232

1.2.1 *β-Peptides*

A new dimension to the field of biomimetic structures has been introduced by Seebach,[12] through the recognition that the repertoire of polypeptide conformations can be greatly expanded by the creation of structures that incorporate backbone homologated amino acids,[13] synthetically accessible from the proteinogenic amino acids. β-Peptides consists of homologated amino acids, the new carbon atom expands the possibilities of functionalization and the stereochemical aspect of this class of building blocks. This is very important in medicinal chemistry because natural-like (i.e. β-hPhe, β-hTrp) and unnatural side chains can occupy much more different spatial positions while interacting with receptors. The employment of β-amino acids in peptidomimetic chemistry offer many advantages, such as an high stability towards proteolytic enzymes, more possibility of chemical diversity and, in most cases, more predictable secondary structures.[14] In addition, quite recently, Gellman outlined the numerous advantages of heterogeneous (mixed α- and β-) backbone peptidomimetics with respect to homogeneous ones.[15] In fact, the heterogeneous approach allows many different combinations, starting from α- and β-amino acid building blocks, each of which offers a potentially distinctive way to project sets of side chains in space and to generate preferential conformations.[16]

β-amino acids and β-peptides with proteinogenic side chains R can be divided into three main types (**Figure 7**): β^3 and β^2, insertion of a CH_2 group between the CO and the α-carbon and between the α-carbon and the nitrogen, respectively; $\beta^{2,3}$, β-amino acid with an additional proteinogenic side chain (for example, Me) in the α-position with *syn* (*R,R* or *S,S*) or *anti* (*R,S* or *S,R*) configuration; finally $\beta^{2,2}$ or $\beta^{3,3}$ with a double substitution on the same carbon atom. Such substitution might be identical, leading to an achiral β amino-acid, or different.

[12] (a) Seebach D., Gardiner J. "β-Peptidic Peptidomimetics" *Acc. Chem. Res.*, **2008**, *41*, 1366-1375 (b) Wu Y.D., Han W., Wang D.P., Gao Y., Zhao Y.L. "Theoretical Analysis of Secondary Structures of β-Peptides" *Acc. Chem. Res.*, **2008**, *41*, 1418-1427.

[13] Giannis A., Kolter T. "Peptidomimetics for Receptor Ligands – Discovery, Development and Medical Perspectives" *Angew. Chem., Int. Ed.*, **1993**, *32*, 1244-1267

[14] Grauer A., König B. "Peptidomimetics – A Versatile Route to Biologically Active Compounds" *Eur. J. Org. Chem.*, **2009**, *30*, 5099-5111

[15] Horne W.S., Gellman S. "Foldamers with Heterogeneous Backbones" *Acc. Chem. Res.*, **2008**, *41*, 1399-1408

[16] Vasudev P.G., Chatterjee S., Shamala N., Balaram P. "Structural Chemistry of Peptides Containing Backbone Expanded Amino Acid Residues: Conformational Features of β, γ, and Hybrid Peptides" *Chem. Rev.*, **2011**, *111*, 657-687
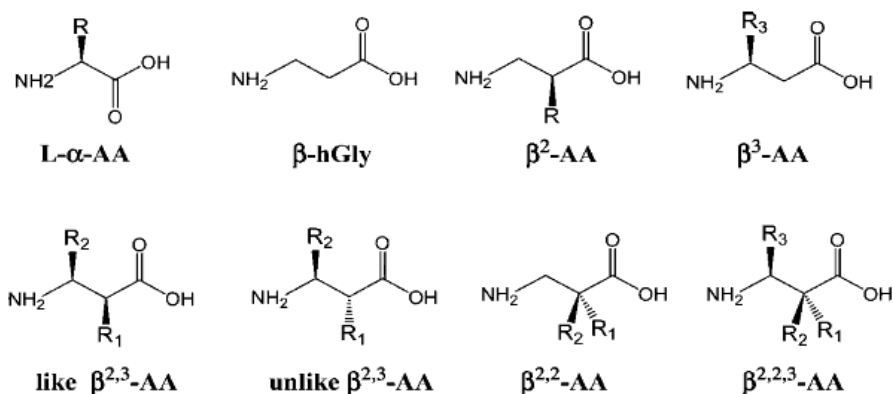
Figure 7. Generic β-Amino acids.

C3-substituted β-amino acid may be prepared by homologation of α-amino acids via Arndt-Eistert homologation,[17] by mean of a more classical Kolbe protocol,[18] or by a number of other practical routes,[19] providing a convenient and highly diverse source of enantiomerically pure monomers possessing proteinogenic-like or unnatural side chains. C2-substituted β-amino acid synthesis have been fully explored and a recent review covers most of the synthetic approaches.[20] Evans' oxazolidinones methodology remain one of the most exploited method for enantioselective synthesis of pure β²-amino acids.[21]

The conformations of β-peptides can be analyzed in terms of the main chain torsional angles, which are assigned the angles ω, φ, θ, and ψ (**Figure 8**) in the convention of Balaram.
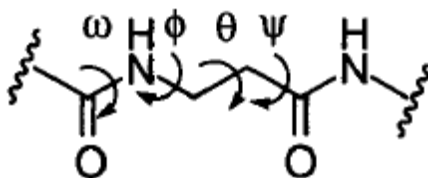
Figure 8. Definition for the torsional angles in β-peptides.

[17] Hughes A.B., Sleebs B.E. "Effective Methods for the Synthesis of N-Methyl b-Amino Acids from All Twenty Common a-Amino Acids Using 1,3-Oxazolidin-5-ones and 1,3-Oxazinan-6-ones" *Helv. Chim. Acta*, **2006**, *89*, 2611-2637

[18] Sobolewski D., Kowalcyzk W., Prahl A., Derdowska I., Slaninova J., Zaborcki J., Lammek B. "Analogues of arginine vasopressin and its agonist and antagonist modified in the *N*-terminal part of the molecule with L-β-homophenylalanine" *J. Peptide Res.* **2005**, *65*, 465-471

[19] Juaristi, E. "Enantioselective Synthesis of β-Amino Acids" Wiley-VCH: New York, **1997**

[20] Lelais G., Seebach D. "β²-Amino acids – Synthesis, Occurance in Natural Products and Components of β-Peptides" *Biopolymers*, **2004**, *76*, 296-243

[21] Gessier F., Schaeffer L., Kimmerlin T., Flogel O., Seebach D. "Preparation of b2-Amino Acid Derivatives (β²hThr, β²hTrp, β²hMet, β²hPro, β²hLys, Pyrrolidine-3-carboxylic Acid) by Using DIOZ as Chiral Auxiliary" *Helv. Chim. Acta*, **2005**, *88*, 2235-2249

β-Peptides offer various secondary structures, even in a four to six small peptide, unaccessibile to α-amino acids. In particular the typical α-helix can be expanded to different intramolecular hydrogen bonds stabilizing helical structures. These are summarized in **Figure 9** and they are strictly related to the absolute and relative configuration of the monomers. Secondary structures of α-peptides are significantly affected by side chain properties, on the other hand the secondary structure of β-peptides seems to be mainly determined by the substitution patterns. Peptides formed from β³-amino acids derived from natural L-amino acids adopt preferentially left-handed 14-helices. β-Peptides with alternating β²- and β³-monosubstituted residues can adopt the 10/12-helix conformation.[22] The characteristic feature of this helix is an intertwined network of 10- and 12- membered hydrogen-bonded rings.

α-Peptide	β-Peptides		
α-Helix poly-Ala	14-Helix poly-β³-hAla	12-Helix poly-β³-hAla	10/12-Helix poly-(β³-hAla-β²-hAla)
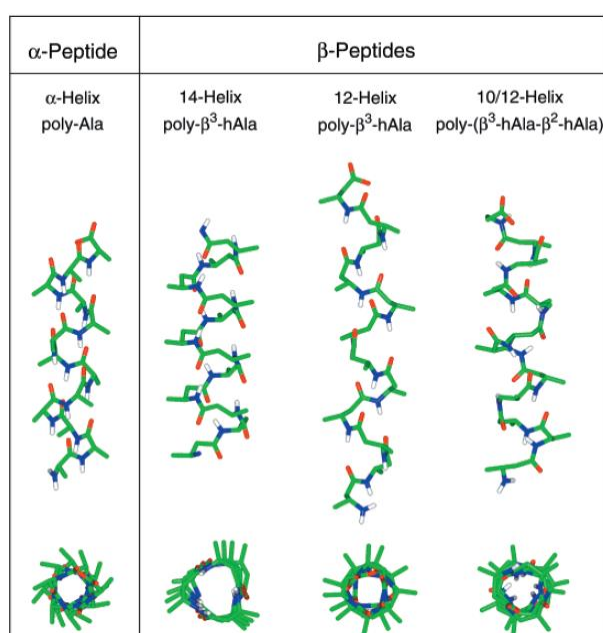
Figure 9. Structure of the α-helix, 14-helix, 12-helix and 10/12-helix.

β-Peptides carrying proteinogenic side chains can mimic their progenitors, the α-peptides. Helical mimics will be likely to consist of six or more β-amino acid residues, while turn and hairpin-mimicking β-peptides might consist of as few as two β-amino acid moieties. As demonstrated with a β-peptidic tetrapeptide, there is a chance that the short-chain β-peptides are orally bioavailable and are excreted within a reasonably short half-life, a prerequisite considered essential for a drug candidate by most

[22] Seebach D., Abele S., Gademann K., Guichard, G., Hintermann T., Jaun B., Matthews, J.L., Schreiber, J.V., Oberer L., Hommel U., Widmer H. "β2- and β3-Peptides with Proteinaceous Side Chains: Synthesis and solution structures of constitutional isomers, a novel helical secondary structure and the influence of solvation and hydrophobic interactions on folding" *Helv. Chim. Acta* **1998**, *81*, 932

medicinal chemists and clinical researchers. Proteolytic cleavage and metabolic processes do not seem to be an issue with β-peptides.[23]

In **Figure 10** is summarized the hydrogen bonding pattern for most common helices secondary structures accessible to β-peptides. This pattern becomes much more interesting because β-amino acid building blocks offer an higher degree of diversification. Moreover an heterogeneous backbone allows chemists to rationally design synthetic oligomers that exhibit natural biopolymer conformational behavior.
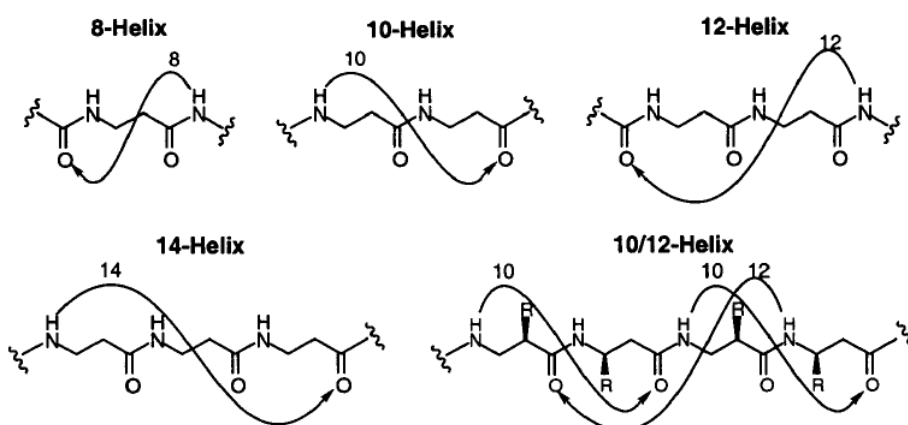
Figure 10. Hydrogen bonding pattern for β-peptides.

[23] Nunn C., Langenegger M.R.D., Schuepbach E., Kimmerlin T., Micuch P., Hurth K., Seebach D., Hoyer D. "β2/β3-Di- and α/β3-Tetrapeptide Derivatives as Potent Agonists of Somatostain sst4 Receptors" *Naunyn-Schmiedeberg's Arch. Pharmacol.* **2003**, *367*, 95–103

1.2.2 *Aromatic AAs based Scaffolds*

In the field of phenylalanine there are several possible modification reported and applied in many research topics, in particular medicinal chemistry. We can divide such mimics into two main categories: the linear one and the conformationally constrained. Among the linear mimics, one of the most exploited is the β-Methyl substitution[24] and the aromatic ring methylation.[25] The introduction of a new stereogenic center gives more tools for a structure-activity relationship investigation. Since methods of asymmetric synthesis of β-methyl aromatic amino acids have been developed, serial substitutions of biologically important aromatic amino acids with four β-methylated stereoisomers became an important tool for investigating topographical requirements of peptide receptors for the side chain conformations.[26] The β-methyl derivatives of Phe, Tyr, and Trp have been incorporated into various biologically active peptides[27] to better understand structure-activity relationship.
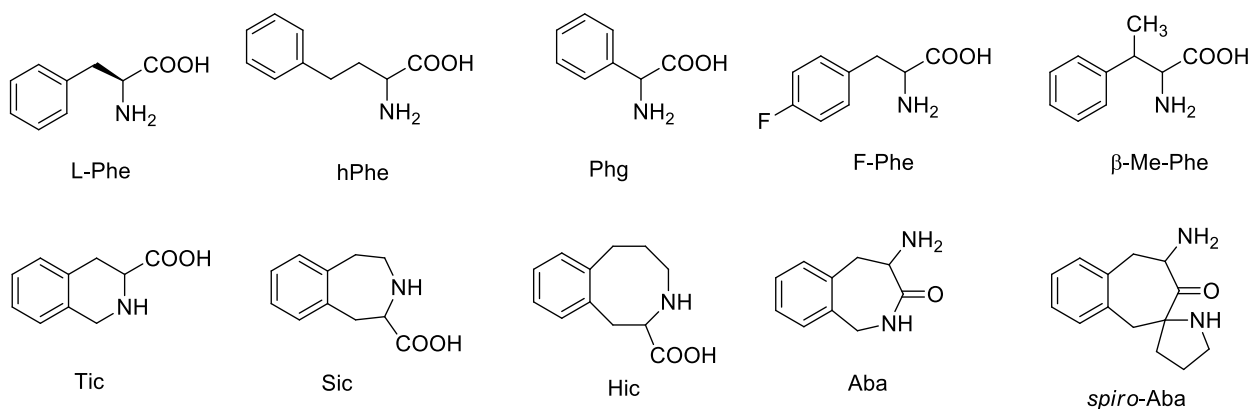
Figure 11. Linear and constrained Phenylalanine mimics.

[24] Azizeh B.Y., Shenderovich M.D., Trivedi D., Li G., Sturm N.S., Hruby V.J., "Topographical Amino Acid Substitution in Position 10 of Glucagon Leads to Antagonists/Partial Agonists with Greater Binding Differences" *J. Med. Chem.* **1996**, *39*, 2449–2455

[25] Haskell-Luevano C., Toth K., Boteju L., Job C., Castrucci A., Hadley M.E., Hruby V.J. "β-Methylation of the Phe7 and Trp9 Melanotropin Side Chain Pharmacophores Affects Ligand–Receptor Interactions and Prolonged Biological Activity" *J. Med. Chem.* **1997**, *40*, 2740–2749

[26] Hruby, V.J. "Conformational and Topographical Considerations in the Design of Biologically Active Peptides" *Biopolymers* **1993**, *33*, 1073-1082

[27] Toth G., Russell, K.C., Landis G., Kramer T. H.; Fang, L., Knapp R., Davis, P., Yamamura H. I.; Hruby V.J. "Ring Substituted and Other Conformationally Constrained Tyrosine Analogues of [D-Pen2, D-Pen5]enkephalin with δ–Opioid Receptor Selectivity" *J. Med. Chem*. **1992**, *35*, 2384-2391

On the other hand phenylalanine is a suitable starting point for the synthesis of conformationally constrained peptidomimetics which may drive the aromatic ring orientation in the proper hydrophobic region.

Within natural amino-acids, phenylalanine, tryptophan and tyrosine play a fundamental role in molecular recognition events because of aromatic ring presence. Giving also a more lipophilic profile to the peptide and being involved in π-interaction or hydrophobic cavity insertion. It is known that a good peptidomimetic drug candidate must cross the blood-brain barrier (BBB) or cell wall due to its intrinsic lipophilicity, when active transport is not a solution.

Benzazepinones have been widely studied as well. Specially for conformational and structural investigation within small peptides.[28] Recently, Tourwé and co-workers observed that in a series of Ac-Aba-Xaa-NHMe containing tetrapeptide models, the spirocyclic derivative, Ac-spiro-Aba-Gly-NHMe exclusively formed a β-turn, while other lactams, such as Ac-Aba-Gly-NHMe adopted mainly an extended conformation.[29]

Furthermore, in a recent work,[30] a combination of these common Phe mimics were exploited for the synthesis of a potent DOR radioantagonist. In particular a systematic combination of β-methyl substituted Phe stereoisomers coupled with Tic nucleus; proving how many efforts are dedicated to the synthesis of conformationally constrained peptidomimetics in the drug discovery process related to GPCRs ligands. Similarly this article reviews the emergence of derivatives based on the Tyr-Tic and Dmt-Tic pharmacophores as lead structures, and discusses potential clinical and therapeutic applications.[31]

Generally, these compounds are synthesized, also as pure enantiomers, with the Pictet-Spengler reaction in its variations from Phe, Tyr, *m*-Tyr, Trp and His, which allows to obtain the desired product in good yields. Approaches using more complex building blocks have been also proposed, involving the generation of benzenoid systems

[28] Tömböly Cs., Ballet S., Feytens D., Kover K.E., Borics A., Lovas S., Al-Khrasani M., Furst Z., Toth G., Benyhe S., Tourwé D. "Endomorphin-2 with a β-Turn Backbone Constraint Retains the Potent *μ*-Opioid Receptor Agonist Properties" *J. Med. Chem.* **2008**, *51*, 173-177

[29] Van Rompaey K., Ballet S., Tömböly Cs., De Wachter R., Vanommeslaeghe K., Biesmans M., Willem R., Tourwé D. "Synthesis and evaluation of the β-turn properties of 4-amino-1,2,4,5-tetrahydro-2-benzazepin-3-ones and of their spirocyclic derivative" *Eur.J. Org. Chem.* **2006**, *13*, 2899–2911

[30] Birkas E., Kertesz I., Toth G., Bakota L., Gulya K., Szucs M. "Synthesis and pharmacological characterization of a novel, highly potent, peptidomimetic delta-opioid radioantagonist, [3H]Tyr-Tic-(2S,3R)-beta-MePhe-Phe-OH" *Neuropeptides*, **2008**, *42 (1)*, 57-67

[31] Lazarus L.H., Bryant S.D., Cooper P.S., Guerrini R., Balboni G., Salvadori S. "Design of δ-opioid peptide antagonists for emerging drug applications" *Drug Discovery Today* **1998**, *3 (6)*, 284-294

through cycloaddition reactions. This may solve problems connected with the use of less nucleophilic substrates, substituted with electron withdrawing groups.[32]

The Tic skeleton (Tic = 1,2,3,4-tetrahydroisoquinoline-3-carboxylic acid) is probably the structure which, in recent years and in this context, was more developed and studied.[33] Many conformational analyses of this compound and of its derivatives are in fact available.[34] Tic containing peptidomimetics have often been used effectively in studies of the quantitative structure-activity relationship (QSAR). The tetrahydroisoquinoline unit is an important structural element in many alkaloids and pharmaceuticals. The Tic skeleton has been used many times as a rigid analogue of Phe and Tyr, for example in the design of peptidic antagonists of opioid receptors, showing useful therapeutic applications.

The Tic skeleton, in fact, allows to limit the torsional dihedral angle ψ, blocking the conformation of the side chain and bringing an hydrophobic aromatic residual important to cross the blood-brain barrier.

The Tic structure resulted for these reasons unique in its effects, even in comparison to potential promising residues, being crucial in the process of recognition of the ligand by the receptor. Modular aspects that have proved to be decisive for the activity are: the α stereogenic center, the hydrophobicity of the side chains, the derivatization of nitrogen and carbon terminal atoms, the reduction of some amide bonds of the peptidic chain and the possibility to use vinyl homologues.

The Pictet-Spengler cyclization[35] is an intramolecular reaction, promoted by acidic conditions, between a nucleophilic aromatic ring and an electrophilic iminium ion or acyl iminium ion. A new carbon-carbon bond is formed, increasing the skeleton complexity, and a new stereocenter is present when using any aldehyde but

[32] Sambasivarao K. "The Building block Approach to unusual α-amino acid derivatives and peptides" *Acc. Chem. Res.* **2002**, *36*, 342-351

[33] (a) Liskamp R.M.J. "Conformationally restricted amino acids and dipeptides, peptidomimetics and secondary structure mimetics" *Recl. Trav. Chim. Pays-Bas.* **1994**, *113*, 1-19. (b) Grieco P., Campiglia P., Gomez-Monterrey I., Novellino E. "Synthesis of new β-turn dipeptide mimetic based on tetrahydroisoquinoline moiety" *Tetrahedron Lett.* **2002**, *43* (36), 6297-6299. (c) Gibson S.E., Guillo N., Jones J.O., Buck I.M., Kalindjian S.B., Roberts S., Tozer M.J. "CCK2 receptor antagonists containing the conformationally constrained phenylalanine derivatives, including the new amino acid Xic" *Eur. J. Med. Chem.* **2002**, *37 (5)*, 379-389.

[34] (a) Lesma G., Meschini E., Recca T., Sacchetti A., Silvani A. "Synthesis of tetrahydroisoquinoline-based pseudopeptides and their characterization as suitable reverse turn mimetics" *Tetrahedron* **2007**, *63*, 5567–5578 (b) Landoni N., Lesma G., Sacchetti A., Silvani A. "Pyrroloisoquinoline-based tetrapeptide analogues mimicking reverse-turn secondary structures" *J. Org. Chem.* **2007**, *72*, 9765-9768 (c) Arbor S., Marshall G.R. "A virtual library of constrained cyclic tetrapeptides that mimics all four side-chain orientations for over half the reverse turns in the protein data bank" *J. Comput. Aided. Mol. Des.* **2009**, *23*, 87–95.

[35] (a) Pictet A., Spengler T. *Ber. Dtsch. Chem. Ges.* **1911**, *44*, 2030-2036 (b) Tatsui G.J. *Pharm. Soc. Jpn.* **1928**, *48*, 92

formaldehyde. Most of the peptidomimetic synthesized in this project rely on this strategy for the introduction of a conformational restriction.

This reaction is widely employed in the synthesis of tetrahydro-isoquinolines and tetrahydro-carbolines where the nucleophile is a phenyl ring or an indole.[36] Depending on the activation of the nucleophile, reaction conditions go from room temperature and acid catalysis (formic acid) to stronger conditions like refluxing solvent and strong acid (trifluoroacetic).

Nucleophilicity can be summarized with the following ascending order:

Phenyl < MeO-Phenyl < Indole

These aromatic rings can be traced to natural amino acids like Phe, Tyr, Dopa and Trp.

Most indicated electrophiles come from aldehydes, or acetals, affording products in good yield instead of ketones which tend to give lower conversion and longer reaction time. In Scheme 1a and 1b are described the general reaction mechanisms for the synthesis of *N*-acyl-Tic and *N*-acyl-Thbc skeletons. These chemical modifications occur also on the amines, with no need for a coupling, however it is more peculiar for activated aromatic ring like indole instead of phenyl.
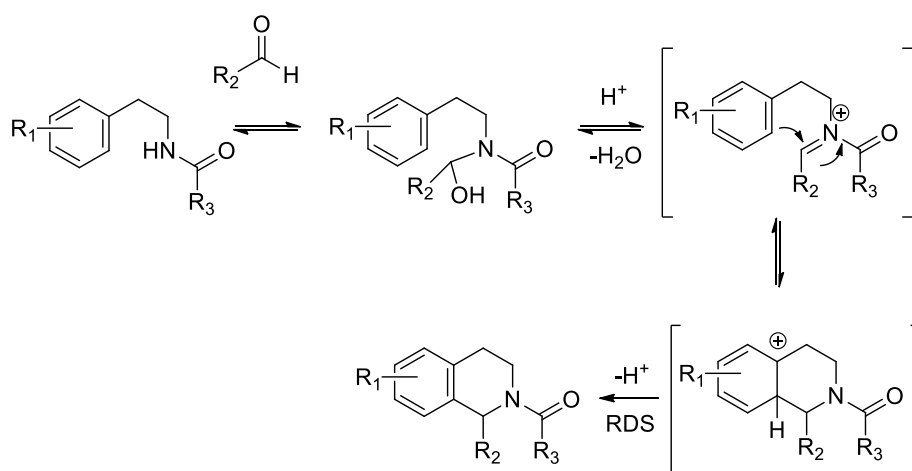
Scheme 1a. Reaction Mechanism for *N*-acyl iminium ion.

The first step is the formation of an iminium ion, the dehydration process is fundamental for the formation of such intermediate and is more evident in the *N*-acyl iminium pathway. This step is followed by electrophilic substitution at the position 2. The desired product is formed after deprotonation, to restore aromaticity and obtain a neutral derivative. This reaction is a classical favored 6-endo-trig cyclization.

[36] Cox E.D., Cook J.M. "The Pictet-Spengler condensation: a new direction for an old reaction" *Chem. Rev.* **1995**, *95*, 1797-1842

Stereocontrol of the new stereocenter is a demanding task. Usually is very difficult for phenylalanine derivatives, whereas enantiopure tryptophan are more inclined to afford the kinetically favored *cis* diastereomer for structural reasons. Quite recently have been developed a catalytic system to promote enantioselectively the PS cyclization.[37] Till now, there are few stereoselective catalytic examples and often they require difficult reaction conditions (long time, low temperature), whereas the substrate scope is limited.

The PS cyclization on the indole ring is slightly different (Scheme 1b) because of the indolic nitrogen participating in the mechanism. There are two possible mechanism, the C2 and the C3 addition. C2 addition is the favored pathway and leads to the desired tetrahydro-β-carboline core. C3 addition is non productive and leads to a spiroindolinone intermediate. This intermediate is reversible and might undergo a ring opening and then a productive C2 addition. When position C2 is substituted, C3 addition becomes favored and spiro derivatives can be isolated. However, C3 addition is in general disfavored because is a 5-endo-trig cyclization and is disallowed according to Baldwin's rules.
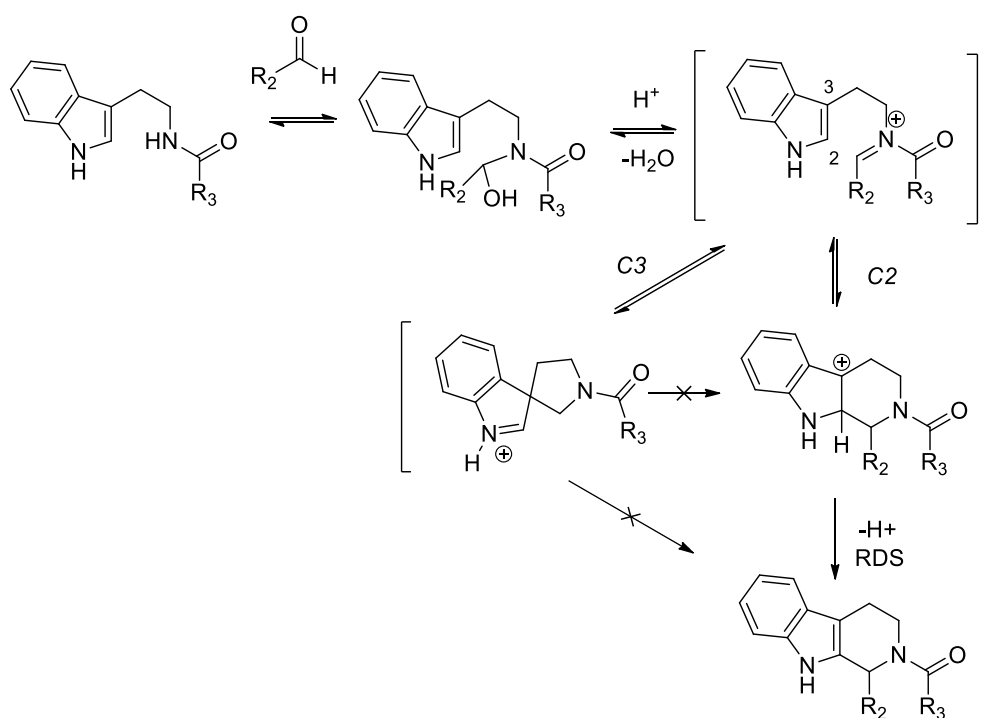
Scheme 1b. Reaction Mechanism for *N*-acyl iminium ion on Trp.

[37] (a) Seayad J., Seayad A.M., List B. "Catalytic Asymmetric Pictet-Spengler Reaction" *J. Am. Chem. Soc.* **2006**, *128*, 1086-1087 (b) Raheem I.T., Thiara P.S., Peterson E.A., Jacobsen E.N. "Enantioselective Pictet–Spengler-Type Cyclizations of Hydroxylactams: H-Bond Donor Catalysis by Anion Binding" *J. Am. Chem. Soc.* **2007**, *129*, 13404-13405

1.3 *G-Protein Coupled Receptors*

G-protein-coupled receptors (GPCRs) are a family of biological receptors constituted by seven transmembrane segments (α-helices), located on the cell surface. They are able to mediate cellular responses to extracellular stimuli, both endogenous chemicals or exogenous (external environmental agents). Once triggered by an extracellular signal, GPCRs activates heterotrimeric G proteins, which interact with different receptors, including guanosine nucleotides GTP and GDP, and with the GPCR itself at the level of the third long cytoplasmic loop, corresponding to the region of the molecule which is coupled to the G protein. The G protein activated, in fact, exchanges the bound GDP with the GTP. Then the GTP-protein dissociates from the occupied receptor, binding itself to another adjacent receptor and altering its activity. An important aspect of the signaling mechanism is that the ligand does not pass through the membrane. Instead, the signal is transferred to the inside of the cell by conformational changes in the receptor protein, which are coupled to ligand-binding events.
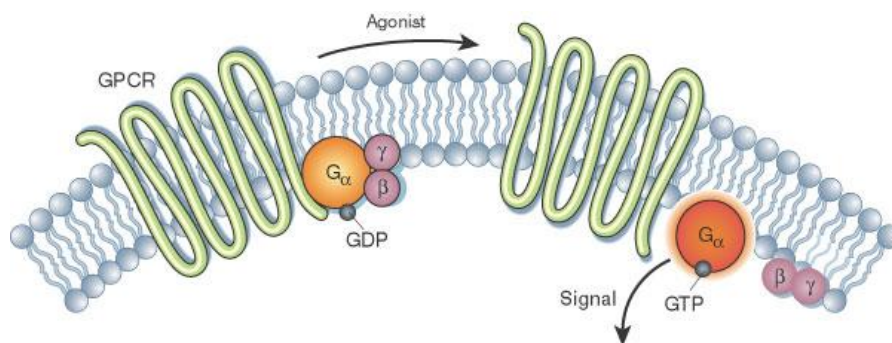
Figure 12. Activation of the G alpha subunit of a GPCR.

The activation of a GPCR triggers a cascade intracellular transduction of the signal, with numerous internal messengers, which produce the cellular change that characterizes or begins the physiological process. The human genome encodes between 700 and 1000 members of this family of receptors. About 60% of the known GPCRs represent sensory receptors, associated with taste, sight and smell; while only 300-400 GPCRs have a non-sensory function. Of these last category, about 175 receptors are considered "orphans", that is still devoid of an identified ligand.

The GPCRs are generally formed of a single polypeptidic chain of approximately 400-3000 amino-acidic residues, consisting of an extracellular N-terminal residue of variable length (7-3000 AAs), seven transmembrane α-helices (20-27 AAs), three *endo-* and three *exo-*loops (5-250 AAs) and an intracellular C-terminal residues (12-400 AAs) (**Figure 12**). The region of the seven transmembrane α-helices (7TM) is usually highly conserved, whereas other domains considerably vary among different GPCRs.

Historically, G protein-coupled receptors have been grouped in three classes but, up to now, were also identified other receptors that cannot properly be included in these.

The "Class A" is the largest group of GPCRs, most of which have a N-terminal residue very short and a highly conserved 7TM region. These receptors are structurally related to rhodopsin or adrenergic receptors and bind several amines, purines, and peptidic ligands. About 900 olfactory receptors belong to this class.

The "Class B" consists of the secretin-related receptors, which have six conserved cysteine and a binding domain for an hormonal ligand in their long N-terminal residue. These receptors bind large peptidic ligands such as glucagon.

To the "Class C" belong neurotransmitter receptors with long N-terminal residues (500-600 aa) and without homology in the 7TM region with other families of GPCRs. To this family belong for example the GABA and the Ca^{2+} receptors.

In addition to these three families it is possible to find many more recent introductions like the "Class D", which reunites the STE2 GPCRs containing a large amount of hydrophobic residues grouped into seven domains, the "Class E" to which belongs the cAMP receptors and the "Class F" which comprises GPCR Frizzled/TAS2.[38]

Almost half of the drugs currently registered exerts its therapeutic effect by binding to GPCRs, but the target receptors are limited to about thirty, over a total of thousand, and only few of these are peptide-activated. A lot of drugs used today binds with the hydrophobic transmembrane region of the GPCRs, but it's supposed that the majority of extracellular peptidic ligands interact primarily with the extracellular loops or with the *N*-terminal domain of the GPCR. For these reasons, a better knowledge of the protein-protein interactions, which are usually very complex and involve large surface areas, it's important to design new drugs that are able to interact at the best with these receptors.[39]
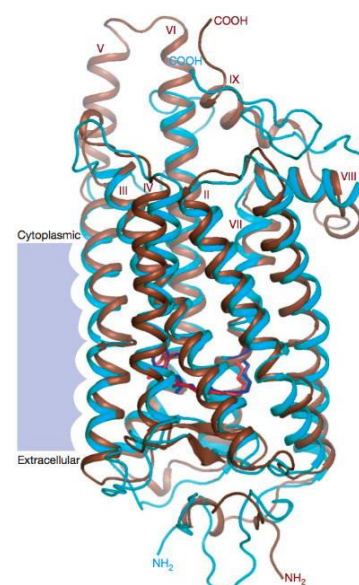
Figure 13. The bovine rhodopsin GPCR.

[38] (a) Attwood T.K., Findlay J.B. "Fingerprinting G-protein-coupled receptors" *Protein Eng.* **1994**, *7 (2)*, 195–203. (b) Dann C.E., Hsieh J.C., Rattner A., Sharma D., Nathans J., Leahy D. J. "Insights into Wnt binding and signaling from the structures of two Frizzled cysteine-rich domains" *Nature*, **2001**, *412*, 86–90. (c) Foord S.M., Bonner T.I., Neubig R.R., Rosser E.M., Pin J.P., Davenport A.P., Spedding M., Harmar A. "J. International Union of Pharmacology. XLVI. G protein-coupled receptor list" *Pharmacol. Rev.* **2005**, *57 (2)*, 279–88. (d) Kolakowski L.F. Jr. "GPCRDb: a G-protein-coupled receptor database" *Receptors Channels*, **1994**, *2 (1)*, 1–7.

[39] Tyndall J.D.A., Pfeiffer B., Abbenante G., Fairlie D.P. "Over one hundred peptide-activated G Protein-Coupled Receptors recognize ligands with turn structure" *Chem. Rev.* **2005**, *105*, 793-826.

Since few three-dimensional structure of a GPCR (the photoactivated bovine rhodopsin reported into **Figure 13**) are currently known, and only in its inactive state, the development of drugs that interact with G protein-coupled receptors is heavily based on ligand-based drug design. This strategy considers the structure of certain known ligands, basing the design of the new drug on these, rather than on the structure of the GPCR, less easy to interpret. Analyzing the main ligands for a wide range of GPCRs can be observed an universal recognition element: the reverse turn motif, generally adopted in solution by these ligands and closely associated with the binding capacity and therefore with the bioactivity.

In contrast with α-helices and β-sheets, turns are irregular secondary structures, sites where the polypeptidic chain turns down on itself and also responsible for the globularity of the proteins. In particular, β-turns are a specific secondary structure motif which is commonly recognized by most of the GPCRs family.

The geometric characteristics observed for a structure which can actually be considered as a good β-turn mimic are: dα distance between C$_\alpha$ atoms of the first and last residue respectively; the absolute value of the virtual torsion angle β defined as C$_{(1)}$-C$_{\alpha(2)}$-C$_{\alpha(3)}$-N$_{(4)}$ and the presence of the characteristic hydrogen bond C$_{(1)}$O$^{...}$HN$_{(4)}$.

The usually adopted classification criterion was proposed by Ball and co-workers. According to that, each tetrapeptidic sequence in which the distance C$_{\alpha(1)}$-C$_{\alpha(4)}$ appears
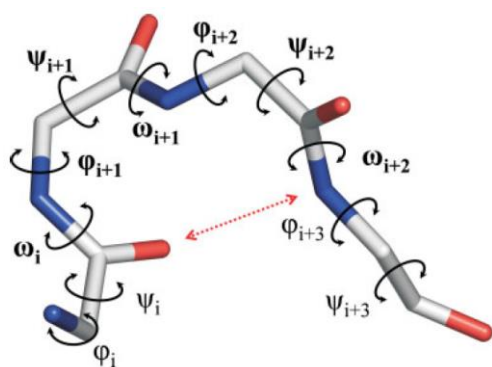
Figure 14. β-turn parameters.

to be less than 7 Å and in a region that lacks of α-helices, may be described as a β-turn.[40] The specific type of β-turn (**Figure 14**) is then classified according to the peptide geometry.

The geometric characteristics observed for a structure which can actually be considered as a good β-turn mimic are: dα distance between C$_\alpha$ atoms of the first and last residue respectively; the absolute value of the virtual torsion angle β defined as C$_{(1)}$-C$_{\alpha(2)}$-C$_{\alpha(3)}$-N$_{(4)}$ and the presence of the characteristic hydrogen bond C$_{(1)}$O$^{...}$HN$_{(4)}$.

[40] Ball J.B., Hughes R.A., Alewood P.F., Andrews P.R. "β-turn topography" *Tetrahedron*, **1993**, *49 (17)*, 3467-3478
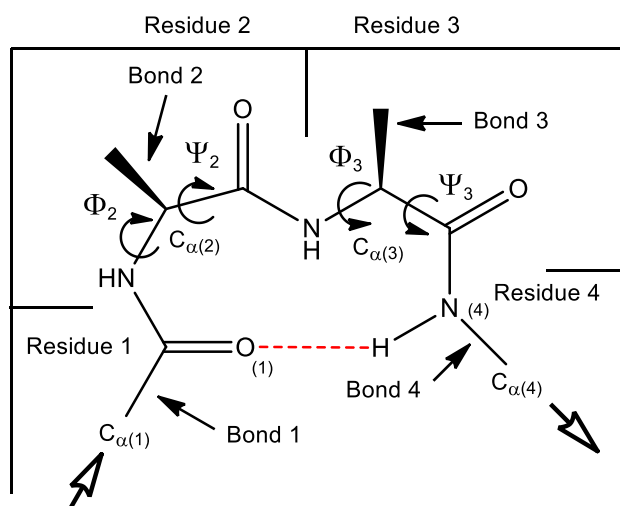
Figure 15. β-turn structure.

Although there are slight variations in the β-turn classification of based on the torsion angles φ and ψ, similar distributions of β-turns were identified, as well as a large number (30-50%) of non-ideal or distorted β-turns (usually defined as β-turns having only one torsion angle that differs by 45-50° from ideal values) and one or more categories not well defined (types VI and VII). In type I and type II β-turn peptide skeleton adopts an "U-shaped" conformation. These motifs are characterized by specific angular and torsional parameters in addition to an important 10-membered intramolecular H-bond that orient two peptide units from each end. It's so possible, with the synthesis of structurally constrained dipeptides, mimic the scaffold structure of the natural β-turns in a given target molecule, exploiting two features of the peptidomimetic (an amine group and a carboxylic group) to replicate the constriction deriving from the hydrogen bond. The presence of substituent functional groups on the chosen ring as base system or the presence within it of heteroatoms provide another opportunity for diversification. The nature of these substituents can be varied to direct the hydrophobic or hydrophilic interactions in the molecule in order to maximize the affinity for the biological target. There is a clear evidence that shows how the side chain of the peptide is often extremely important in the peptide-receptor interactions.

Today there is a growing interest towards this type of peptidomimetics since it was established that the conformational constriction has an important role in the biological activity of peptides, making them more potent agonists or antagonists against certain receptors. There is also a net gain in terms of specificity and stability against organic proteases. In this way it's possible to overcome most of the problems in the therapeutic use of these molecules. These mimetics may also be interesting for the conformational study of the ligand-receptor system and the bioactive structure.

In the next chapters I will present the thesis goal based on the information gathered. This work concerns the synthesis of peptidomimetics, some of them possessing a specific reverse-turn conformation, as potentially active ligands for well defined GPCRs and proteases. Peptidomimetics' strategy relies on three main ideas which can be summarized into three concepts: β-amino acids based, conformational restriction through side chain cyclization and secondary structure inducers.

CHAPTER II: ENDOMORPHIN-2 MIMICS

2.1 *Opioid Receptors*

The opioid receptors,[41] belonging to the class of GPCRs, are widely distributed in the nervous system and in the peripheral tissues of animals. An accurate evaluation at the molecular level of the ligand binding pathways into these receptors may play a key role in the design of new molecules with more desirable properties and reduced side effects. Agonists of these receptors have the ability to attenuate the acute and chronic pain, while antagonists may alleviate the reliance on opiate alkaloids and alcohol; they can be used as immunosuppressants after transplantation and are effective in the treatment of autism and the Tourette syndrome.[42] Gene disruption studies in mice show that the target for the majority of the effects of opioid alkaloids, whether beneficial or adverse, is the μ-OR^2. The μ-OR belongs to the γ subfamily of "Class A" G-protein-coupled receptors with two closely related family members known as the δ- and κ-opioid receptors. The μ-OR constitutes the main opioid target for the management of new drug candidates.

The opioid receptors are divided into three classes: δ, μ and κ, which differ for the bond profile with the ligand molecule. Morphine and codeine are the main active opioid alkaloids in opium and they possess an high affinity with almost no selectivity over all opioid receptors. Whereas the endogenous opioid ligands of mammals as enkephalin, endorphins and dynorphin, are not particularly selective in respect of the different classes of receptors, but endomorphin and deltorphin are respectively μ- and δ-selective, with a high biological stability and the ability to cross the blood-brain barrier. These peptides are then the starting point for a drug design leading to the preparation of analogous molecules with agonist or antagonist activity respect to these receptors. However, opioid drugs are highly addictive, with the acetylated form of morphine, heroin, being the best-known example. Because of this, the clinical efficacy of opioid drugs is often limited by the development of tolerance and dependence.

The first example of synthesis of a selective antagonist of receptor δ has involved the replacement, within peptides derived from the amphibian skins, of the amino acid in position two with a Tic skeleton. This allows for the generation of short-chain peptides with a total selectivity towards the δ receptors. These peptides show a lot of advantages such as low molecular weight, the ability to cross the blood-brain barrier, a limited number of conformations and a good resistance towards the proteolytic degradation.

[41] Stevens C.W. "The evolution of vertebrate opioid receptors" *Front. Biosci.* **2009**, *14*, 1247–1269

[42] Masakazu E. "Recent advances in selective opioid receptor agonist and antagonist", *Med. Res. Rev.* **2004**, *24 (2)*, 182-212

Starting from these results the tetrahydroisoquinolinic skeleton assumed a lead role in the study of strategies for the synthesis of opioid receptors structure.

Given the importance of DOR, MOR, and KOR in modulating opioid analgesia, it comes as no surprise that they have been the subject of intense research for developing potent opioid analgesics with fewer unwanted side effects. These side effects include sedation, euphoria, changes in thermoregulation, inhibition of gastrointestinal motility, respiratory depression, muscle rigidity and physical dependence.

However, to better understand the structural basis for MOR function, very recently a crystallographic study of this receptor has been performed.[43] In **Figure 16** is reported the overall view of the mouse MOR complexed with an irreversible morphinan agonist. This discovery is going to modify the entire drug discovery approach towards new analgesics. Shifting from a ligand-based drug design, established for the past decades on SAR studies, supported by deep computational and NMR-based conformational analysis, to a structure-based drug design, assisted by a more reliable and effective docking study, a useful tool for prediction in computer aided drug design (CADD).
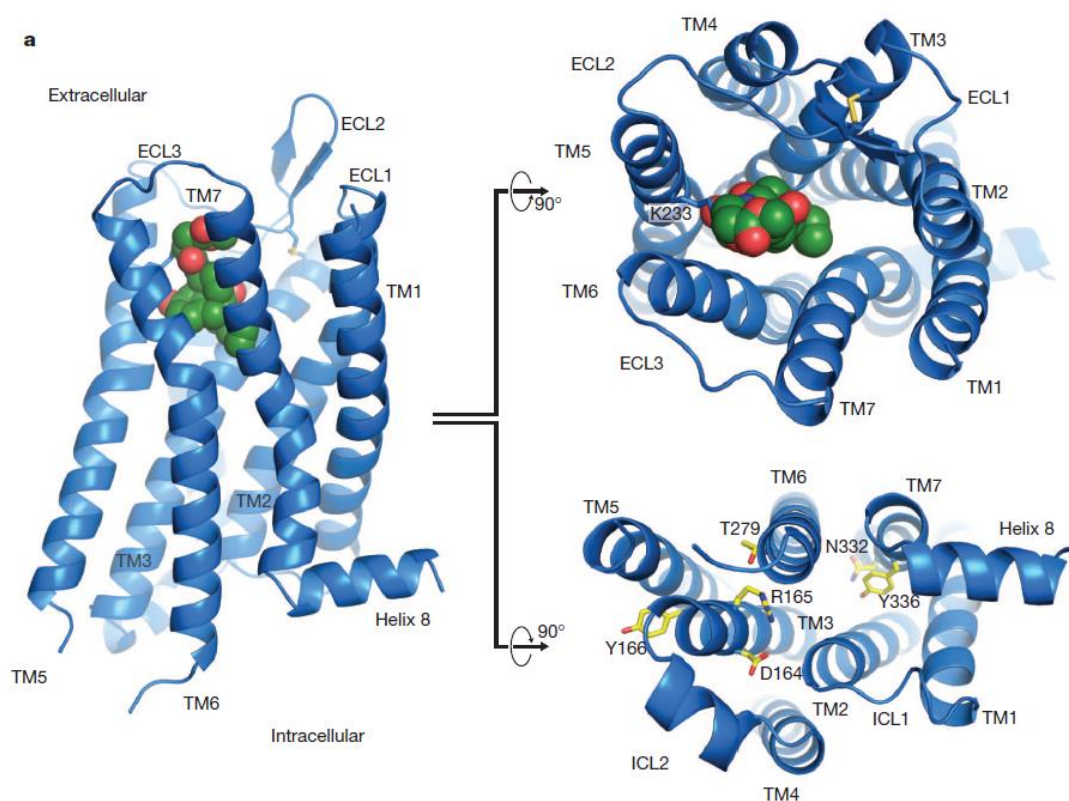
Figure 16. Overall view of the μ-OR structure bound to morphinan.

[43] (a) Manglik A., Kruse A.C., Kobilka T.S., Thian F.S., Mathiesen J.M., Sunahara R.K., Pardo L., Weis W.I., Kobilka B.K. Granier S. "Crystal structure of the μ-opioid receptor bound to a morphinan antagonist" *Nature*, **2012**, *485*, 321-327 (b) Granier S., Manglik A., Kruse A.C., Kobilka T.S., Thian F.S., Weis W.I., Kobilka B.K. "Structure of the δ-opioid receptor bound to naltrindole" *Nature*, **2012**, *485*, 400-404

Surprisingly MOR crystallizes as a dimeric structure, this suggests that the association may represent a higher-order oligomer in mammals. Consistent with a role for oligomerization in MOR function, the authors observed that the amino acids involved in the dimer interface display a high degree of homology with the DOR. Replacing the residues of MOR with the corresponding residues from DOR would not be predicted to interfere with dimer formation. This analysis also suggests that a μ-OR–δ-OR dimer could share the same interface. Interestingly, in the μ-OR TM5–TM6 dimer, the two binding sites are coupled through a network of packing interactions at the dimeric interface. This network could provide a structural explanation for the distinct pharmacological profiles obtained for μ-OR heterodimers and for the allosteric effects of one protomer on the pharmacological properties of the other. This dimeric interface thus provides potential insights into the mechanism of allosteric regulation of one GPCR protomer by the other.

These crystallographic data are very recent and, till now, not yet exploited for computational design. During next years, these worthy piece of information will be the starting point for drug candidates screening and for a much more faithful structure-activity relationship investigation.

2.2 *Endomorphins*

Among the endogenous peptides active towards GPCRs, in particular opioid receptors, there are several small molecules recently discovered: Endorphins, Endomorphins, Enkephalins, Dynorphin or Nociceptin. They are all involved in the pain perception biological process. In particular, Endomorphins are small tetrapeptide isolated from mammalian brain in 1997.[44] Endomorphins are two derivative which differ for the third residue, in EM-2 the Trp is replaced by a Phe.

Endomorphin-2 (H-Tyr-Pro-Phe-Phe-NH$_2$, EM-2) is a highly potent and selective μ-opioid receptor agonist neuropeptide. The amidated Endomorphin-2 (EM-2) tetrapeptide has been shown to be μ-opioid receptor agonist exhibiting a very high μ-receptor affinity and selectivity.[45] Because of the C-terminal amidation, EMs display the longest proteolytic half-lives among the known endogenous opioid peptides.

Metabolism of EMs is first the cleavage of Pro^2-Trp^3 and Pro^2-Phe^3 peptide bonds by the intervention of Serine Proteases. This family of proteolytic enzyme is known to metabolize most of the proline based neuropeptides. Among this family, Prolyl OligoPeptidease (POP) has been implicated in many physiological processes and is supposed to play a role in EMs metabolism.[46]

Since the μ-opioid receptor agonists display the most potent antinociceptive activity, EM-2 is an important model in the search towards new analgesics. Despite of the recent advances in the structural investigation of complex molecules, the comprehension of the 3D features for the interaction between opioid peptides and receptors remains an elusive task. This has to be attributed to the opioid peptides' nature which can assume different conformations and to opioid receptors' flexibility. Due to this inherent mobility of the ligand-receptor system massive efforts devoted to the definition of a rigid bioactive
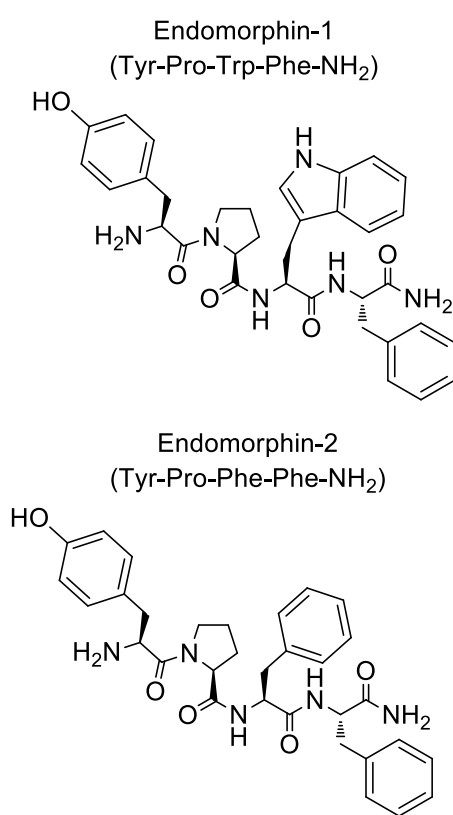
Figure 17. Endomorphins.

[44] Zadina J.E., Hackler L., Ge L.J., Kastin A.J. "A potent and selective endogenous agonist for the μ-opiate receptor" *Nature*, **1997**, *386*, 499-502

[45] Horvath G. "Endomorphin-1 and endomorphin-2: pharmacology of the selective endogenous μ-opioid receptor agonists" *Pharmacology & Therapeutics*, **2000**, *88*, 437-463

[46] Garcia-Horsman J.A., Mannisto P.T., Venalainen J.I. "On the role of Prolyl Oligopeptidase in health and disease" *Neuropeptides*, **2007**, *41*, 1-24

conformation might be overstressed.[47] Structural investigation of EM-2 reveals the high conformational freedom of the Phe side chains and also the inherent flexibility of the peptide backbone, indicating many probable bioactive conformations, ranging from β-turns to extended conformations.[28,48] The relevant role of the proper spatial orientation of the aromatic rings and in particular of the benzylic side chains at position 3 and 4 is well established, but not fully clarified.

Three main structural features must be undisclosed: the "message-address" concept, the pharmacophore elements and the *cis-trans* isomerisation about the Tyr[1]–Pro[2] peptide bond.[49]

EMs can be divided into two main portion: the message fragment are the N-terminal Tyr[1]-Pro[2]-Trp[3] and Tyr[1]-Pro[2]-Phe[3] tripeptide units. The address fragment is the remaining C-terminal Phe[4]-NH$_2$ peptide. These two sequences play a key role in the molecular recognition and binding event. The 3D structure of the message fragment is supposed to contribute to the bioactive conformation and to the binding process. On the other hand the message fragment might contribute to the structural stability and to the selectivity.

The pharmacophore unit are mainly related to hydrophobic interaction of the aromatic ring, the hydroxyl function of Tyr[1] and the amine which interacts with Asp147. Pro[2] is considered to be a stereochemical spacer and is responsible for the correct orientation of the pharmacophore groups.[50] Moreover is responsible to induce a *cis-trans* isomerisation.

Indeed, these tetrapeptides exist as an equilibrium mixture between the two isomers. The interconversion barrier is sufficiently low to allow a reversible conformational transition. The ratio of the two isomers depends on the solvent, but the *trans*-conformation is considered to be the bioactive form.

[47] Gentilucci L., Tolomelli A. "Recent Advances in the Investigation of the Bioactive Conformation of Peptides Active at the μ-opioid Receptor. Conformational Analysis of Endomorphins" *Curr. Top. Med. Chem*. **2004**, *4*, 105-121

[48] (a) Torino D., Mollica A., Pinnen F., Feliciani F., Lucente G., Fabrizi G., Portalone G., Davis P., Lai J., Ma S.W., Porreca F., Hruby V.J. "Synthesis and Evaluation of New Endomorphin-2 Analogues Containing (Z)-α,β-Didehydrophenylalanine (ΔZPhe) Residues" *J. Med. Chem*. **2010**, *53*, 4550-4554 (b) Keresztes A., Szűcs M., Borics A., Kövér K.E., Forró E., Fülöp F., Tömböly C., Péter A., Páhi A., Fábián G., Murányi M., Tóth G. "New Endomorphin Analogues Containing Alicyclic β-Amino Acids: Influence on Bioactive Conformation and Pharmacological Profile" *J. Med. Chem.* **2008**, *51*, 4270-4279

[49] Leitgeb B. "Structural Investigation of Endomorphins by Experimental and Theoretical Methods: Hunting for the Bioactive Conformation" *Chem & Biodiv.* **2007**, *4*, 2703-2724

[50] Paterlini M.G., Avitable F., Ostrowski B.G., Ferguson D.M., Portoghese P.S. "Stereochemical requirements for receptor recognition of the mu-opioid peptide endomorphin-1" *Biophys. J.* **2000**, *78*, 590-599

2.2.1. *Endomorphins Mimics: State of the art*

During the past years a lot of efforts have been spent in the synthesis of EMs analogues with the aim to achieve a better structure-activity information.[51]

Modifications at Tyr[1]- and *N*-terminal positions require caution because of their pharmacological relevance.[52] Usually the phenolic moiety is kept intact while alkylation of the Tyr[1] aromatic ring is quite usual. The most exploited Tyr mimic is Dmt (dimethyl tyrosine) which showed in many cases a maintenance for opioid receptor affinity because of a better hydrophobic interaction in the binding pocket.[53]
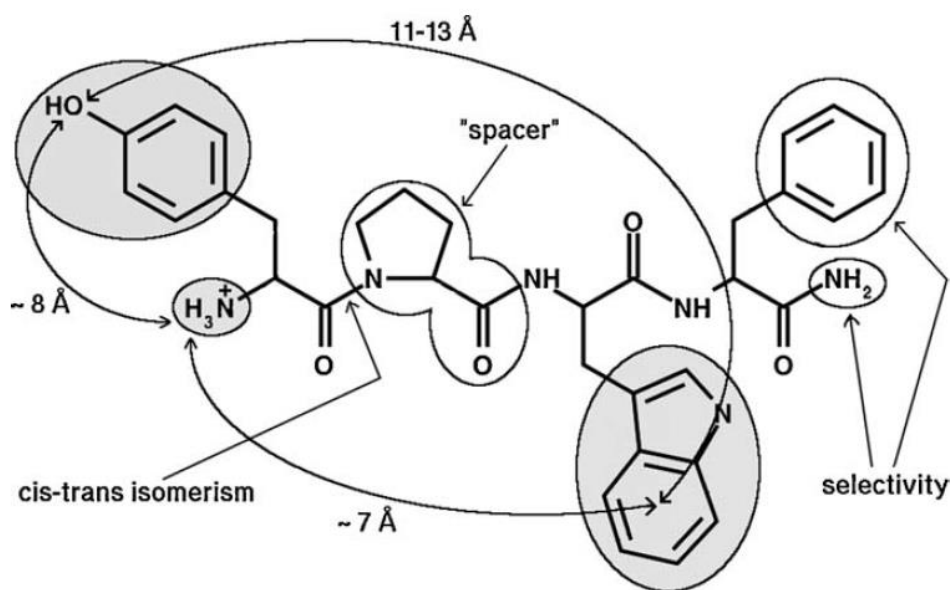
Figure 18. General structural features for EM-1 (EM-2).

Regarding Pro[2], modifications have been performed with the aim of a better proteolytic stability and to force the Tyr[1] pharmacophore residue in a specific 3D conformation. Replacement with unnatural D isomer (D-Pro[2]) lead to a remarkable longer half-life and a new 3D shape of the molecule. However, an extensive investigation using β-Pro derivative has been performed.[54] Moreover β-Pro offers a good systematic

[51] Keresztes A., Borics A., Toth G. "Recent Advances in Endomorphin Engineering" *Chem. Med. Chem.* **2010**, *5*, 1176-1196

[52] Szatamari I., Biyashev D., Tomboly C., Toth G., Macsai M., Szabo G., Borsodi A., Lengyel I. "Influence of degradation on binding properties and biological activity of endomorphin-1" *Biochem Biophys. Res. Commun.* **2001**, *284*, 771-776

[53] (a) Li. T., Fujita Y., Tsuda Y., Miyazaki A., Ambo A., Sasaki Y., Jinsma Y., Bryant S.D., Lazarus L.H., Okada Y. "Development of potent µ-opioid receptor ligands using unique tyrosine analogues of Endomorphin-2." *J. Med. Chem.* **2005**, *48*, 586-592 (b) Jinsmaa Y., Marczak E., Fujita Y., Shiotani K., Miyazaki A., Li T., Tsuda Y., Ambo A., Sasaki Y., Bryant S.D., Okada Y., Lazarus L.H. "Potent in vivo antinociception and opioid receptor preference of the novel analogue [Dmt[1]]Endomorphin-1" *Pharmacol Biochem Behav.* **2006**, *84*, 252-258

[54] Fulop F., Martinek T.A., Toth G.K. "Application of alicyclic β-amino acids in peptide chemistry" *Chem. Soc. Rev.* **2006**, *35*, 323-334

manipulation tool for EMs secondary structure depending on the absolute and relative configuration; inducing a bent structure instead of an extended one. A very recent work exploited this strategy and the author were also able to preferentially induce a *trans-*conformation around the Pro[2] peptide bond.[55] On the other hand, a systematic study on the ring size of the βPro and its stereochemical configuration showed analogues with a very high affinity and selectivity towards MOR.[48b]

A contemporary double replacement of the dipeptide Tyr[1]-Pro[2] with Dmt-βPro and other isomers displayed, in one case, one of the highest MOR affinities ever observed, in the very low nanomolar scale. Apparently, active compounds substituted by a βPro prefer a bent conformation instead of an extended structure.[56]

Summarizing, Pro-targeting single and multiple modifications result in proteolytically stable analogues and maintaining, in most cases, a biological activity comparable to EM-1 and EM-2.
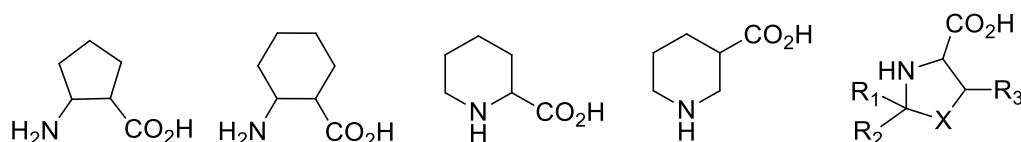
Figure 19. Proline based amino acids incorporated in place of Pro[2].

The last point of functionalization is the Phe[3]-Phe[4] residue bearing the carboxy amide pendant. I reported previously some common example for Phe replacement. It's very important to remember that Phe[3] aromatic ring is mandatory for MOR binding. Furthermore, the aromaticity cannot be replaced by an hydrophobic ring such as cyclohexil. Application of the Phe mimetic Phg and Hfe at position 3 and 4 resulted in equally or less potent analogues relative to EM-2.[57] In general has been observed that the presence of an hydrophobic aromatic ring is highly recommended for maintaining a good opioid affinity, while the proper spatial orientation might reach a low nanomolar interaction and a higher selectivity. Incorporation of β-MePhe at either position 3 or 4 alters the population of rotamers and involves the research for the most suitable

[55] Borics A., Mallareddy J.R., Timari I., Kővér K.E., Keresztes A., Tóth G. "The Effect of Pro[2] Modifications on the Structural and Pharmacological Properties of Endomorphin-2" *J. Med. Chem.* **2012**, *55*, 8418-8428

[56] Mallareddy J.R., Borics A., Keresztes A., Kővér K.E., Tourwé D., Tóth G. "Design, Synthesis, Pharmacological Evaluation, and Structure-Activity Study of Novel Endomorphin Analogues With Multiple Structural Modifications" *J. Med. Chem.* **2011**, *54*, 1462-1472

[57] Gao Y., Liu X., Liu W., Qi Y., Liu X., Zhou Y., Wang R. "Opioid receptor binding and antinociceptive activity of the analogues of endomorphin-2 and morphiceptin with phenylalanine mimics in the position 3 or 4" *Bioorg. Med. Chem. Lett.* **2006**, *16*, 3688-3692

diasteromeric couple.[58] Author observed that only the replacement of Phe[4] with the (2*S*,3*S*)-β-MePhe lead to peptides which exhibited MOR affinities higher than parent endomorphins 1 and 2, also increasing enzymatic stability.

A systematic study on the aromatic ring spatial orientation was performed by constraining Phe side chains with dehydrophenylalanine in configuration Z alternatively at position 3, 4 or both.[48a] This work suggests that Phe[3] aromatic ring requires a certain flexibility and the conformationally constrained Phe[4] inducing an extended conformation.

With the aim of contemporary replace the Pro[2]-Phe[3] portion of EM-2, Tourwé and co-workers exploited a well known conformationally constrained Phe mimic, that is spiro-Aba.[28] Secondly, such substitution in a very small tetrapeptide was able to block the *trans*-conformation around Tyr[1]-Pro[2] bond and also to induce a stable β-turn. The small library of synthesized analogues, possessing different configuration, revealed to be slightly active, only with the Tyr-(*R*)-spiro-Aba-Gly-Phe-NH$_2$ derivative. However it showed a high selectivity toward MOR.

Phe[4] is a critical part of the address sequence as well. The aromatic ring is required for binding and EMs analogues without an hydrophobic aromatic residue, properly oriented, suffers a lower potency. However, the C-terminal amide has been deeply modified in order to understand its possible implication in the binding process. Comparison of the binding results revealed that a polar function maintains or increases the affinity while a bulky or non-polar termination does not favor MOR binding.[59]

Surprisingly, the exploitation of β-amino acids for Trp or Phe replacement has been poorly investigated. The main reason relies on the poor biological results obtained so far. Gentilucci and co-workers systematically replaced each amino acid of EM-1 with a β-Xaa or β-homo-Xaa.[60] This strategy allowed to obtain a series of derivative which displayed a good proteolytic stability, an extensive pharmacokinetic study supports this statement, whereas the MOR affinity in the nanomolar range was comparable to reference only for β-L-hPro[2] containing peptidomimetic. Same approach was not

[58] Tomboly C., Kover K.E. Antal P., Tourwé D., Biyashev D., Benyhe S., Borsodi A., Al-Khrasani M., Ronai A.Z., Toth G. "Structure-Activity Study on the Phe Side Chain Arrangement of Endomorphins Using Conformationally Constrained Analogues" *J. Med. Chem.* **2004**, *47*, 735-743

[59] Wang C., Yao J., Yua Y., Shao X., Cui Y., Liu H., Lai L., Wang R. "Structure–activity study of endomorphin-2 analogues with C-terminal modifications by NMR spectroscopy and molecular modeling" *Bioorg. Med. Chem.* **2008**, *16*, 6415-6422

[60] (a) Cardillo G., Gentilucci L., Melchiorre P., Spampinato S. "Synthesis and Binding Activity of Endomoprhin-1 Analogues Containing β-Amino Acids" *Bioorg. Med. Chem. Lett.* **2000**, *10*, 2755-2758 (b) Cardillo G., Gentilucci L., Qasem A.R., Sgarzi F., Spampinato S. "Endomorphin-1 Analogues Containing β-Proline are µ-Opioid Receptor Agonists and Display Enhanced Enzymatic Hydrolysis Resistance" *J. Med. Chem.* **2002**, *45*, 2571-2578

employed in the synthesis of EM-2 mimetics, probably due to the lack of encouraging results.

In this biological and chemical context, we started our research conjugating different ideas in order to synthesize EM-2 analogues possessing three main features. They should be β-amino acid based, with a proteinogenic like side chain. So we focused our attention to β^2-hPhe and β^3-hPhe. Moreover, they present a conformational restriction on the corresponding Phe^4 portion, to possibly induce a preferential turn conformation, and not constrained on Phe^3 because of previous mimics synthesized by Hruby and co-workers which displayed a decrease in potency. In comparison to other research groups, we also planned to simultaneously replace the Phe^3-Phe^4 portion of EM-2 and to give a synergic positive effect to the resulting analogues library. Working on both the residues, we were able to specifically tune relative aromatic ring distance and spatial orientation due to the stereochemical configuration and conformational restriction.

2.3 *Computational Design*

Focusing our attention on β^2-hPhe- and β^3-hPhe-based dipeptide mimics, a computer-assisted conformational analysis was performed[61] on compounds **1**-**4**, in order to evaluate the reverse turn-like mimicry, bearing in mind that an important feature in stabilizing the reverse turn conformation is the presence of intramolecular hydrogen bonds. For homodipeptide segments, two hydrogen bonded rings can in principle be formed, with hydrogen bond directionalities that run in normal direction (4-1, 12-membered hydrogen bond) and reversed direction (1-2, 10-membered hydrogen bond). According to the literature, a β^2-aa-β^3-aa segment should favor folding with formation of a 10-membered hydrogen-bonded ring. On the other hand, a β^3-aa-β^2-aa segment should stabilize 12-membered hydrogen-bonded conformations.

The computational procedure consisted in an unconstrained Monte Carlo/Energy Minimization conformational search using the molecular mechanics MMFF94 force field,[62,63] *in vacuo*. For each compound only conformations within 6 kcal/mol of the global minimum were kept. Results are reported in Table 1 as percentage of conformers which show an intramolecular hydrogen bond. The conformational analysis shows that homologated dipeptide derivatives **1** and **3** seem to prefer 8-membered H-bond conformations, while constrained segments **2** and **4** are more inclined to reverse turn conformations, with prevalence of 12-membered H-bonds in both cases.

---

[61] In collaboration with Dr. A. Sacchetti, Politecnico di Milano.

[62] Halgren T.A. "Merck molecular force field: I. Basis, form, scope, parameterization and performance of MMFF94" *J. Comput. Chem.* **1996**, *17*, 490-519

[63] Hydrogen bonds are defined as non-bonded contacts between a nitrogen or oxygen and an hydrogen attached to nitrogen or oxygen, separated by a distance ranging from 1.6Å to 2.1Å and making an X-H--Y (X,Y = N,O) angle >120°.
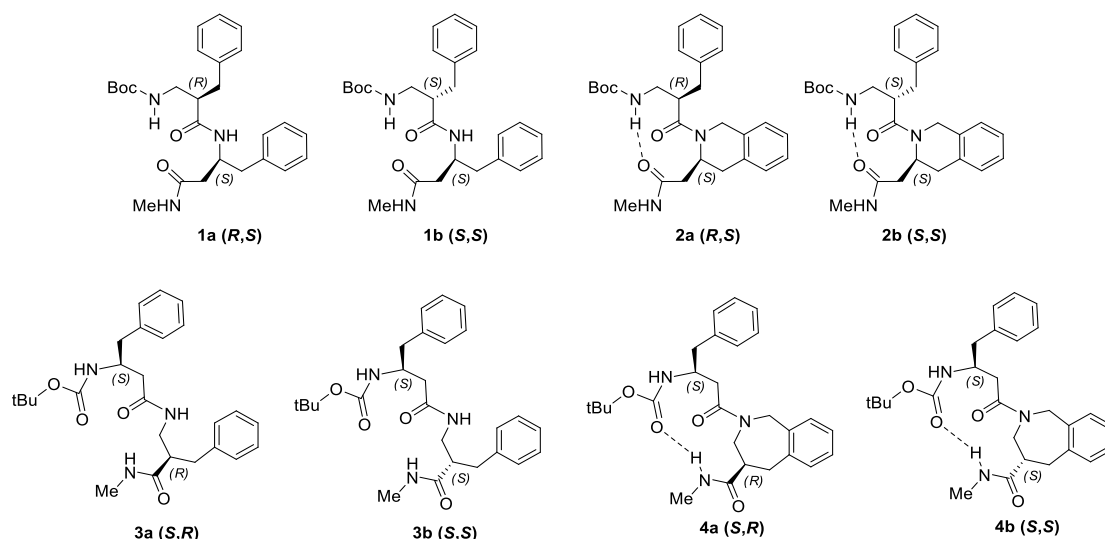
Figure 20. Dipeptides computer assisted design.

Table 1. Conformers Distribution.

H Bond (directionality)	1a	1b	2a	2b	3a	3b	4a	4b
n° of conf. < 6Kcal/mol	23	32	29	35	36	41	36	34
8H Ring (4-2)	11%,#	16%	37%	23%	45%, #	19%	0%	9%
8H Ring (3-1)	26%,#	19%, #	--	--	17%	19%, #	--	--
10H Ring (1-2)	0%	3%	0%	3%	0%	2%	0%	0%
12H Ring (4-1)	4%	16%, #	20% ,#	3%,#	14%	7%, #	25%, #	6%, #

H bond present in the energy minimum

Because of these promising data, I planned a synthetic pathway to verify the dipeptides secondary structure. Same scaffolds, as methyl esters, were also inserted in EM-2 tetrapeptide and subjected to biological evaluation.

General disconnection involves the coupling between two β-hPhe monomers protected as Boc or methyl ester. Thus the conformational restriction occurs on a single β-hPhe exploiting a PS cyclization to give a six or seven member ring depending on the building block employed.

2.4 Synthesis

The target compounds **1-4** were synthesised from the key precursors β³-hPhe and β²-hPhe. Preparation of variously protected β³-hPhe derivatives **10** and **11** was accomplished following the protocol of stereospecific classical homologation of the corresponding L-αPhe, by means of Kolbe reaction (Scheme 2).[60a] The whole synthetic pathway has been optimized and it is column-free until compound **9**. Reduction of nitrile **9**, with contemporary Boc deprotection, occurs under strong acidic condition in good chemical yield. Free amine is obtained by basic extraction of AcOEt solution with NaHCO₃ ss.
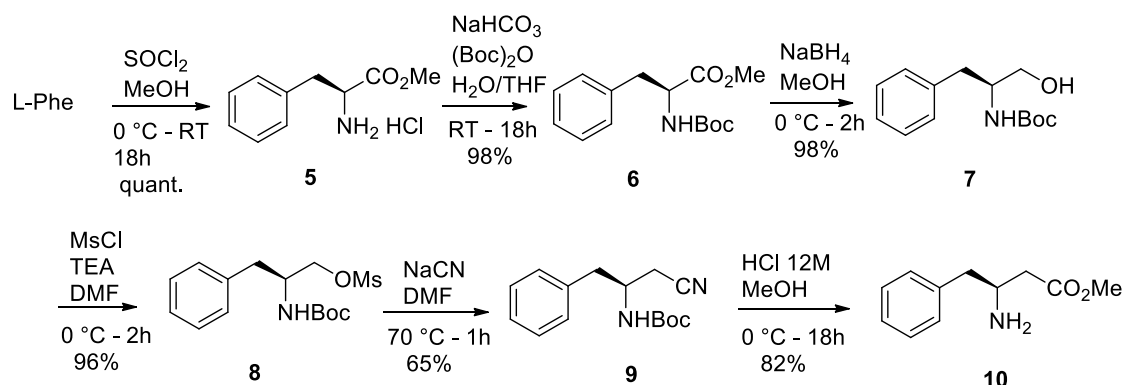
Scheme 2. Synthesis of β³-hPhe.

Direct Pictet-Spengler condensation on compound **10** to afford **14**, does not occur even under strong acidic conditions. I suppose that the lack of iminium ion stabilization, present in α-AAs, is the main reason. Indeed, after protection of the amino group with a temporary protective group, stable under acidic conditions (i.e. Cbz), the PS cyclization undergoes smoothly in decent yield, using trioxane as formaldehyde source. The reaction is followed by Cbz deprotection and allowed us to obtain the homo-Tic derivative **14** (Tic = 1,2,3,4-tetrahydroisoquinoline-3-carboxylic acid).
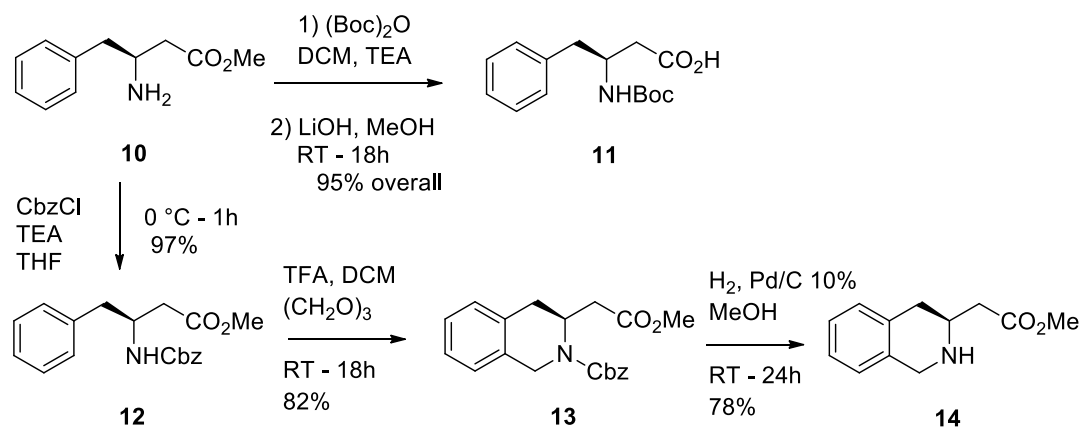
Scheme 3. β³-hPhe building blocks preparation.

At the very beginning, I also planned to synthesize β^3-hPhe derivatives using a faster Arndt-Eistert homologation procedure,[64] but the overall yield were not suitable for a gram scale synthesis. Mainly because of the usage of TMSCHN$_2$ instead of diazomethane. Because of the synthetic issues previously described in the PS cyclization step, I also tried the Arndt-Eistert homologation on a Tic protected derivative but it seemed completely unreactive under this conditions.[65]
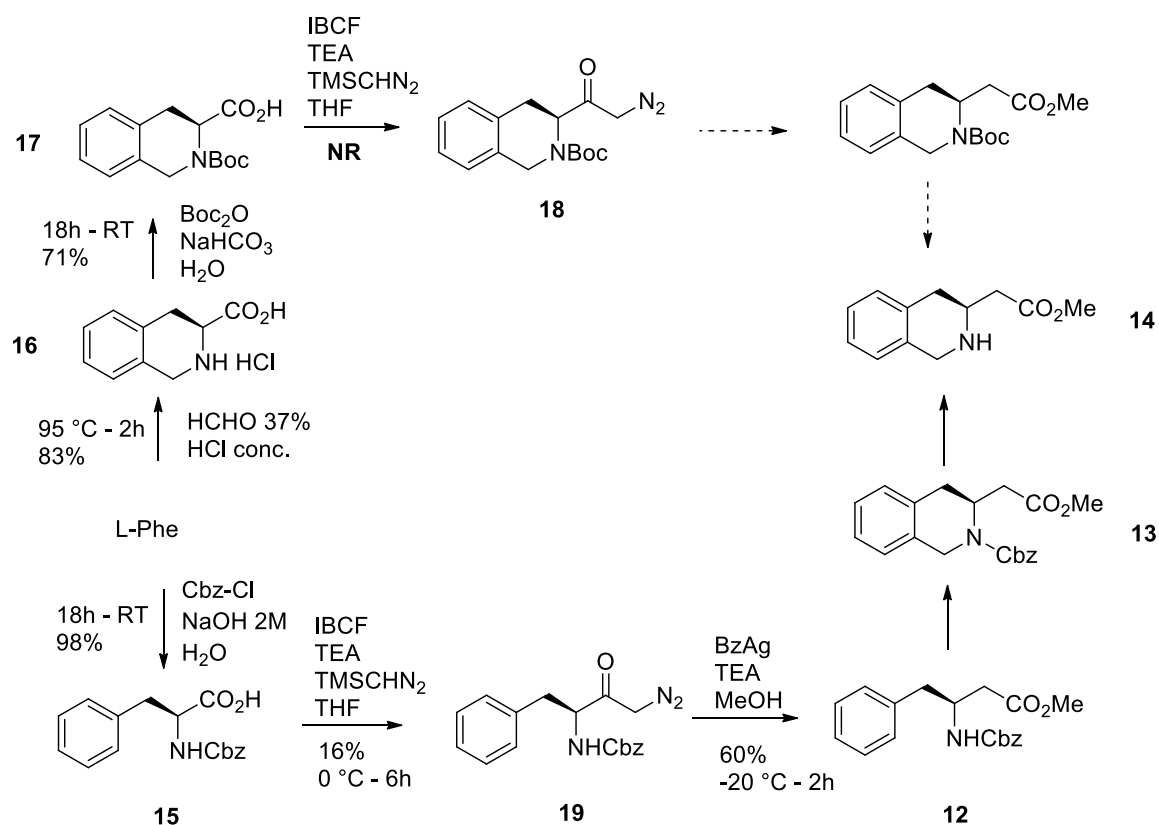
Scheme 4. Arndt-Eistert alternative route.

β^2-hPhe could be obtained in both the enantiomeric forms following an efficient protocol developed by Gellman[66] which relies on the synthetic sequence depicted in Scheme 5. Key step is the Michael addition of a chiral hydroxylamine to the α-benzylacrylate **22.** Procedure has been improved by using just 1 equivalent of precious auxiliary at 45 °C instead of 2 eq. at room temperature. The addition is followed by cyclization to give a diastereomeric mixture of α-substituted isoxazolidinones **24a** and

[64] Arvidsson P.I., Frackenpohl J., Seebach D. "Syntheses and CD-Spectroscopic Investigations of Longer-Chain β-Peptides: Preparation by Solid-Phase Couplings of Single Amino Acids, Dipeptides, and Tripeptides" *Helvetica Chim. Acta* **2003**, *86*, 1523-1553

[65] Cesar J., Dolenc M.S. "Trimethylsilyldiazomethane in the preparation of diazoketones via mixed anhydride and coupling reagent methods: a new approach to the Arndt-Eistert synthesis" *Tetrahedron Lett.* **2001**, *42*, 7099-7102

[66] Lee H.S., Park J.S., Kim B.M., Gellman S.H. "Efficient Synthesis of Enantiomerically Pure β2-Amino Acids via Chiral Isoxazolidinones" *J. Org. Chem.* **2003**, *68*, 1575-1578

24b, separable by column chromatography. After hydrogenolytic removal of chiral auxiliary and ring opening, β²-hPhe unprotected amino acids were recovered as optically pure enantiomers.
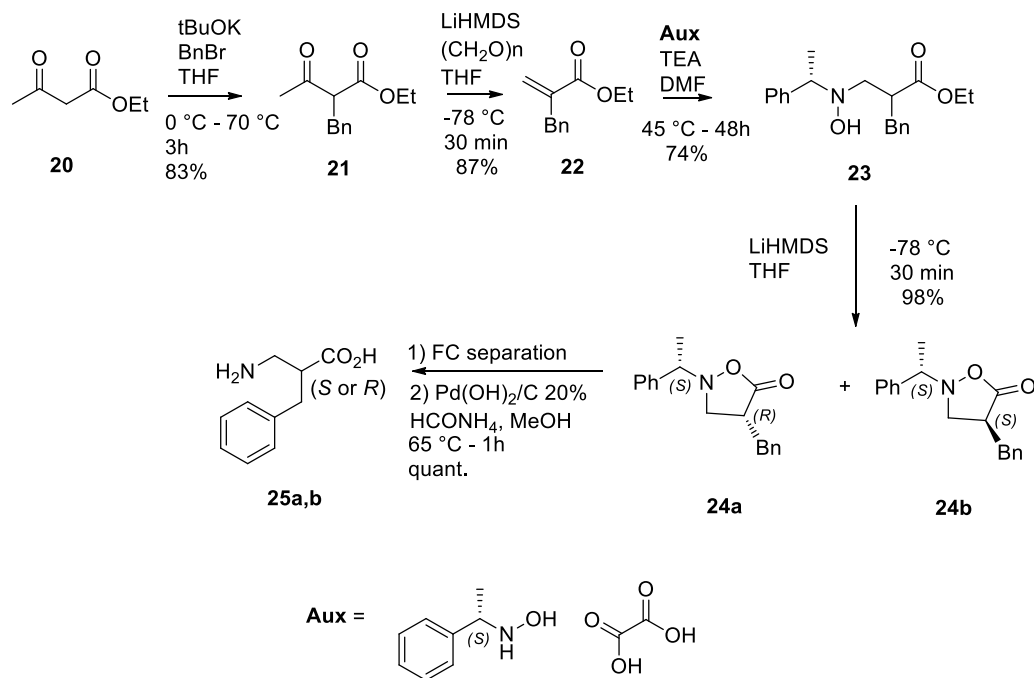
Scheme 5. Synthesis of β²-hPhe.

Derivatives **25a,b** were alternatively protected at the acidic or aminic position for peptide coupling and afforded **26a,b** and **27a,b**. Compounds **27a,b** were then converted to the corresponding Cbz-protected **28a,b** and subjected to Pictet-Spengler reaction, affording in good yield benzazepines **29a,b**. The cyclization is stereoretentive, it requires the presence of a stabilizing carbamate and occurs in short time with reasonable yield. Cbz group is removed with Pd/C 10% under hydrogen atmosphere in six hours, to prevent hydrogenation of the benzylic bond. Longer reaction time showed the presence of a toluene derivative, identified by ^{1}H NMR presence of a methyl signal.

PS cyclization directly on dipeptides worked sluggishly, with lower yields and regioselectivity issues to be taken in account. That's why, in all the examples presented, I prepared the cyclized β-hPhe and then coupled to a second monomer. Moreover, to induce the desired regioselectivity, amino groups have to be protected as imides which are not as easy as Boc to be installed and removed.
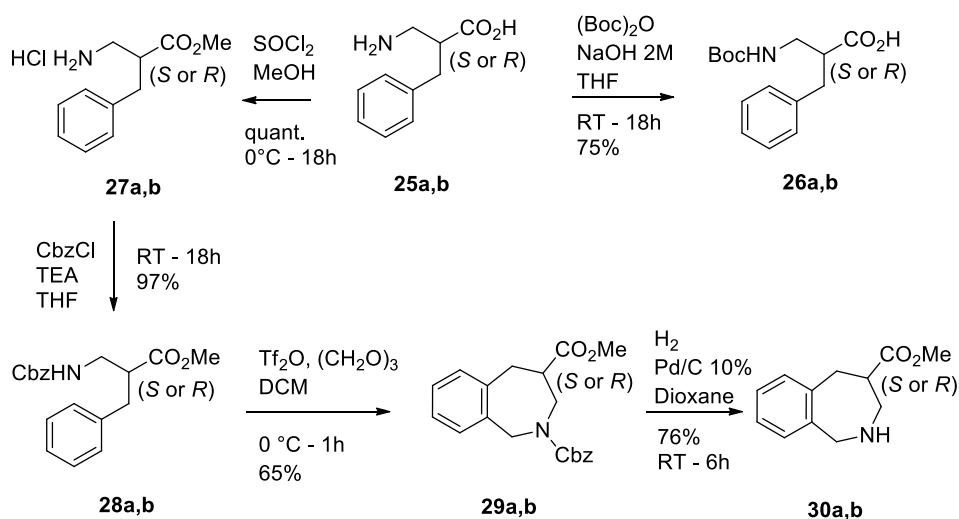
Scheme 6. β²-hPhe building blocks preparation.

With β²-hPhe, β³-hPhe and the corresponding constrained derivatives available, I pursuit the synthesis of different dipeptidomimetic scaffolds **31**-**37**, by standard peptide coupling chemistry (Scheme 7-8). In addition to the planned constrained and linear dipeptides, I also synthesized β³-hPhe-β³-hPhe **33** and **36** and β²-hPhe-β²-hPhe **37**.
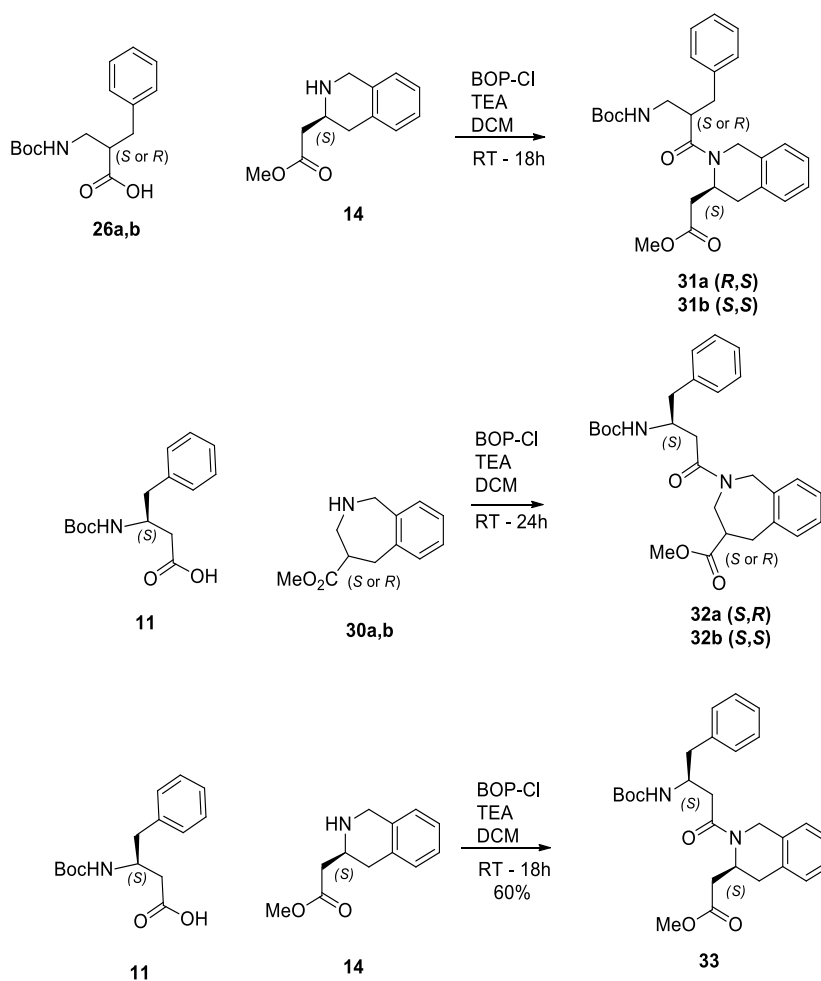
Scheme 7. Peptide Coupling – Constrained scaffolds.
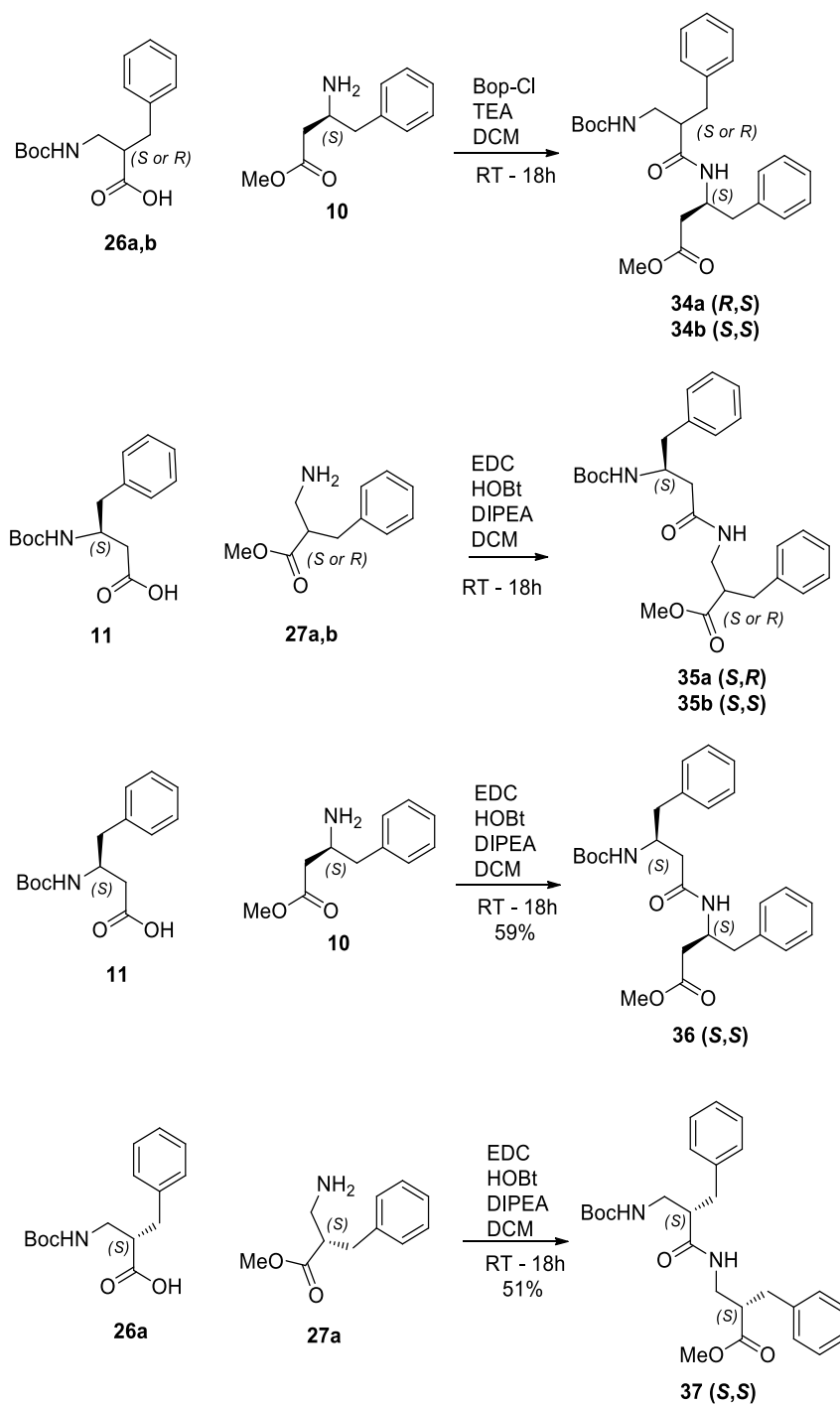
Scheme 8. Peptide Coupling – Linear scaffolds.

The aim was to extend the chemical space in our β-amino acid containing EM-2 peptidomimetics and evaluate most of the possible combinations.

I observed, from a preliminary coupling agent screening, that for cyclic derivatives BOP-Cl is the most suitable reagent, while for linear one, the cheap and well known EDC – HOBt couple is sufficient for reasonable yield.

Compounds **31a,b** and **32a,b** were then converted into methyl amide using a solution of methylamine in ethanol. I investigated the secondary structure conformation by employing a combination of different techniques and instrumentation: ^{1}H NMR, VT-NMR and IR. Results will be presented in next paragraph.
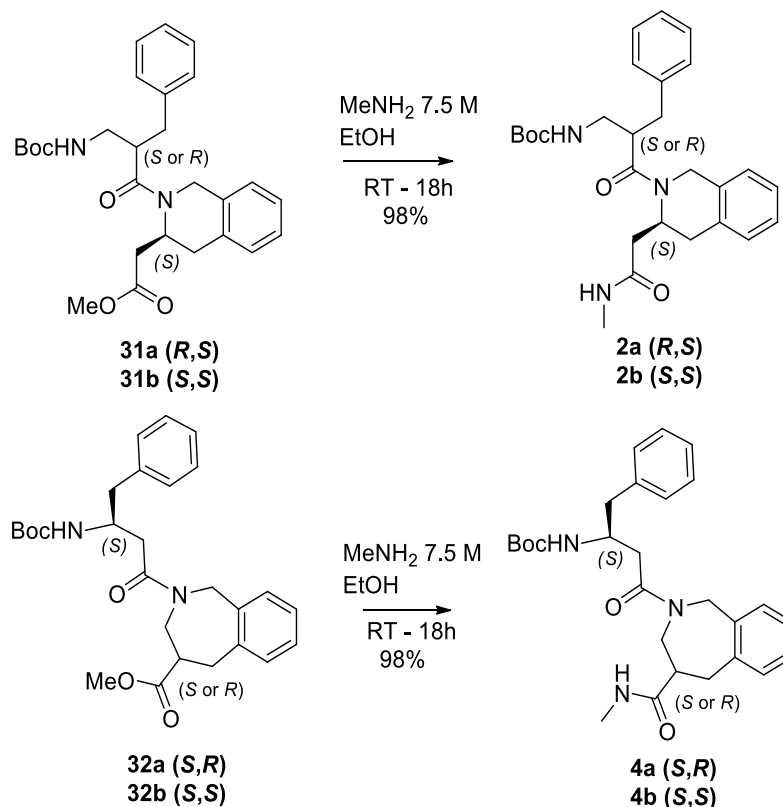
Scheme 9. Synthesis methyl amides.

With the aim of introducing new modifications in the field of β-amino acids peptidomimetics I also tried to focus on benzazepinonic scaffolds. This strategy was an extension of existing methodologies for the synthesis of α-amino acid based benzazepinones.[67] The idea was to isolate an intramolecular source of formaldehyde, masked as six member ring 1,3-oxazinan-6-one aminal (**41**), then subject such intermediate to a PS cyclization. In order to prevent regioselectivity issues, β^2-hPhe amino group was doubly protected as imide; reaction conditions for **41** might promote a PS cyclization on the same amino acid. So I chose phthalimide as protective group. Synthesis of desired linear dipeptide **40** went easily until I tried different reaction condition to promote the cyclization.

---

[67] (a) Ballet S., De Wachter R., Bert U.W., Tourwé D. "Derivatization of 1-phenyl substituted 4-amino-2-benzazepin-3-ones: evaluation of Pd-catalyzed coupling reactions" *Tetrahedron*, **2007**, *63*, 3718-3727 (b) Severino B., Fiorino F., Esposito A., Frecentese F., De Angelis F., Perissutti E., Caliendo G., Santagada F. "Efficient microwave-assisted synthesis of 4-amino-2-benzazepin-3-ones as conformationally restricted dipeptide mimetics" *Tetrahedron*, **2009**, *65*, 206-211
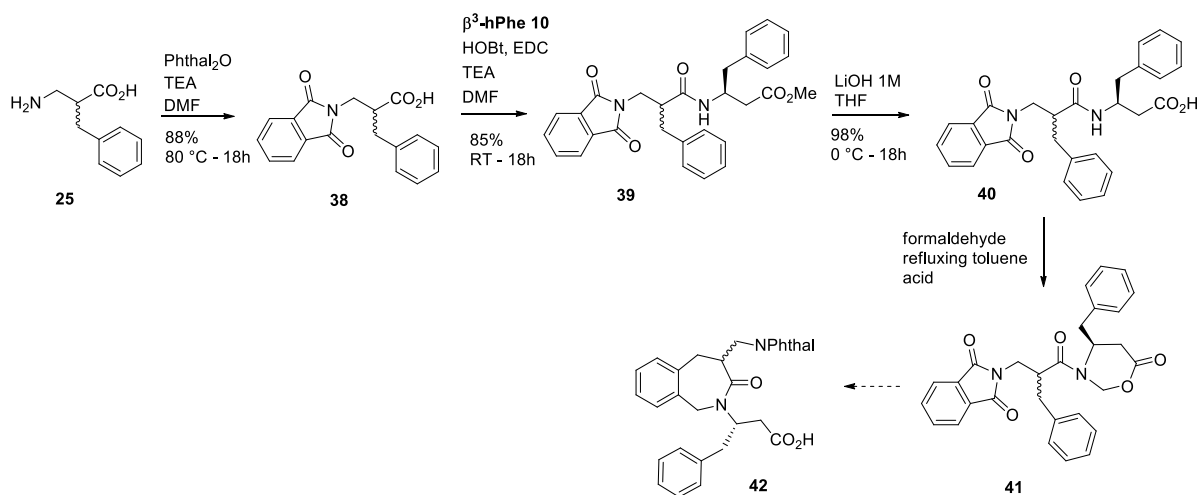
Scheme 10. Benzazepinones synthesis.

Unfortunately, ring closure on a dipeptide skeleton was not straightforward, specially for Phe analogues. We were warned of possible synthetic difficulties because of recent literature discoveries,[68] where the six member ring oxazinanone formation was difficult, with low yields even on a single amino acid. Applying the same approach used for oxazolidinones,[67b] I was unable to isolate any product corresponding to compound **41**. Starting material was recovered unreacted in most cases. Aldehyde sources exploited were paraformaldehyde and trioxane, in presence of molecular sieves 4Å. Protic acids exploited to promote the intramolecular cyclization were CSA, pTSA, TFA and TfOH.

[68] (a) Govender T., Arvidsson P.I. "Facile Synthesis of FmoC N-methylated α- and β- amino acids" *Tetrahedron Lett.* **2006**, *47*, 1691-1694 (b) Hughes A.B., Sleebs B.E. "Effective Methods for the Synthesis of *N*-Methyl β-Amino Acids from All Twenty Common α-Amino Acids Using 1,3-Oxazolidin-5-ones and 1,3-Oxazinan-6-ones" *Helvetica Chim. Acta*, **2006**, *89*, 2611-2637

2.5 *Conformational Analysis*

Conformational analysis on compound **2a,b** and **4a,b** was performed in order to verify if such structures were able to induce reverse turn secondary conformation as good as predicted by computational study. ^{1}H NMR spectra were recorded in the polar aprotic CH$_3$CN-d_3 solvent and all analyses were performed on 2.0 mM solutions, that is, in the absence of a significant aggregation. To ascertain if amide protons are involved in intramolecular hydrogen bonds, the ^{1}H NMR chemical shifts of the amide protons and their temperature dependence ($\Delta\delta/\Delta T$) have been evaluated. Even if NMR studies were made complicated by the presence of multiple rotamers in solution, an essential extended conformation could be deduced for compounds **2a,b**, while a situation of equilibrium between extended and 12-membered H-bonded conformations could be invoked for **4a** and, to a less extent, for **4b**. IR analyses seems to confirm such attitudes.
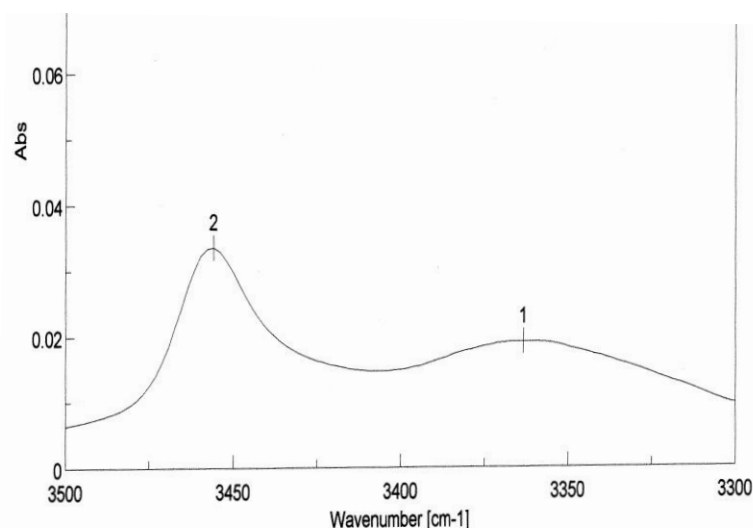
Figure 21. IR Spectrum of **2a**.

The IR spectrum of **2a** exhibits a shoulder at 3350 cm^{-1} (hydrogen-bonded state) together with a band at 3433 cm^{-1} (non-hydrogen-bonded state). This observation suggests an extended conformation in solution for these small dipeptides. Same conclusions were drawn for analogue **2b**. These piece of information were in agreement with NH ^{1}H NMR chemical shift, in fact the amidic proton were found in a range between 6.5 and 6.0 ppm. Such chemical shift, $\delta < 7.0$, is significant of a non-hydrogen bonded amide proton.[69] NH-Boc amidic proton was not predicted for any hydrogen bonded state, indeed its chemical shift was below 6 ppm.

---

[69] Lesma G., Meschini E., Recca T., Sacchetti A., Silvani A. "Synthesis of tetrahydroisoquinoline-based pseudopeptides and their characterization as suitable reverse turn mimetics" *Tetrahedron*, **2007**, *63*, 5567-5578

On the other hand, IR analysis of compounds **4a,b** exhibited a similar pattern, even if the conformational equilibrium is more balanced and the presence of a hydrogen bonded state is more evident. The IR spectrum of **4b** exhibits a shoulder at 3350 cm^{-1} (hydrogen-bonded state) together with a band at 3433 cm^{-1} (non-hydrogen-bonded state).
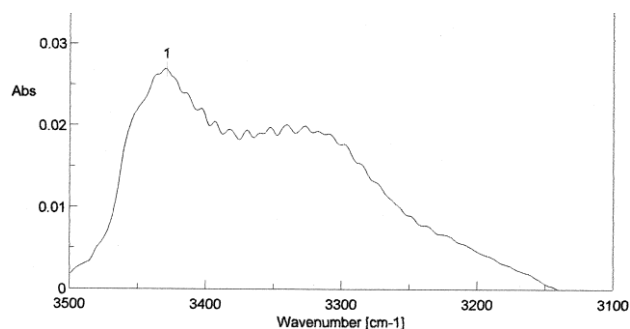
Figure 22. IR Spectrum of **4b**.

I also performed a VT-NMR analysis on compound **4b** because the IR spectrum was promising. The temperature dependence of amidic protons (two conformers) observed is -2.2 ppb/K for the major conformer and -4.5 ppb/K for the minor conformer. This variation, related to the NH chemical shift of 6.64 ppm, is in agreement with an equilibrium state between extended and reverse turn conformation. The amidic proton is then involved in a 12 membered ring.
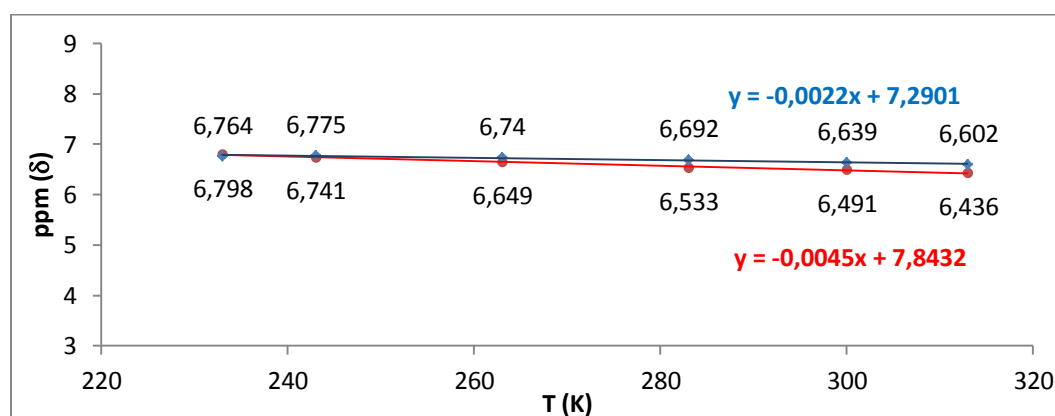
Figure 23. VT-NMR for NH-Me (CD₃CN, 2mM, **4b**).

We reasoned that the propensity of compounds of type **2** to induce a well defined folded structure could be better evaluated in α,β hybrid tetrapeptide mimics. I pursuit the synthesis of **43** (**Figure 24**), adding two L-alanines to starting compound **31a**, by standard peptide chemistry (Scheme 11). We chose to elongate **31a**, bearing *R,S* configuration, because it was predicted by computational analysis to be more prone to a 12 membered intramolecular H-bond, favouring folded conformation, than parent compound **2b**.
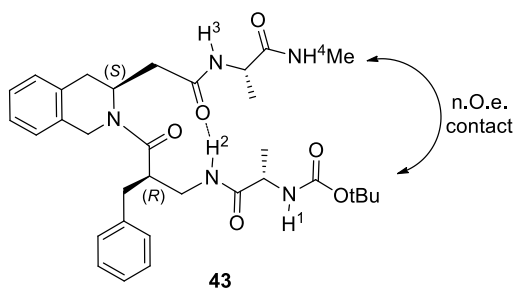
Figure 24. α,β hybrid tetrapeptide **43**.

Table 2. Conformers Distribution.

H Bond	2a (*R,S*)	2b (*S,S*)	43
8H Ring	37 %	23 %	
10H Ring	0 %	3 %	
12H Ring	20 %	3 %	88 %
16H Ring			100 %
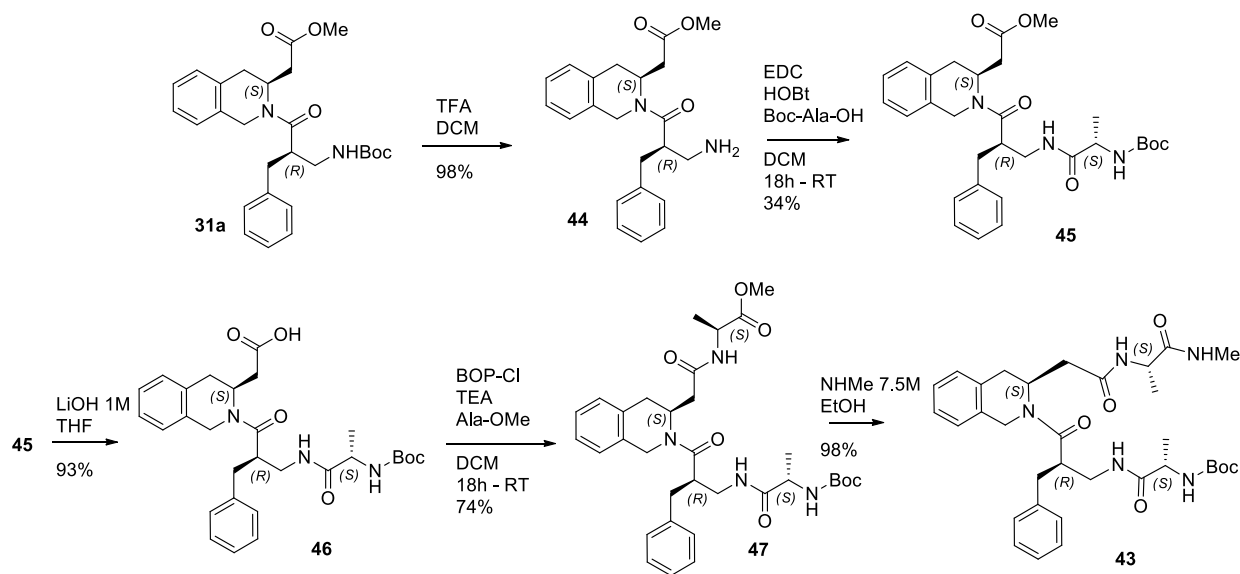
Scheme 11. Synthesis of **43**.

NMR analysis on **43** revealed an intramolecular hydrogen-bonded state for N-H^2, supported both by downfield chemical shift (7.47 ppm at room temperature) and by a reasonably low temperature dependence (-3.8 ppb/K). (**Figure 25**)

The presence of an interstrand n.O.e. contact between Boc and Me terminal groups also strongly supports a folded conformation for **43**, most likely involving a 10-membered H-bonded ring.
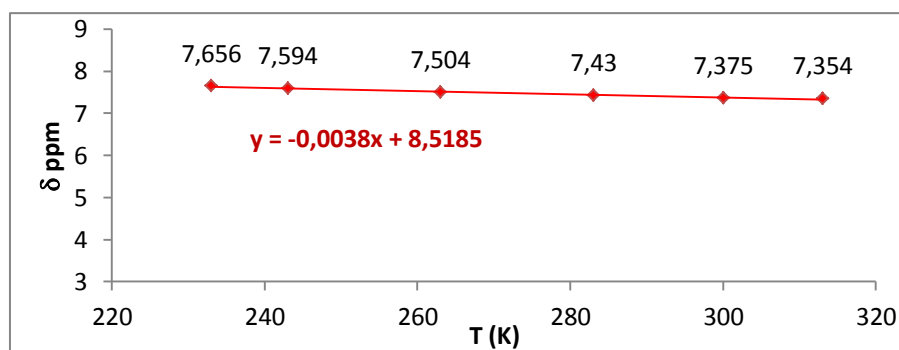
Figure 25. VT-NMR for N-H^2 (CD$_3$CN, 2mM, **43**).

Finally, the CD spectrum of **43**, measured in methanol, displays a quite similar behavior with respect to literature data[70] pertinent to β^2-aa-β^3-aa segment containing peptidomimetics.
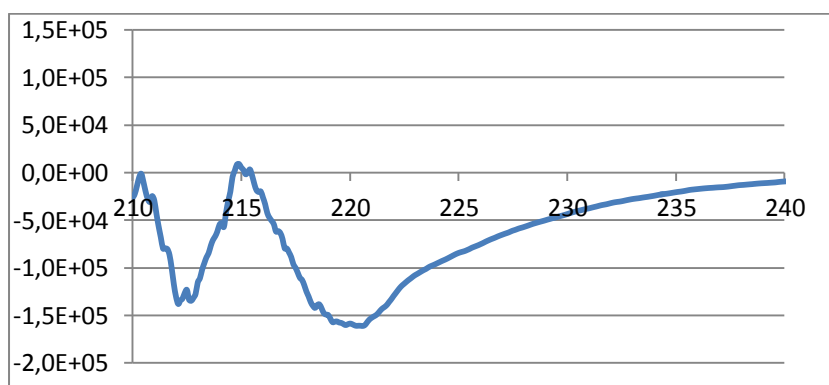
Figure 26. CD spectrum of **43**.

The reverse turn conformation can be figured out from the CD spectrum of **43** (MeOH, 2 mM) which indicates the typical wavelengths of a β^2-Xaa-β^3–Xaa backbone assuming such secondary structure:

- Minimum at 212 nm
- Maximum at 215 nm
- Minimum at 220 nm

[70] Seebach D., Jaun B., Sebesta R., Mathad R.I., Flogel O., Limbach M., Sellner H., Cottens S. "Synthesis, and Helix or Hairpin-Turn Secondary Structures of 'Mixed' α/β-Peptides Consisting of Residues with Proteinogenic Side Chains and of 2-Amino-2-methylpropanoic Acid (Aib)" *Helv. Chim. Acta*, **2006**, *89*, 1801-1825

2.6 *Biological Evaluation*

Starting from dipeptides **31**-**37**, endomorphin-2 analogues were obtained by functionalization of the carboxy terminal moiety with isobutyl chloroformate and ammonia, followed by peptide coupling with Tyr-Pro, in presence of condensating agent, and then isolated as TFA salts.[71]

Peptidomimetics based on β^2hPhe-β^3hPhe scaffolds were synthesized in a first time, while β^3hPhe-β^2hPhe containing scaffolds were prepared as a consequence of the preliminary biological results obtained. In this "second generation" family, I expanded the conformational space by synthesizing analogues bearing the same substitution pattern, β^3-β^3 and β^2-β^2 like compounds **53** and **54**. These combinations provide an further source of investigation in the aromatic rings distance analysis.

31a (*R*,*S*)
31b (*S*,*S*)

a, b, c, d, e

H-Tyr-Pro-(*R*)-β^2hPhe-(*S*)-β^3hTic-NH$_2$ (**48a**)
H-Tyr-Pro-(*S*)-β^2hPhe-(*S*)-β^3hTic-NH$_2$ (**48b**)

34a (*R*,*S*)
34b (*S*,*S*)

a, b, c, d, e

H-Tyr-Pro-(*R*)-β^2hPhe-(*S*)-β^3hPhe-NH$_2$ (**49a**)
H-Tyr-Pro-(*S*)-β^2hPhe-(*S*)-β^3hPhe-NH$_2$ (**49b**)
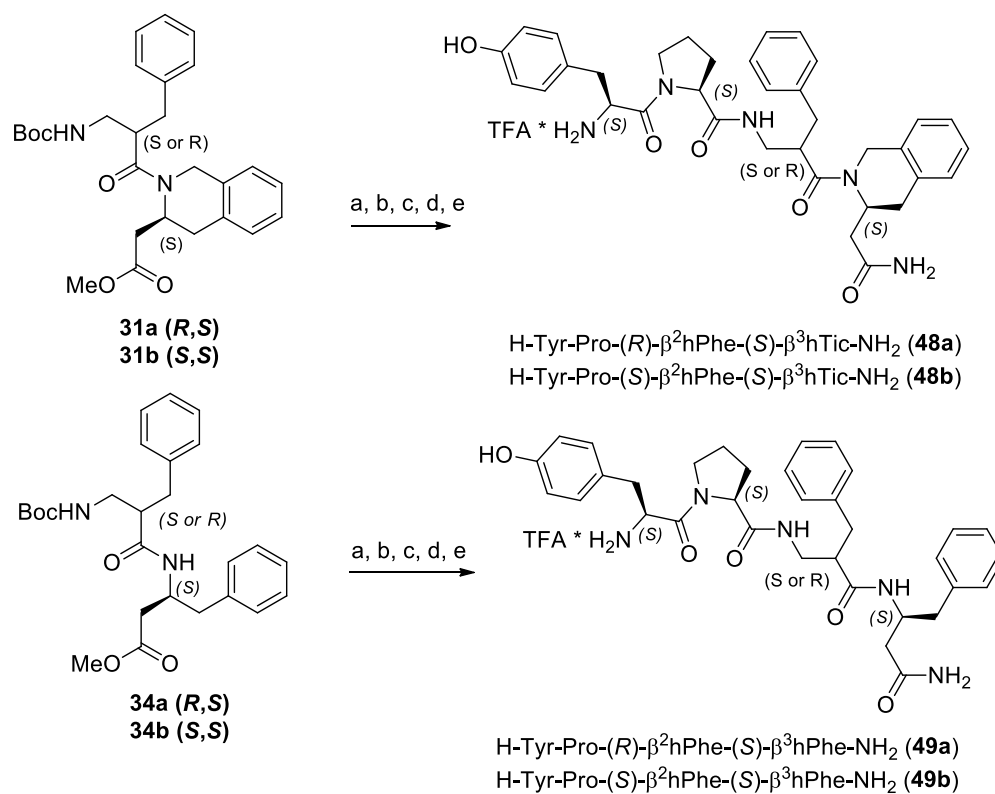
a) NaOH 1N. b) IBCF, NH$_3$. c) TFA. d) Boc-Tyr-Pro-OH, EDC/HOBt. e) TFA.

Scheme 12. EM-2 Analogues – First Generation.

[71] In Collaboration with Prof. Gianfranco Balboni – Università degli Studi di Ferrara.

32a (*S*,*R*)
32b (*S*,*S*)

H-Tyr-Pro-(*S*)-β³hPhe-(*R*)-β²hTbac-NH₂ (**50a**)
H-Tyr-Pro-(*S*)-β³hPhe-(*S*)-β²hTbac-NH₂ (**50b**)

35a (*S*,*R*)
35b (*S*,*S*)

H-Tyr-Pro-(*S*)-β³hPhe-(*R*)-β²hPhe-NH₂ (**51a**)
H-Tyr-Pro-(*S*)-β³hPhe-(*S*)-β²hPhe-NH₂ (**51b**)

33

H-Tyr-Pro-(*S*)-β³hPhe-(*S*)-β³hTic-NH₂ (**52**)

36 (*S*,*S*)

H-Tyr-Pro-(*S*)-β³hPhe-(*S*)-β³hPhe-NH₂ (**53**)

37 (*S*,*S*)

H-Tyr-Pro-(*S*)-β²hPhe-(*S*)-β²hPhe-NH₂ (**54**)
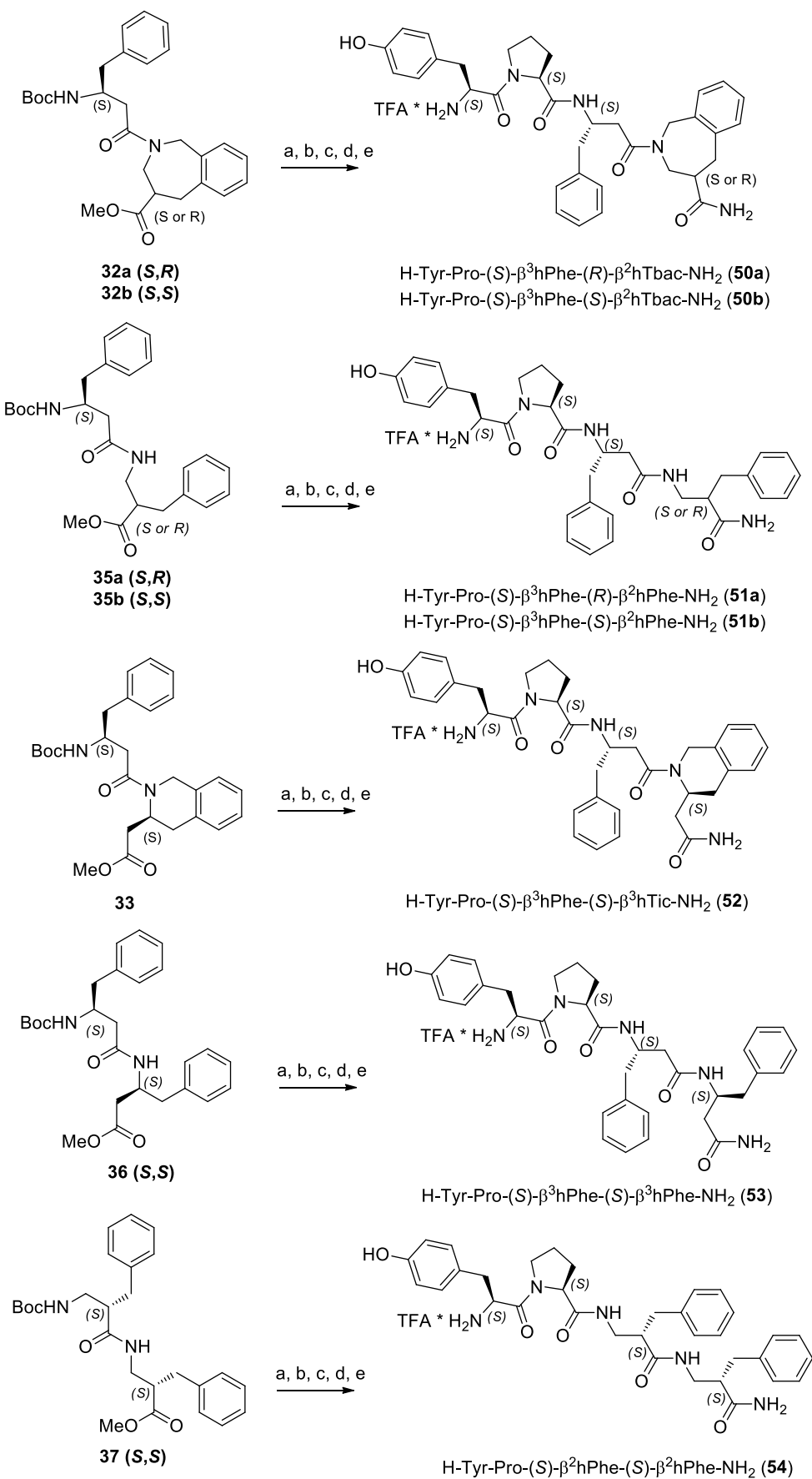
a) NaOH 1N. b) IBCF, NH₃. c) TFA. d) Boc-Tyr-Pro-OH, EDC/HOBt. e) TFA.

Scheme 13. EM-2 Analogues – Second Generation.

The new endomorphin-2 analogues were evaluated for their affinity and selectivity for µ- and δ- opioid receptors using Chinese hamster ovary (CHO) cell membranes stably expressing the opioid receptors. The data are summarized in Table 3 and 4. The new compounds **48b** and **49a**, despite the important modifications at their C-termini maintained a significant affinity especially for δ receptors; their affinities for this receptor increased of more than 2 order of magnitude.[72] On the other hand the µ affinity decreased 100 (**48b**) and 30 fold (**49a**) in comparison to the reference EM-2.[73] Considering the difficulty to obtain endomorphin analogues able to maintain opioid affinity, here I report for the first time the synthesis of new derivatives in which the C-terminal Phe-Phe dipeptide is simultaneously substituted by a peptidomimetic structure with the maintenance of opioid affinity. This type of modification is able to completely abate the high µ selectivity of EM-2 providing compounds endowed with a little preference for δ- receptors. On the basis of very simple considerations about the stereochemical configuration of these EM-2 analogues, their activities seem to be correlated to the spatial disposition of the third Phe side chain.

Table 3. Opioid Receptor Binding Affinities and Selectivities of EM-2 Analogues.[a]

Compounds	Selectivity		Affinity - K_i (nm) ± SEM	
	K_i^{μ}/K_i^{δ}	K_i^{δ}/K_i^{μ}	[³H]DAMGO (µ)	[³H]Ile^{5,6}Dt-2 (δ)
EM-2	$6.1*10^{-4}$	1630	3.24 ± 1.05	5280 ± 1257
48a	0.97	1.03	1001 ± 222	1034 ± 254
48b	7.65	0.13	338 ± 37	44.2 ± 17.1
49a	2.13	0.47	102 ± 28	47.8 ± 22.7
49b	1.04	0.96	1652 ± 885	1589 ± 299

[a] Receptor binding data are presented as the means ± SEM of two or three independent assays. [³H]DAMGO as µ ligand and [³H]Ile^{5,6}-deltorphin-2 as δ ligand were used.

The second series of EM-2 mimics was evaluated for DOR and MOR affinities in radioligand binding assays under standard conditions using cloned receptors stably

[72] In collaboration with Prof. Engin Bojnik. (Institute of Biochemistry, Biological Research Centre, Hungarian Academy of Sciences, Szeged)

[73] Lesma G., Salvadori S., Airaghi F., Bojnik E., Borsodi A., Recca T., Sacchetti A., Balboni G., Silvani A. "Synthesis, Pharmacological Evaluation and Conformational Investigation of Endomorphin-2 Hybrid Analogues" *Mol. Divers.* **2012**, DOI: 10.1007/s11030-012-9399-5

expressed on Chinese hamster ovary (CHO) cells and [³H]DPDPE (cyclo[D-Pen2,DPen5]enkephalin) and [³H]DAMGO ([D-Ala2,NMePhe4,glyol5-enkephalin), respectively, as the radioligands.[74]

In Table 4 are reported the biological results.

Table 4. Opioid Receptor Binding Affinities and Selectivities of EM-2 Analogues.

Compounds	Selectivity		Affinity - K_i (nm)	
	$K_i{}^\mu/K_i{}^\delta$	$K_i{}^\delta/K_i{}^\mu$	[³H]DAMGO (μ)	[³H]DPDPE (δ)
EM-2	0.002	639	5.3	3385
50a	0.03	33	21	695
50b	0.075	13	14	187
51a	0.004	245	**5.5**	1347
51b	0.007	140	**3.3**	463
52	0.012	83	20	1650
53	0.007	147	19	2798
54	0.011	9	101	922

With regard to **50-54**, relying on preliminary data, these compounds show a very good affinity towards μ-opioid receptor, in the low nanomolar scale for the most active **51a** and **51b**. In particular, molecule **51a** has almost the same affinity and selectivity of the reference compound. For an EM-2 analogue with multiple structural modifications in the Phe-Phe portion, a such high μ-opioid affinity and μ/δ selectivity is rather uncommon. Other compounds shows a good nanomolar affinity and selectivity towards μ-opioid receptor, but one order of magnitude less than EM-2. Less potent derivative is **54** which is 2 orders of magnitude less active than reference.

Surprisingly the conformationally constrained scaffold are not as active as **51a** and **51b**, confirming that the proper aromatic ring distance and spatial orientation are highly influencing the binding process, discriminating a potent lead from a completely inactive derivative.

[74] In collaboration with Prof. Thomas F. Murray. (Department of Pharmacology, Creighton University Schcol of Medicine, Omaha - Nebraska)

Structural studies, in particular 2D proton NMR and docking analysis, have been performed in order to fully investigate the three dimensional properties of all the analogues synthesized.

2.7 Structural Study: ^{1}H NMR

Compounds **48a,b** and **49a,b** were studied in their conformational behavior by means of NMR spectroscopy and computational tools. Due to the poor solubility of our molecules in apolar solvents, we performed NMR studies in DMSO-d_6 solution. This solvent offers some additional advantages in studying biologically active molecules since it is considered a good physical approximation of transport fluids environments.[75] A very recent comparative structural analysis of MOR ligands with similar affinity and selectivity confirmed that DMSO may be a better approximation for the mechanical and electrostatic environment of binding to the MOR than D2O is.[76] Moreover, being a good hydrogen bond acceptor, it induces rather inter- than intramolecular interactions, which may reveal intrinsic conformational preferences and may mimic the physical circumstances of receptor-ligand interactions. Proton resonances were assigned using a combination of COSY, TOCSY, NOESY, ROESY and HSQC experiments.[77] (see Table 5)

The spectra show the presence of two conformers (*cis* and *trans* with respect to the Tyr-Pro peptide bond) for **49a** and **49b**, and four conformers (two *cis* and two *trans*[78]) for **48a** and **48b**. A higher prevalence of the *trans* conformers (*trans/cis* ratio ranging from 2:1 for **49a,b** to mainly *trans* for **48a,b**) has been observed according to the intensities of NH peaks in ^{1}H NMR spectra, in line with the reported outcome for the parent EM-2. The question whether endomorphins adopt the *cis* or *trans* configuration of Tyr-Pro peptide bond, when bound to the receptor, is far from being answered. However, relying on total energy measurements, it was recently proposed that the *trans* isomer of EM-2 and analogues could be the mainly bioactive form and that the *cis* isomer is mainly an artifact under the solution conditions.[79]

[75] Albrizio S., Carotenuto A., Fattorusso C., Moroder L., Picone D., Temussi P.A., D'Ursi A. "Environmental Mimic of Receptor Interaction: Conformational Analysis of CCK-15 in Solution" *J. Med. Chem.* **2002**, 45, 762–769

[76] Borics A., Toth G. "Structural comparison of m-opioid receptor selective peptides confirmed four parameters of bioactivity" *J. Mol. Graph. Modell.* **2010**, *28*, 495-505

[77] NMR protons labeling for EM-2 hybrid analogues (e.g. compound **48**).
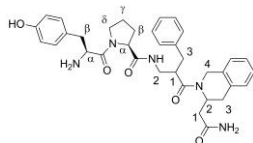
[78] The additional conformational isomerism was ascribed to the presence of the tertiary amide in the β-hTic moiety.

[79] (a) Shao X., Gao Y., Zhu C., Liu X., Yao J., Cui Y., Wang R. "Conformational analysis of Endomorphin-2 analogues with phenylalanine mimics by NMR and molecular modeling" *Bioorg. & Med. Chem.* **2007**, 15, 3539–3547 (b) Grathwohl C., Wüthrich K. "Nmr studies of the rates of proline *cis–trans* isomerization in oligopeptides" *Biopolymers*, **1981**, *20*, 2623–2633

Table 5. Proton attribution for compounds **48-49**.

Compd.	Residue	NH	δHα	δHβ	δHγ	δHδ	δH1	δH2	δH3	δH4	δH(OH)
48a	Tyr[1]										
	(*trans1*)	8.02	4.25	3.08; 2.81							9.36
	(*trans2*)										
	Pro[2]										
	(*trans1*)		4.37	2.12; 1.80	1.93; 1.81	3.68; 3.30					
	(*trans2*)		4.23	1.90; 1.58	1.76; 1.70	3.61; 3.19					
	β-hPhe[3]										
	(*trans1*)	7.94					3.45	3.34; 3.27	2.80; 2.70		
	(*trans2*)	8.11						3.35	2.75		
	β-hTic[4]										
	(*trans1*)						1.90	4.04	2.85; 2.67	5.02; 4.09	
	(*trans2*)										
48b	Tyr[1]										
	(*trans1*)	8.02	4.25	3.07; 2.85							9.36
	(*trans2*)	8.00	4.20	3.01; 2.79							8.79
	Pro[2]										
	(*trans1*)		4.37	2.12; 1.80	1.93; 1.81	3.68; 3.30					
	(*trans2*)		4.23	1.90; 1.58	1.76; 1.70	3.61; 3.19					
	β-hPhe[3]										
	(*trans1*)		7.98				3.33	3.34; 3.25	2.75; 2.81		
	(*trans2*)		7.89				3.50	3.33; 3.13	2.72; 2.90		
	β-hTic[4]										
	(*trans1*)						2.10 1.90	4.94	3.12; 2.68	5.20; 4.05	
	(*trans2*)						2.10; 1.89	4.88	3.00; 2.72	5.11; 4.05	
49a	Tyr[1]										
	(*cis*)	8.17	3.69	2.87; 2.81							9.41
	(*trans*)	8.00	4.2	3.01; 2.79							9.35
	Pro[2]										
	(*cis*)		3.75	1.70; 1.61	1.70; 1.60	3.41; 3.26					
	(*trans*)		4.33	1.98; 1.75	1.88; 1.78	3.63; 3.21					
	β-hPhe[3]										
	(*cis*)	8.12					2.57	3.26; 2.97	2.77; 2.58		
	(*trans*)	7.82					2.62	3.22; 2.98	2.73; 2.60		
	β-hPhe[4]										
	(*cis*)	7.93					2.15	4.21	2.72		
	(*trans*)	7.81					2.12; 2.08	4.21	2.71		
49b	Tyr[1]										
	(*cis*)	8.23	3.85	2.95; 2.84							9.35
	(*trans*)	7.98	4.24	3.06; 2.82							8.73
	Pro[2]										
	(*cis*)		3.68	1.81; 1.61		3.45;					

					3.27				
(*trans*)		4.35	2.08; 1.81	1.91; 1.83	3.67; 3.27				
β-hPhe³									
(*cis*)	7.80								
(*trans*)	7.84					2.62	3.16	2.63; 2.70	
β-hPhe⁴									
(*cis*)	7.91					2.20	4.25	2.72; 2.60	
(*trans*)	7.73					2.20	4.25	2.72; 2.60	
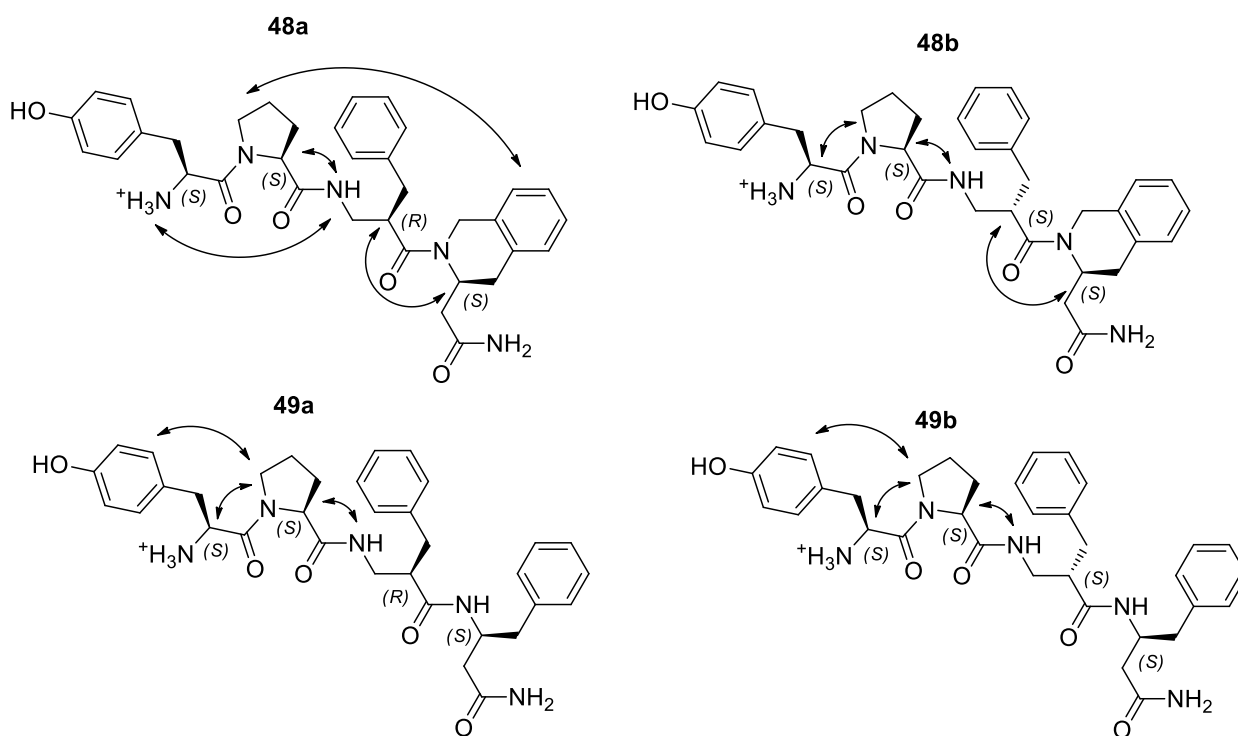
Figure 27. Relevant Inter-residue Correlations, from ROESY Experiments.

Some non sequential NOE cross-peaks were observed (**Figure 27**), which highlight a few common conformational behaviors: in most products, the Tyr¹ aromatic ring seems to be folded over the Pro² segment and the NH of the β-hPhe³ interacts with the Pro's H-α. The most unique interaction for conformationally constrained **48a,b** is the one between β-hTic⁴ H-2 and β-hPhe³ H-1. However, since NMR gave elusive elements about conformation (for instance, no strong internal hydrogen bonds could be detected by VT-NMR in DMSO-d_6, 2 mM solution) a computer aided conformational search has been performed, using the observed NOE cross peaks to generate distance constraints.

Regarding the second series of EM-2 analogues tested (**50-54**), the same conformational issues is present. The *trans/cis* isomerism around the Pro² peptidic bond, plus the isomerism due to the conformational restriction. This restriction led to a tertiary amide present in solution as two energetically stable isomers. In **Figure 28** are summarized the

relevant inter-residue NOE interactions. Compounds **50a** and **50b** present quite unique and unusual interactions, in the first case involving the β^2-hTbac[4] aromatic ring and the benzylic side chain of β^3-hPhe[3]. **50b** presents a clear set of signals which underlines a Phe[3]-Phe[4] overlap. However, we did not observed any significant inter-residue NOE interaction for linear derivatives, revealing preferentially extended conformation. The only exceptions regards analogue **53** where the Tyr[1] seems completely folded over Pro[2] and the overall structure is quite compressed. Comparing these observations to biological results, we can deduce that the aromatic rings require a certain degree of flexibility in order to fit positively in the hydrophobic pockets and, at the same time, require a correct relative placement on the backbone. Indeed only **51a** and **51b**, bearing the β^3-hPhe-β^2-hPhe inserted scaffolds can reach the low nanomolar scale. Compound **54** is 2 orders of magnitude less active even though there is a minimal difference, but sufficiently important to determine such behavior.
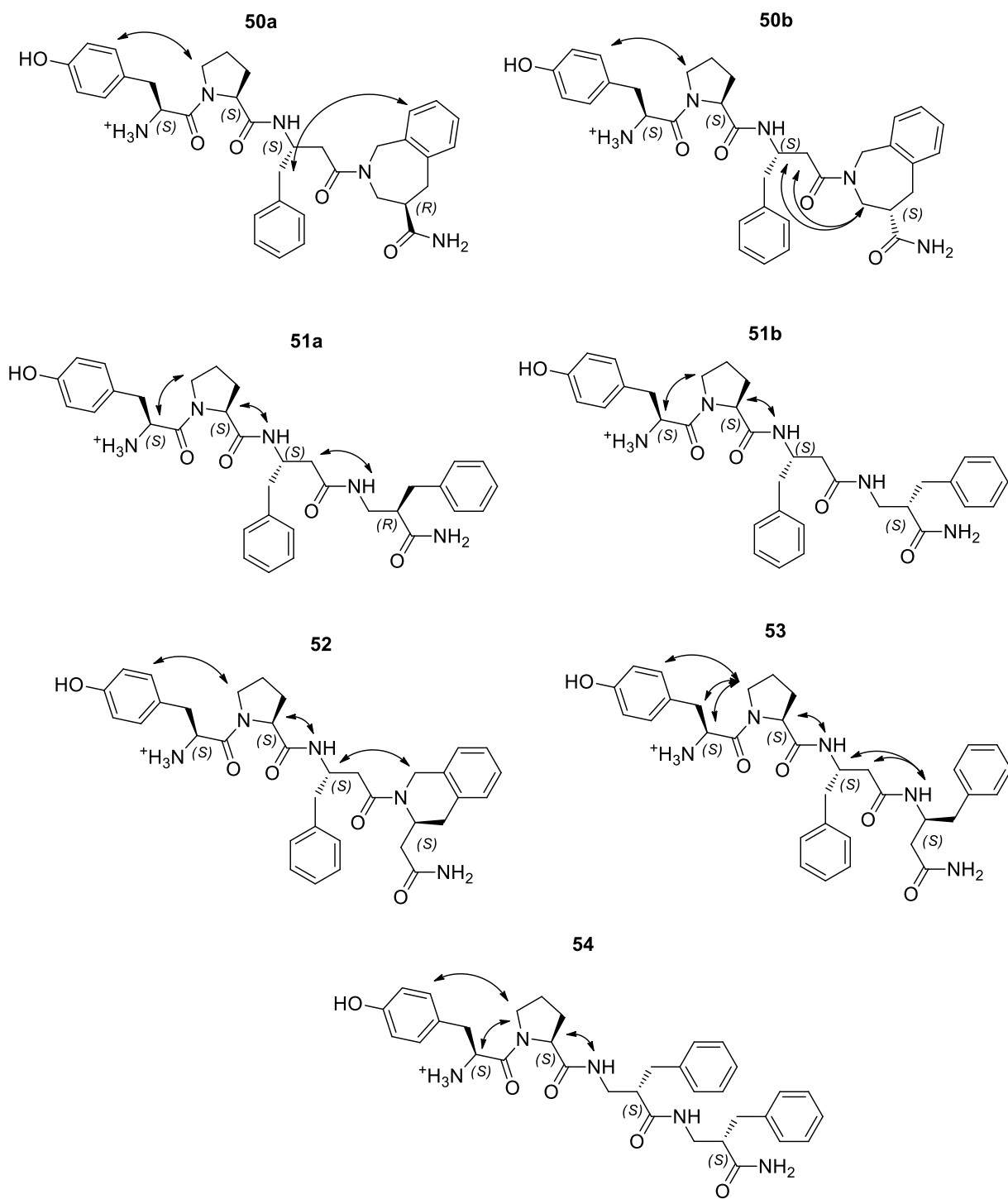
Figure 28. Relevant Inter-residue Correlations, from ROESY Experiments.

2.8 *Structural Study: Docking*

Since the crystal structure of the μ-opioid receptor bound to a morphinan antagonist became available[43a] only during the final writing of this thesis, and the same happened for the crystal structure of the δ-receptor bound to naltrindole,[43b] our investigation of possible binding modes of the most active ligands **48b** and **49a** was performed in the absence of this data, relying on a rhodopsin-based receptor-ligand homology model.[80]

From previous investigations on the binding mode of EM-1 and EM-2 on the MOR model[81] it seems that endomorphins bind in the core of transmembrane helix 3, 5 and 6, with the Tyr[1] residue lying at the bottom of the binding site, interacting with the carboxyl of Asp147. Many interactions between the aromatic portions of the ligands and the receptor are present, together with a hydrogen bond involving the terminal NH amide of Phe[4] and the carbonyl of Glu229.

Our docking studies were performed with the software Glide. As starting points for both compounds, we used the global minima obtained from the conformational analysis performed as previously described, without introducing constraints derived from NMR experiments. The structures were docked flexibly in the XP mode on the active form of the MOR model[82] and the docking score was calculated using the default score functions. The obtained values correlate well with the biological data, the best value (-13.43) being obtained for **49a**. The score was -12.68 for **48b**.

A visual inspection of the binding modes shows that both compounds bind to the receptor similarly to EM-2, with the Tyr[1] residue placed at the bottom of the binding site and bearing a hydrogen bond with Asp147 (**Figure 29**). The phenyl moiety of Tyr[1] lies in a hydrophobic region, and interactions with Phe237 and Phe152 are present. Two more hydrogen bonds are present between the terminal β-hPhe[4] and Thr307 and Asn230. Favorable interactions between the phenyl of the terminal β-hPhe[4] and a number of aromatic groups (Phe221, His223) in a lipophilic pocket can also be

[80] Mosberg H.I., Fowler C.B. "Development and validation of opioid ligand-receptor interaction models: the structural basis of μ vs δ selectivity" *J. Pept. Res.* **2002**, *60*, 329–335

[81] (a) Gentilucci L., Tolomelli A., De Marco R., Artali R. "Molecular Docking of Opiates and Opioid Peptides, a Tool for the Design of Selective Agonists and Antagonists, and for the Investigation of Atypical Ligand-Receptor Interactions" *Curr. Med. Chem.* **2012**, *19*, 1587–1601 (b) Liu X., Kai M., Jin L., Wang R. "Molecular modeling studies to predict the possible binding modes of endomorphin analogues in μ opioid receptor" *Bioorg. Med. Chem. Lett.* **2009**, *19*,5387–5391 (c) Liu X., Kai M., Jin L., Wang R. "Computational study of the heterodimerization between μ and δ receptors" *J. Comput. Aid. Mol. Des.* **2009**, *23*, 321–332

[82] The receptor model used is the OPRM_MOUSE_AD_JOM6 obtained by the web site http://mosberglab.phar.umich.edu.

evidenced. Notably relevant portions of the two molecules occupy the same receptor regions (see **Figure 30** for superimposition of docked conformations).
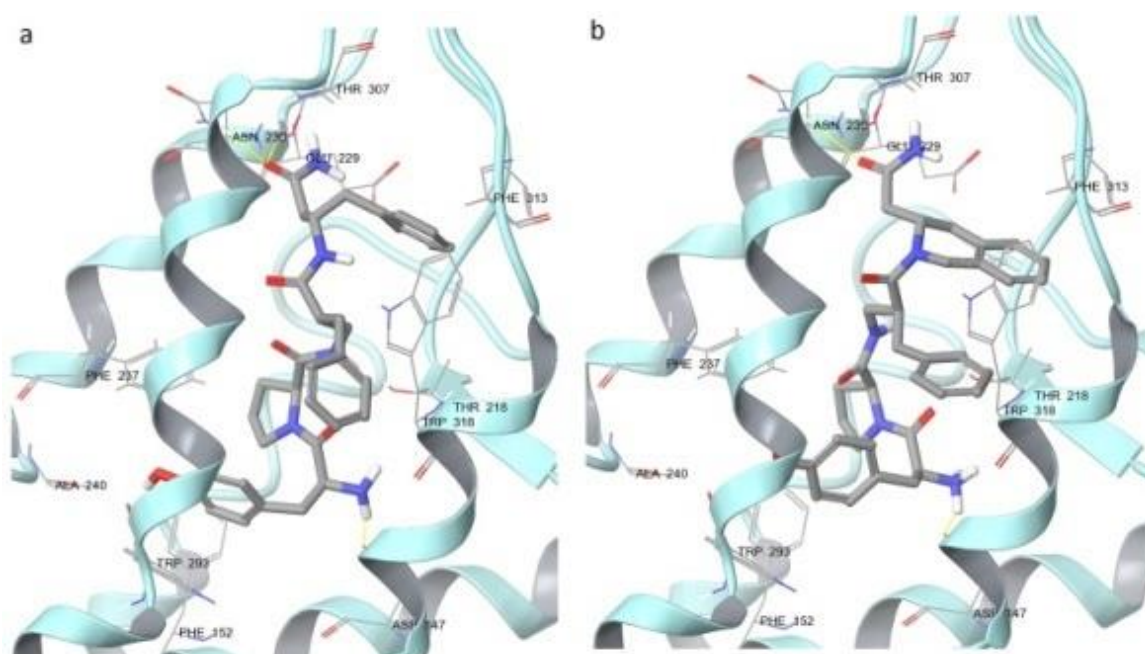
Figure 29. Binding mode towards the MOR Model; a) **49a**, b) **48b**.
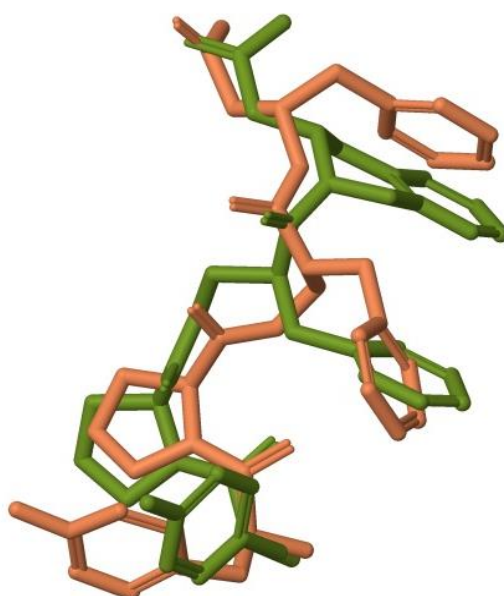
Figure 30. Superimposition of the Docked Conformations of **49a** (Orange) and **48b** (Green) (RMSD of amide backbone is 1.3Å).

This binding analogy was quite unpredictable on the basis of structural elements. In fact, the two compounds have an opposite configuration at the β-hPhe³ stereocenter (*R* for **49a** and *S* for **48b**) and the terminal residue is a β-hPhe⁴ for **49a** and a constrained β-hTic⁴ for **48b**. The bound conformations for both ligands **49a** and **48b** resulted quite different if compared with the free state conformations, as resulted from NMR and

conformational analysis. While in the free state these compounds tend to adopt bent conformations (with the presence of different intramolecular hydrogen bonds), the docked conformations are more extended and no intramolecular hydrogen bonds are present. In this case the docking experiment seems to be more able in giving explanation about bioactivity, with respect to the conformational studies performed by NMR and molecular modeling.

The docking studies were performed with the use of the Molegro 4.0 suite, having MolDock as integrated docking software. We decided to switch to a different docking software because we observed an higher accuracy. The docking scoring function of MolDock is an extension of the piecewise linear potential (PLP) including new hydrogen bonding and electrostatic terms.[83]

As receptor models we decided to use both the recently isolated crystal structure of the μ-opioid receptor bound to a morphinan antagonist (PDB code: 4DKL) and a rhodopsin-based receptor-ligand homology model as comparison. Results are reported as the Moldock score as implemented in the software. It has to be noticed that the two receptors have some significant discrepancy due to the different orientation of some residues. The alignment of the two receptor models is quite good with an RMSD of 1.046Å (in the common region from residue 64 to 286). The binding sites look very similar, but some evident differences appear in the orientation of residues Trp318, Gln 124 and Tyr128. These residues play an important role in defining the cavity space and the shape of the binding site thus affecting the binding modes of the ligands.

The two receptors' binding site region has been aligned from x-ray structure and from homology model. There is a good overlap between the two structures, in particular related to the common amino acids involved in binding.

The use of the receptor modeled from the x-ray structure gave results which are consistent with the biological data. Compound **51b** resulted to have the lowest docking score followed by EM2. However the two molecules bind to the receptor in quite different ways as showed by the ligand-receptor interaction diagrams. On the other hand, results from the homology model were not in agreement with the biological data.

	MolDock score:	
	Crystal Structure	Homology Model
EM2	-154.2	-131.5
51a	-151.7	-162.6
51b	-156.4	-151.2

[83] Thomsen R., Christensen M.H. "MolDock: A New Technique for High-Accuracy Molecular Docking" *J. Med. Chem.* **2006**, *49*, 3315-3321

MolDock score puts in evidence the lower accuracy of the homology model.

In the following pages I report the docking analysis using the homology model and the crystallized receptor to enlighten the most important binding differences observed for EM-2 and active compound **51b**.
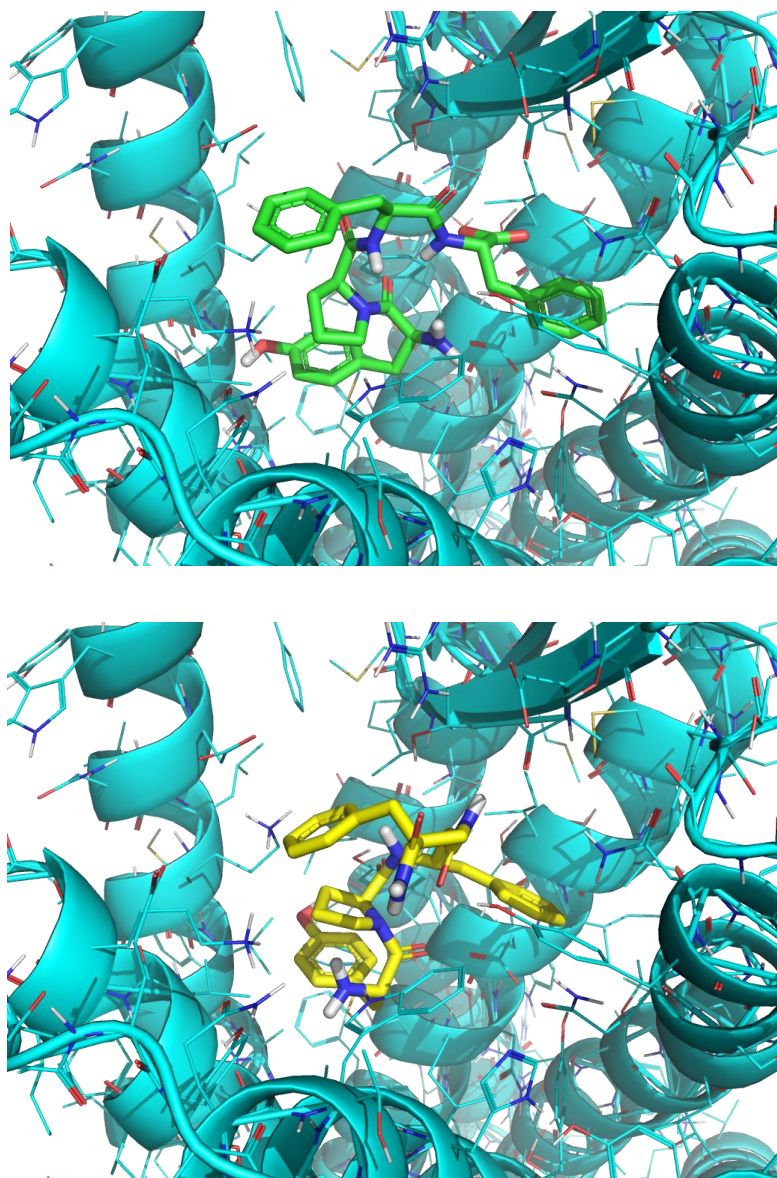
Figure 31. Binding mode towards the MOR (EM-2, **51b**). (Homology Model)
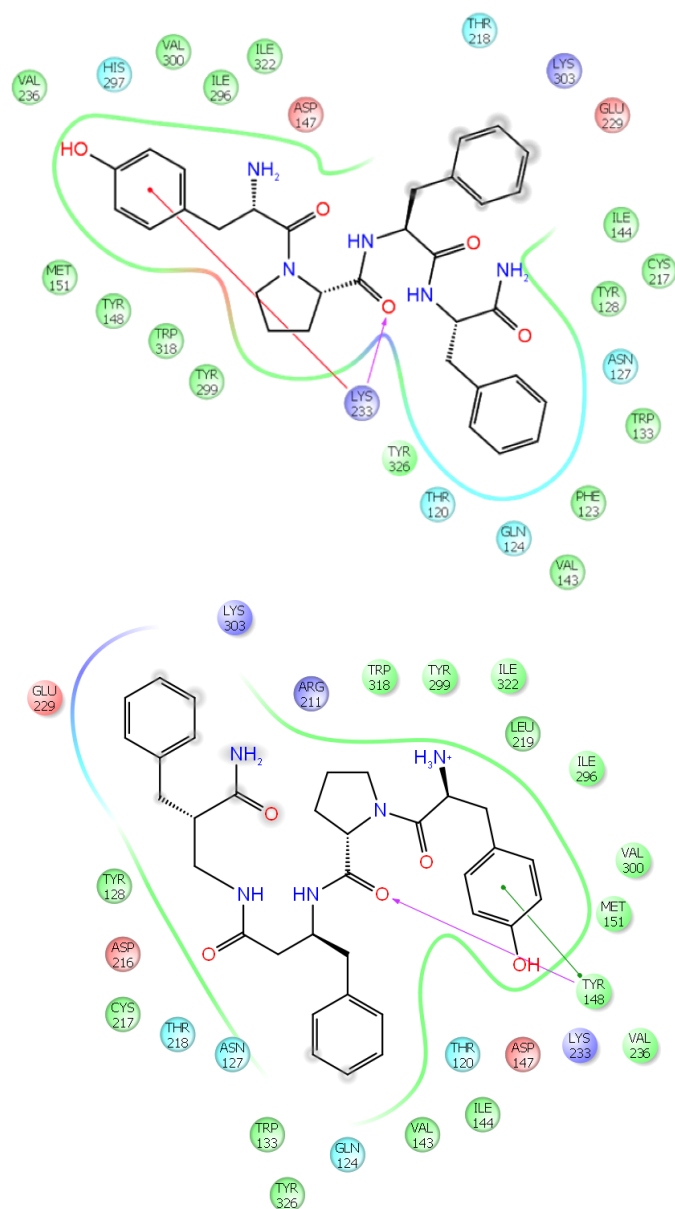
Figure 32. 2D Ligand-Protein interaction of EM-2 and **51b**. (Homology Model)

According to the homology model, Asp147 is no more a determinant interaction, while Tyr[1] seems placed in the same hydrophobic pocket. Comparing the two diagrams, **51b** is able to fold up better because of the elongated structure. These observations are in contrast with the commonly accepted EM-2 binding mode.
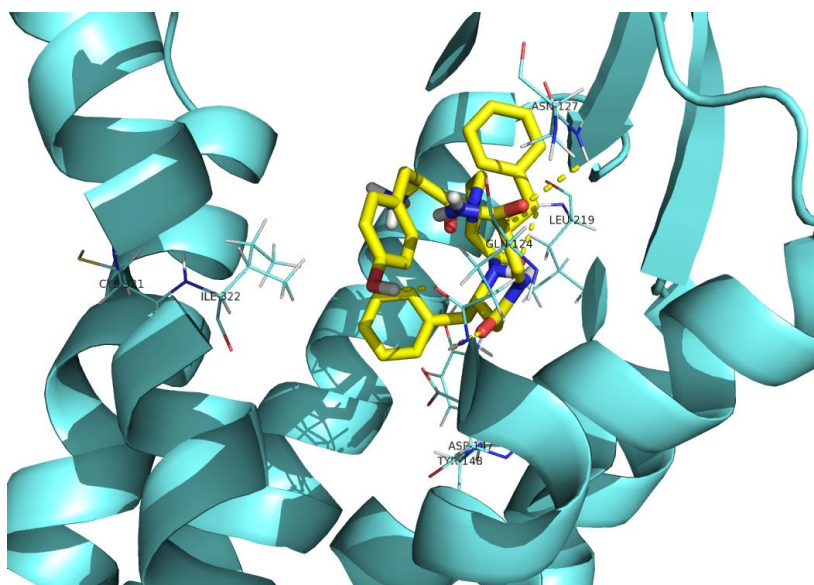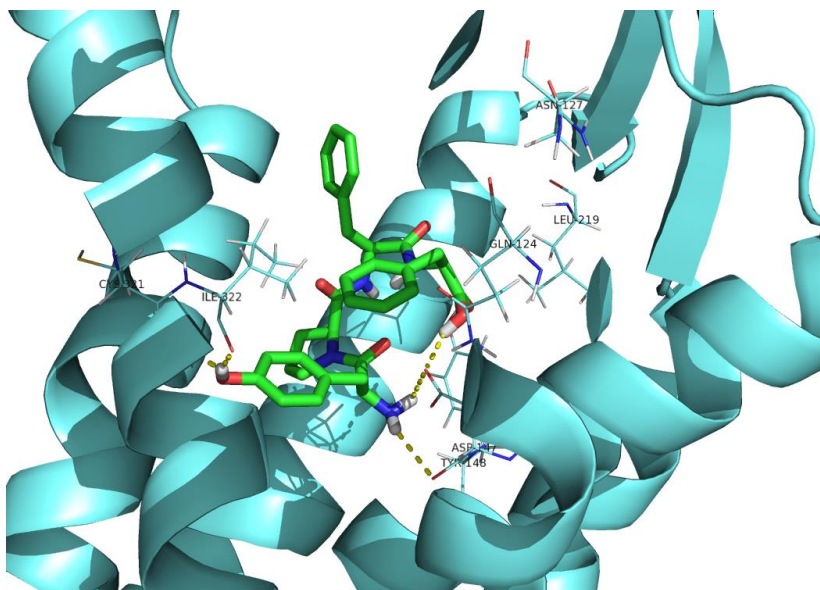
Figure 33. Binding mode towards the MOR (EM-2, **51b**). (Crystal Structure)
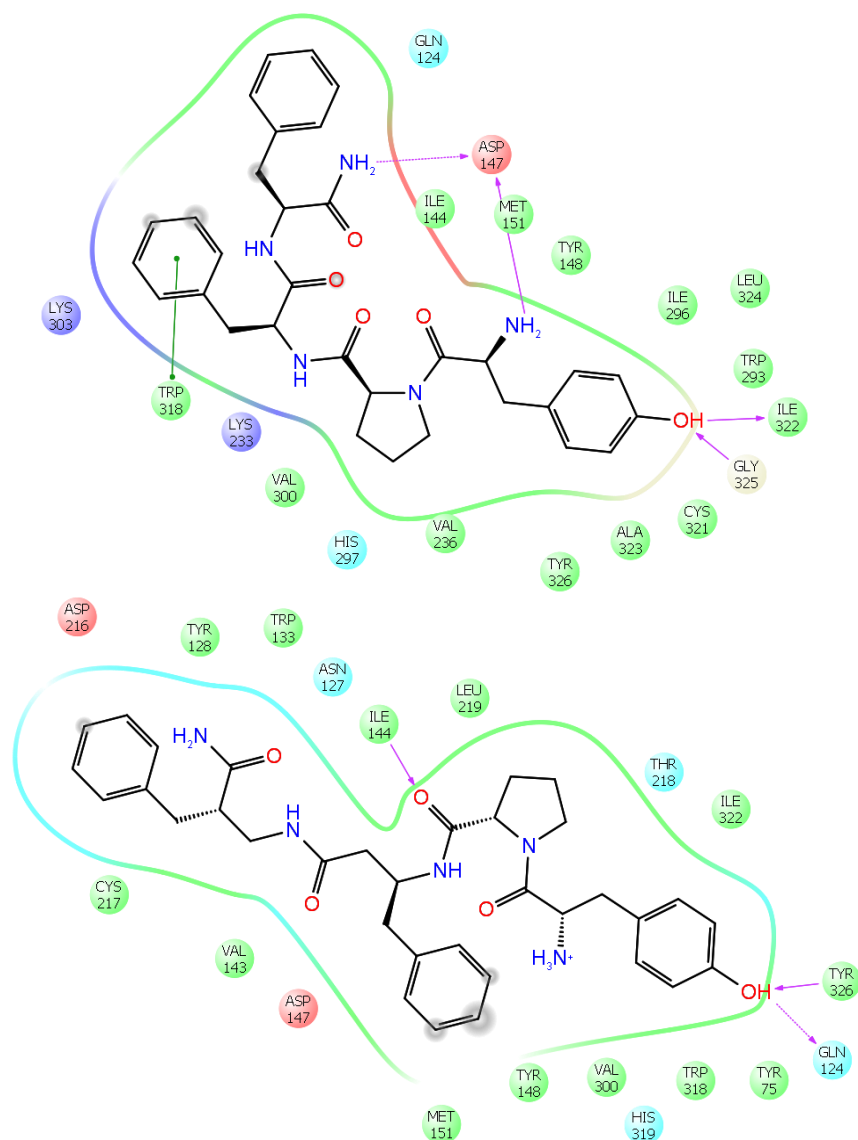
Figure 34. 2D Ligand-Protein interaction of EM-2 and **51b**. (Crystal Structure)

Exploiting the downloaded PDB structure of μ-opioid receptor, the docking analysis is now more reliable. Apparently, EM-2 has important interactions in the hydrophobic cavity occupied by Trp318 and an acid/base equilibrium with Asp147, as previously reported in literature. However, the new compound **51b** seems bind differently. Still Tyr[1] phenolic moiety has electrostatic interactions, even though amino acids involved are different. This preliminary analysis is peculiar because differs from the well established EM-2 binding mode. Apparently, the extended conformation of **51b**, due to the homologation, is helpful for a better fitting.

2.9 _Conclusions_

We investigated the biological activity and the conformational requirements of hybrid EM-2 analogues, by NMR spectroscopy, molecular modeling and docking studies. On the basis of all data, some considerations can be drawn. Compounds **48b** and **49a** are among the few examples of EM-2 analogues in which the C-terminal Phe[3]-Phe[4] dipeptide is simultaneously substituted by a peptidomimetic structure with the maintenance of opioid affinity. Besides, this type of modification is able to completely abate the high μ selectivity of EM-2 providing compounds endowed with a slight preference for δ receptors.

Molecular modeling, which was performed taking into account distance restraints from NMR, suggests a high propensity of all first generation analogues for various turn structures. Since conformational studies were performed on isolated molecules in the absence of their receptor and therefore the most populated conformational family does not necessarily correspond to the bioactive structure, we also performed docking studies in order to elucidate the binding mode for their action. The docking procedure strongly highlights a common binding mode for **48b**, **49a** confirming the necessity for specific binding interactions, for instance between Asp147 and Tyr[1], already identified in recent studies.[84]

On the other hand, a second generation of EM-2 analogues has been prepared and tested (**50-54**). According to preliminary biological results, compounds **51a** and **51b** displayed a low nanomolar affinity for μ-opioid receptor, in particular **51a** showed an high degree of selectivity for MOR. Docking studies on the new receptor's crystal structure enlighten some differences between the standard key interaction for EM-2 and the active analogues. This piece of information might help explaining the biological outcome and the resulting bioactive conformations.

Finally, we should bear in mind the hypothesis that GPCRs, including opioid receptors, exist as dynamic entities that can occupy multiple conformations, depending on the accessory proteins within the signaling complex, but also on the ligand.[85] On the basis of this argument, caution must be used in providing key structural parameters for bioactivity versus opioid receptors.

---

[84] Liu X., Kai M., Jin L., Wang R. "Molecular modeling studies to predict the possible binding modes of endomorphin analogues in μ- opioid receptor" _Bioorg. Med. Chem. Lett._ **2009**, _19_, 5387-5391

[85] Urban J.D., Clarke W.P., Von Zastrow M., Nichols D.E., Kobilka B., Weinstein H., Javitch J.A., Roth B.L., Christopoulos A., Sexton P.M., Miller K.J., Spedding M., Mailman R.B. "Functional Selectivity and Classical Concepts of Quantitative Pharmacology" _J. Pharmacol. Exp. Ther._ **2007**, _320_, 1–13

2.10 *Experimental Details*

Chemistry

All solvents were distilled and properly dried, when necessary, prior to use. All chemicals were purchased from commercial sources and used directly, unless otherwise indicated. All reactions were run under nitrogen atmosphere, unless otherwise indicated. All reactions were monitored by thin layer chromatography (TLC) on precoated silica gel 60 F_{254}; spots were visualized with UV light (254 nm) and by treatment with 1% aqueous $KMnO_4$ solution, Ninhydrin solution in ethanol or Cerium-ammonium-molybdate (CAM) reactive. Products were purified by flash chromatography on silica gel 60 (230-400 mesh). ^{1}H and ^{13}C NMR spectra were recorded with 300 and 400 Mhz spectrometers using chloroform-*d* (CDCl$_3$), dimethylsulfoxide-*d$_6$* (DMSO-*d$_6$*), acetonitrile-*d$_3$* (CD$_3$CN) or methanol-*d$_4$* (CD$_3$OD). Chemical shifts (δ) are expressed in ppm relative to TMS at δ = 0 ppm for ^{1}H NMR and relative to CDCl$_3$ at δ = 77.16 ppm for ^{13}C NMR. High-resolution MS spectra were recorded with a FT-ICR (Fourier Transform Ion Ciclotron Resonance) instrument, equipped with an ESI source, or a standard MS instrument, equipped with an EI source. Specific rotations were measured by a polarimeter "P-1030 Jasco" with 10 cm Optical path cells and 1 ml capacity.

Radioligand Binding Assays[86]

Rat brain membranes were prepared from Wistar rat brain. The binding experiments were performed in 50 mM Tris·HCl buffer, pH 7.4, at a final volume of 1 ml containing 200-300 μg protein. In competition experiments the following conditions were used for incubations: [^{3}H]DAMGO (35 °C, 45 min), [^{3}H]Ile^{5,6}-deltorphin-2 (35 °C, 45 min). Incubations were started by the addition of the membrane suspension and terminated by rapid filtration through Whatman GF/C glass fiber filters using Brandel M24R Cell Harvester. The filters were washed three times with ice cold Tris·HCl buffer and dried for 3 h at 37 °C, and the radioactivity was measured in UltimaGOLD scintillation cocktail using a Packard TriCarb 2300 TR counter. Affinities of competing ligands were determined by co-incubation with 10^{-12}-10^{-5} M freshly prepared solution of the unlabeled peptides with 0.5-1 nM tritiated ligand. Nonspecific binding was defined as a

[86] (a) Nevin S.T., Kabasakal L., Otvös F., Tóth G., Borsodi A. "Binding characteristics of the novel highly selective delta agonist, [^{3}H]Ile^{5,6}deltorphin II" *Neuropeptides*, **1994**, *26*, 261–265 (b) Tóth G., Ioja E., Tömböly C., Ballet S., Tourwé D., Péter A., Martinek T., Chung N.N., Schiller P.W., Benyhe S., Borsodi A. "β-Methyl Substitution of Cyclohexylalanine in Dmt-Tic-Cha-Phe Peptides Results in Highly Potent δ Opioid Antagonists" *J. Med. Chem.* **2006**, *50,* 328–333

radioactivity bound in the presence of 10 μM naloxone. All assays were performed in duplicate and repeated several times. Experimental data were analyzed by GraphPad Prism 2.01 software.

Computational details

Conformational analysis was performed with the software Spartan '08[87] using a MC/MM protocol with the application of NOE constraints as obtained by NMR. The obtained conformers were then optimized with the semiempirical method AM1. The structures were then analyzed and clustered according to their secondary structure motifs. For docking studies, we used the structure of the mouse μ- opioid receptor model (active state) with JOM6 as ligand, obtained from the Mosberg lab (mosberglab.phar.umich.edu). The complex was prepared with the "protein preparation wizard" tool as implemented in Maestro 9.0 (Schrodinger)[88] using the OPLS2001 force field for the minimization. The receptor grid was generated with Glide 5.5 (Schrodinger)[89,90] around the JOM6 ligand (a 40x30x50 Å box was used). The ligands were docked flexibly into the receptor grid using the extra-precision mode. Up to ten poses for each ligand were analyzed and docking scores were generated using the standard functions as implemented in the software. The poses were visualized with the Maestro 9.0 graphical interface.

[87] Spartan '08, Wavefunction, Inc. Irvine, CA

[88] Maestro, version 9.0, Schrödinger, LLC, New York, NY, 2011

[89] Glide, version 5.5, Schrödinger, LLC, New York, NY, 2011

[90] Friesner R.A., Murphy R.B., Repasky M.P., Frye L.L., Greenwood J.R., Halgren T.A., Sanschagrin P.C., Mainz D.T. "Extra Precision Glide: Docking and Scoring Incorporating a Model of Hydrophobic Enclosure for Protein–Ligand Complexes" *J. Med. Chem.* **2006**, *49*, 6177–6196

Synthesis of 2:

MeNH₂ 7.5 M
EtOH
RT - 18h
98%

31a (*R,S*)
31b (*S,S*)

2a (*R,S*)
2b (*S,S*)
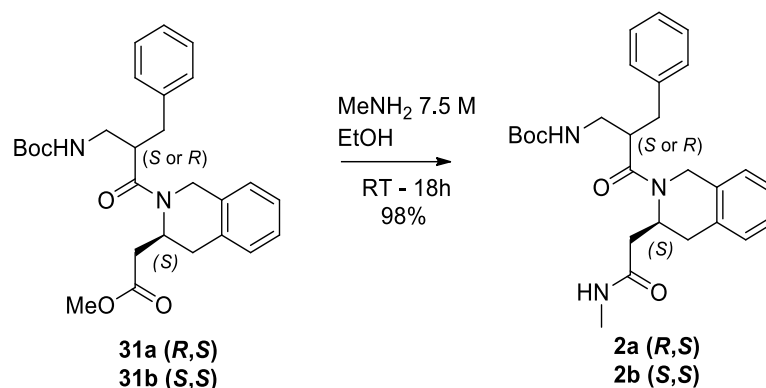
tert-butyl **((*R*)-2-benzyl-3-((*S*)-3-(2-(methylamino)-2-oxoethyl)-3,4-dihydroisoquinolin-2(1H)-yl)-3-oxopropyl) carbamate (2a)**

Compound **31a** (20 mg, 0.045 mmol) was dissolved at room temperature in a solution of methylamine in EtOH (2 ml, 7.5 M). The reaction mixture was stirred for 18 h and evaporated to give **2a** (19 mg, 98%) as a white solid.

$[\alpha]_D^{25}$ = +38,6 (*c* 1.0, CHCl₃). ¹H NMR (400 MHz, CD₃CN) δ 7.42 – 6.91 (m, 9H), 6.51 (s, 1H), 6.01 (s, 1H), 5.13 (d, 1H, *J* = 18.1 Hz), 4.57 (dd, 1H, *J* = 12.9, 6.4 Hz), 4.10 (d, 1H, *J* = 18.3 Hz), 3.56 (d, 1H, *J* = 4.5 Hz), 3.50 – 3.29 (m, 1H), 3.29 – 3.03 (m, 2H), 3.03 – 2.49 (m, 4H), 2.36 (d, 1H, *J* = 16.2 Hz), 2.31 – 2.24 (m, 1H), 2.11 (dd, 1H, *J* = 14.9, 5.8 Hz), 1.87 (dd, 1H, *J* = 13.4, 7.7 Hz), 1.42 (s, 9H). ¹³C NMR (101 MHz, CD₃CN) δ 174.3, 172.2, 151.9, 140.9, 133.8, 133.7, 130.6, 130.4, 129.9, 129.8, 129.7, 127.9, 127.9, 127.8, 127.5, 79.7, 50.2, 44.7, 44.1, 42.4, 40.0, 39.0, 34.2, 29.2, 26.9. HRMS (ESI) calcd. for [C₂₇H₃₅N₃O₄]⁺: 465.2628, found 466.2234. (MH⁺)

tert-butyl ((*S*)-2-benzyl-3-((*S*)-3-(2-(methylamino)-2-oxoethyl)-3,4-dihydroisoquinolin-2(1H)-yl)-3-oxopropyl) carbamate (2b)

Compound **31b** (20 mg, 0.045 mmol) was dissolved at room temperature in a solution of methylamine in EtOH (2 ml, 7.5 M). The reaction mixture was stirred for 18 h and evaporated to give **2b** (19 mg, 98%) as a white solid. The following data has been collected on a 1:1 rotamer mixture.

$[\alpha]_D^{25}$ = +38,0 (*c* 1.25, CHCl₃). ¹H NMR (400 MHz, CDCl₃) δ 7.40 – 7.26 (m, 3H), 7.26 – 7.07 (m, 4H), 7.06 – 6.99 (m, 2H), 6.43 (bs, 0.5H), 6.21 (bs, 0.5H), 5.91 (bs, 0.5H), 5.50 (bs, 0.5H), 5.31 – 5.18 (m, 1H), 4.93 (dd, 0.5H, *J* = 12.2, 6.2 Hz), 4.46 (s, 1H), 4.15 – 4.02 (m, 1H), 3.61 – 3.51 (m, 0.5H), 3.44 – 3.27 (m, 1H), 3.27 – 3.06 (m, 2.5H), 2.99 - 2.68 (m, 2H),

2.69 – 2.58 (m, 3H), 2.26 – 2.13 (m, 1H), 2.09 (ddd, 1H, J = 14.7, 6.8, 2.6 Hz), 1.83 (dd, 0.5H, J = 14.6, 7.3 Hz), 1.43 (s, 4.5H), 1.34 (s, 4.5H). ^{13}C NMR (101 MHz, CDCl$_3$) δ 174.6, 174.5, 172.5, 171.6, 157.6, 157.3, 141.6, 140.9, 134.2, 134.1, 133.8, 133.6, 130.8, 130.7, 130.6, 130.4 (2C), 129.8 (2C), 129.7 (2C), 128.3, 128.0, 127.8 (2C), 127.7 (2C), 127.6 (2C), 127.5, 79.8 (2C), 50.3, 46.9, 45.5, 45.3, 44.7, 44.4, 44.0, 42.6, 39.8, 39.2, 37.8 (2C), 35.1, 34.0, 29.2, 29.1, 26.8, 26.7. HRMS (ESI) calcd. for [C$_{27}$H$_{35}$N$_3$O$_4$]$^+$: 465.2628, found 466.2655. (MH$^+$)

¹H and ¹³C NMR of compound **2a**

¹H and ¹³C NMR of compound **2b**
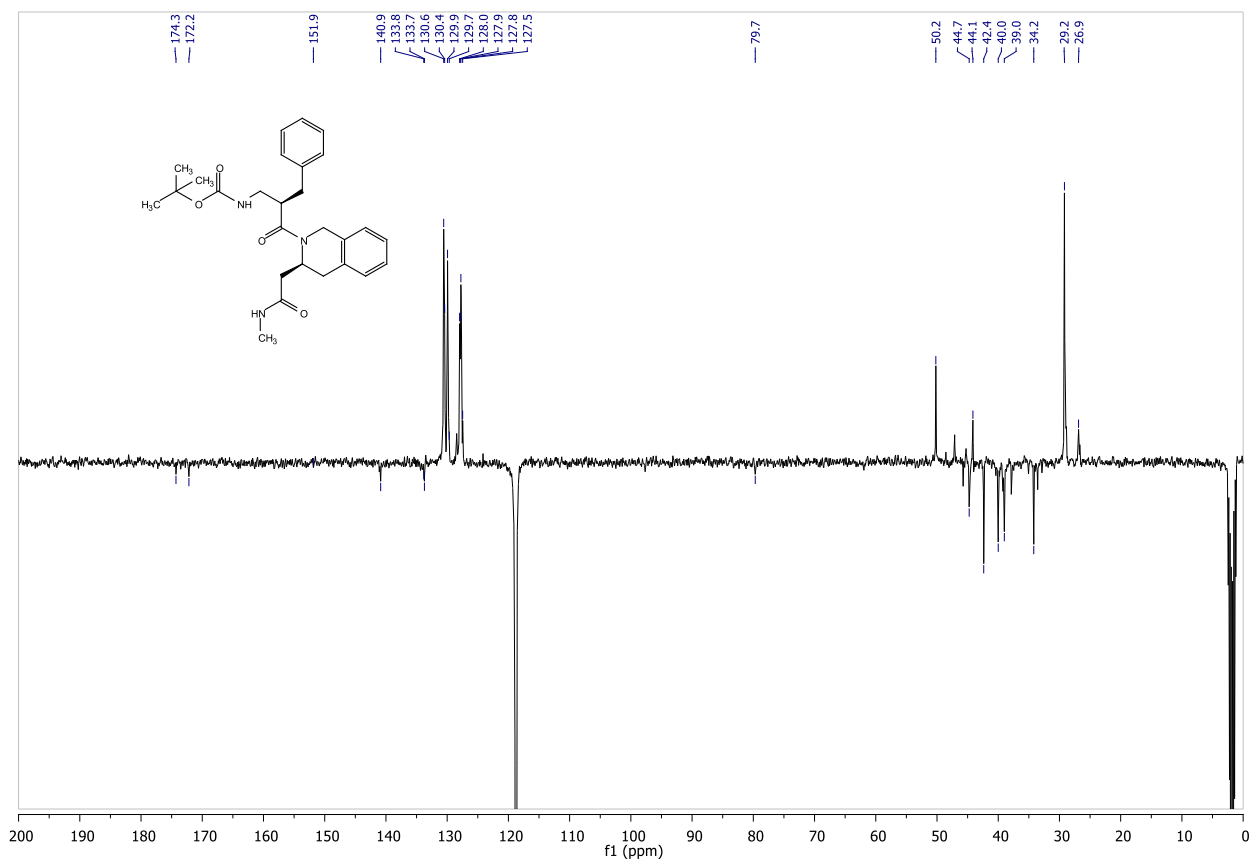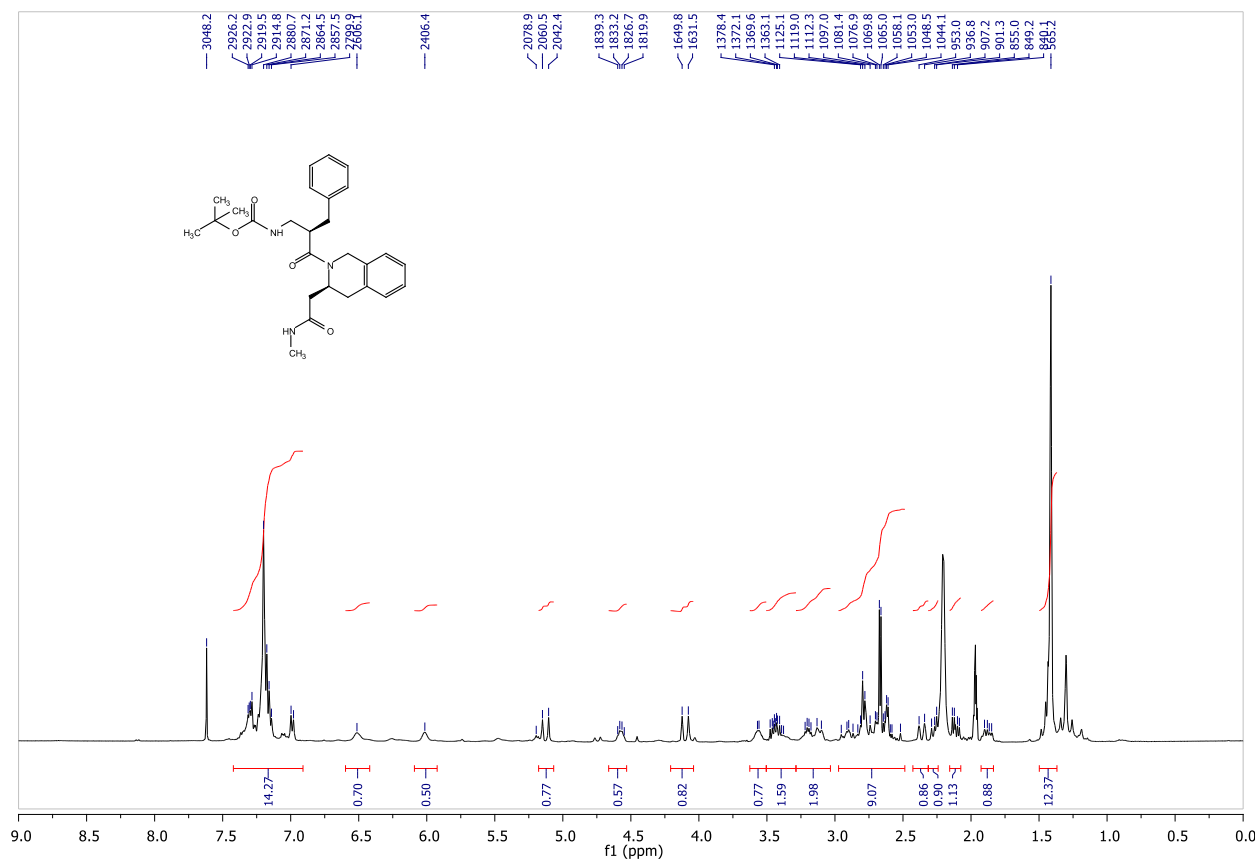
Synthesis of 4:
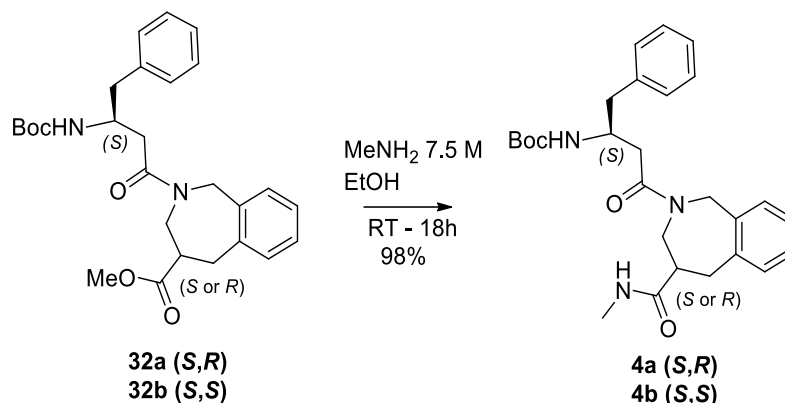
tert-butyl ((*S*)-4-((*R*)-4-(methylcarbamoyl)-4,5-dihydro-1H-benzo[c]azepin-2(3H)-yl)-4-oxo-1-phenylbutan-2-yl)carbamate (4a)

Compound **32a** (20 mg, 0.045 mmol) was dissolved at room temperature in a solution of methylamine in EtOH (2 ml, 7.5 M). The reaction mixture was stirred for 18 h and evaporated to give **4a** (18 mg, 98%) as a white solid. The following data has been collected on a 1:1 rotamer mixture.

$[\alpha]_D^{25}$ = -21,6 (*c* 0.5, CHCl$_3$). ^{1}H NMR (400 MHz, CD$_3$CN) δ 7.39 – 7.28 (m, 2H), 7.28 – 7.05 (m, 6H), 6.95 (d, 1H, *J* = 5.9 Hz), 6.63 (bs, 0.5H), 6.51 (bs, 0.5H), 5.56 (d, 0.5H, *J* = 7.8 Hz), 5.48 (bs, 0.5H), 4.99 (d, 0.5H, *J* = 14.0 Hz), 4.61 (d, 0.5H, *J* = 16.1 Hz), 4.49 (d, 0.5H, *J* = 16.0 Hz), 4.34 (d, 0.5H, *J* = 13.8 Hz), 4.16 (dd, 0.5H, *J* = 10.7, 6.4 Hz), 4.08 – 3.90 (m, 1H), 3.72 – 3.47 (m, 1H), 3.46 – 3.20 (m, 1.5H), 2.97 (d, 1H, *J* = 14.8 Hz), 2.83 – 2.60 (m, 4.5H), 2.56 – 2.23 (m, 3.5H), 1.42 – 1.27 (m, 9H). ^{13}C NMR (101 MHz, CD$_3$CN) δ 172.9, 172.7, 170.6, 169.5, 155.2 (2C), 139.8, 139.6, 139.2, 139.0, 138.5, 137.9, 130.7, 129.8, 129.5, 129.3 (2C), 129.1, 128.4 (2C), 128.3 (2C), 127.8, 127.5 (2C), 126.6 (2C), 126.3, 126.2, 126.1, 79.8 (2C) 53.4, 52.5, 50.2 (2C), 49.9, 49.7, 45.8, 44.2, 40.1, 39.6, 38.0, 37.5, 37.3, 36.8, 29.9, 27.6 (2C), 25.2 (2C). HRMS (ESI) calcd. for [C$_{27}$H$_{35}$N$_3$O$_4$]$^+$: 465.2628, found 466.2339. (MH$^+$)

tert-butyl ((*S*)-4-((*S*)-4-(methylcarbamoyl)-4,5-dihydro-1H-benzo[c]azepin-2(3H)-yl)-4-oxo-1-phenylbutan-2-yl)carbamate (4b)

Compound **32b** (20 mg, 0.045 mmol) was dissolved at room temperature in a solution of methylamine in EtOH (2 ml, 7.5 M). The reaction mixture was stirred for 18 h and evaporated to give **4b** (18 mg, 98%) as a white solid. The following data has been collected on a 1:1 rotamer mixture.

$[\alpha]_D^{25}$ = -25,3 (*c* 0.5, CHCl₃). ¹H NMR (400 MHz, CD₃CN) δ 7.37 − 7.08 (m, 8H), 7.03 - 6.95 (m, 1H), 6.72 (bs, 0.5H), 6.57 (bs, 0.5H), 5.55 (d, 0.5H, *J* = 6.9 Hz), 5.34 (bs, 0.5H), 4.88 (d, 0.5H, *J* = 14.4 Hz), 4.51 (s, 1H), 4.41 − 4.16 (m, 1H) 4.15 - 3.87 (m, 1.5H), 3.77 − 3.58 (m, 1H), 3.58 − 3.09 (m, 2.5H), 2.94 (dd, 1H, *J* = 27.3, 15.4 Hz), 2.86 − 2.55 (m, 5.5H), 2.55 − 2.29 (m, 1H), 1.34 (s, 4.5H), 1.31 (s, 4.5H). ¹³C NMR (101 MHz, CD₃CN) δ 175.1, 174.5, 172.2, 171.1, 156.6 (2C), 141.3, 140.6, 140.5, 140.2, 139.8, 139.3, 132.3, 131.3, 131.2, 131.2, 130.8 (2C), 130.2, 129.8 (2C), 129.8 (2C), 129.4, 129.0, 128.1 (2C), 127.8, 127.7, 127.6, 79.8, 79.7, 56.5, 54.8, 54.1, 52.1, 51.5, 51.3, 47.2, 46.0, 45.9, 41.8, 41.6, 39.4, 39.0, 38.6, 29.1 (2C), 26.7 (2C). HRMS (ESI) calcd. for $[C_{27}H_{35}N_3O_4]^+$: 465.2628, found 466.2651. (MH⁺)
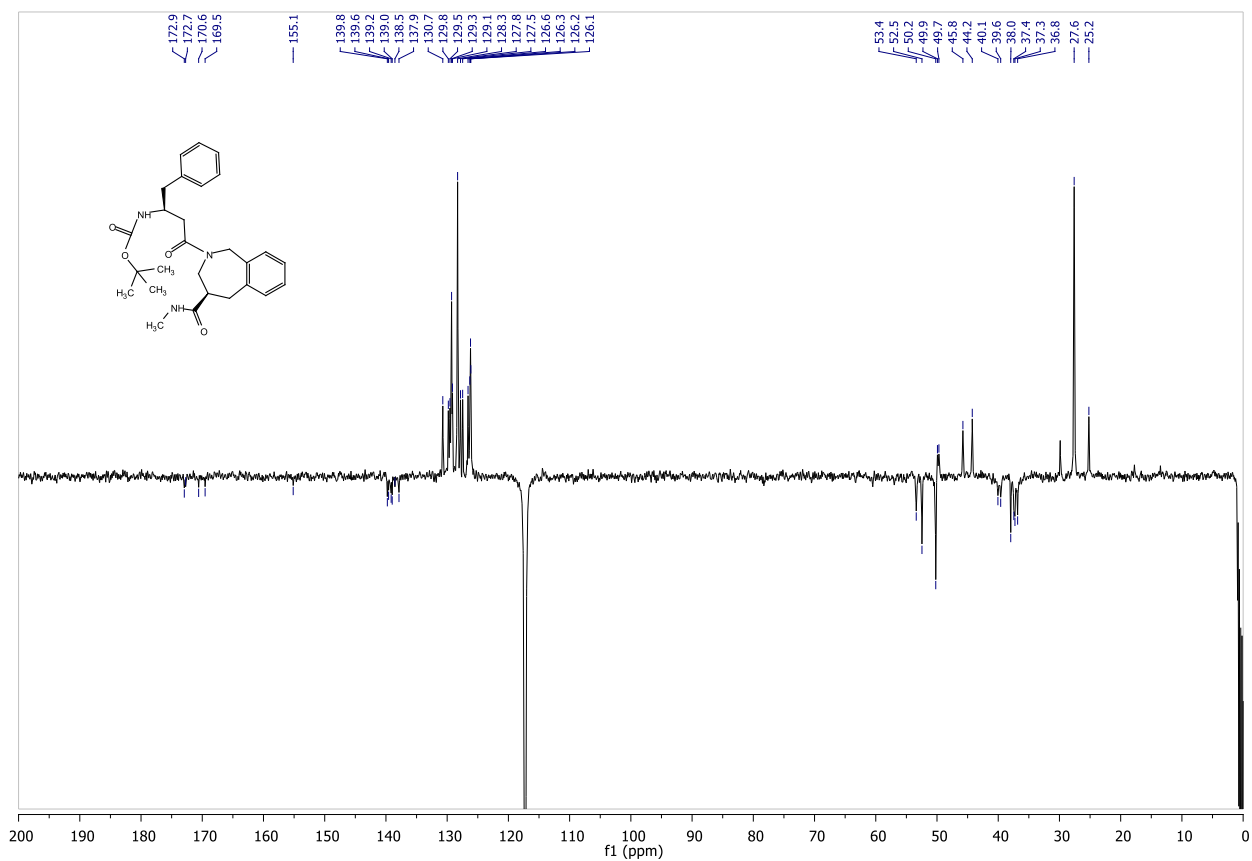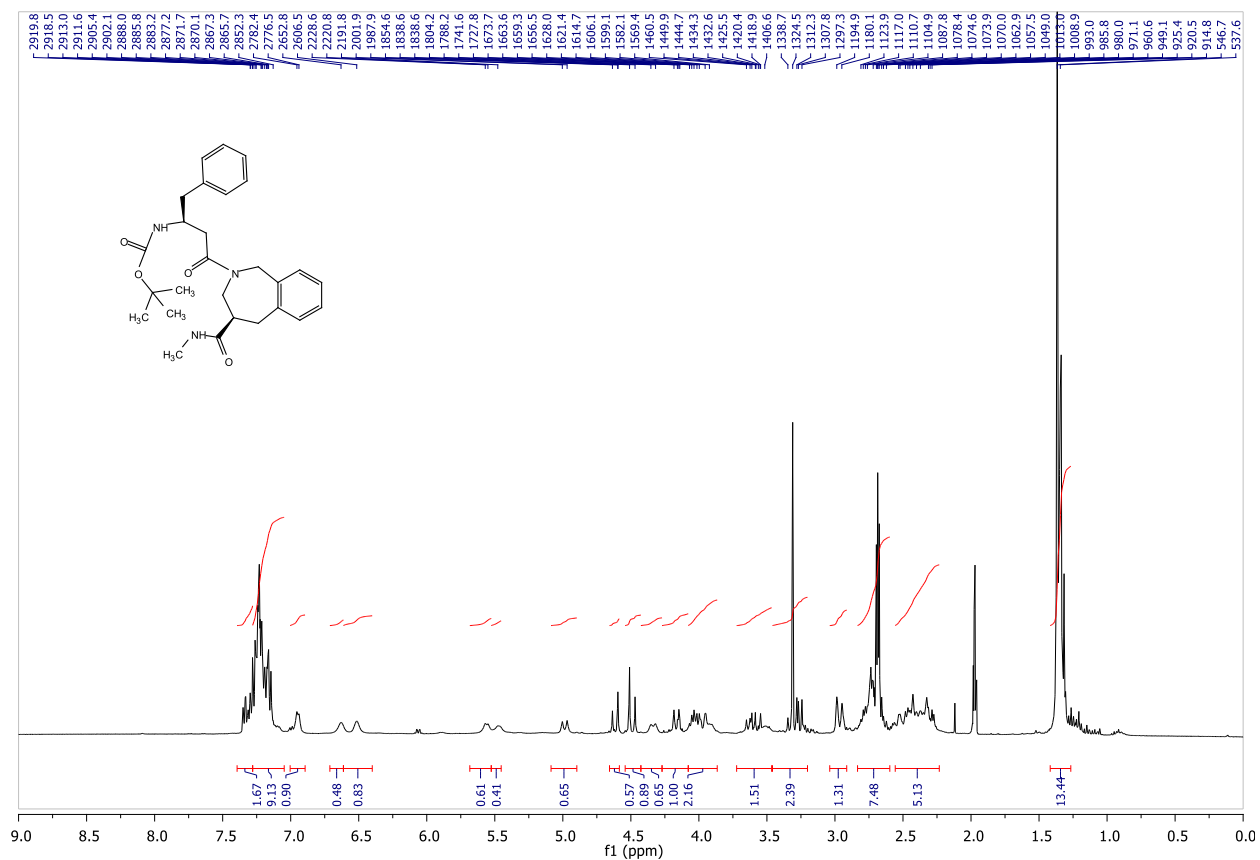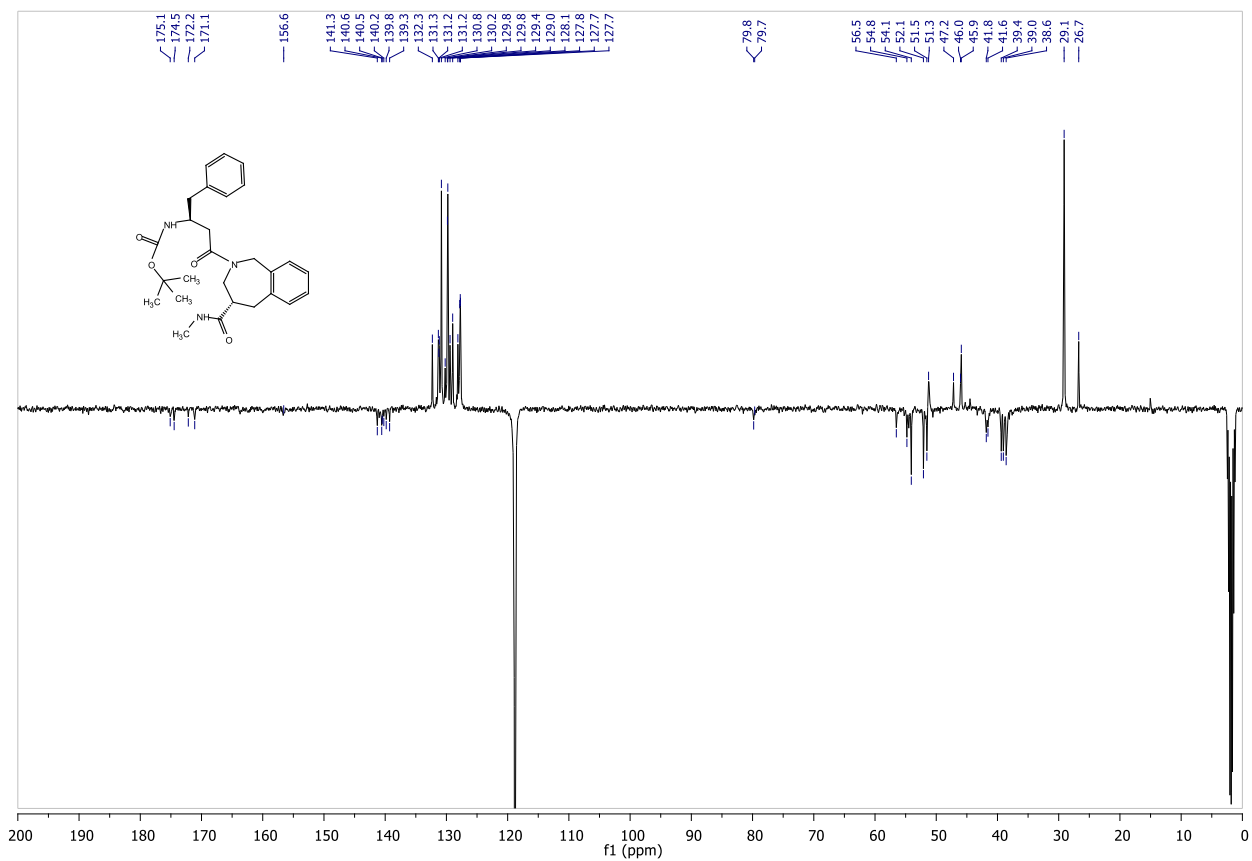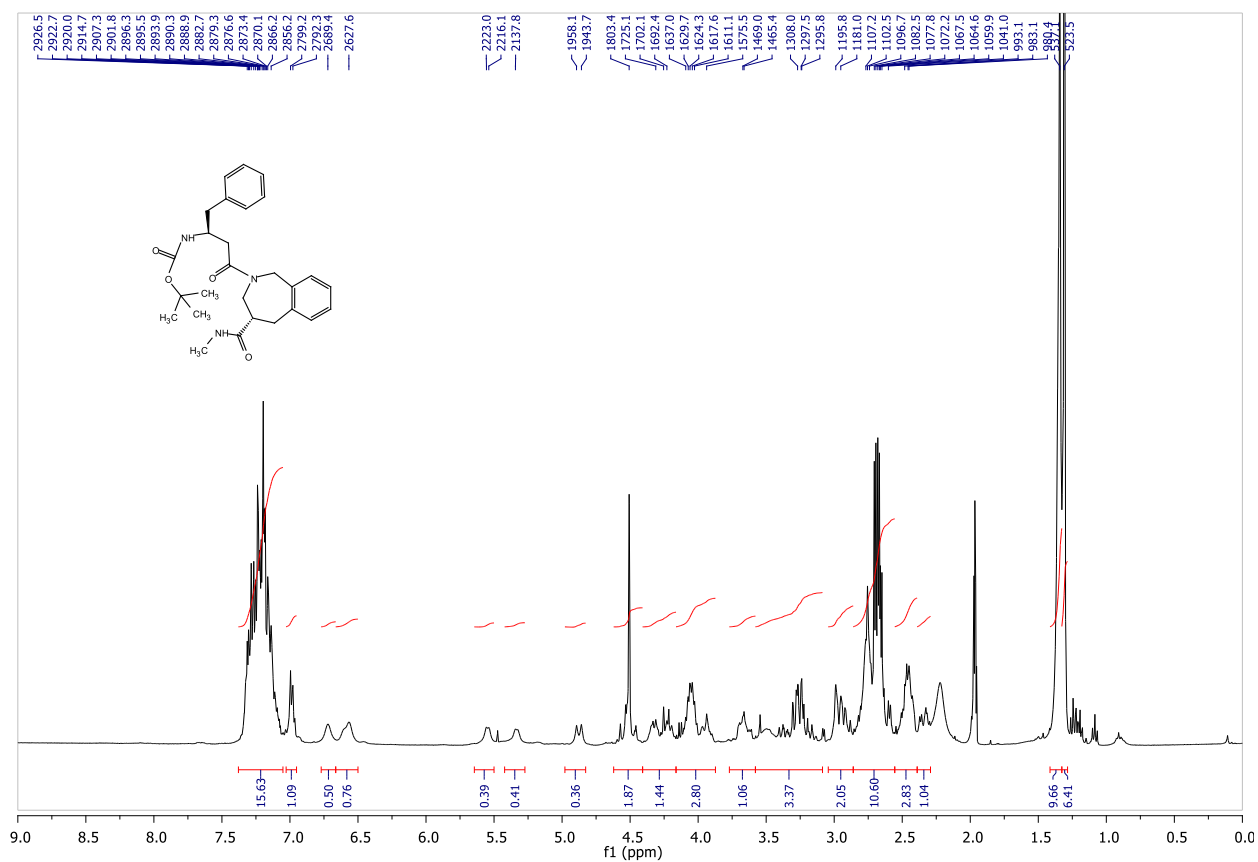
Synthesis of 14:
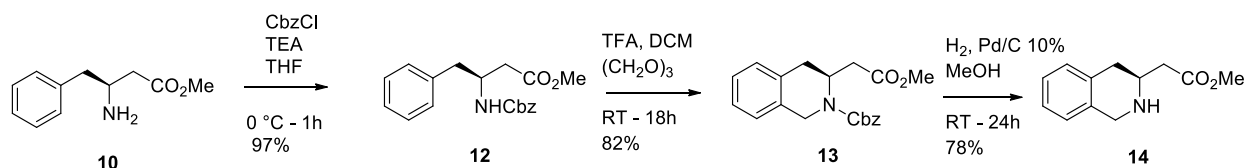
A solution of **10** (882 mg, 4.56 mmol) in THF (30 ml) was cooled to 0°C. Then triethylamine (700 μl, 5.02 mmol) and CbzCl (652 μl, 4.56 mmol) were added. The reaction was quenched after 1h with H_2O. The pH was driven to acidic by means of a solution of $NaHSO_4$ 1M and the mixture was partitioned between AcOEt and H_2O. The organic layer was washed with H_2O, dried (Na_2SO_4), filtered and concentrated to afford crude N-Cbz-β^3-hPhe methylester (1,49 g) as a foam.

^{1}H NMR (400 MHz, CDCl$_3$) δ 7.40 - 7.10 (m, 10H), 5.32 (d, 1H, J = 7.5 Hz), 5.07 (s, 2H), 4.25 - 4.20 (m, 1H), 3.67 (s, 3H), 2.95 (dd, 1H, J = 13.5, 7.2 Hz), 2.83 (dd, 1H, J = 13.3, 7.7 Hz), 2.60 - 2.40 (m, 2H).

(S)-benzyl 3-(2-methoxy-2-oxoethyl)-3,4-dihydroisoquinoline-2(1H)-carboxylate (13)

A solution of the crude N-Cbz-β^3-hPhe methylester (107 mg, 0.33 mmol) in CH_2Cl_2 (3 ml) was cooled to 0° C. Trioxane (59 mg, 0.65 mmol) and TFA (378 μl, 4.9 mmol) were added. The reaction was stirred at room temperature for 18h, then quenched with water and the pH adjusted with $NaHCO_3$ saturated solution. The mixture was partitioned between CH_2Cl_2 and H_2O. The organic layer was washed with H_2O, dried (Na_2SO_4), filtered and concentrated. The residue was purified by flash column chromatography (hexane/AcOEt 85:15) to afford the N-Cbz-β^3hTic-OMe (89 mg, 82% yield) as a foam.

$[\alpha]_D^{25}$ = +49,4 (c 0.6, CHCl$_3$). ^{1}H NMR (400 MHz, CDCl$_3$) δ 7.50 - 7.10 (m, 9H), 5.20 (s, 2H), 4.98 (bs, 1H), 4.85 (d, 1H, J = 16.8 Hz), 4.40 (d, 1H, J = 16.9 Hz), 3.59 (s, 3H), 3.14 (dd, 1H, J = 16.0, 5.5 Hz), 2.77 (d, 1H, J = 15.8 Hz), 2.52 (dd, 1H, J = 14.9, 6.7 Hz), 2.33 (dd, 1H, J = 14.9, 7.7 Hz). ^{13}C NMR (101 MHz, CDCl$_3$) δ 172.1, 155.9, 137.4, 133.1, 132.8, 129.8, 129.1, 128.6, 128.5, 127.6, 127.2, 126.8, 67.9, 52.2, 48.1, 43.9, 37.7, 33.8. FAB-MS-LR m/z 340.15 (MH$^+$).

(S)-methyl 2-(1,2,3,4-tetrahydroisoquinolin-3-yl) acetate (14)

To a solution of N-Cbz-β^3hTic-OMe (837 mg, 2.46 mmol) in MeOH (10 ml), Pd/C 10% (80 mg) was added and the reaction was put under H_2 atmosphere at room temperature

for 6 hours. The crude was filtered over celite and purified by flash column chromatography (Hex/AcOEt 1:1) to afford amine **14** (393 mg, 78% yield) as a colorless oil.

$[\alpha]_D^{25}$ = -52,6 (*c* 1.0, CHCl$_3$). ^{1}H NMR (400 MHz, CDCl$_3$) δ 7.24 - 6.92 (m, 4H), 4.15 (d, 1H, *J* = 15.9 Hz), 4.05 (d, 1H, *J* = 15.9 Hz), 3.71 (s, 3H), 3.45 - 3.25 (m, 1H), 2.81 (dd, 1H, *J* = 16.1 Hz, *J* = 3.9 Hz), 2.61 - 2.39 (dd, 1H, *J* = 19.0, 9.8 Hz), 2.57 – 2.54 (m, 2H). ^{13}CNMR (101 MHz, CDCl$_3$) δ 172.5, 135.1, 133.9, 129.1, 126.1, 125.9, 51.7, 50.5, 48.1, 40.6, 34.8. HRMS (ESI) calcd. for $[C_{12}H_{15}NO_2]^+$: 205.1103, found 206.1132. (MH$^+$)

¹H and ¹³C NMR spectra of compound **14**
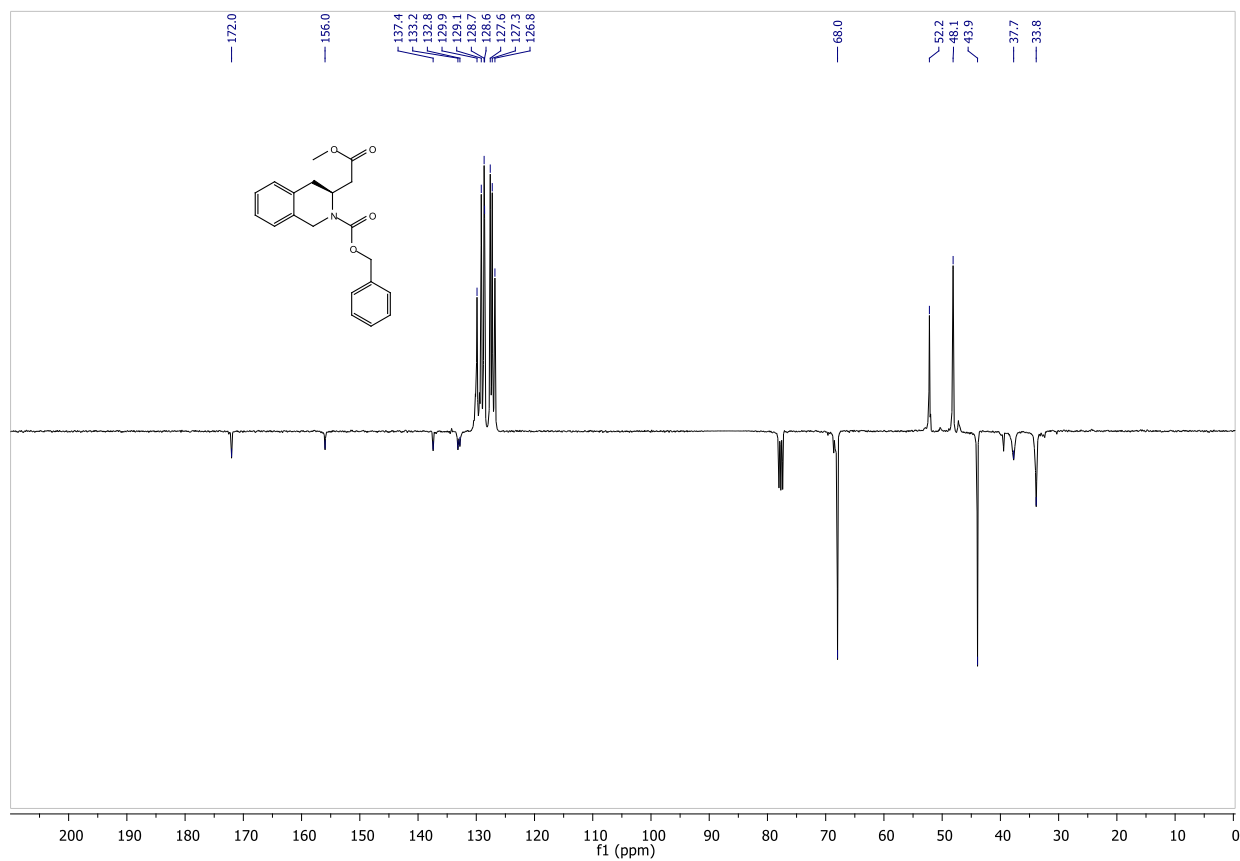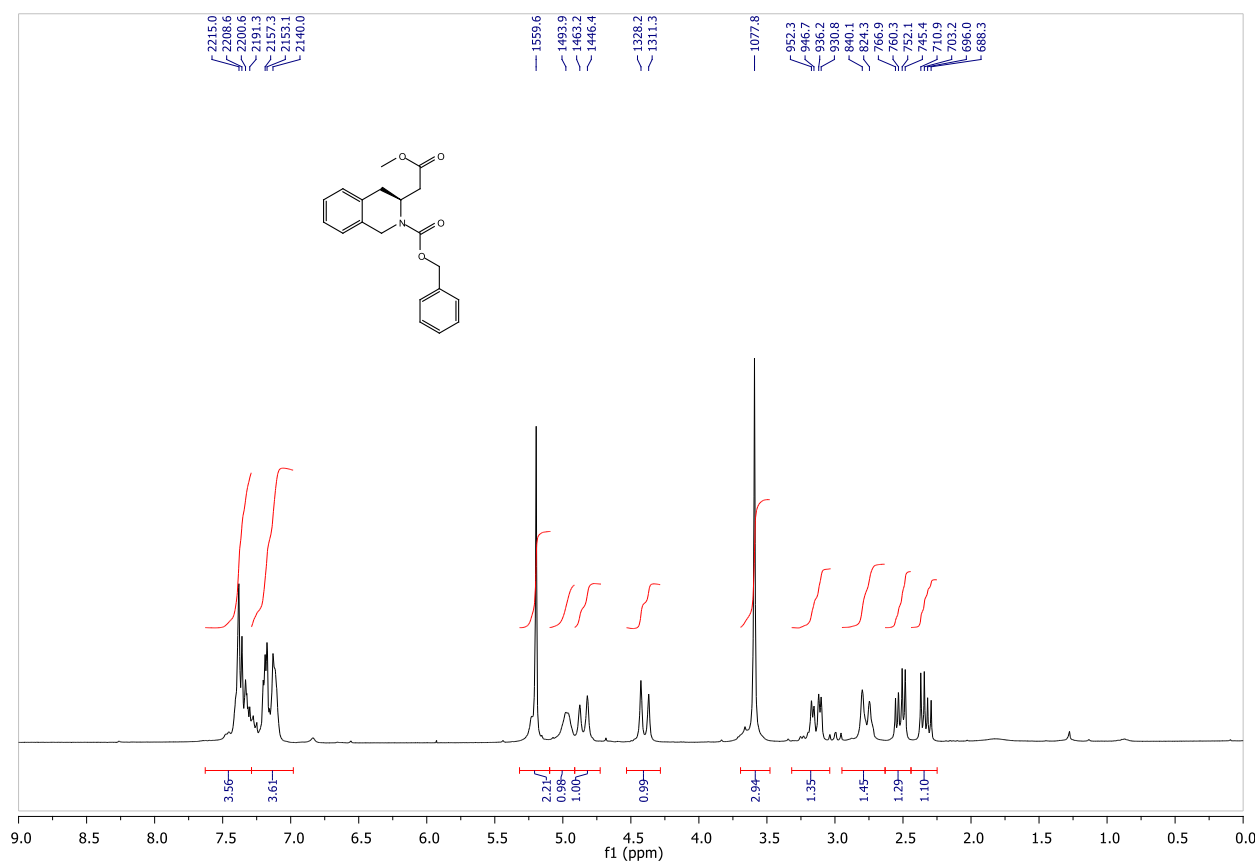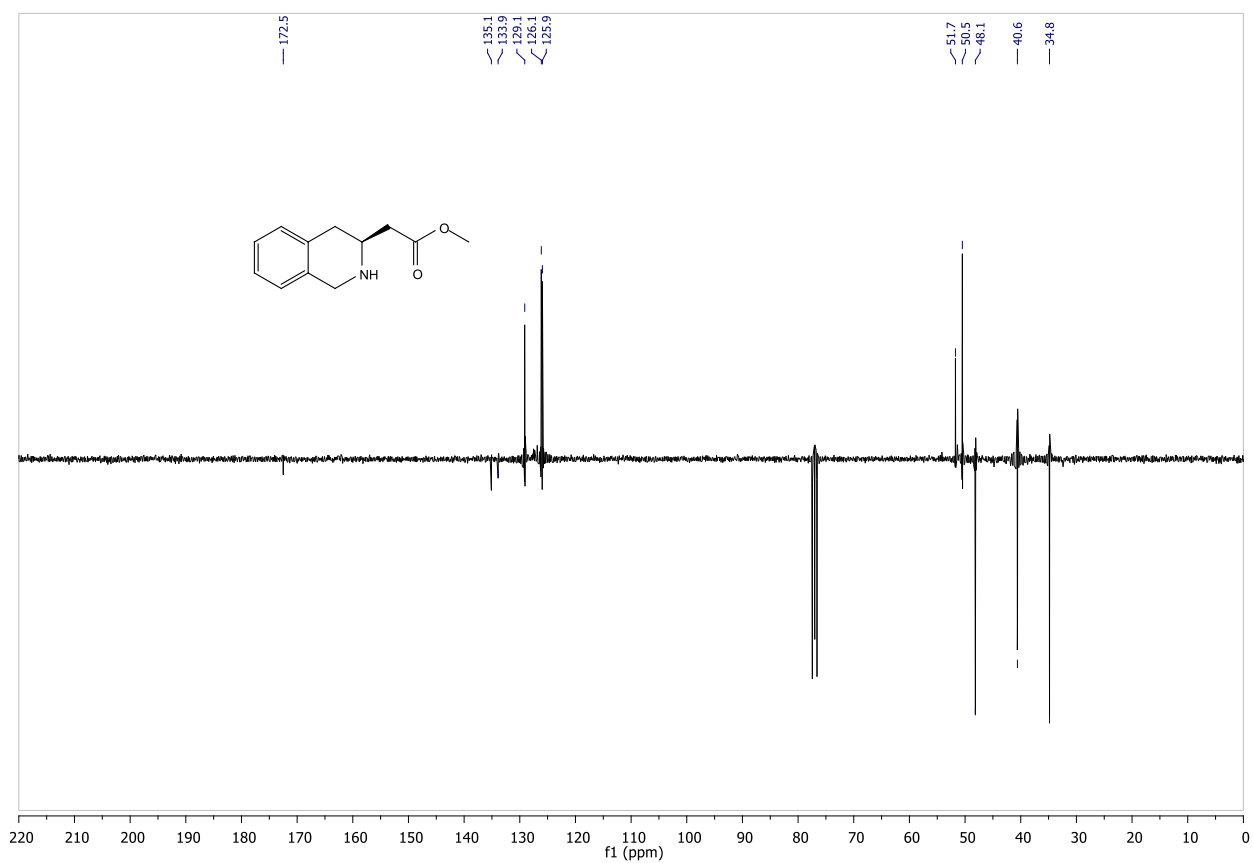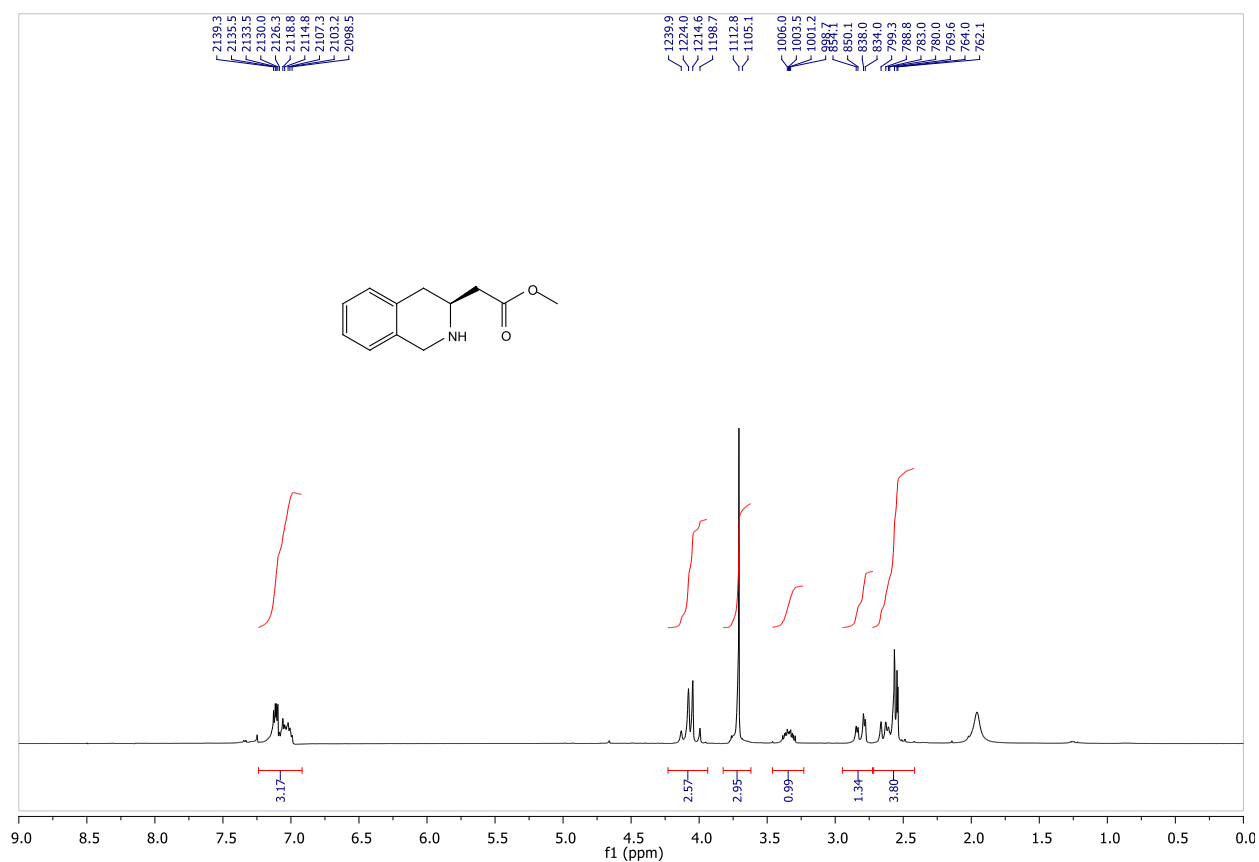
Synthesis of 30:
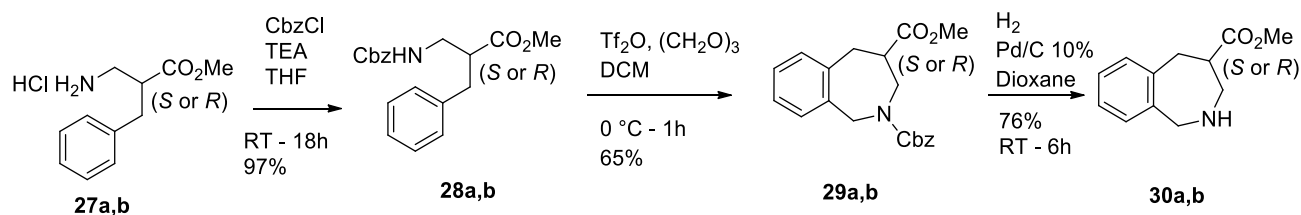
(R)-methyl 2-benzyl-3-(benzyloxycarbonylamino) propanoate (28a)

β^2-hPhe (137 mg, 0.71 mmol) is dissolved in THF and cooled to 0 °C. TEA (108 µl, 0.78 mmol) was added followed by CbzCl (111 µl, 0.78 mmol). After 2 hours the pH is adjusted to acidic by adding NaHSO$_4$ 1M. The reaction is extracted with AcOEt and washed with brine, water, dried over Na$_2$SO$_4$, filtered and concentrated under reduced pressure. The crude was purified by flash chromatography (Hex/AcOEt 8:2) to afford the product as a colorless oil (225 mg, 97%).

Rf = 0.28 (Hex/AcOEt 8:2). $[\alpha]_D^{25}$ = +1.3 (c 0.6, CHCl$_3$). ^{1}H NMR (400 MHz, CDCl$_3$) δ 7.39 – 6.97 (m, 10H), 5.14 – 4.94 (m, 3H), 3.54 (s, 3H), 3.45 – 3.31 (m, 1H), 3.30 – 3.19 (m, 1H), 2.95 – 2.80 (m, 2H), 2.80 – 2.64 (m, 1H). ^{13}C NMR (101 MHz, CDCl$_3$) δ 174.5, 156.3, 138.1, 136.5, 128.8 (2C), 128.6 (3C), 128.1 (3C), 126.7 (2C), 66.8, 51.8, 47.2, 41.9, 35.8. HRMS (ESI) calcd. for [C$_{19}$H$_{21}$NO$_4$]$^+$: 327.1471, found 328.1459. (MH$^+$)

(S)-methyl 2-benzyl-3-(benzyloxycarbonylamino) propanoate (28b)

β^2-hPhe (112 mg, 0.58 mmol) is dissolved in THF and cooled to 0 °C. TEA (90 µl, 0.64 mmol) was added followed by CbzCl (91 µl, 0.64 mmol). After 2 hours the pH is adjusted to acidic by adding NaHSO$_4$ 1M. The reaction is extracted with AcOEt and washed with brine, water, dried over Na$_2$SO$_4$, filtered and concentrated under reduced pressure. The crude was purified by flash chromatography (Hex/AcOEt 8:2) to afford the product as a colorless oil (185 mg, 98%).

Rf = 0.28 (Hex/AcOEt 8:2). $[\alpha]_D^{25}$ = -2.8 (c 0.45, CHCl$_3$). ^{1}H NMR (400 MHz, CDCl$_3$) δ 7.39 – 6.97 (m, 10H), 5.14 – 4.94 (m, 3H), 3.54 (s, 3H), 3.45 – 3.31 (m, 1H), 3.30 – 3.19 (m, 1H), 2.95 – 2.80 (m, 2H), 2.80 – 2.64 (m, 1H). ^{13}C NMR (101 MHz, CDCl$_3$) δ 174.5, 156.3, 138.1, 136.5, 128.8 (2C), 128.6 (3C), 128.1 (3C), 126.7 (2C), 66.8, 51.8, 47.2, 41.9, 35.8. HRMS (ESI) calcd. for [C$_{19}$H$_{21}$NO$_4$]$^+$: 327.1471, found 328.1439. (MH$^+$)

^{1}H and ^{13}C NMR spectra of compound 28
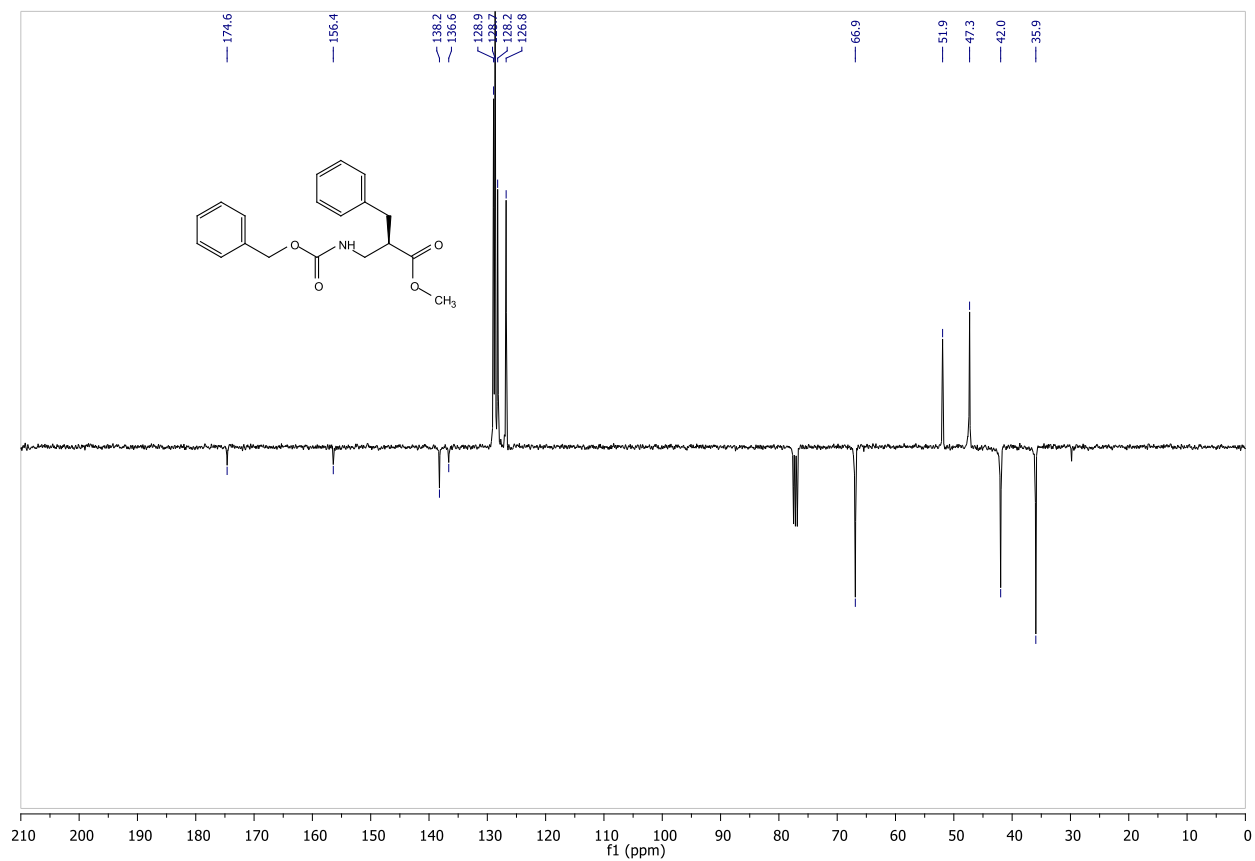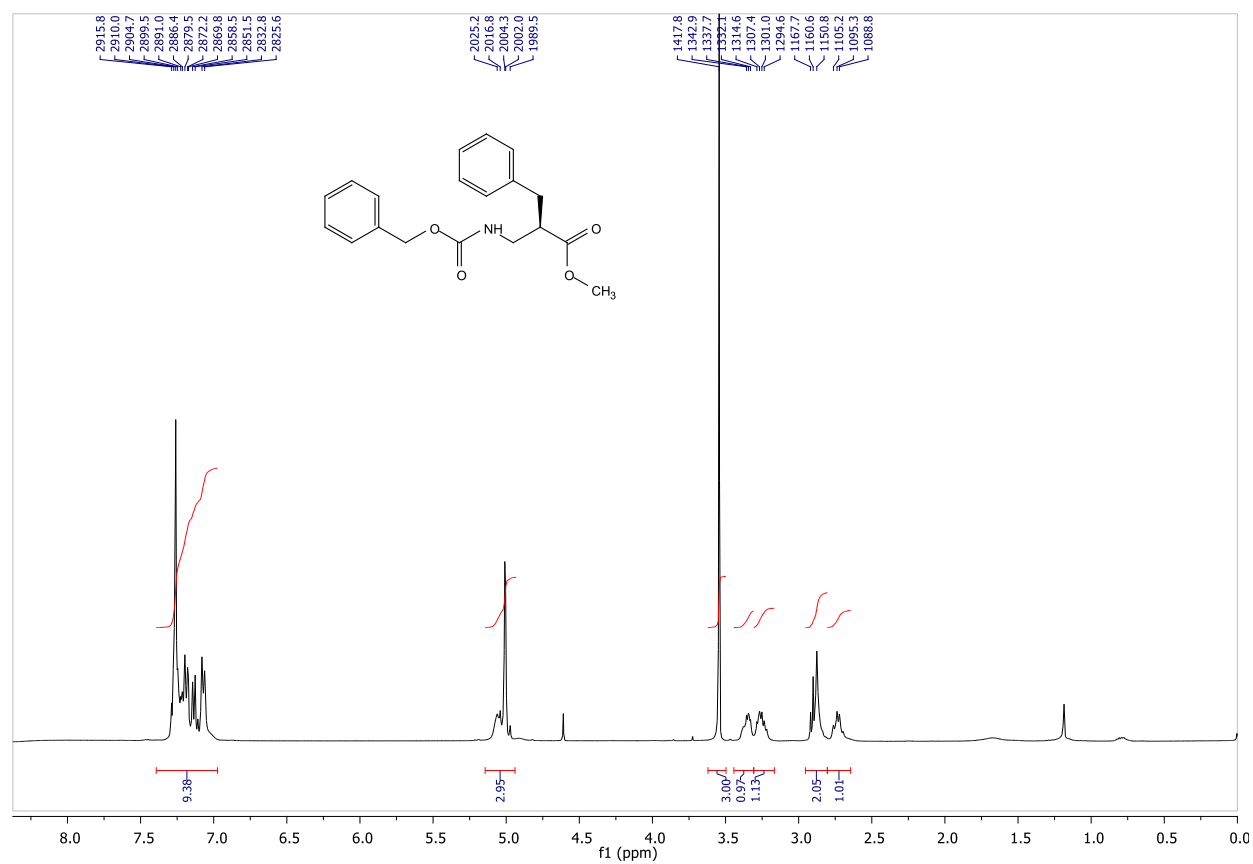
(*R*)-2-benzyl 4-methyl 4,5-dihydro-1H-benzo[c]azepine-2,4(3H)-dicarboxylate (29a)

A solution of β^2-hPhe (102 mg, 0.31 mmol) in CH_2Cl_2 (1 ml) was cooled to 0 °C, then trioxane (111 mg, 1.24 mmol) was added, followed by triflic anhydride dropwise (109 μl, 0.62 mmol). The mixture was stirred for 60 minutes at 0 °C. The reaction is stopped by adding $NaHCO_3$ ss, extracted with CH_2Cl_2, dried over Na_2SO_4, filtered and concentrated under reduced pressure. The crude was purified by flash chromatography (Hex/AcOEt 8:2) to afford the product as a colorless oil (67 mg, 64%).

The following data has been collected on a 1:1 rotamer mixture. Rf = 0.31 (Hex/AcOEt 8:2). $[\alpha]_D^{25}$ = -22.9 (*c* 0.3, CHCl$_3$). ^{1}H NMR (CDCl$_3$, 400 MHz) δ 7.4-7.1 (m, 9H), 5.2 (d, 1H, *J* = 13.0 Hz), 5.1 (d, 1H, *J* = 13.1 Hz), 4.8 (d, 0.5H, *J* = 14.9 Hz), 4.70 (d, 0.5H, *J* = 15.0 Hz), 4.5 (d, 1H, *J* =15.1 Hz), 4.37 – 4.29 (m, 1H), 3.72 (s, 1.5H), 3.68 (s, 1.5H), 3.54 – 3.51 (m, 0.5H), 3.47 – 3.44 (m, 0.5H), 3.25 – 3.17 (m, 2H), 2.92 – 2.61 (m, 1H). ^{13}C NMR (CDCl$_3$, 101 MHz) δ 175.4, 175.2, 155.8, 155.3, 138.6, 137.9, 137.7, 137.4, 136.7, 136.6, 130.1, 130.0 (2C), 129.4 (2C), 129.1 (2C), 128.7 (2C), 128.4 (2C), 128.1 (2C), 128.0 (2C), 127.0 (2C), 126.7, 67.5, 67.3, 52.6, 52.1, 51.9, 51.6, 51.3, 50.4, 43.9, 43.3, 37.3, 36.9. HRMS (ESI) calcd. for $[C_{20}H_{21}NO_4]^+$: 339.1471, found 340.1442. (MH$^+$)

(*S*)-2-benzyl 4-methyl 4,5-dihydro-1H-benzo[c]azepine-2,4(3H)-dicarboxylate (29b)

A solution of β^2-hPhe (88 mg, 0.27 mmol) in CH_2Cl_2 (1 ml) was cooled to 0 °C, then trioxane (96 mg, 1.07 mmol) was added, followed by triflic anhydride dropwise (91 μl, 0.54 mmol). The mixture was stirred for 60 minutes at 0 °C. The reaction is stopped by adding $NaHCO_3$ ss, extracted with CH_2Cl_2, dried over Na_2SO_4, filtered and concentrated under reduced pressure. The crude was purified by flash chromatography (Hex/AcOEt 8:2) to afford the product as a colorless oil (60 mg, 65%).

The following data has been collected on a 1:1 rotamer mixture. Rf = 0.31 (Hex/AcOEt 8:2). $[\alpha]_D^{25}$ = +10.0 (*c* 1.0, CHCl$_3$). ^{1}H NMR (400 MHz, CDCl$_3$) δ 7.49 – 7.05 (m, 9H), 5.17 (d, 1H, *J* = 10.6 Hz), 5.08 (d, 1H, *J* = 13.7 Hz), 4.81 (d, 0.5H, *J* = 14.8 Hz), 4.73 (d, 0.5H, *J* = 15.1 Hz) 4.48 (dd, 0.5H, *J* = 13.9, 3.3 Hz), 4.36 - 4.24 (m, 1.5H), 3.74 (s, 1.5H), 3.68 (s, 1.5H), 3.63 – 3.49 (m, 0.5H), 3.44 (dd, 0.5H, *J* = 13.9, 10.2 Hz), 3.31 – 3.09 (m, 2H), 2.88 – 2.71 (m, 1H). ^{13}C NMR (101 MHz, CDCl$_3$) δ 173.4, 173.3, 155.5, 155.2, 138.6, 138.1, 137.9, 137.4, 136.7, 136.6, 130.2 (2C), 130.1 (2C), 129.4 (2C), 129.1 (2C), 128.4 (2C), 128.0 (2C), 127.9 (2C), 127.0 (2C), 126.7 (2C), 67.4, 67.2, 52.5, 52.0, 51.9, 51.7, 51.4, 50.3, 43.9, 43.3, 37.2, 36.7. HRMS (ESI) calcd. for $[C_{20}H_{21}NO_4]^+$: 339.1471, found 340.1495. (MH$^+$)

¹H and ¹³C NMR spectra of compound **29**
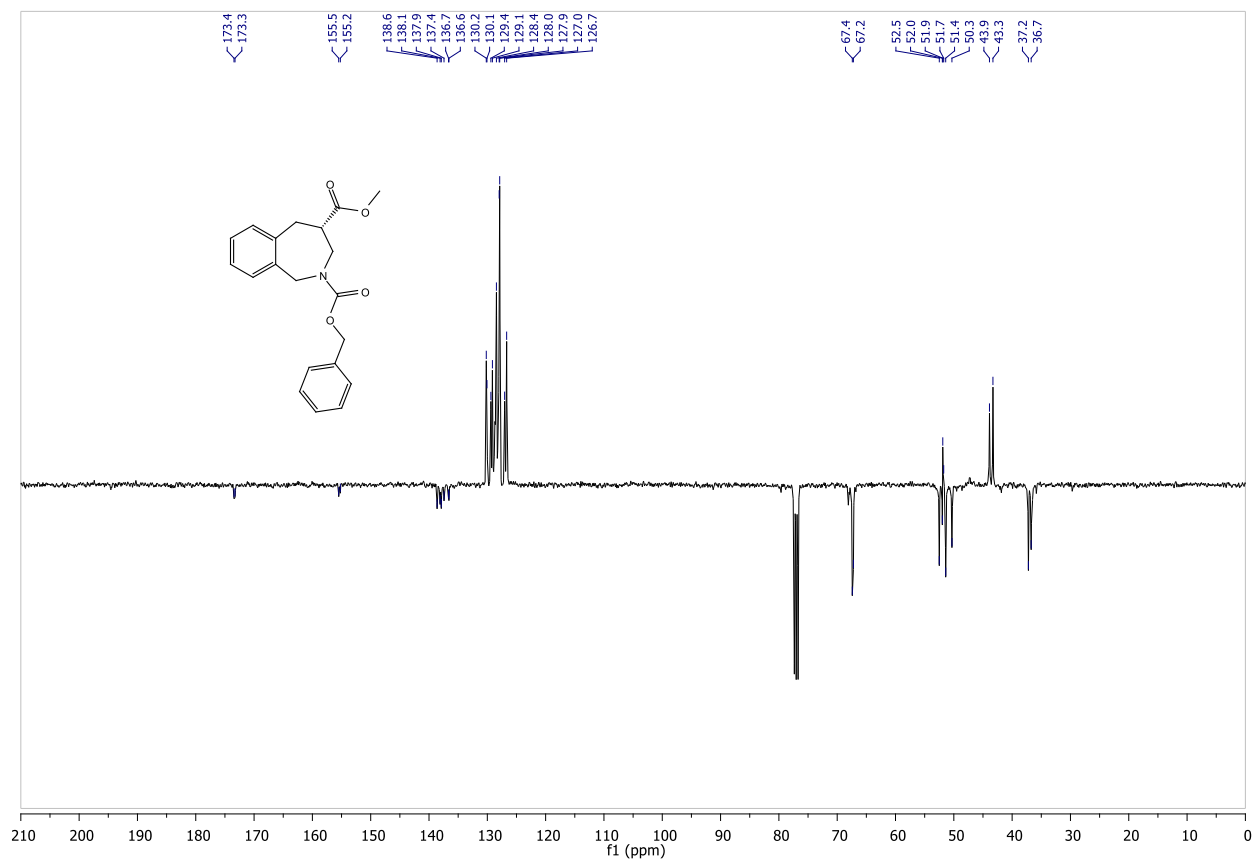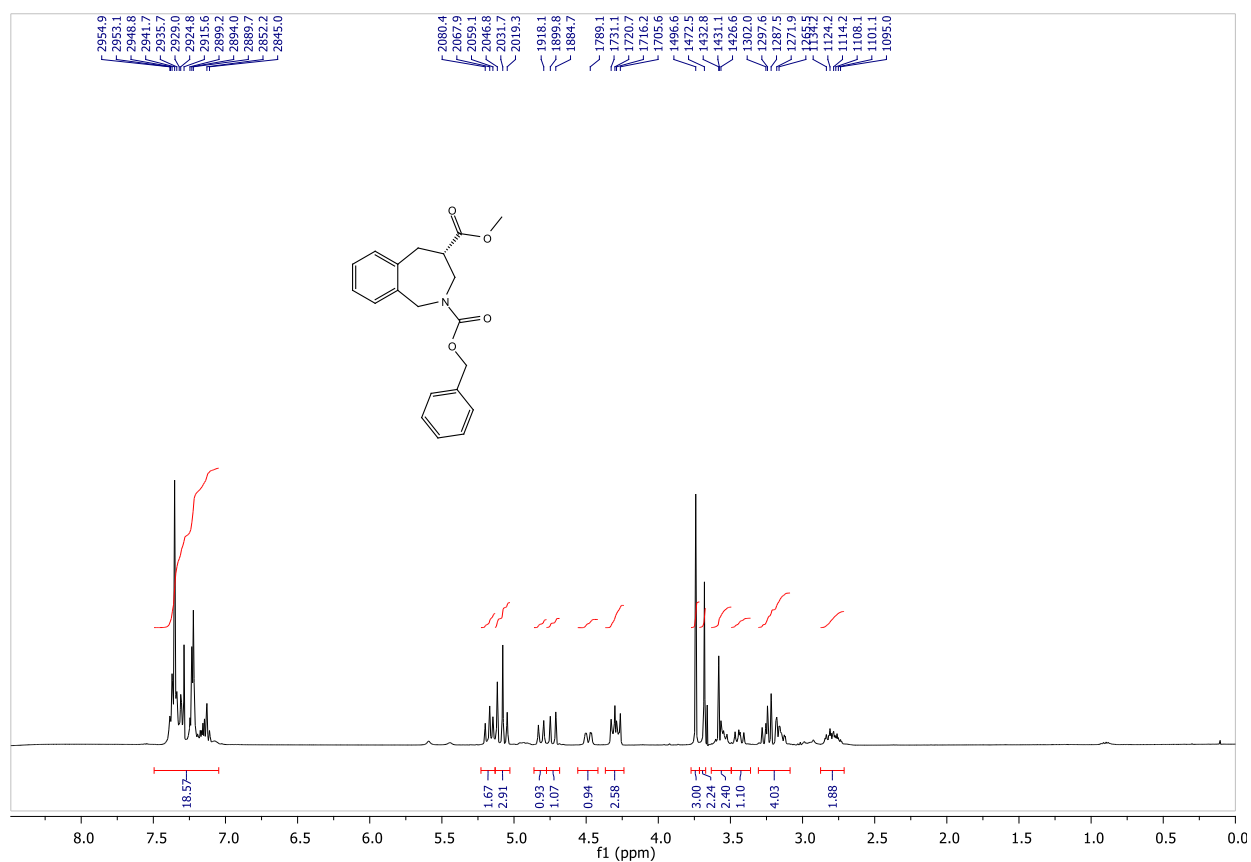
(*R*)-methyl 2,3,4,5-tetrahydro-1H-benzo[c]azepine-4-carboxylate (30a)

Compound **29a** (177 mg, 0.52 mmol) was dissolved in dioxane (5 ml). Pd/C 10% (30 mg) and AcOH were added. The reaction was stirred under hydrogen atmosphere at rt for 18h. The mixture was filtered through celite pad and concentrated. The residue was purified by flash chromatography to give colorless oil (64 mg, 60%).

Rf = 0.34 (Hex/AcOEt/TEA 1:1:0.1). $[\alpha]_D^{25}$ = +37.9 (*c* 1.0, CHCl$_3$). ^{1}H NMR (CDCl$_3$, 400 MHz) δ: 7.2-7.05 (m, 4H), 3.98 (s, 2H), 3.65 (s, 3H), 3.40 (d, 2H, *J* =5.85 Hz), 3.25 - 3.20 (m, 2H), 2.69 – 2.61 (m, 1H), 2.53 (s, 1H). ^{13}C NMR (CDCl$_3$, 101 MHz) δ: 173.5, 141.5, 138.7, 130.0, 128.0, 126.9, 126.5, 76.2, 54.0, 51.9, 44.1, 38.5. HRMS (ESI) calcd. for [C$_{12}$H$_{15}$NO$_2$]$^+$: 205.1103, found 228.1127. (MNa$^+$)

(*S*)-methyl 2,3,4,5-tetrahydro-1H-benzo[c]azepine-4-carboxylate (30b)

Compound **29b** (92 mg, 0.27 mmol) was dissolved in dioxane (5 ml). Pd/C 10% (9 mg) and AcOH were added. The reaction was stirred under hydrogen atmosphere for 18h at rt. The mixture was then filtered through celite pad and concentrated. The residue was purified by flash chromatography (Hex/AcOEt/TEA 1:1:0.1) to give a colorless oil (42 mg, 76%).

Rf = 0.34 (Hex/AcOEt/TEA 1:1:0.1). $[\alpha]_D^{25}$ = -31.4 (*c* 1, CHCl$_3$). ^{1}H NMR (CDCl$_3$, 400 MHz) δ: 7.20 -7.05 (m, 4H), 3.98 (s, 2H), 3.65 (s, 3H), 3.40 (d, 2H, *J* = 5.85 Hz), 3.25 - 3.20 (m, 2H), 2.69 – 2.64 (m, 1H), 2.53 (bs, 1H). ^{13}C NMR (CDCl$_3$, 101 MHz) δ: 173.5, 141.5, 138.7, 130.0, 128.0, 126.9, 126.5, 76.2, 54.0, 51.9, 44.1, 38.5. HRMS (ESI) calcd. for [C$_{12}$H$_{15}$NO$_2$]$^+$: 205.1103, found 228.1131. (MNa$^+$)

General Procedure for Peptide Coupling:
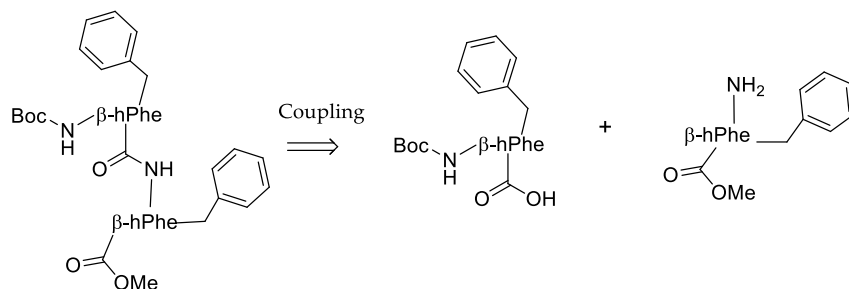
PROCEDURE A:

To a suspension of β-hPhe (acid) in dry CH₂Cl₂ under nitrogen atmosphere was added DIPEA (1.1 - 2.0 equiv.). The reaction mixture was cooled to 0°C, HOBt (1.2 equiv.) and EDC (1.2 equiv.) were added, after 45 minutes a solution of β-hPhe (amine) with DIPEA (1.1 - 2.0 equiv.) in CH₂Cl₂ was added and the reaction was stirred overnight at room temperature. The mixture was then diluted with water, extracted with CH₂Cl₂ and washed with 1.0 M HCl, saturated NaHCO₃, dried over anhydrous Na₂SO₄, filtered and concentrated *in vacuo*.
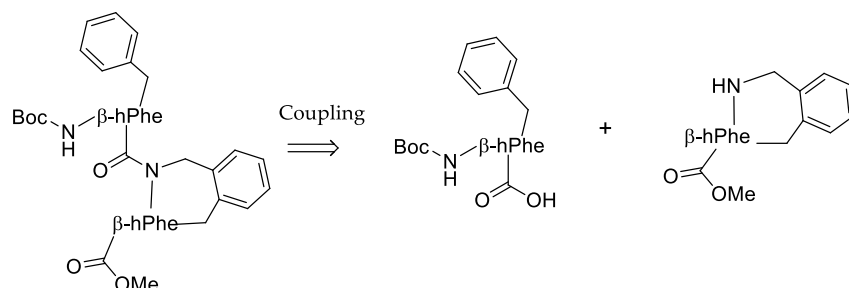
PROCEDURE B:

To a suspension of β-hPhe (acid) in dry CH₂Cl₂ under nitrogen atmosphere was added TEA (1.1 - 2.0 equiv.). The reaction mixture was cooled to 0°C and BOP-Cl (1.5 equiv.) was added, after 45 minutes a solution of β-hPhe (amine) with TEA (1.1 - 2.0 equiv.) in CH₂Cl₂ was added and the reaction was stirred overnight at room temperature. The mixture was then diluted with water, extracted with CH₂Cl₂ and washed with 1.0 M HCl, saturated NaHCO₃, dried over anhydrous Na₂SO₄, filtered and concentrated *in vacuo*.
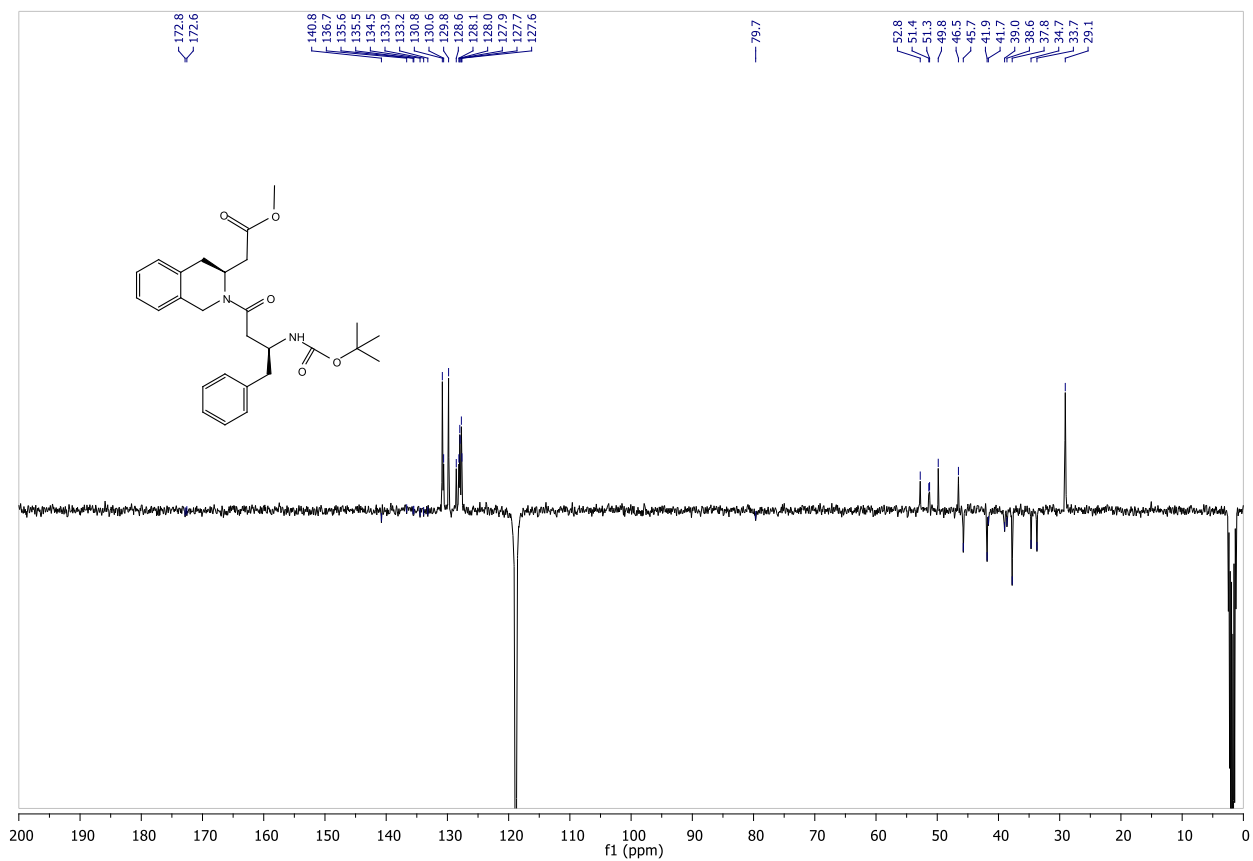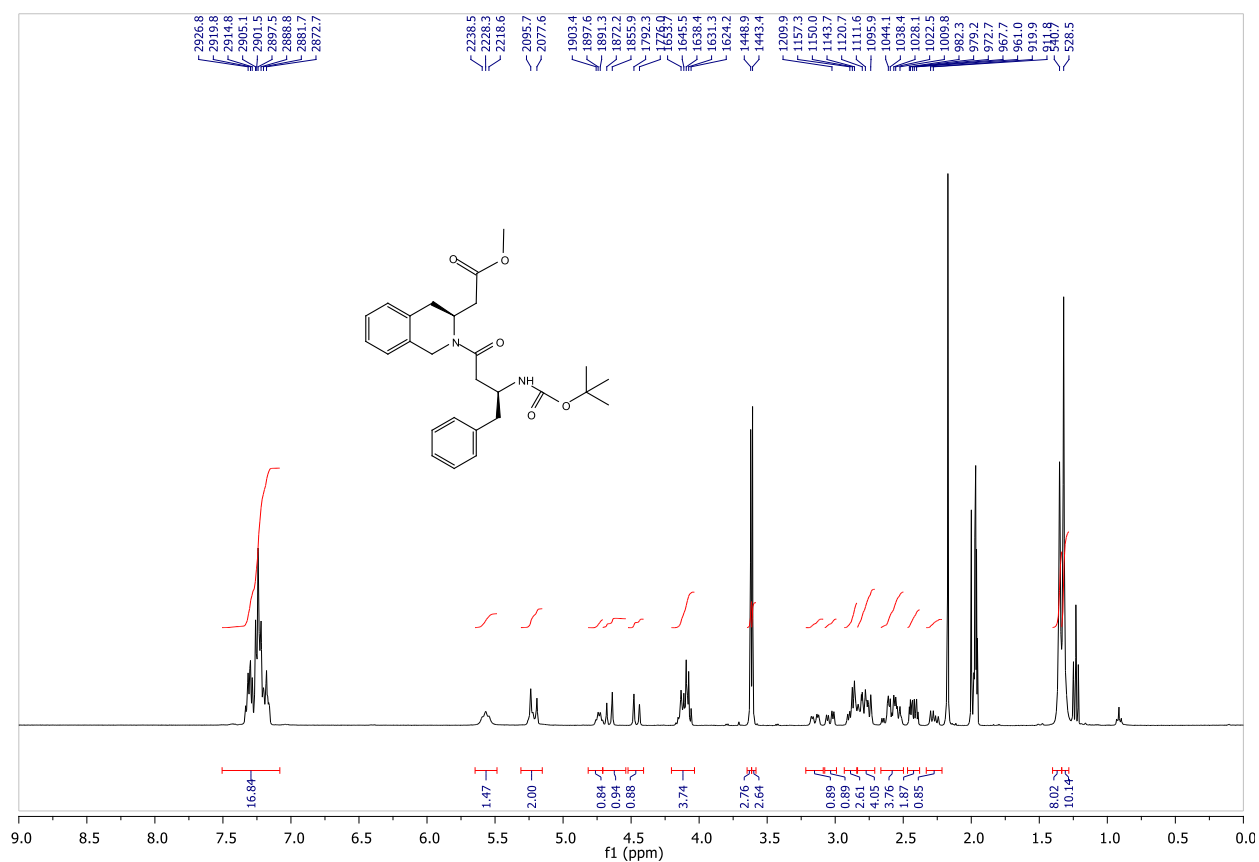
Synthesis of 31:
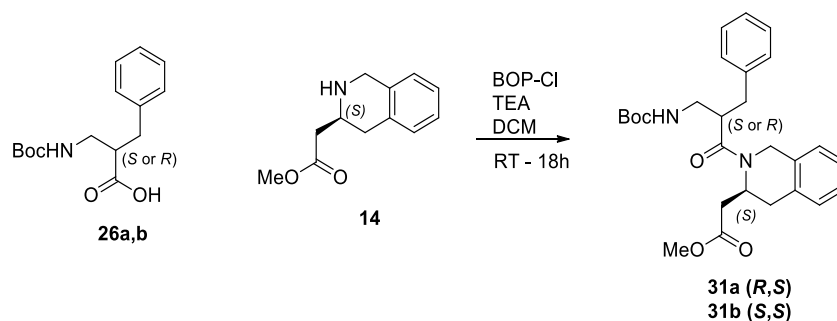
Methyl 2-((*S*)-2-((*R*)-2-benzyl-3-(tert-butoxycarbonylamino)propanoyl)-1,2,3,4-tetrahydroisoquinolin-3-yl) acetate (31a).
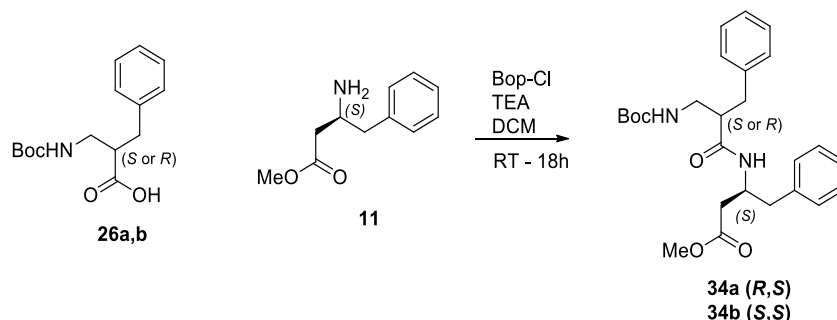
Following the general procedure **B** for peptide coupling. Acid **26a** (81 mg, 0.29 mmol), amine **14** (60 mg, 0.29 mmol), TEA (90 µl, 0.64 mmol), BOP-Cl (111 mg, 0.44 mmol) and CH_2Cl_2 (1.5 ml) afforded after flash chromatography (Hex/AcOEt 75:25) a foam (111 mg, 82%).

$[\alpha]_D^{25}$ = +43,3 (*c* 0.5, CHCl$_3$). ^{1}H NMR (400 MHz, CD$_3$CN, mixture of two conformers in ratio 1:1) δ 7.38 - 6.95 (m, 9H), 5.21 - 5.19 (m, 0.5H), 5.02 (d, 0.5H, *J* = 17.8 Hz), 4.75 (d, 0.5H, *J* = 16.1 Hz), 4.50 - 4.45 (m, 0.5H), 4.17 (d, 0.5H, *J* = 17.9 Hz), 4.12 (d, 0.5H, *J* = 16.1 Hz), 3.64 (s, 1.5H), 3.61 (s, 1.5H), 3.54 - 3.15 (m, 3H), 3.00 (dd, 0.5H, *J* = 16.1, 5.5 Hz), 2.85 (dd, 0.5H, *J* = 16.1, 9.2 Hz), 2.80 - 2.65 (m, 2H), 2.52 - 2.40 (m, 1H), 2.31 (dd, 0.5H, *J* = 16.1 Hz, 9.2 Hz), 2.24 (dd, 0.5H, *J* = 16.1, 5.5 Hz), 2.16 (dd, 1H, *J* = 16.3 Hz, 4.7 Hz), 2.06 (dd, 1H, *J* = 15.0 Hz, 9.1 Hz), 1.45 (s, 4.5H), 1.43 (s, 4.5H). ^{13}C NMR (101 MHz, CD$_3$CN, mixture of two conformers in ratio 1:1) δ 172.9, 171.3, 155.9, 139.5, 139.2, 132.9-126.0 (10C), 78.3, 51.4 and 51.2, 48.3, 45.2 and 43.7, 44.2, 41.3, 37.0, 36.9 and 36.3, 35.9 and 32.5, 27.6 and 27.5 (3C). HRMS (ESI) calcd. for [C$_{27}$H$_{34}$N$_2$O$_5$]$^+$: 466.2468, found 467.2496. (MH$^+$)

Methyl 2-((*S*)-2-((*S*)-2-benzyl-3-(tert-butoxycarbonylamino)propanoyl)-1,2,3,4-tetrahydroisoquinolin-3-yl) acetate (31b).

Following the general procedure **B** for peptide coupling. Acid **26b** (89 mg, 0.32 mmol), amine **14** (67 mg, 0.32 mmol), TEA (101 µl, 0.52 mmol), BOP-Cl (124 mg, 0.49 mmol) and CH_2Cl_2 (1.5 ml) afforded after flash chromatography (Hex/AcOEt 75:25) a foam (109 mg, 73%).

$[\alpha]_D^{25}$ = +42,3 (*c* 0.5, CHCl$_3$). ^{1}H NMR (400 MHz, CD$_3$CN, mixture of two conformers in ratio 1:1) δ 7.3 - 7.0 (m, 9H), 5.6 - 5.5 (m, 0.5H), 5.34 - 5.08 (m, 0.5H), 4.82-4.78 (m, 0.5H), 4.42 (d, 0.5H, *J* = 16.3 Hz), 4.37 (d, 0.5H, *J* = 16.3 Hz), 4.03 (d, 0.5H, *J* = 18.1 Hz), 3.61 (s, 1.5H), 3.58 (s, 1.5H), 3.55 - 3.48 (m, 1H), 3.45 - 3.35 (m, 1H), 3.3 - 3.15 (m, 1.5H), 3.10 (d,

0.5H, J = 15.1 Hz), 2.92 (dd, 0.5H, J = 14.8, 7.5 Hz), 2.83 - 2.65 (m, 2.5H), 2.37 (dd, 0.5H, J = 14.8, 7.2 Hz), 2.24 (dd, 0.5H, J = 14.8, 7.5 Hz), 2.16 (dd, 1H, J = 8.8 Hz, 7.5 Hz), 1.63 (dd, 1H, J = 16.0, 5.4 Hz), 1.42 (s, 4.5H), 1.36 (s, 4.5H). ^{13}C NMR (101 MHz, CD_3CN, mixture of two conformers in ratio 1:1) δ 174.7 and 174.3, 173.2 and 172.6, 155.9, 141.5, 140.8, 134.1-127.5 (10C), 79.9, 52.8, 49.7, 46.6 and 45.3, 45.6, 44.5 and 44.3, 42.5, 37.9 and 37.8, 34.6 and 33.7, 29.2 and 29.1 (3C). HRMS (ESI) calcd. for $[C_{27}H_{34}N_2O_5]^+$: 466.2468, found 467.2438. (MH$^+$)

^{1}H and ^{13}C NMR of compound **31a**
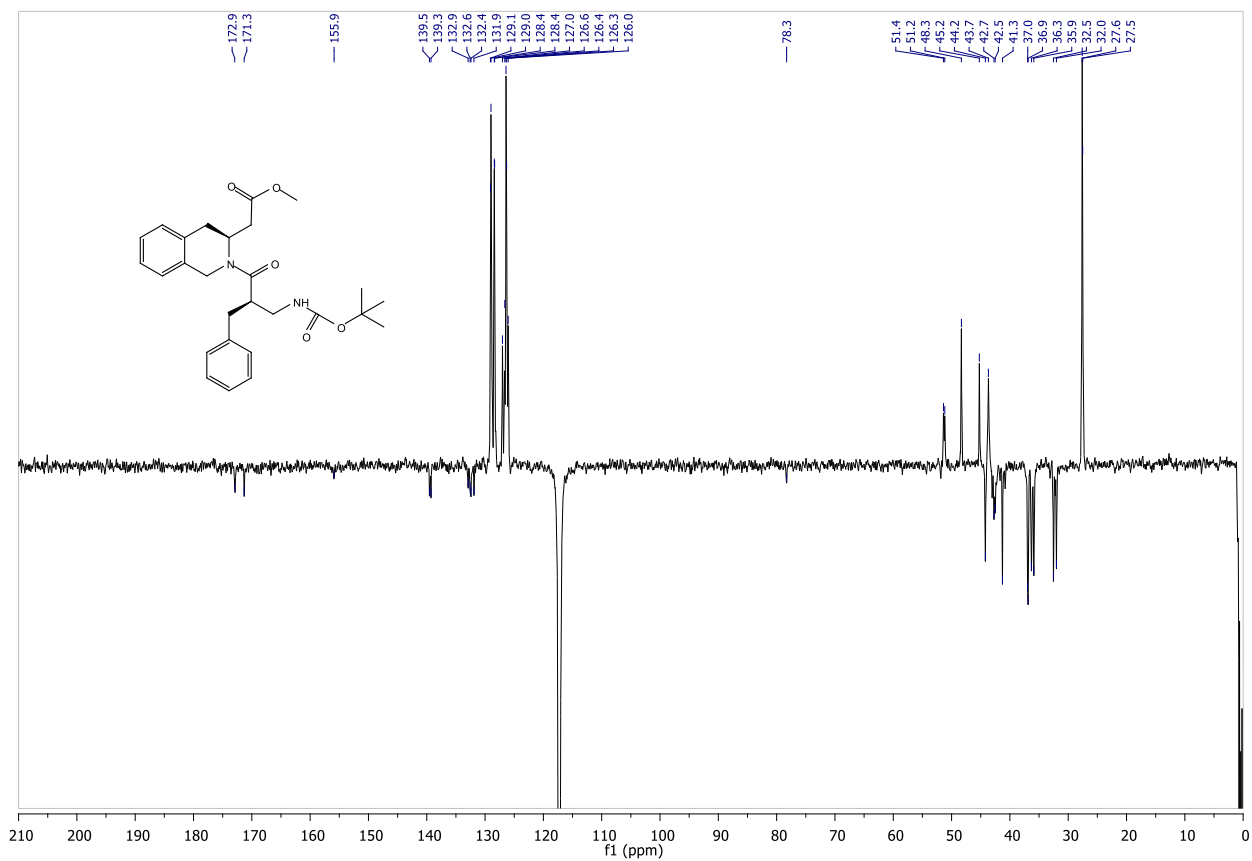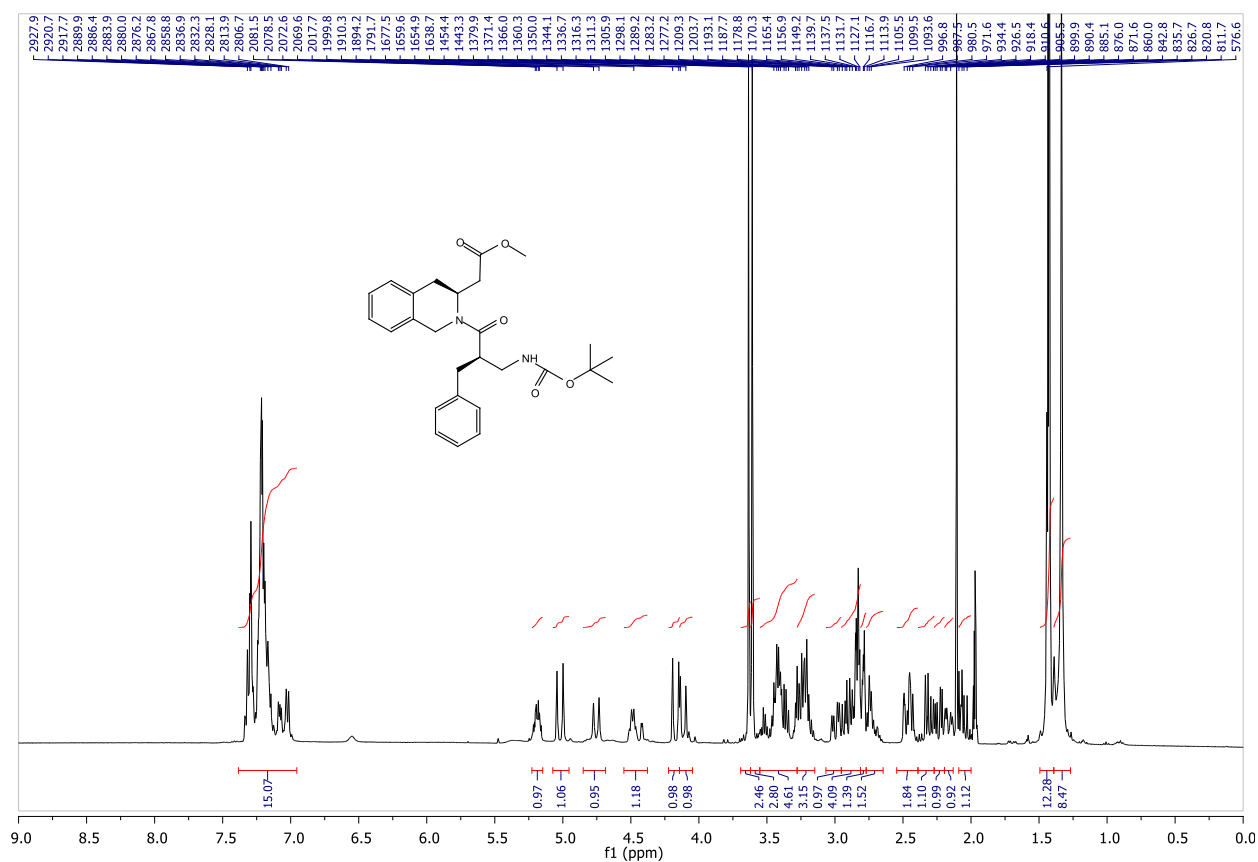
¹H and ¹³C NMR of compound **31b**
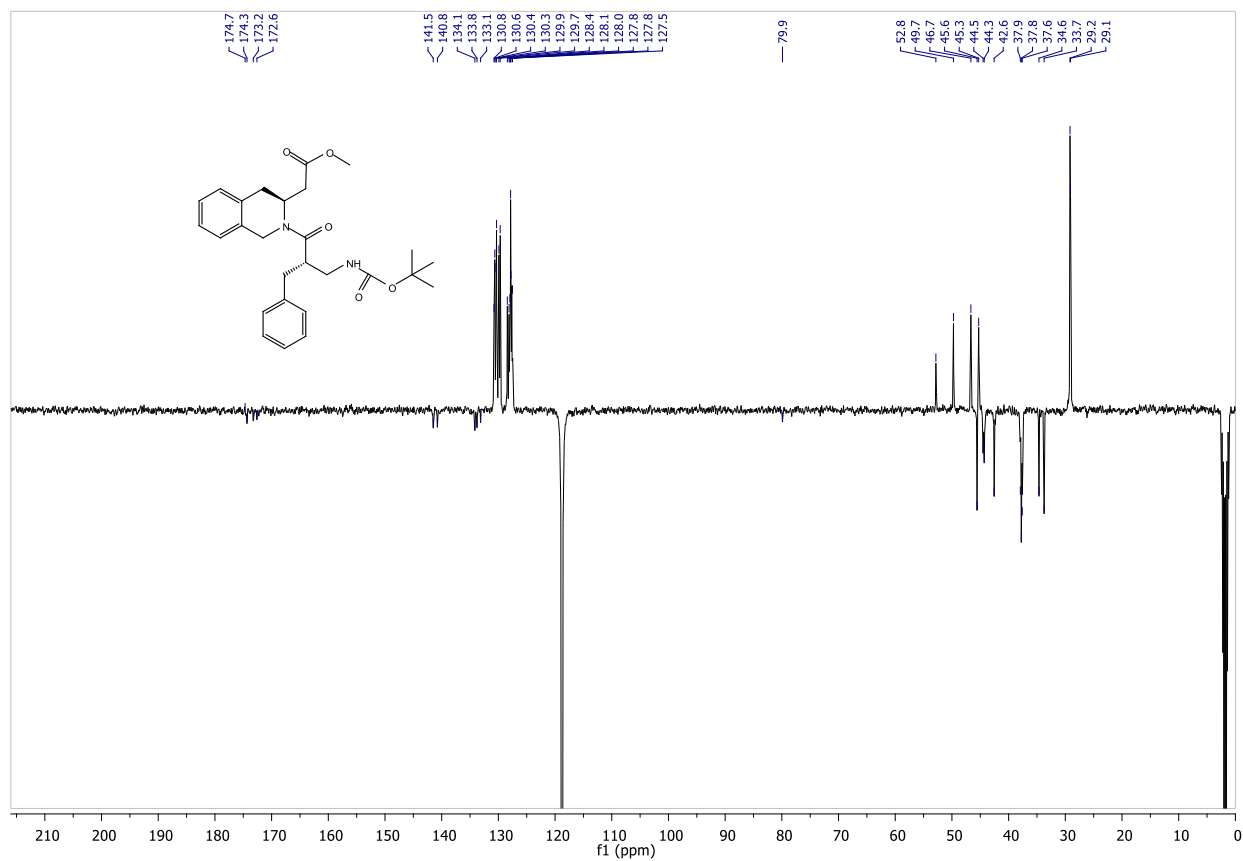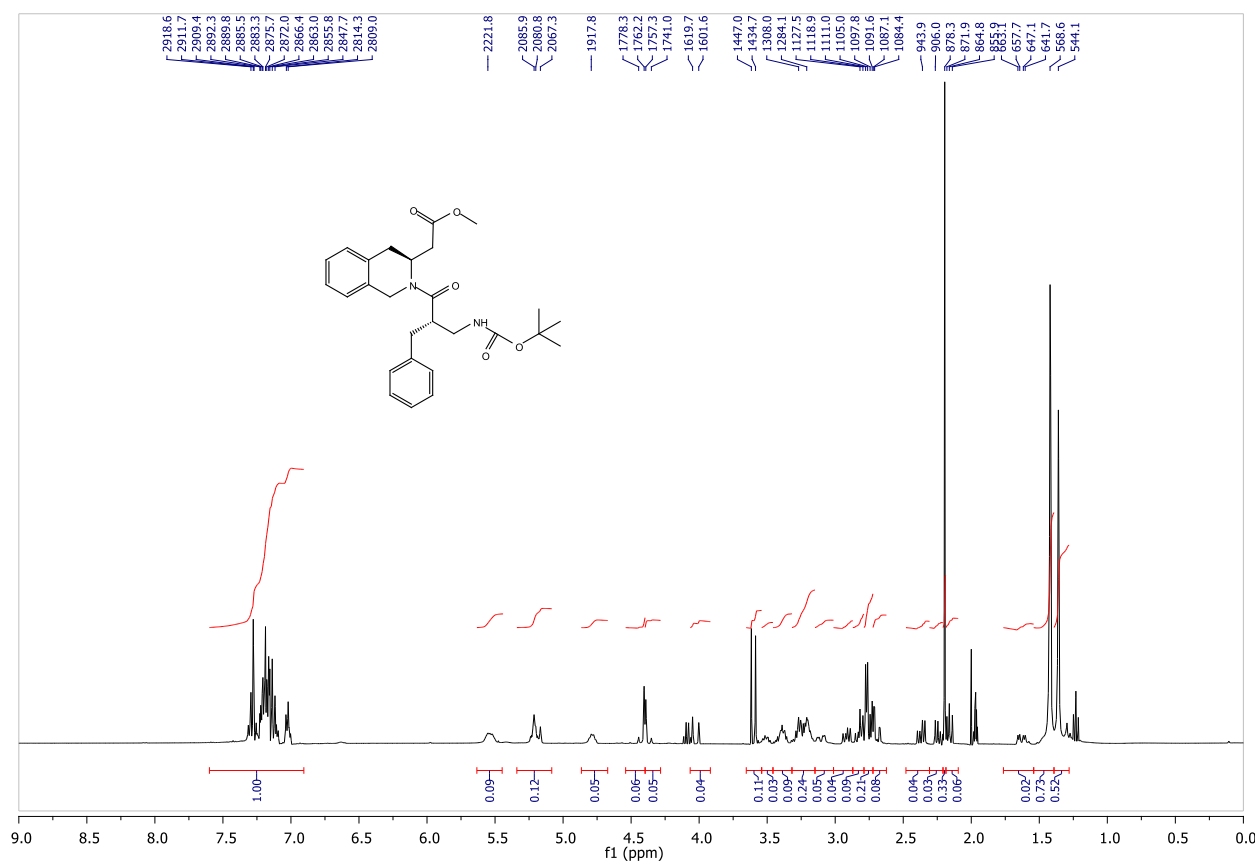
Synthesis of 32:
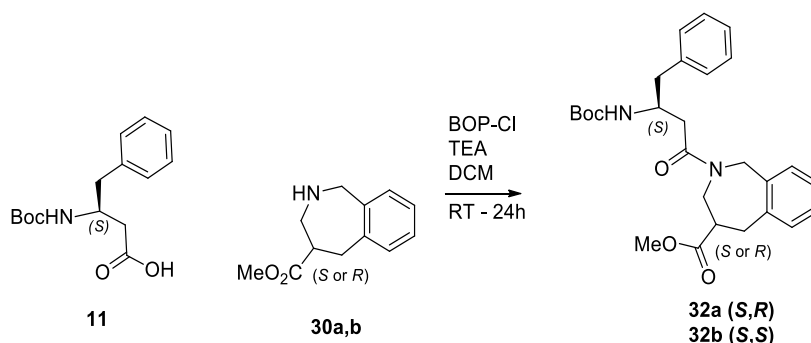
(*R*)-methyl 2-((*S*)-3-(tert-butoxycarbonylamino)-4-phenylbutanoyl)-2,3,4,5-tetrahydro-1H-benzo[c]azepine-4-carboxylate (32a)
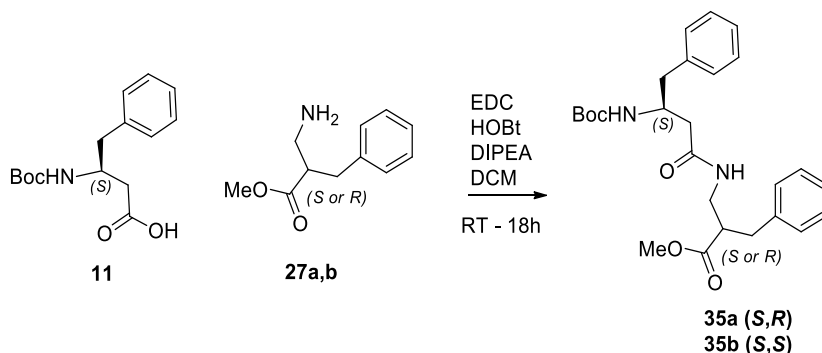
Following the general procedure **B** for peptide coupling. Acid **11** (88 mg, 0.31 mmol), amine **30a** (64 mg, 0.31 mmol), Et₃N (120 μl, 0.86 mmol), BOP-Cl (120 mg, 0.47 mmol) and CH₂Cl₂ (3 ml) afforded after flash chromatography (Hex/AcOEt 6:4) a white solid (98 mg, 68%). The following data has been collected on a 1:1 rotamer mixture.

R*f* = 0.31 (Hex/AcOEt 6:4). $[\alpha]_D^{25}$ = -27.6 (*c* 0.5, CHCl₃). ¹H NMR (400 MHz, CDCl₃) δ 7.49 – 7.04 (m, 8H), 6.99 (d, 0.5H, *J* = 7.3 Hz), 6.87 (bs, 0.5H), 4.99 (d, 0.5H, *J* = 14.4 Hz), 4.64 (d, 0.5H, *J* = 14.0 Hz), 4.46 (d, 0.5H, *J* = 15.7 Hz), 4.35 (d, 0.5H, *J* = 15.7 Hz), 4.22 - 4.06 (m, 1H), 3.84 (d, 0.5H, *J* = 12.3 Hz), 3.75 (s, 1.5H), 3.66 (s, 1.5H), 3.64 – 3.38 (m, 1H), 3.30 – 3.09 (m, 2H), 3.07 – 2.92 (m, 1.5H), 2.91 - 2.73 (m, 2.5H), 2.70 (dd, 0.5H, *J* = 16.0, 4.6 Hz), 2.50 (dd, 0.5H, *J* = 16.4, 4.6 Hz), 2.41 – 2.24 (m, 1.5H), 1.43 (s, 4.5H), 1.41 (s, 4.5H). ¹³C NMR (101 MHz, CDCl₃) δ 173.3, 172.6, 171.1, 170.2, 155.5 (2C), 138.7, 138.6, 138.5, 137.9, 137.4, 136.6, 130.8 (2C), 130.0 (2C), 129.8 (2C), 129.3 (2C), 129.1 (2C), 128.5 (2C), 127.9 (2C), 127.1 (2C), 126.4 (2C), 79.1 (2C), 53.1, 52.0 (2C), 51.6 (2C), 50.8, 49.5, 49.3, 43.5, 42.7, 40.0, 39.6, 37.0, 36.7, 35.3, 34.5, 28.4. HRMS (ESI) calcd. for [C₂₇H₃₄N₂O₅]⁺: 466.2468, found 467.2457. (MH⁺)

(*S*)-methyl 2-((*S*)-3-(tert-butoxycarbonylamino)-4-phenylbutanoyl)-2,3,4,5-tetrahydro-1H-benzo[c]azepine-4-carboxylate (32b)

Following the general procedure **B** for peptide coupling. Acid **11** (68 mg, 0.24 mmol), amine **30b** (50 mg, 0.24 mmol), Et₃N (75 μl, 0.54 mmol), BOP-Cl (93 mg, 0.37 mmol) and CH₂Cl₂ (3 ml) afforded after flash chromatography (Hex/AcOEt 7:3) a white solid (49 mg, 45%). The following data has been collected on a 1:1 rotamer mixture.

Rf = 0.32 (Hex/AcOEt 7:3). [α]$_D^{25}$ = 23.1 (*c* 0.5, CHCl$_3$). ^{1}H NMR (400 MHz, CDCl$_3$) δ 7.34 – 7.02 (m, 9H), 5.04 - 4.88 (m, 0.5H), 4.79 – 4.59 (m, 0.5H), 4.52 – 4.25 (m, 1H), 4.25 – 4.05 (m, 1.5H), 3.75 (s, 1.5H), 3.68 (s, 1.5H), 3.37 – 3.10 (m, 2.5H), 3.10 – 2.92 (m, 1.5H), 2.92 – 2.54 (m, 3H), 2.54 – 2.15 (m, 2.5H), 1.42 (s, 4.5H), 1.38 (s, 4.5H). ^{13}C NMR (101 MHz, CDCl$_3$) δ 173.8, 173.6, 172.8, 170.9, 155.6, 155.5, 138.7, 138.6, 137.9, 137.6, 137.3, 136.8, 130.9, 130.2, 130.1, 129.9, 129.5, 129.4, 128.9, 128.7, 128.4, 128.0, 127.9, 127.3, 126.9, 126.5, 79.3, 54.5, 53.4, 52.2, 52.0, 51.7, 51.1, 49.8, 44.3, 43.2, 43.1, 40.6, 40.4, 37.5, 36.6, 36.5, 28.5. HRMS (ESI) calcd. for [C$_{27}$H$_{34}$N$_2$O$_5$]$^+$: 466.2468, found 467.2444. (MH$^+$)

^{1}H and ^{13}C NMR of compound **32b**
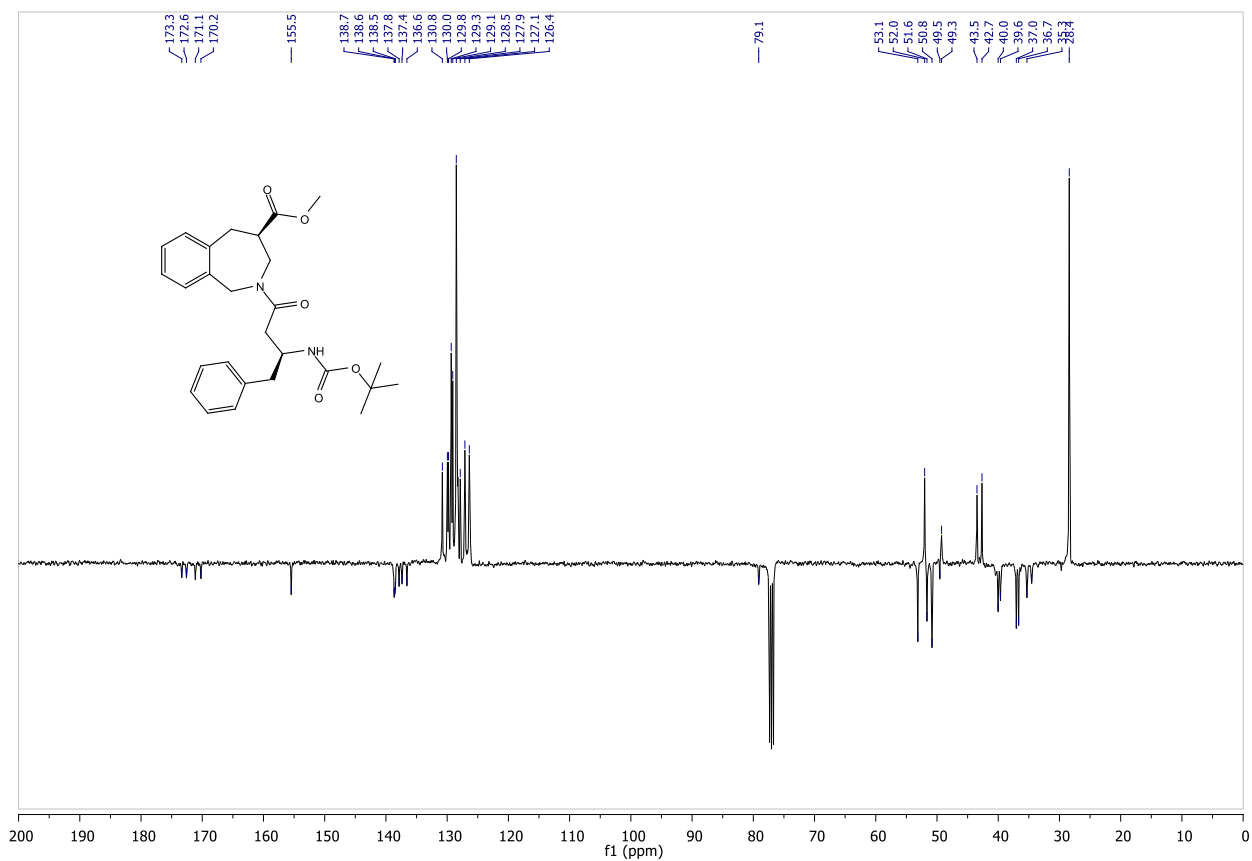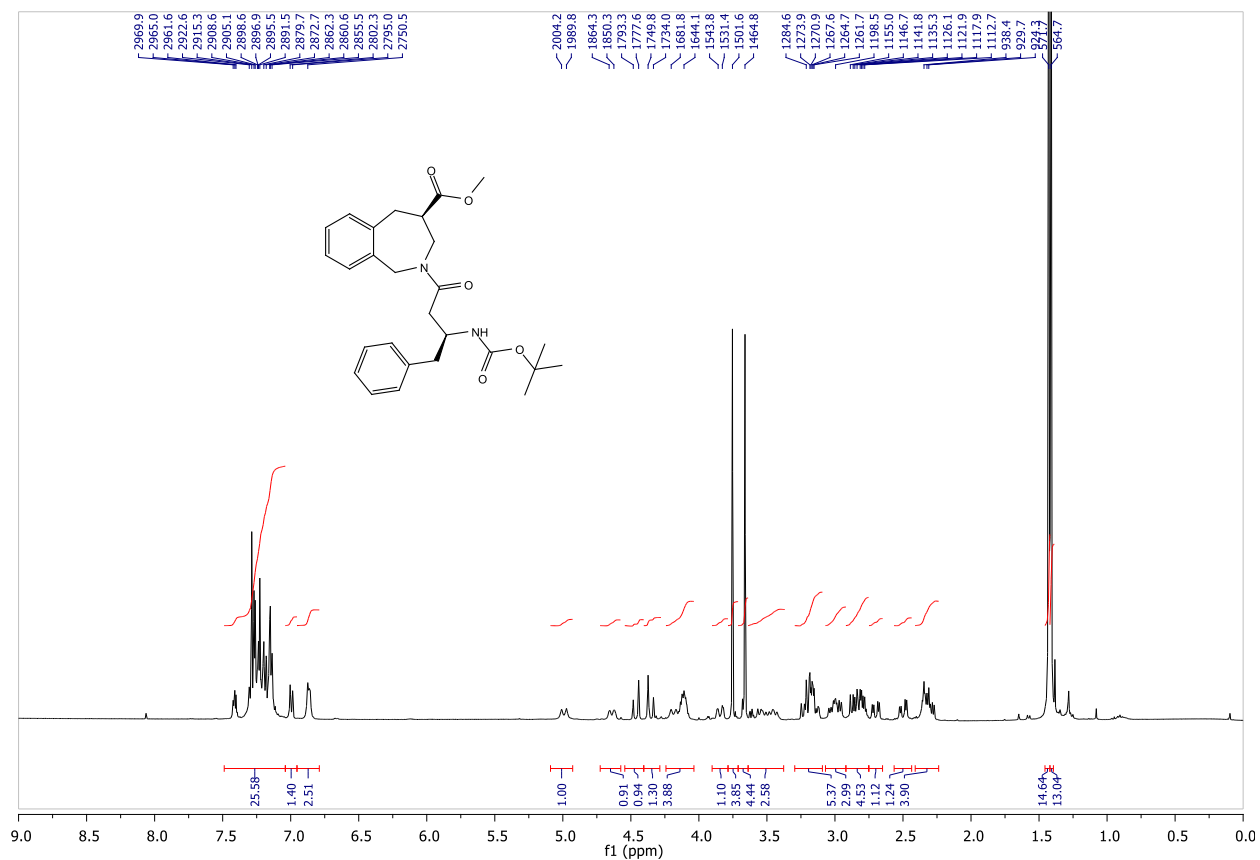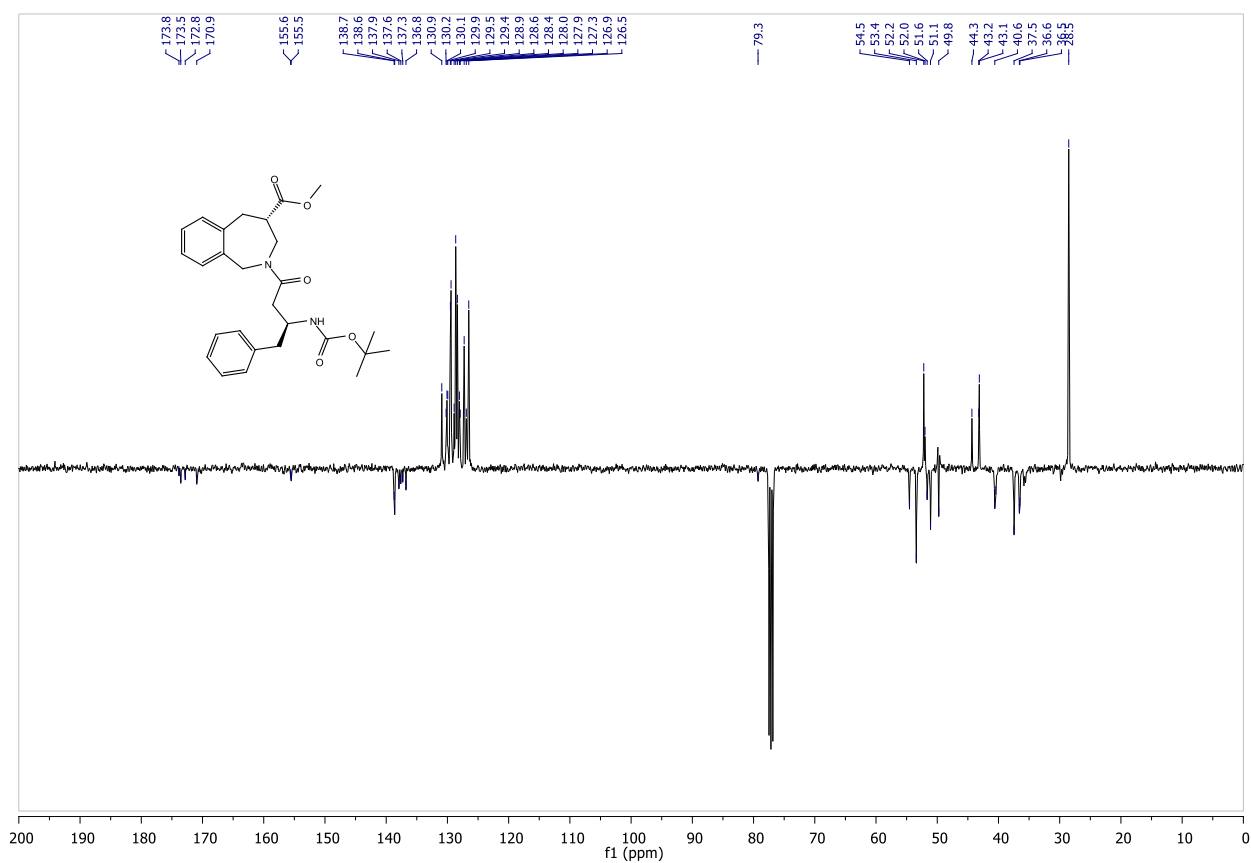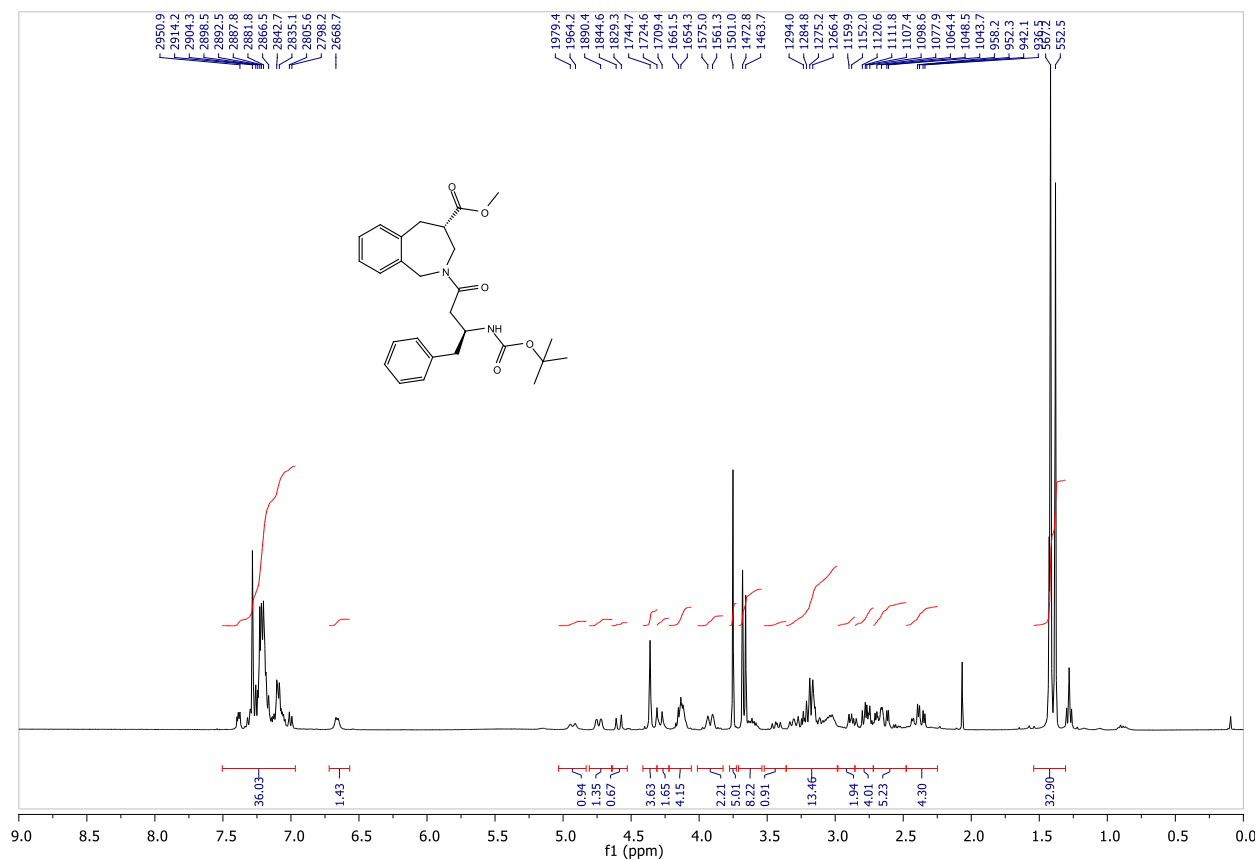
Synthesis of 33:
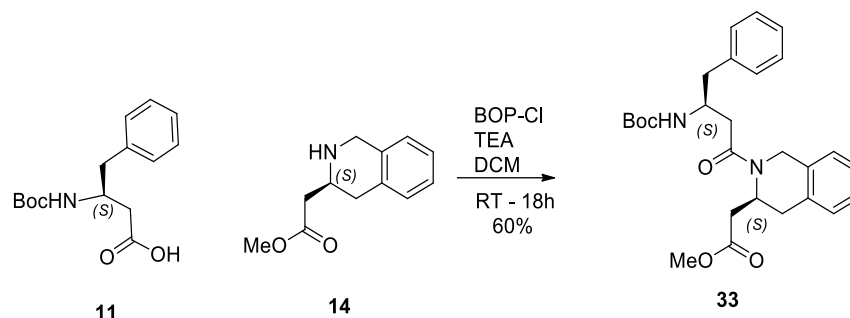
Methyl 2-((*S*)-2-((*S*)-3-(tert-butoxycarbonylamino)-4-phenylbutanoyl)-1,2,3,4-tetrahydroisoquinolin-3-yl) acetate (33).

Following the general procedure **B** for peptide coupling. Acid **11** (58 mg, 0.21 mmol), amine **14** (44 mg, 0.21 mmol), Et₃N (70 µl, 0.47 mmol), BOP-Cl (82 mg, 0.32 mmol) and CH₂Cl₂ (2 ml) afforded after flash chromatography (Hex/AcOEt 7:3) a white solid (59 mg, 60%). The following data has been collected on a 1:1 rotamer mixture.

R*f* = 0.29 (Hex/AcOEt 7:3). $[\alpha]_D^{25}$ = +7.8 (*c* 0.45, CHCl₃). ¹H NMR (400 MHz, CD₃CN) δ 7.51 – 7.08 (m, 9H), 5.57 (t, 1H, *J* = 9.9 Hz), 5.21 (d, 1H, *J* = 18.1 Hz), 4.74 (q, 0.5H, *J* = 5.7 Hz), 4.66 (d, 0.5H, *J* = 16.3 Hz), 4.46 (d, 0.5H, *J* = 16.3 Hz), 4.20 – 4.03 (m, 1H), 3.62 (s, 1.5H), 3.61 (s, 1.5H), 3.15 (dd, 0.5H, *J* = 16.4, 5.5 Hz), 3.04 (dd, 0.5H, *J* = 16.0, 5.6 Hz), 2.93 – 2.85 (m, 1.5H), 2.84 – 2.71 (m, 1.5H), 2.66 – 2.49 (m, 2H), 2.42 (dt, 1H, *J* = 10.6, 3.6 Hz), 2.27 (dd, 0.5H, *J* = 14.7, 8.0 Hz), 1.35 (s, 4.5H), 1.32 (s, 4.5H). ¹³C NMR (101 MHz, CD₃CN) δ 172.9, 172.6, 140.8, 136.7, 135.6, 135.5, 134.5, 133.9, 133.2, 130.8 (2C), 130.6 (2C), 129.8 (2C), 128.6 (2C), 128.1 (2C), 128.0 (2C), 127.9 (2C), 127.7 (2C), 127.6 (2C), 79.7 (2C), 52.8 (2C), 51.4, 51.25, 49.8, 46.5, 45.8, 41.9, 41.7, 39.0, 38.6, 37.8 (2C), 34.7, 33.7, 29.1. HRMS (ESI) calcd. for [C₂₇H₃₄N₂O₅]⁺: 466.2468, found 467.2481. (MH⁺)
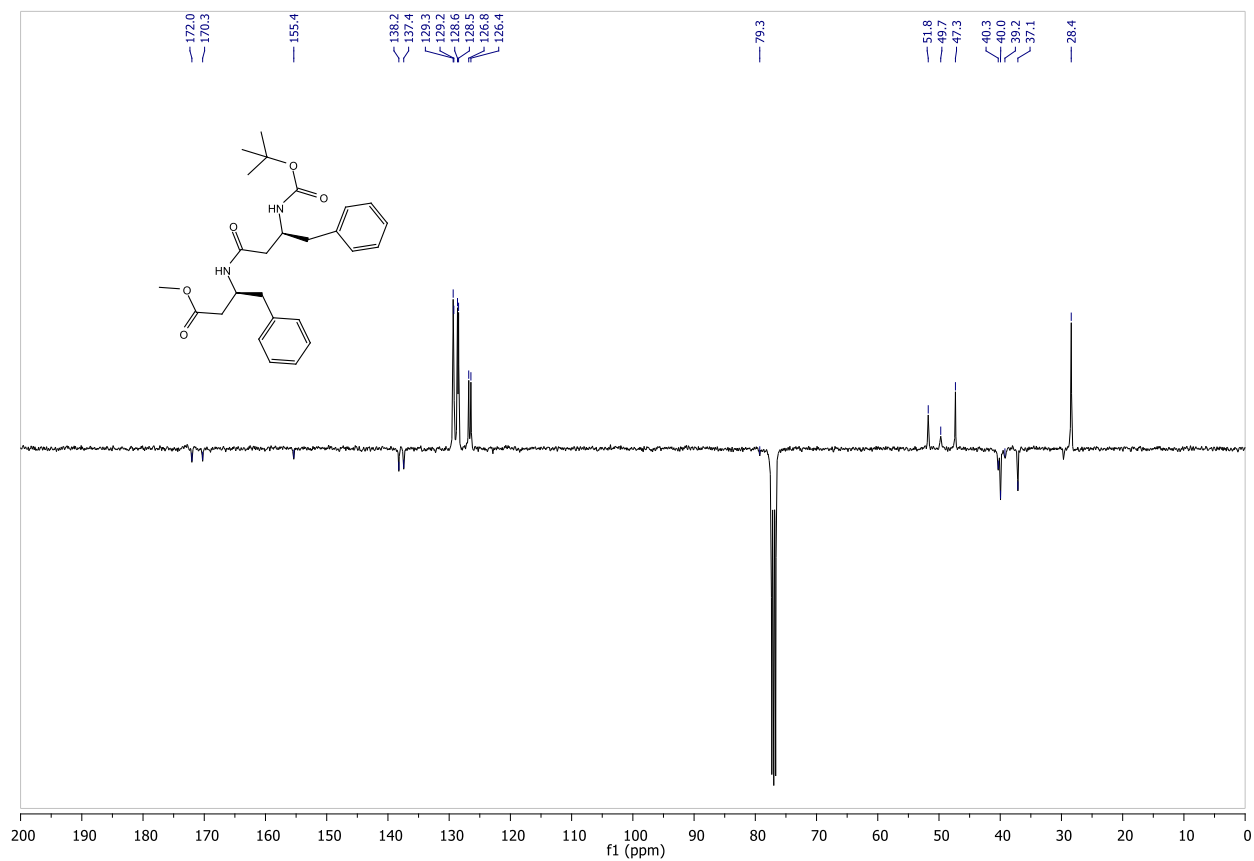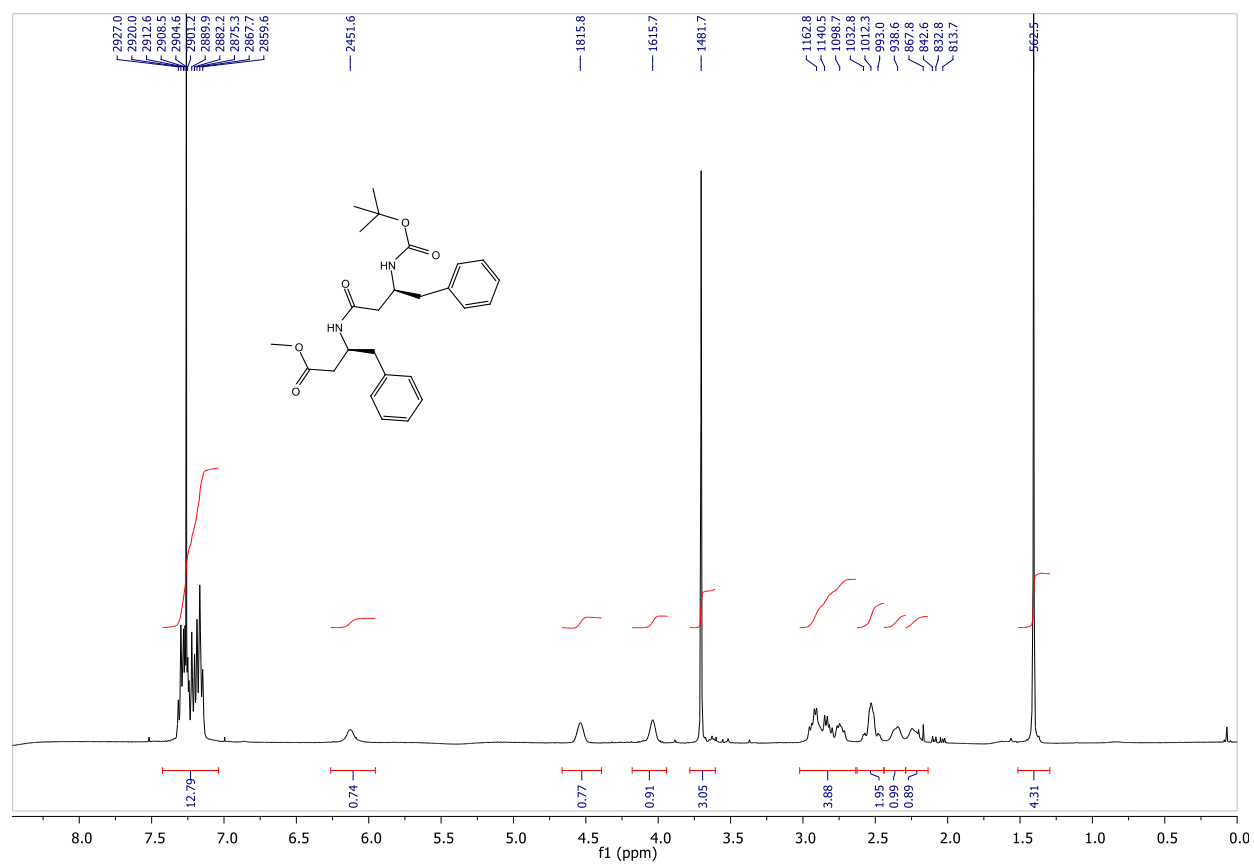
Synthesis of 34:

(S)-methyl-3-((R)-2-benzyl-3-(tert-butoxycarbonylamino)propanamido)-4-Phenyl butanoate (34a).

Following the general procedure **B** for peptide coupling. Acid **26a** (124 mg, 0.44 mmol), amine **11** (86 mg, 0.44 mmol), TEA (136 μl, 0.98 mmol), BOP-Cl (170 mg, 0.67 mmol) and CH₂Cl₂ (2.2 ml) afforded after flash chromatography (Hex/AcOEt 7:3) a foam (149 mg, 75%).

$[\alpha]_D^{25}$ = -24,2 (*c* 0.5, CHCl₃). ¹H NMR (400 MHz, CDCl₃) δ 7.36 - 7.08 (m, 10H), 5.98 (d, 1H, *J* = 9.0 Hz), 4.82 (bs, 1H), 4.45 - 4.35 (m, 1H), 3.65 (s, 3H), 3.55 - 3.45 (m, 1H), 3.4 - 3.3 (m, 1H), 3.25 - 3.15 (m, 1H), 2.85 - 2.7 (m, 3H), 2.64 - 2.5 (m, 1H), 2.29 (dd, 1H, *J* = 16.5, 4.3 Hz), 2.15 - 2.05 (m, 1H), 1.45 (s, 9H). ¹³C NMR (101 MHz, CDCl₃) δ 172.6, 171.9, 156.0, 139, 137.6, 129.1, 128.9, 128.5, 128.4, 126.7, 126.4, 79.3, 51.5, 49.7, 46.7, 42.7, 39.8, 36.7, 36.6, 28.4. HRMS (ESI) calcd. for [C₂₆H₃₄N₂O₅]⁺: 454.2468, found 455.2454. (MH⁺)

(S)-methyl-3-((S)-2-benzyl-3-(tert-butoxycarbonylamino)propanamido)-4-Phenyl butanoate (34b).

Following the general procedure **B** for peptide coupling. Acid **26b** (82 mg, 0.30 mmol), amine **11** (57 mg, 0.30 mmol), TEA (90 μl, 0.64 mmol), BOP-Cl (112 mg, 0.44 mmol) and CH₂Cl₂ (1.5 ml) afforded after flash chromatography (Hex/AcOEt 7:3) a foam (101 mg, 75%).

$[\alpha]_D^{25}$ = +11,6 (*c* 1.0, CHCl₃). ¹H NMR (400 MHz, CDCl₃) δ 7.35-6.97 (m, 9H), 6.95 (d, 1H, *J* = 6.0 Hz), 5.83 (d, 1H, *J* = 8.4 Hz), 5.07 (bs, 1H), 4.50 - 4.40 (m, 1H), 3.67 (s, 3H), 3.48 (dd, 1H, *J* = 14.3, 8.7 Hz), 3.4 - 3.2 (m, 2H), 2.85 (dd, 1H, *J* = 13.4, 9.8 Hz), 2.78 - 2.68 (m, 2H) 2.65 - 2.55 (m, 1H), 2.50 (dd, 1H, *J* = 13.6, 8.0 Hz), 2.44 (dd, 1H, *J* = 15.9 Hz, *J* = 5.1 Hz), 2.31 (dd, 1H, *J* = 15.9, 6.4 Hz), 1.45 (s, 9H). ¹³C NMR (101 MHz, CDCl₃) δ 172.8, 171.7, 156.0, 138.9, 137.1, 129.3, 128.9, 128.6, 126.7, 126.6, 79.3, 51.8, 49.7, 46.9, 42.9, 39.7, 37.0, 36.4, 28.4. HRMS (ESI) calcd. for [C₂₆H₃₄N₂O₅]⁺: 454.2468, found 455.2429. (MH⁺)

¹H and ¹³C NMR of compound **34a**

¹H and ¹³C NMR of compound 34b
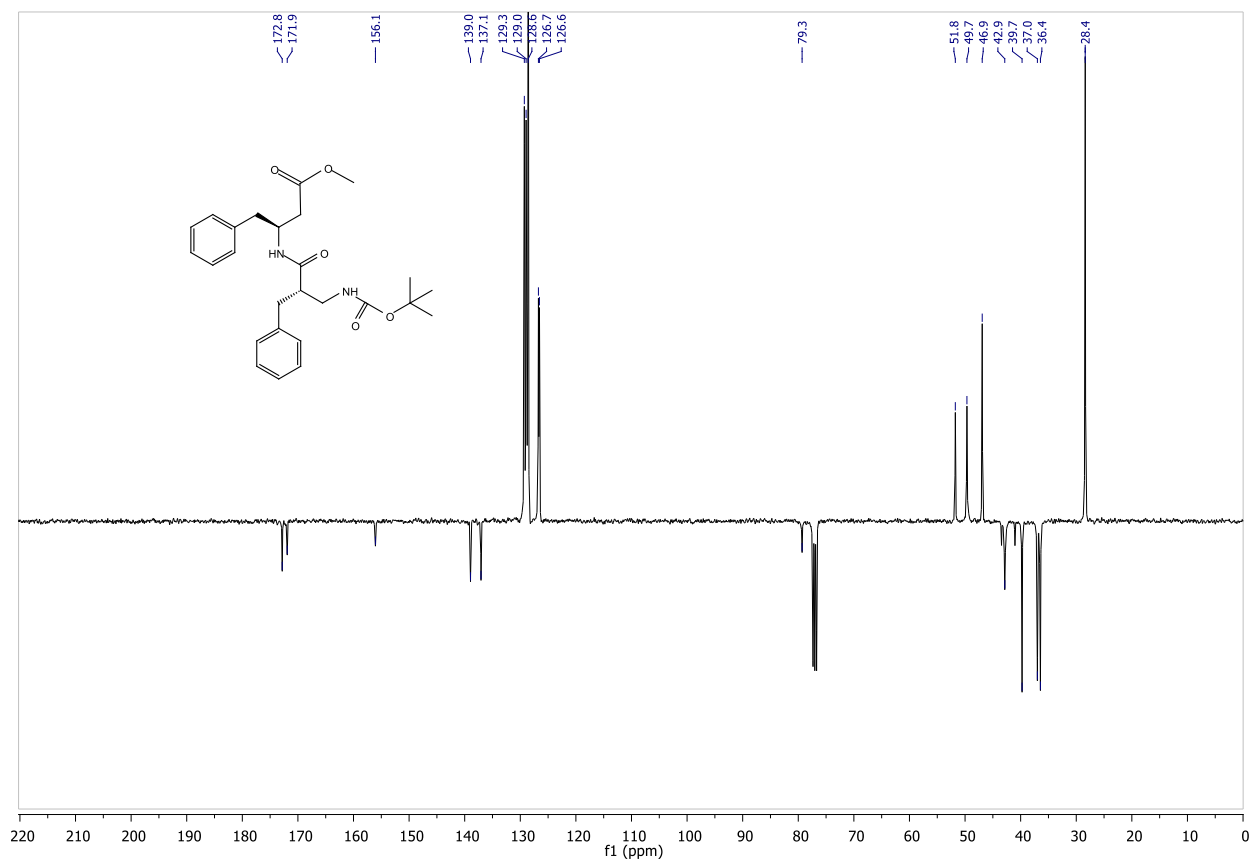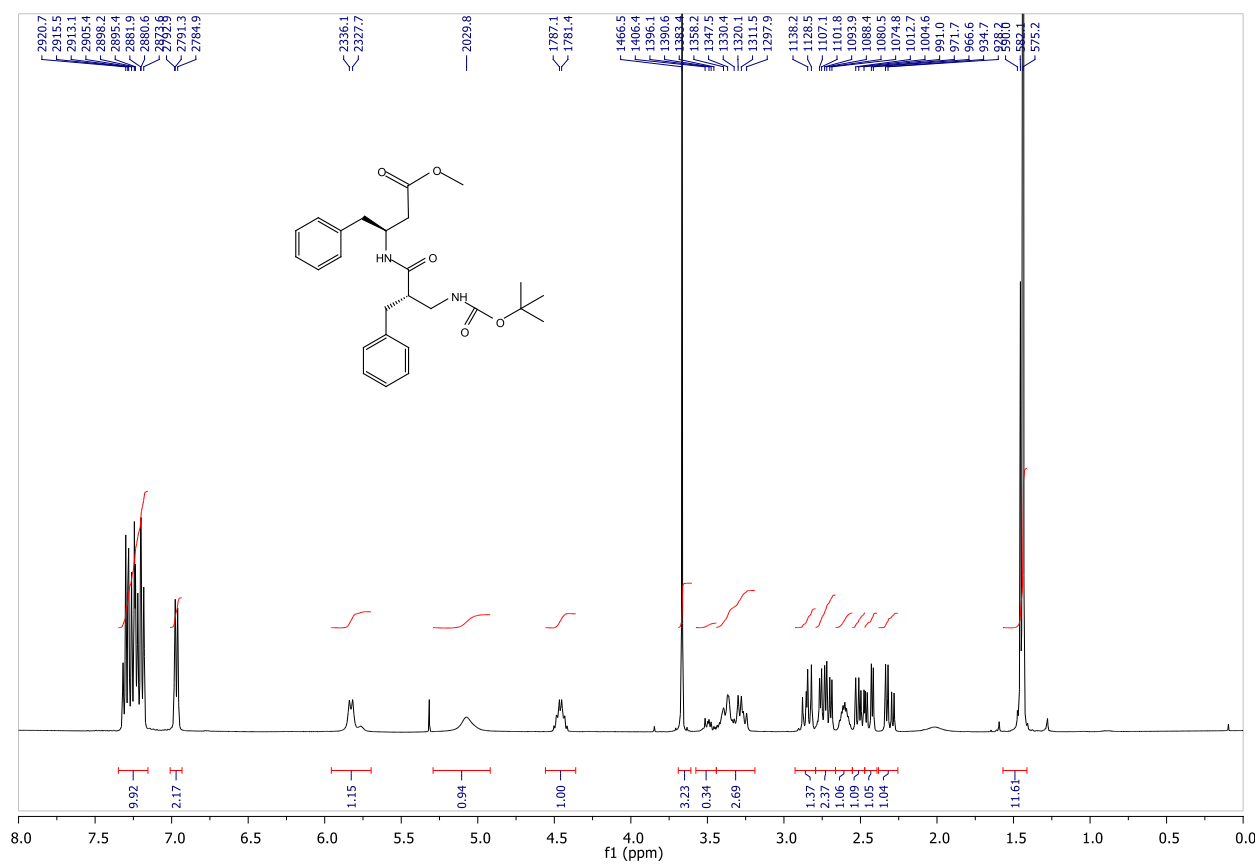
Synthesis of 35:

(R)-methyl 2-benzyl-3-((S)-3-(tert-butoxycarbonylamino)-4-phenylbutanamido) propanoate (35a)
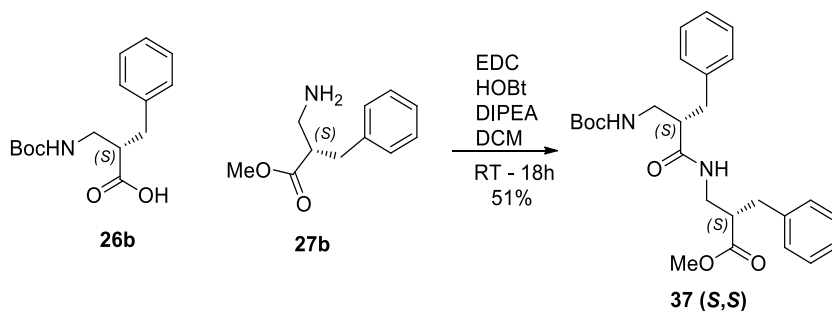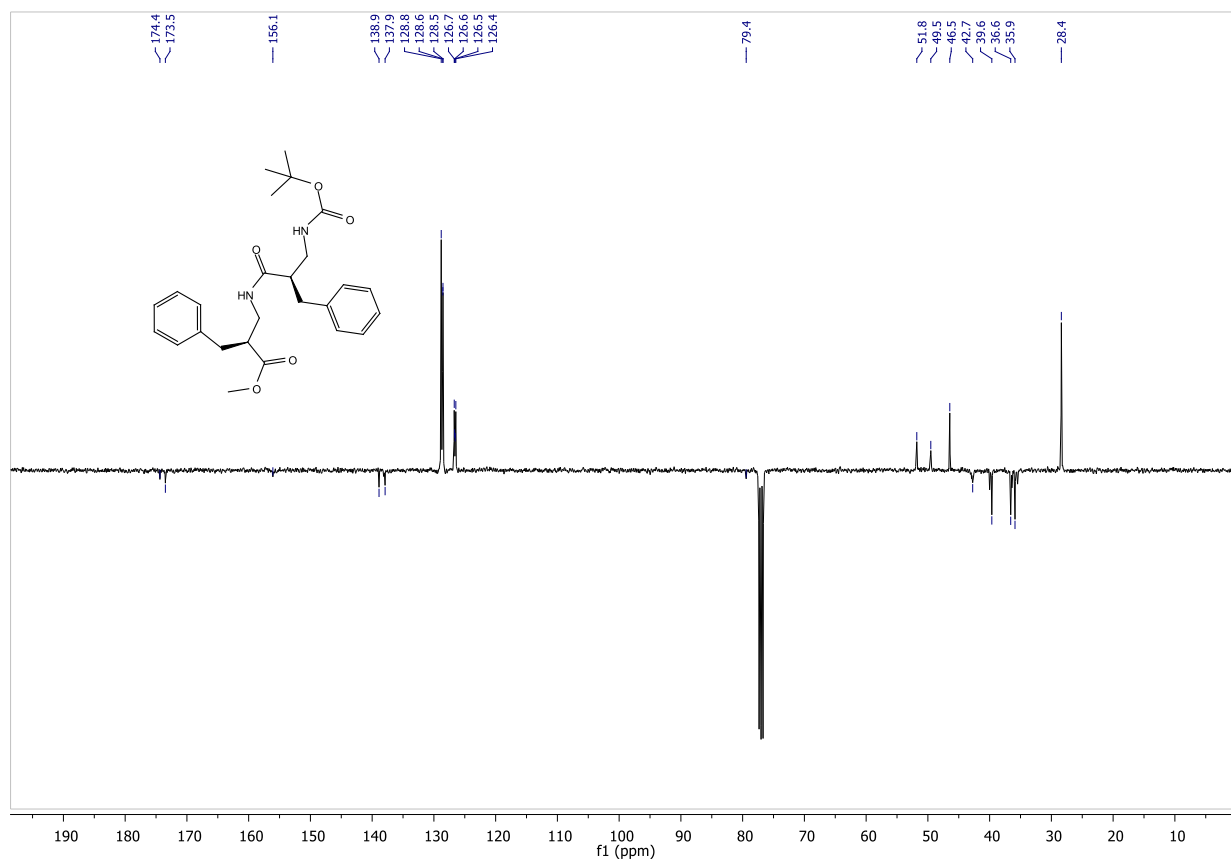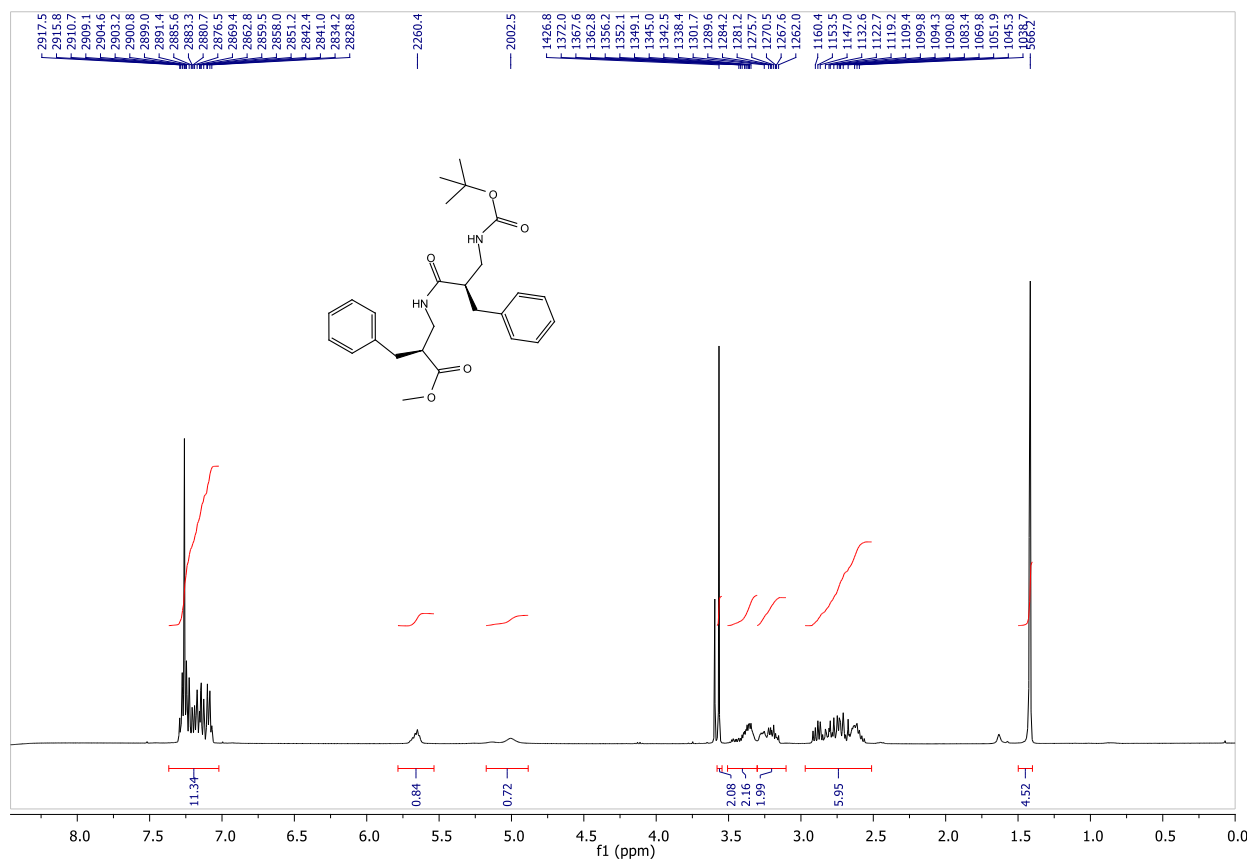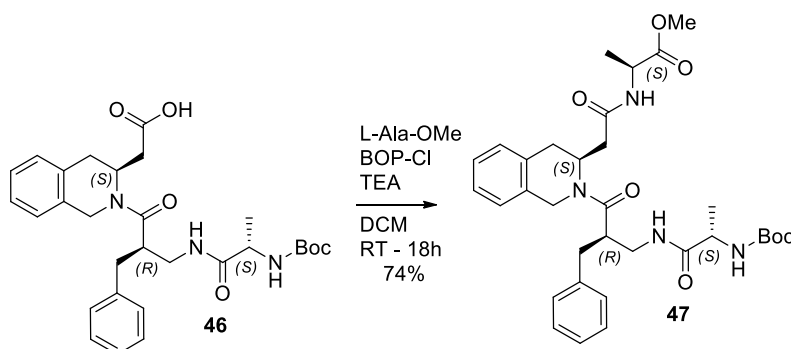
Following the general procedure **A** for peptide coupling. Acid **11** (67 mg, 0.24 mmol), amine **27a** (48 mg, 0.24 mmol), DIPEA (167 µl, 0.96 mmol), HOBt (39 mg, 0.29 mmol), EDC (55 mg, 0.29 mmol) and CH_2Cl_2 (2 ml) afforded after flash chromatography (Hex/AcOEt 6:4) a white solid (49 mg, 45%).

This compound appear as a mixture of conformers due to the Boc protecting group.

Rf = 0.26 (Hex/AcOEt 6:4). $[\alpha]_D^{25}$ = -21.3 (c 0.5, CHCl₃). ¹H NMR (400 MHz, CDCl₃) δ 7.36 – 7.25 (m, 5H), 7.25 – 7.11 (m, 5H), 6.12 (bs, 1H), 6.01 (bs, 1H), 4.09 – 4.00 (m, 2H), 3.65 (s, 3H), 3.64 – 3.47 (m, 3H), 3.35 (ddd, 1H, J = 13.5, 7.3, 6.1 Hz), 3.02 – 2.91 (m, 6H), 2.88 – 2.71 (m, 4H), 2.46 (dd, 1H, J = 15.1, 4.9 Hz), 2.42 – 2.29 (m, 2H), 2.23 (dd, 1H, J = 15.1, 5.7 Hz), 1.41 (s, 9H), 1.40 (s, 9H). ¹³C NMR (101 MHz, CDCl₃) δ 174.6, 171.1, 155.5, 138.2, 138.0, 129.3 (3C), 128.9 (2C), 128.6 (2C), 128.5 (2C), 126.7, 126.6, 126.5, 79.4, 51.9, 49.6, 46.8, 40.5, 40.2, 38.9, 36.1, 28.4. HRMS (ESI) calcd. for $[C_{26}H_{34}N_2O_5]^+$: 454.2468, found 455.2451. (MH⁺)

(S)-methyl 2-benzyl-3-((S)-3-(tert-butoxycarbonylamino)-4-phenylbutanamido) propanoate (35b)

Following the general procedure **A** for peptide coupling. Acid **11** (73 mg, 0.26 mmol), amine **27b** (50 mg, 0.26 mmol), DIPEA (181 µl, 1.04 mmol), HOBt (42 mg, 0.31 mmol), EDC (60 mg, 0.31 mmol) and CH_2Cl_2 (3 ml) afforded after flash chromatography (Hex/AcOEt 1:1) a white solid (72 mg, 61%).

Rf = 0.25 (Hex/AcOEt 1:1). $[\alpha]_D^{25}$ = -10.0 (c 0.5, CHCl₃). ¹H NMR (400 MHz, CDCl₃) δ 7.45 – 7.10 (m, 10H), 5.95 (s, 1H), 4.19 – 3.94 (m, 1H), 3.67 (s, 3H), 3.60 – 3.49 (m, 1H), 3.46 – 3.32 (m, 1H), 3.08 – 2.91 (m, 3H), 2.91 – 2.75 (m, 2H), 2.39 (dd, 1H, J = 15.0, 4.9 Hz), 2.27

(dd, 1H, J = 15.0, 5.7 Hz), 1.42 (s, 9H). ^{13}C NMR (101 MHz, CDCl$_3$) δ 176.1, 172.5, 157.0, 139.7, 139.6, 130.9 (2C), 130.4 (2C), 130.1 (2C), 130.0 (2C), 128.3, 128.0, 80.8, 53.4, 51.2, 48.2, 41.9, 41.6, 40.7, 37.5, 29.9. HRMS (ESI) calcd. for [C$_{26}$H$_{34}$N$_2$O$_5$]$^+$: 454.2468, found 455.2497.

¹H and ¹³C NMR of compound **35a**
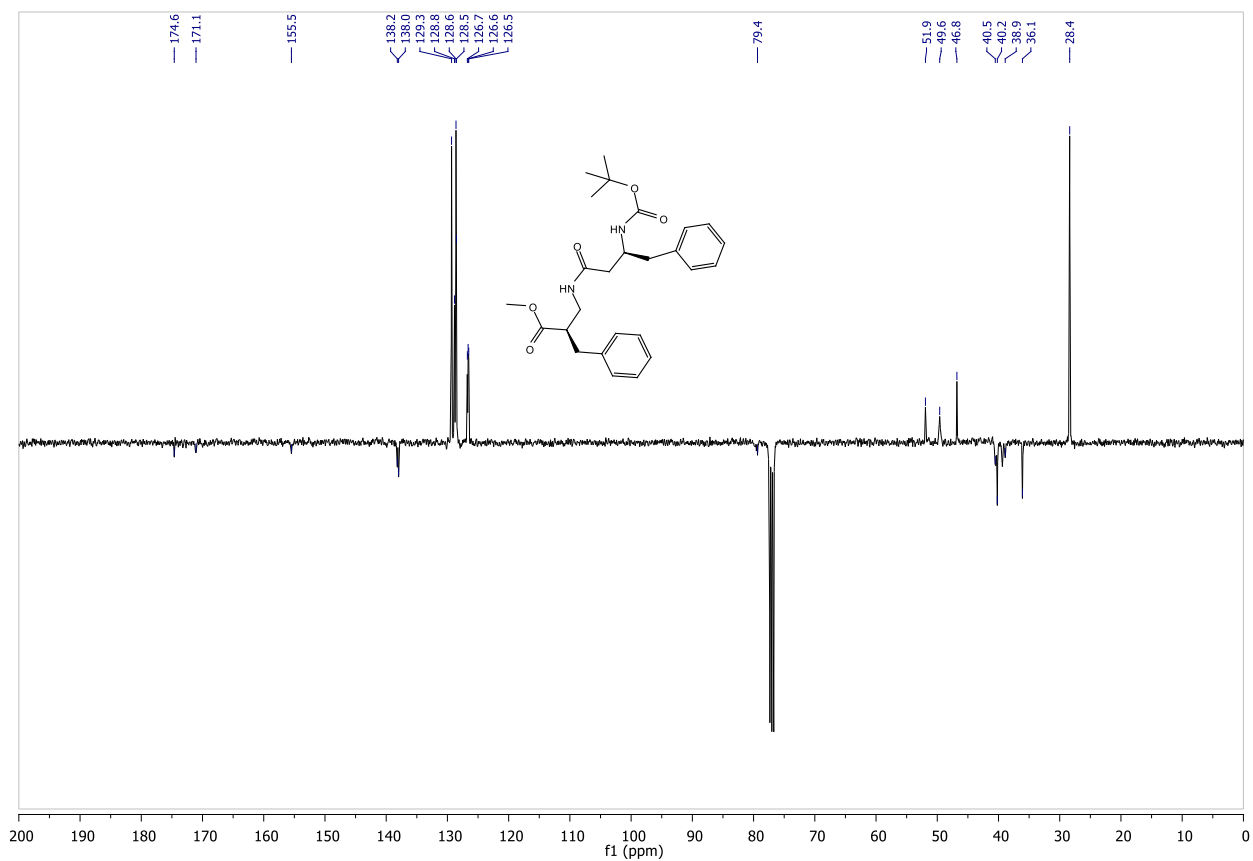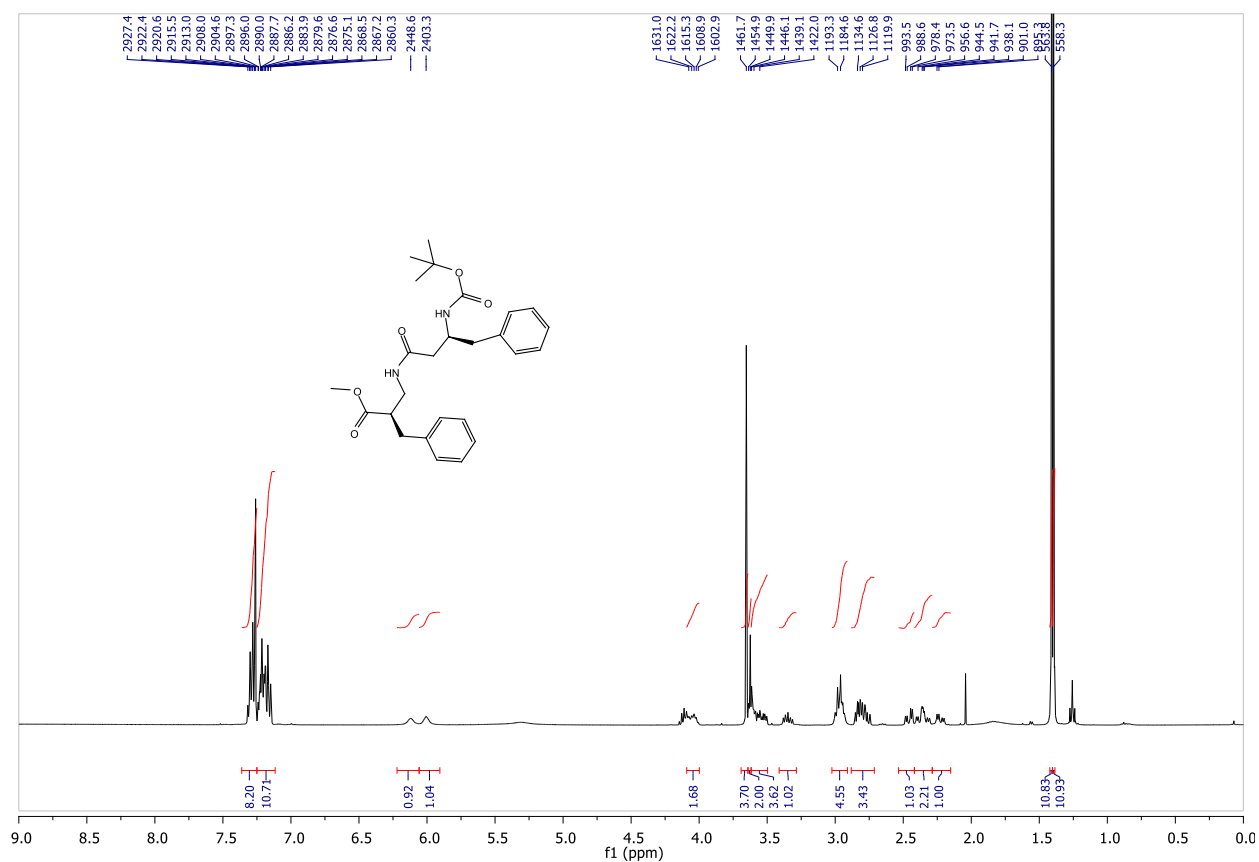
¹H and ¹³C NMR of compound **35b**
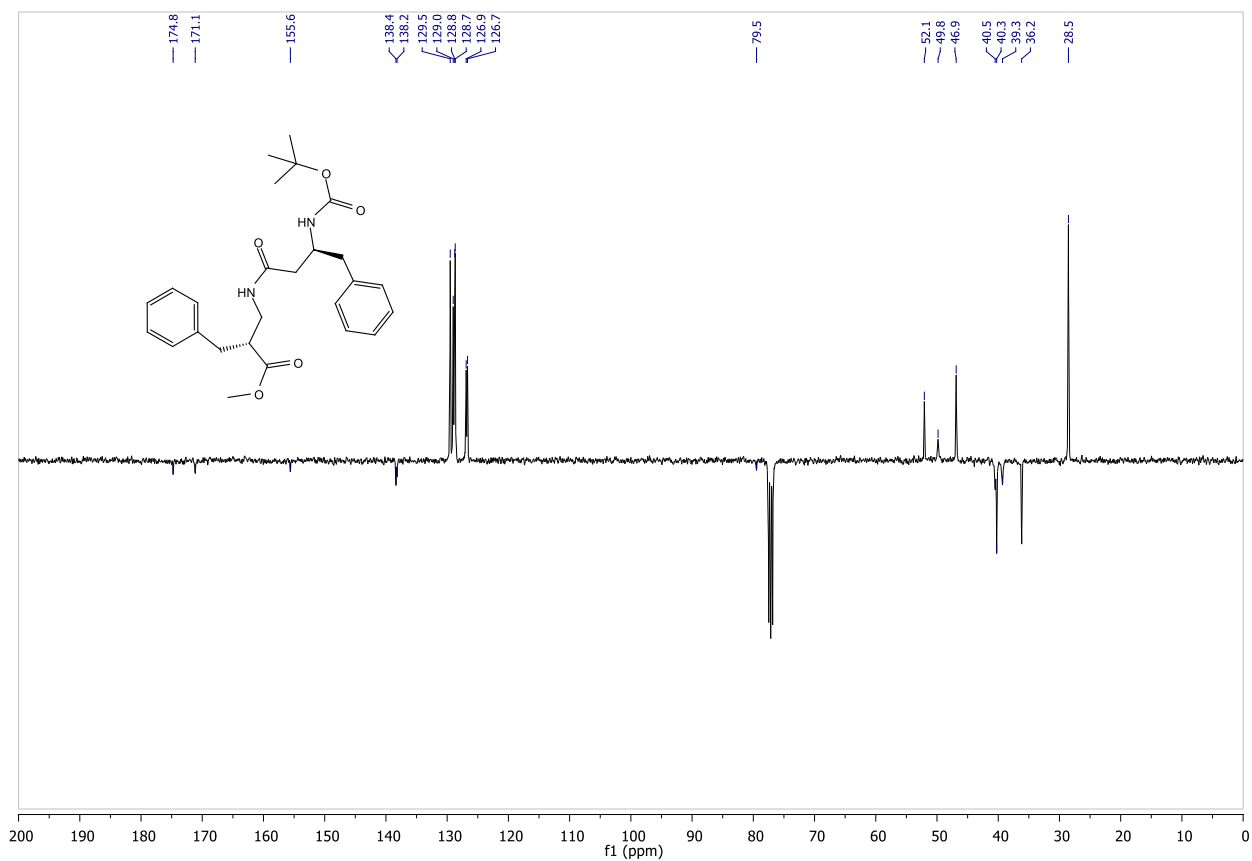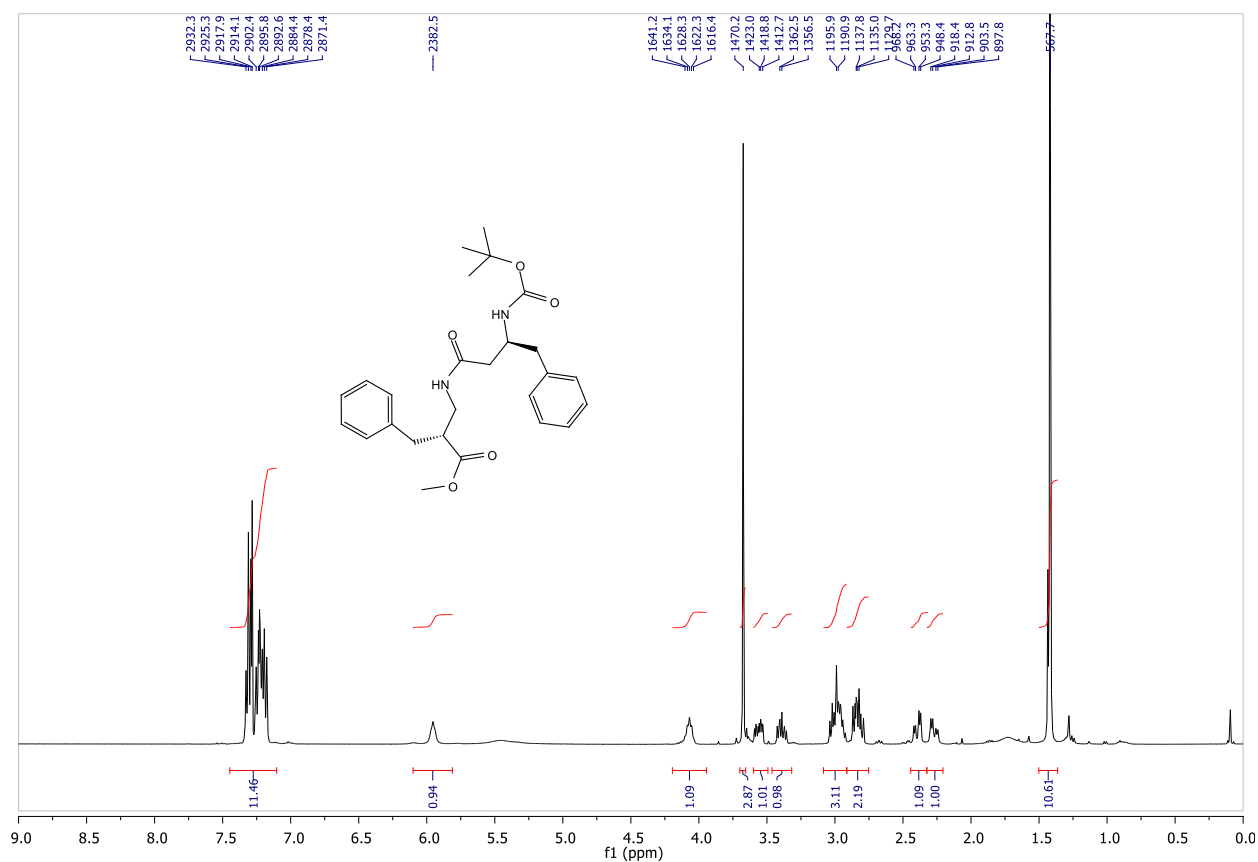
Synthesis of 36:
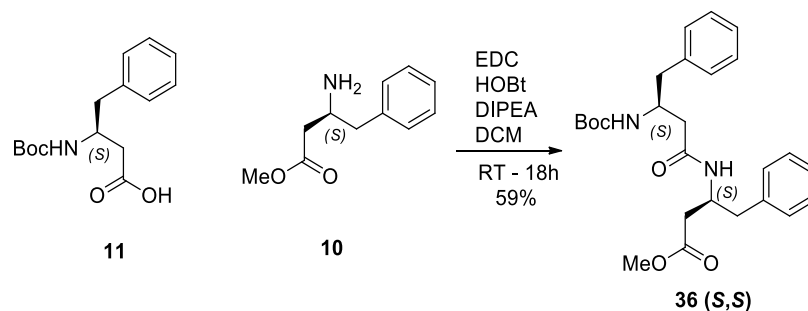
(S)-methyl   3-((S)-3-(tert-butoxycarbonylamino)-4-phenylbutanamido)-4-phenyl butanoate (36)

Following the general procedure **A** for peptide coupling. Acid **11** (66 mg, 0.25 mmol), amine **10** (48 mg, 0.25 mmol), DIPEA (174 µl, 1.0 mmol), HOBt (41 mg, 0.30 mmol), EDC (57 mg, 0.30 mmol)and CH_2Cl_2 (3 ml) afforded after flash chromatography (Hex/AcOEt 6:4) a white solid (65 mg, 59%).

Rf = 0.27 (Hex/AcOEt 6:4). $[\alpha]_D^{25}$ = -14.1 (*c* 0.5, CHCl$_3$). ^{1}H NMR (400 MHz, CDCl$_3$) δ 7.43 – 7.04 (m, 10H), 6.13 (bs, 1H), 4.54 (bs, 1H), 4.04 (bs, 1H), 3.70 (s, 3H), 3.02 – 2.64 (m, 4H), 2.63 – 2.44 (m, 2H), 2.43 – 2.29 (s, 1H), 2.29 – 2.16 (s, 1H), 1.41 (s, 9H). ^{13}C NMR (101 MHz, CDCl$_3$) δ 172.0, 170.3, 155.4, 138.2, 137.4, 129.4 (2C), 129.2 (2C), 128.6 (2C), 128.5 (2C), 126.8, 126.5, 79.3, 51.8, 49.7, 47.3, 40.3, 40.0, 39.2, 37.1, 28.4. HRMS (ESI) calcd. for $[C_{26}H_{34}N_2O_5]^+$: 454.2468, found 455.2489. (MH$^+$)

¹H and ¹³C NMR of compound **36**

Synthesis of 37:

(S)-methyl 2-benzyl-3-((S)-2-benzyl-3-((tert-butoxycarbonyl)amino)propanamido) propanoate (37)

Following the general procedure **A** for peptide coupling. Acid **26b** (67 mg, 0.24 mmol), amine **27b** (48 mg, 0.24 mmol), DIPEA (167 μl, 0.96 mmol), HOBt (39 mg, 0.29 mmol), EDC (55 mg, 0.29 mmol) and CH$_2$Cl$_2$ (2 ml) afforded after flash chromatography (Hex/AcOEt 6:4) a white solid (55 mg, 51%).

Rf = 0.33 (Hex/AcOEt 6:4). [α]$_D^{25}$ = +5.2 (*c* 0.5, CHCl$_3$). ^{1}H NMR (400 MHz, CDCl$_3$) δ 7.37 – 7.02 (m, 10H), 5.65 (bs, 1H), 5.01 (bs, 1H), 3.57 (s, 3H), 3.51 – 3.30 (m, 2H), 3.31 – 3.11 (m, 2H), 2.97 – 2.51 (m, 6H), 1.42 (s, 9H). ^{13}C NMR (101 MHz, CDCl$_3$) δ 174.8, 171.1, 155.6, 138.4, 138.2, 129.5, 129.0 (2C), 128.8 (2C), 128.7 (2C), 126.9, 126.7, 79.5, 52.1, 49.8, 46.9, 40.5, 40.3, 39.3, 36.2, 28.5. HRMS (ESI) calcd. for [C$_{26}$H$_{34}$N$_2$O$_5$]$^+$: 454.2468, found 455.2455. (MH$^+$)

^{1}H and ^{13}C NMR of compound **37**

Synthesis of 46:

(S)-methyl 2-(2-((S)-2-((R)-2-benzyl-3-((S)-2-(tert-butoxycarbonylamino)propanamido) propanoyl)-1,2,3,4-tetrahydroisoquinolin-3-yl)acetamido) propanoate (47)

Following the general procedure **B** for peptide coupling. Acid **46** (18 mg, 0.034 mmol), L-Alanine (5 mg, 0.034 mmol), TEA (16 µl, 0.11 mmol), BOP-Cl (13 mg, 0.05 mmol) and CH₂Cl₂ (1 ml) afforded after flash chromatography (Hex/AcOEt 1:1) a foam (15 mg, 74%). The following data has been collected on a complex conformer mixture.

Rf = 0.36 (Hex/AcOEt 1:1). $[\alpha]_D^{25}$ = +26.4 (*c* 1.0, CHCl₃). ¹H NMR (400 MHz, CD₃CN) δ 7.29 – 7.20 (2m, H), 7.20 – 7.04 (5m, H), 7.04 – 6.93 (2m, H), 6.85 (bs, 1H), 5.53 (bs, 1H), 5.43 (bs, 1H), 5.10 (ddd, 1H, *J* = 9.1, 5.5, 2.5 Hz), 4.97 (d, 1H, *J* = 17.9 Hz), 4.67 (d, 1H, *J* = 16.1 Hz), 4.45 – 4.37 (m, 1H), 4.10 (d, 1H, *J* = 17.9 Hz), 4.04 – 3.91 (m, 2H), 3.84 (t, 1H, *J* = 7.1 Hz), 3.58 (s, 3H), 3.54 (s, 3H), 3.45 – 3.17 (m, 6H), 2.94 (dd, 1H, *J* = 15.8, 5.6 Hz), 2.81 (m, 4H), 2.69 (dd, 1H, *J* = 16.0, 2.8 Hz), 2.47 – 2.33 (m, 2H), 2.30 – 2.14 (m, 2H), 2.04 (dd, 1H, *J* = 16.2, 5.4 Hz), 2.00 – 1.94 (m, 1H), 1.39 (s, 9H), 1.36 (s, 9H), 1.23 (d, 3H, *J* = 7.1 Hz), 1.06 (d, 3H, *J* = 7.1 Hz). ¹³C NMR (101 MHz, CD₃CN) δ 174.0, 173.7, 172.0, 170.4, 159.2, 140.5, 140.3, 134.0, 133.6, 133.4, 132.9, 130.1, 130.1, 129.9, 129.4, 129.4, 128.1, 127.6, 127.4, 127.3, 127.0, 52.4, 52.2, 51.4, 51.2, 49.3, 46.4, 45.2, 44.2, 44.0, 42.2, 42.1, 42.1, 37.8, 37.7, 37.2, 37.0, 33.6, 33.0, 28.6, 18.6 (2C). HRMS (ESI) calcd. for [C₃₃H₄₄N₄O₇]⁺: 608.3210, found 609.3243. (MH⁺)
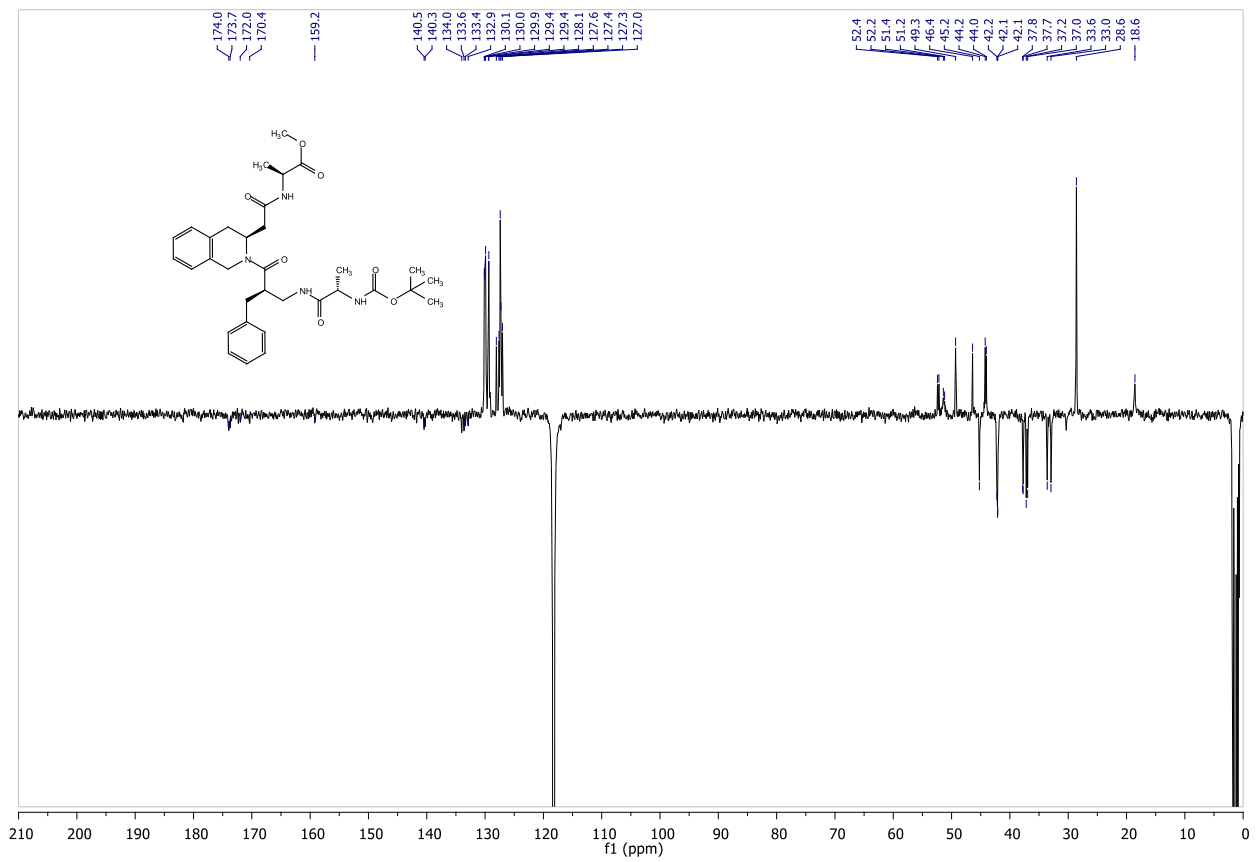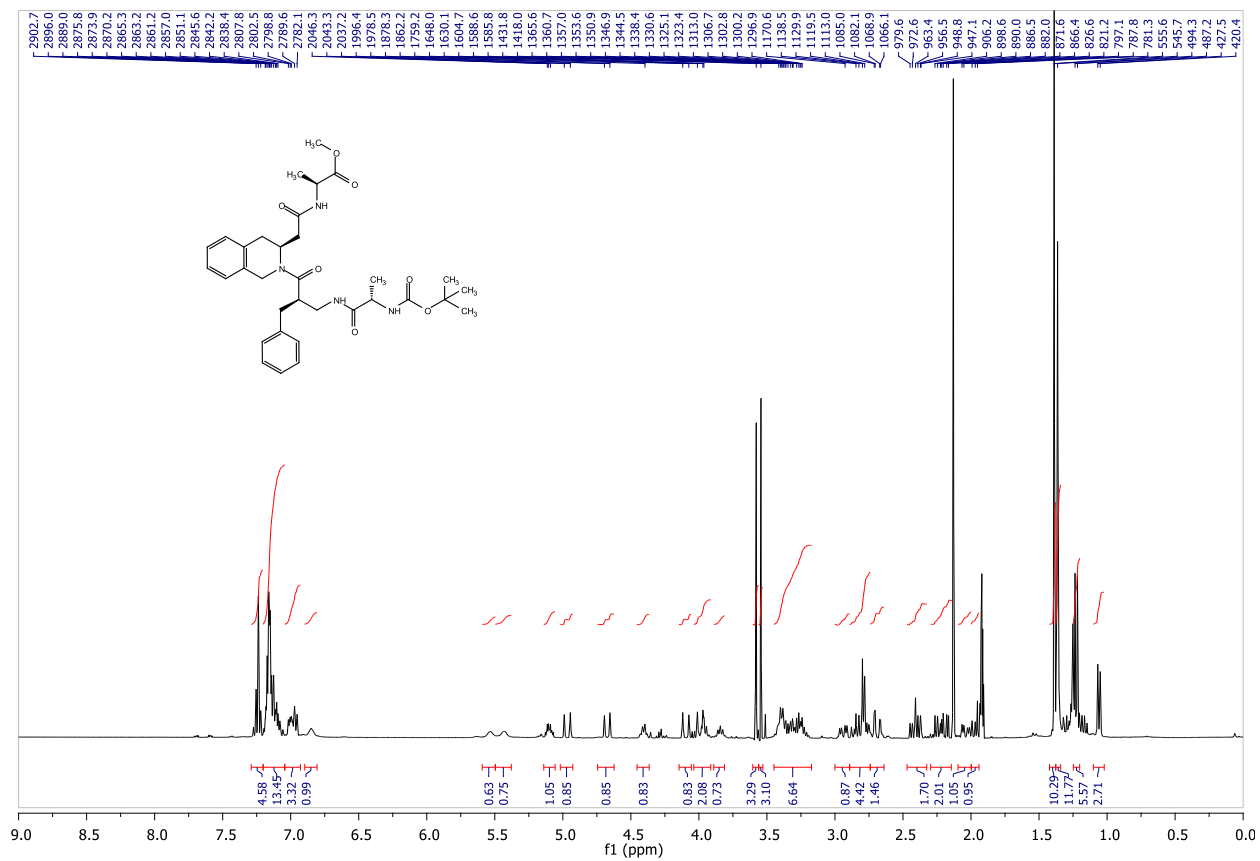
Synthesis of 43:
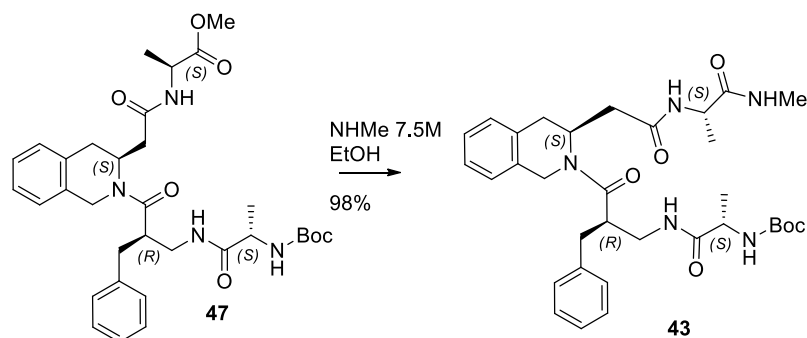
tert-butyl ((S)-1-(((R)-2-benzyl-3-((S)-3-(2-(((S)-1-(methylamino)-1-oxopropan-2-yl)amino)-2-oxoethyl)-3,4-dihydroisoquinolin-2(1H)-yl)-3-oxopropyl)amino)-1-oxopropan-2-yl)carbamate (43)

Compound **47** (8 mg, 0.013 mmol) was dissolved at room temperature in a solution of methylamine in EtOH (1 ml, 7.5 M). The reaction mixture was stirred for 18 h and evaporated to give **43** (8 mg, 98%) as a white solid. The following data has been collected on a complex conformer mixture.

Rf = 0.40 (AcOEt/MeOH 95:5). $[\alpha]_D^{25}$ = +14.5 (c 0.7, CHCl$_3$). ^{1}H NMR (400 MHz, CD$_3$CN) δ 7.40 (bs, 1H), 7.35 – 7.08 (m, 8H), 6.99 (d, 1H, J = 7.3 Hz), 6.91 (bs, 0.5H), 6.69 (bs, 0.5H), 6.24 (bs, 0.5H), 5.70 (bs, 1H), 5.50 (bs, 0.5H), 5.16 (dd, 0.5H, J = 9.0, 2.6 Hz), 5.07 (d, 0.5H, J = 17.6 Hz), 4.72 (d, 0.5H, J = 16.1 Hz), 4.54 – 4.40 (m, 1H), 4.19 – 3.95 (m, 2.5H), 3.66 – 3.46 (m, 1H), 3.41 – 3.19 (m, 1H), 2.82 (d, 1.5H, J = 6.7 Hz), 2.67 (d, 1.5H, J = 4.7 Hz), 2.61 (d, 1.5H, J = 4.7 Hz), 2.57 – 2.00 (m, 5H), 1.92 – 1.78 (m, 0.5H), 1.42 (d, 12H, J = 8.2 Hz), 1.29 (d, 3H, J = 7.0 Hz). ^{13}C NMR (101 MHz, CD$_3$CN) δ 174.7, 174.4, 172.3, 171.9, 156.9, 140.9, 133.9, 133.8, 130.7, 130.6, 129.9, 129.6, 128.5, 128.0, 127.9, 127.7, 127.5, 80.4, 51.9, 50.4, 47.3, 47.0, 45.8, 44.8, 44.3, 43.4, 42.5, 40.0, 39.3, 38.9, 37.8, 34.2, 33.5, 30.9, 29.1, 26.9, 26.7, 19.5, 19.1. HRMS (ESI) calcd. for [C$_{33}$H$_{45}$N$_5$O$_6$]$^+$: 607.3370, found 608.3357. (MH$^+$)

^{1}H and ^{13}C NMR of compound **43**
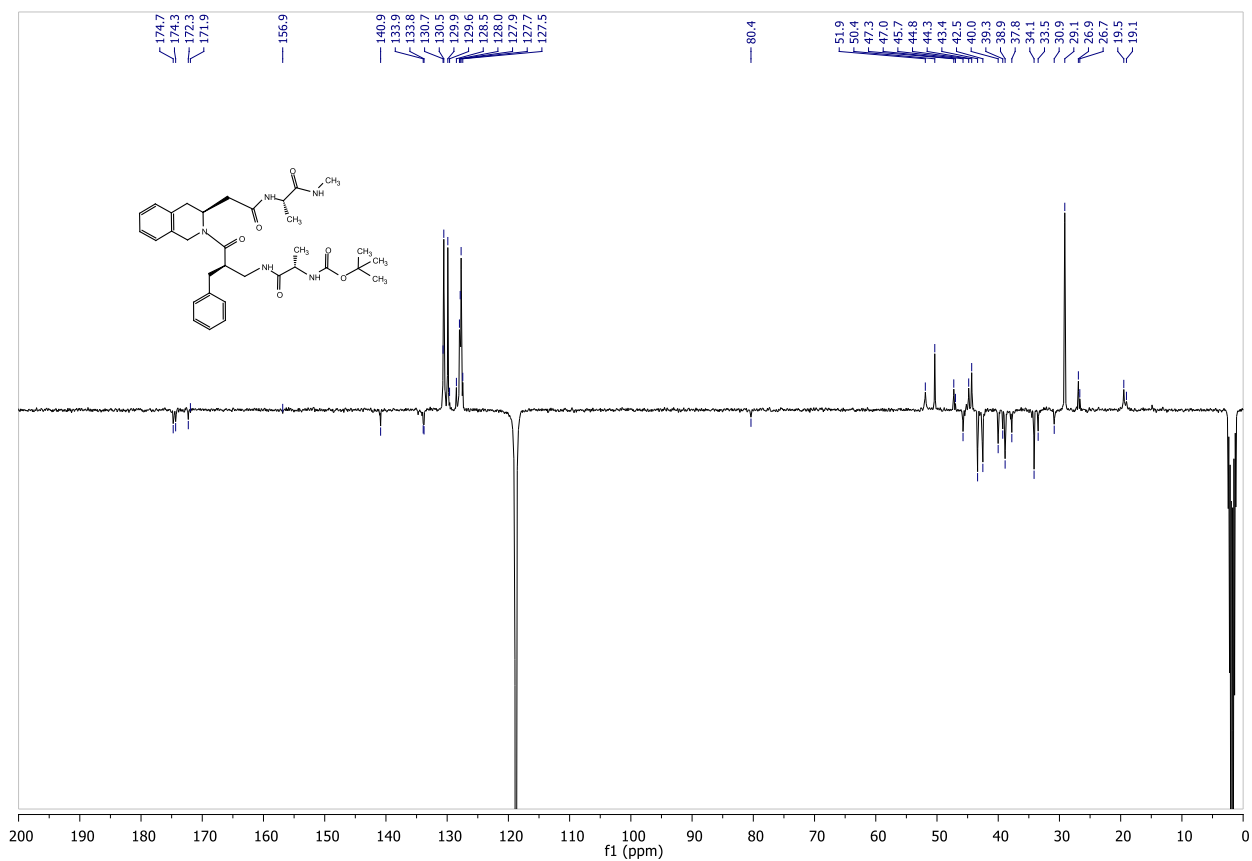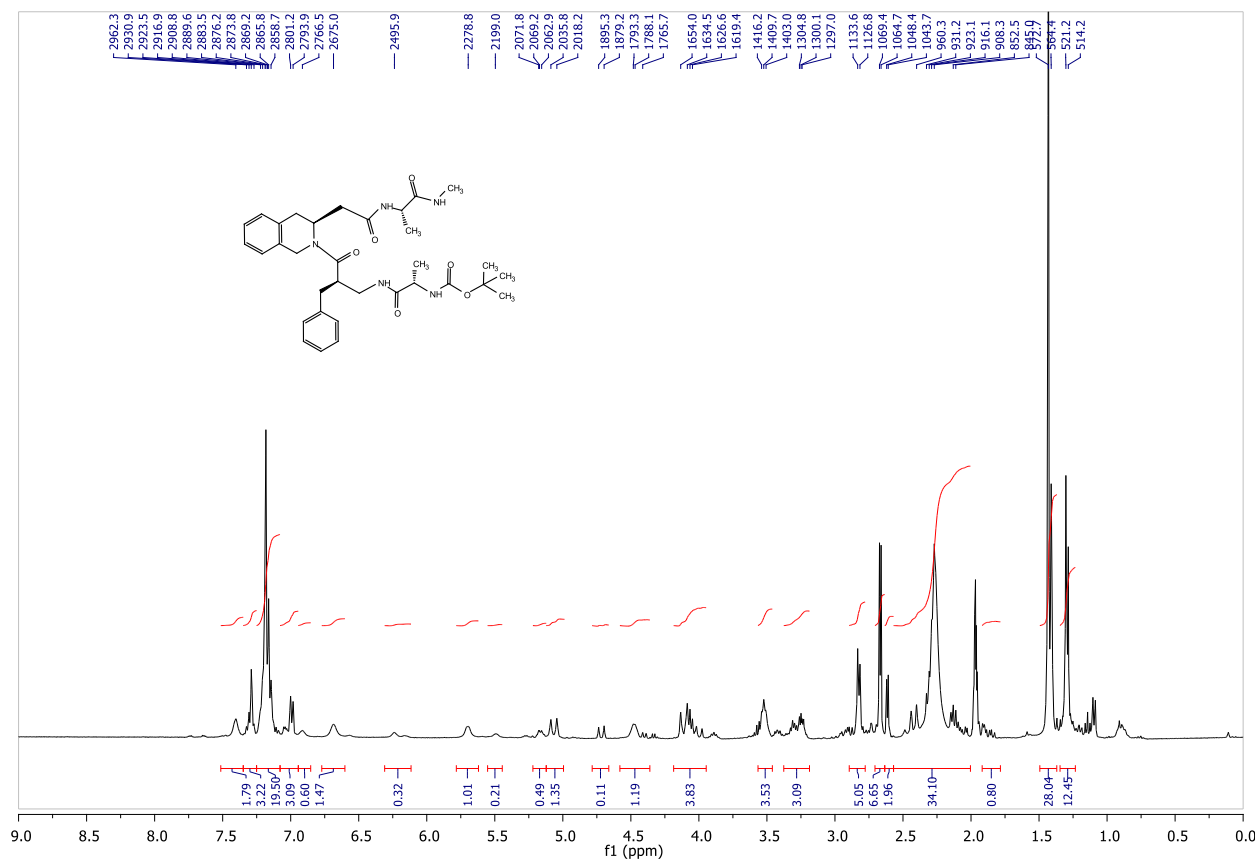
Compound 48a:
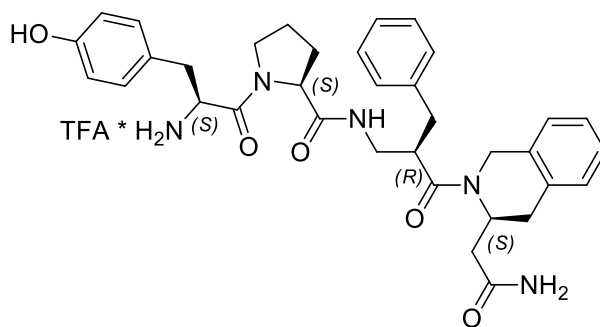
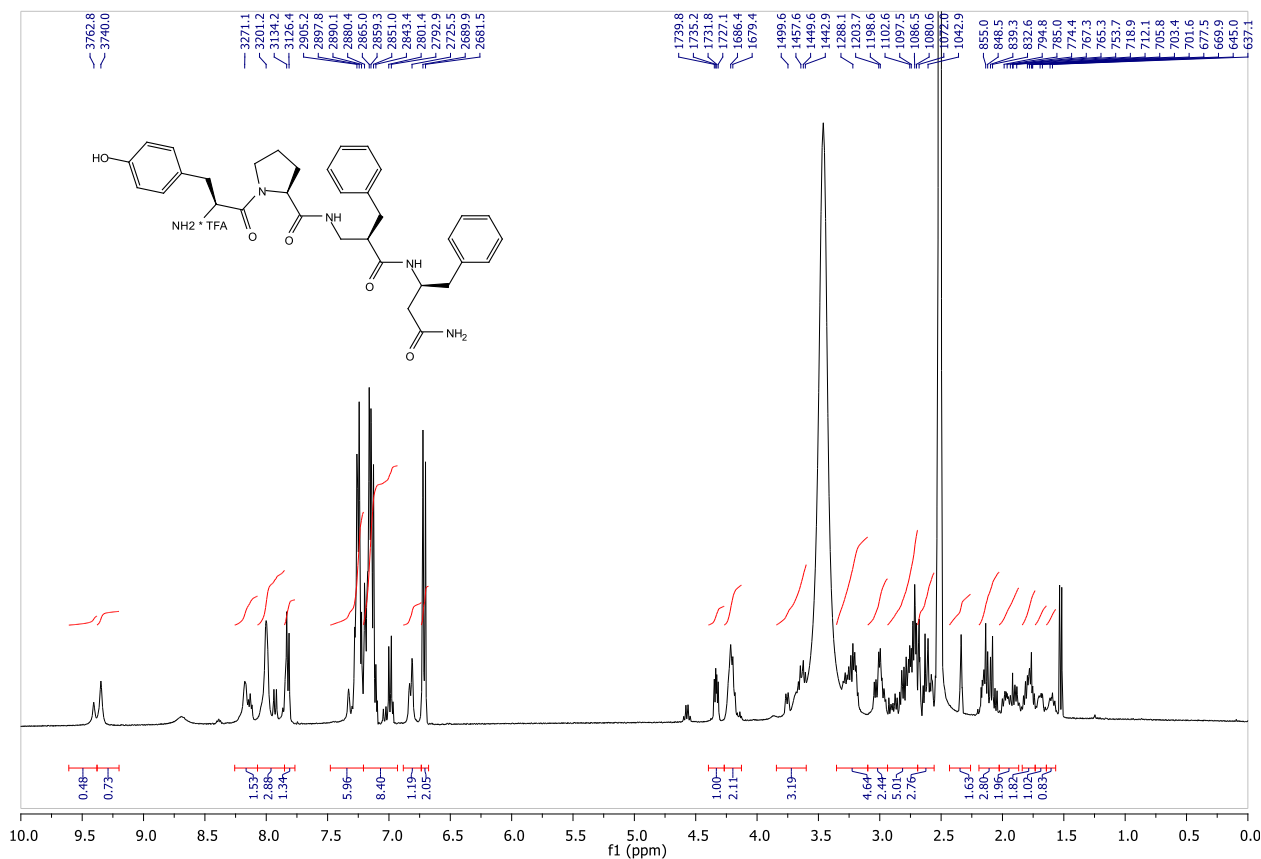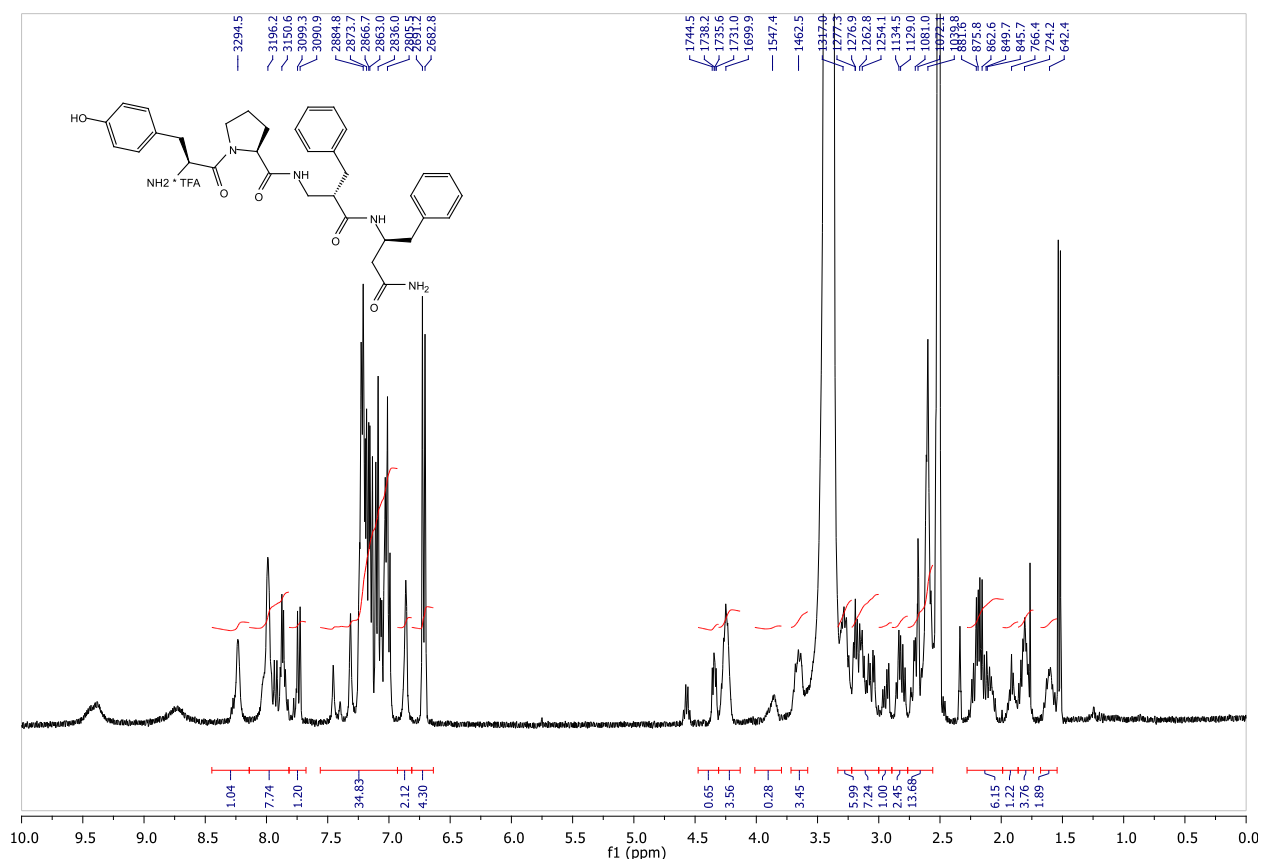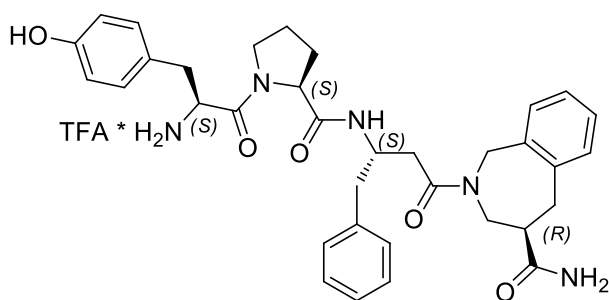

H-Tyr-Pro-(R)-β²hPhe-(S)-β³hTic-NH₂ (**48a**)

The following data has been collected on a complex conformer mixture.

^{1}H NMR (400 MHz, DMSO) δ 9.36 (bs, 2H), 8.74 – 7.80 (m, 3H), 7.59 – 6.81 (m, 18H), 6.81 – 6.55 (m, 8H), 5.37 – 5.13 (m, 1H), 5.05 (dd, 2H J = 25.0, 18.3 Hz), 4.77 – 4.61 (m, 1H), 4.49 – 4.39 (m, 4H), 4.31 – 4.13 (m, 5H), 4.13 – 3.98 (m, 2H), 3.92 (dd, 2H, J = 25.1, 11.9 Hz), 3.82 – 3.60 (m, 3H), 3.21 – 2.94 (m, 4H), 2.94 – 2.60 (m, 6H), 2.46 – 2.21 (m, 4H), 2.21 – 2.01 (m, 3H), 2.01 – 1.59 (m, 4H), 1.40 – 1.15 (m, 3H). HRMS (ESI) calcd. for [$C_{35}H_{41}N_5O_5$]$^+$: 611.3108, found 612.3102. (MH$^+$)
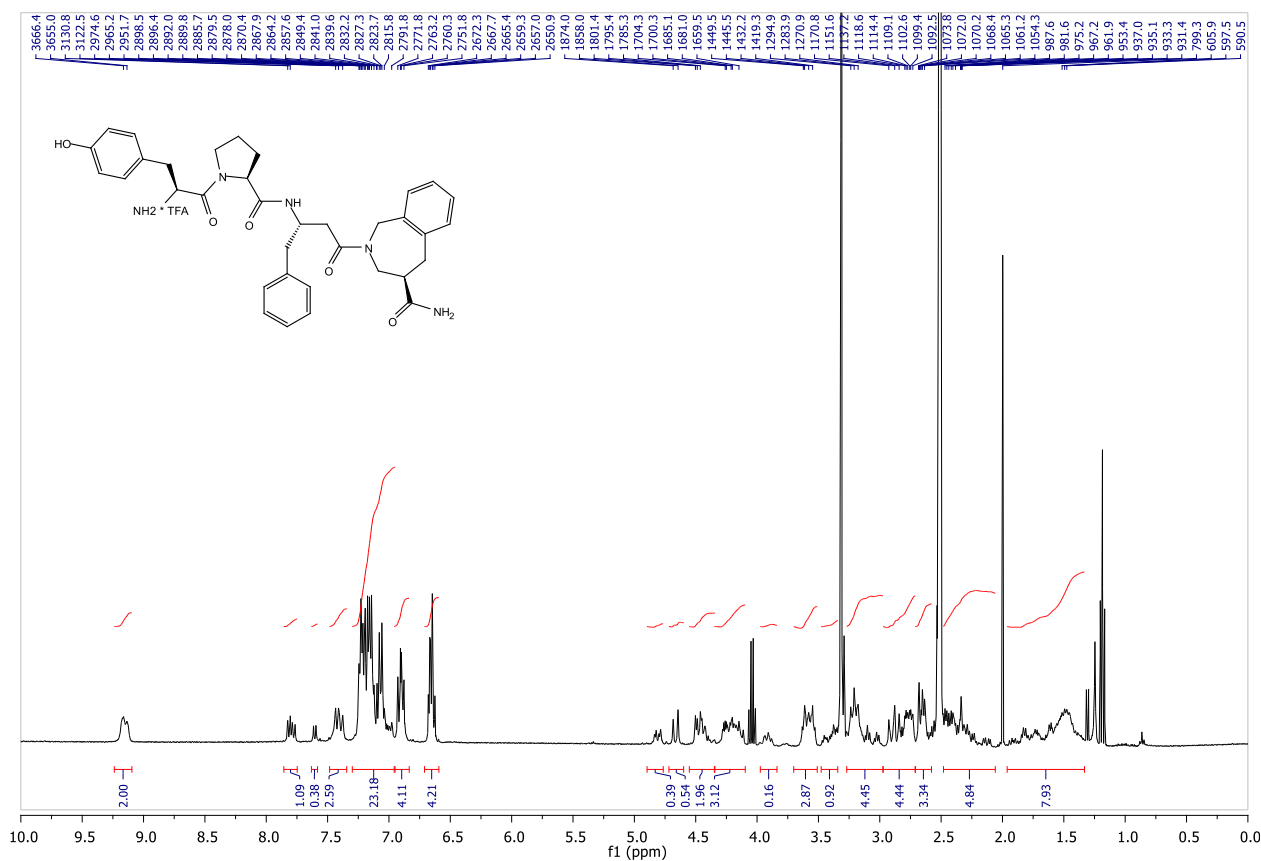
^{1}H NMR of compound **48a**
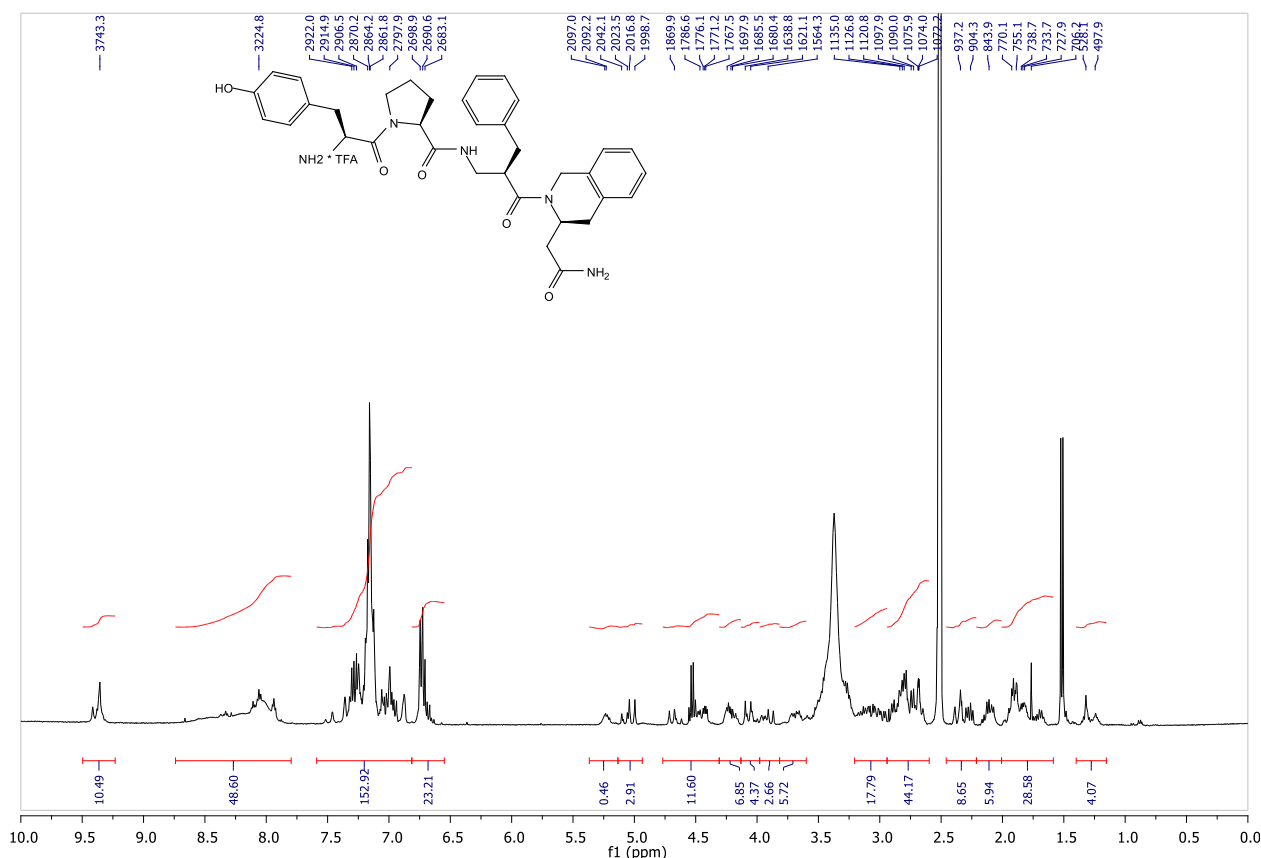
Compound 48b:
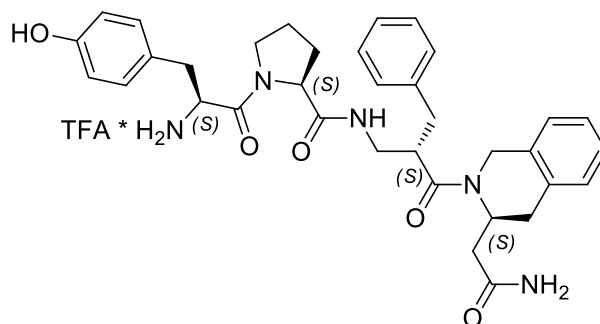
H-Tyr-Pro-(*S*)-β²hPhe-(*S*)-β³hTic-NH₂ (**48b**)

The following data has been collected on a complex conformer mixture.

¹H NMR (400 MHz, DMSO) δ 8.30 – 8.20 (m, 1H), 8.14 – 7.95 (m, 3H), 7.95 – 7.77 (m, 1H), 7.41 – 7.23 (m, 5H), 7.23 – 6.79 (m, 11H), 6.72 (dd, 2H, J = 14.1, 5.5 Hz), 5.39 – 5.03 (m, 1H), 5.03 – 4.82 (m, 1H), 4.53 – 4.30 (m, 2H), 4.23 (dd, 2H, J = 14.0, 5.8 Hz), 4.04 (d, 2H, J = 18.3 Hz), 3.40 – 2.95 (m, 9H), 2.95 – 2.57 (m, 7H), 2.20 – 2.05 (m, 4H), 1.89 (dd, 4H, J = 18.5, 3.9 Hz), 1.83 – 1.62 (m, 4H), 1.59 (dd, 2H, J = 10.9, 6.1 Hz), 1.48 – 1.29 (m, 1H). HRMS (ESI) calcd. for [C₃₅H₄₁N₅O₅]⁺: 611.3108, found 612.3130. (MH⁺)

¹H NMR of compound **48b**
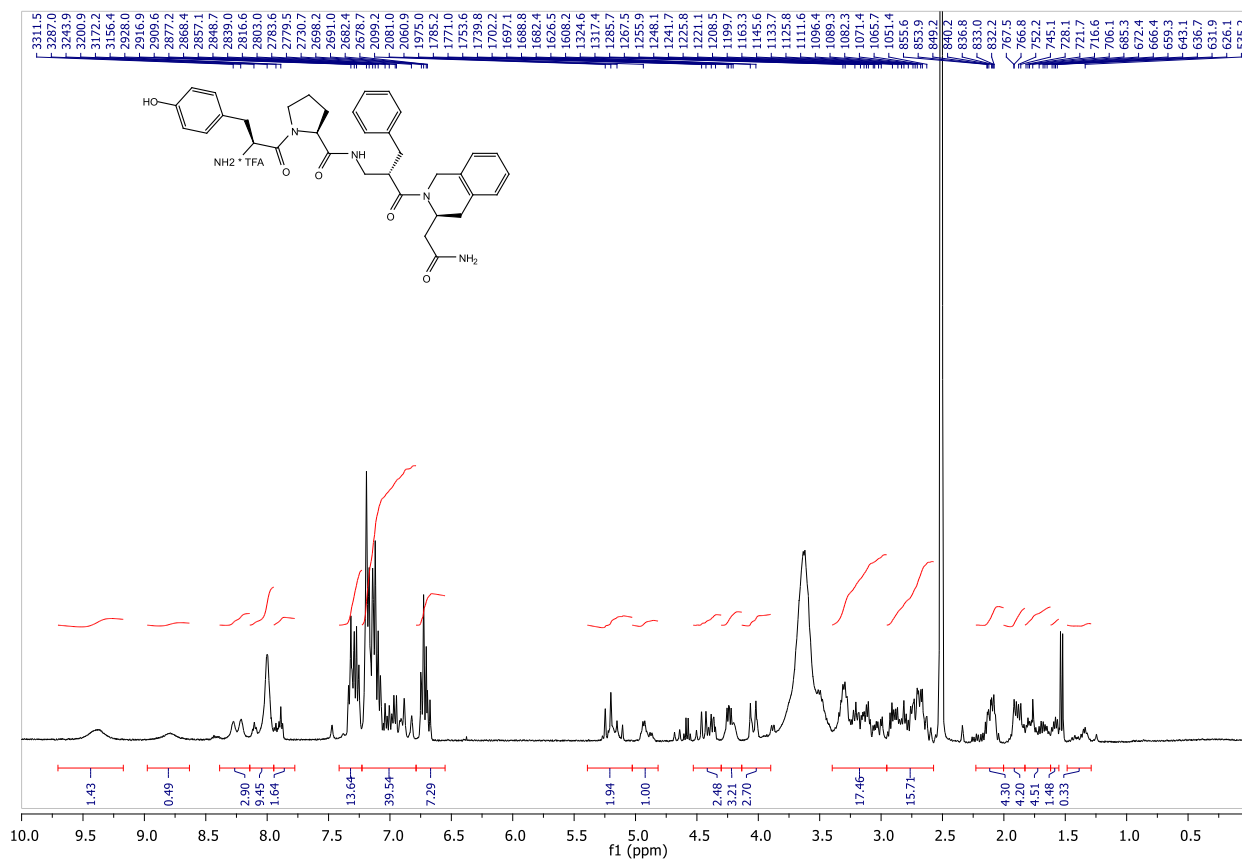
Compound 49a:
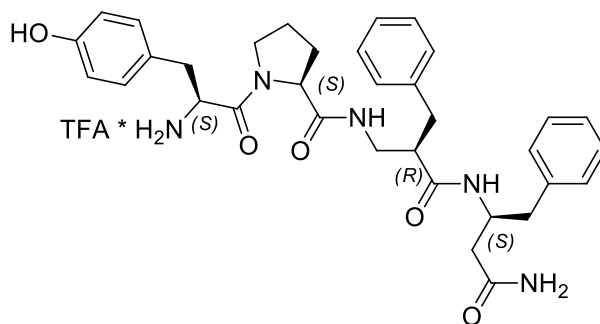
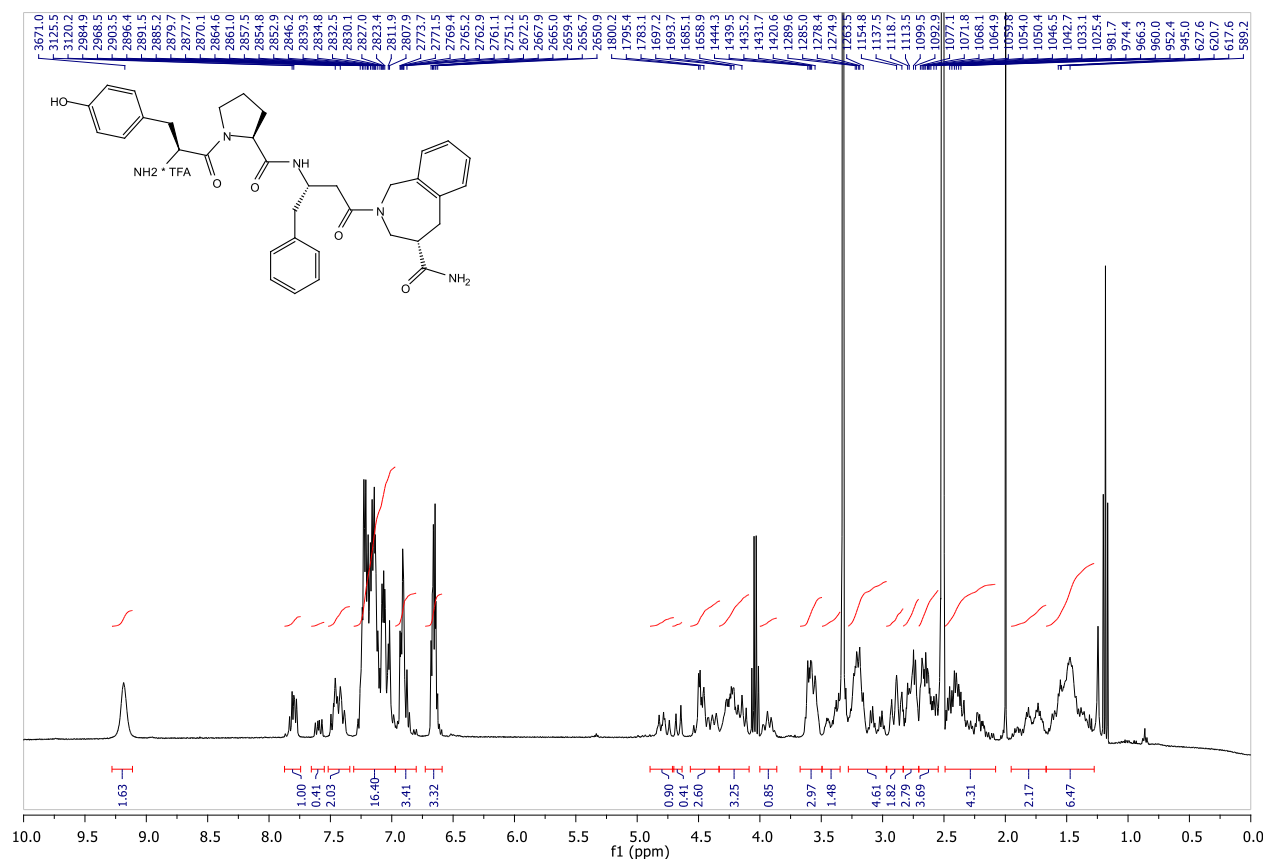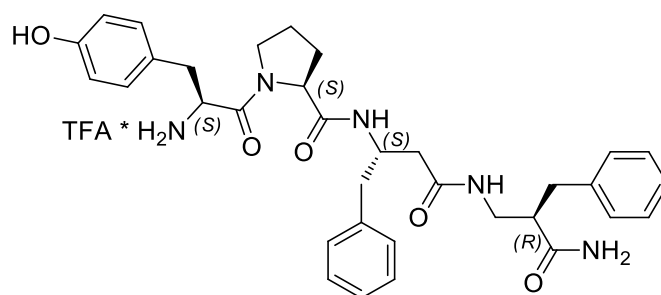H-Tyr-Pro-(*R*)-β²hPhe-(*S*)-β³hPhe-NH₂ (**49a**)

The following data has been collected on a complex conformer mixture.

¹H NMR (400 MHz, DMSO) δ 9.40 (s, 1H), 9.35 (s, 1H), 8.18 (bs, 1H), 8.00 (bs, 2H), 7.82 (d, *J* = 7.8 Hz, 1H), 7.31 – 7.21 (m, 6H), 7.21 – 6.93 (m, 10H), 6.81 (m, 2H), 6.71 (d, 2H, *J* = 8.4 Hz), 4.33 (dd, 1H, *J* = 8.0, 4.6 Hz), 4.24 – 4.18 (m, 2H), 3.90 – 3.60 (m, 3H), 3.35 – 3.10 (m, 5H), 3.02 (dd, 2H, *J* = 14.3, 5.3 Hz), 2.94 – 2.69 (m, 5H), 2.69 – 2.56 (m, 2H), 2.34 (bs, 1H), 2.20 – 2.04 (m, 3H), 2.03 – 1.86 (m, 2H), 1.85 – 1.73 (m, 2H), 1.71 - 1.66 (m, 1H), 1.64 – 1.57 (m, 1H). HRMS (ESI) calcd. for [C₃₄H₄₁N₅O₅]⁺: 599.3108, found 600.3121. (MH⁺)

¹H NMR of compound **49a**

Compound 49b:
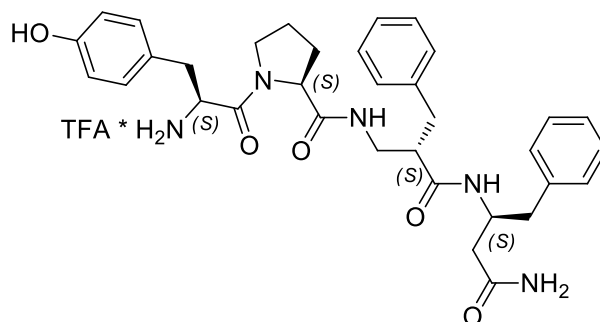
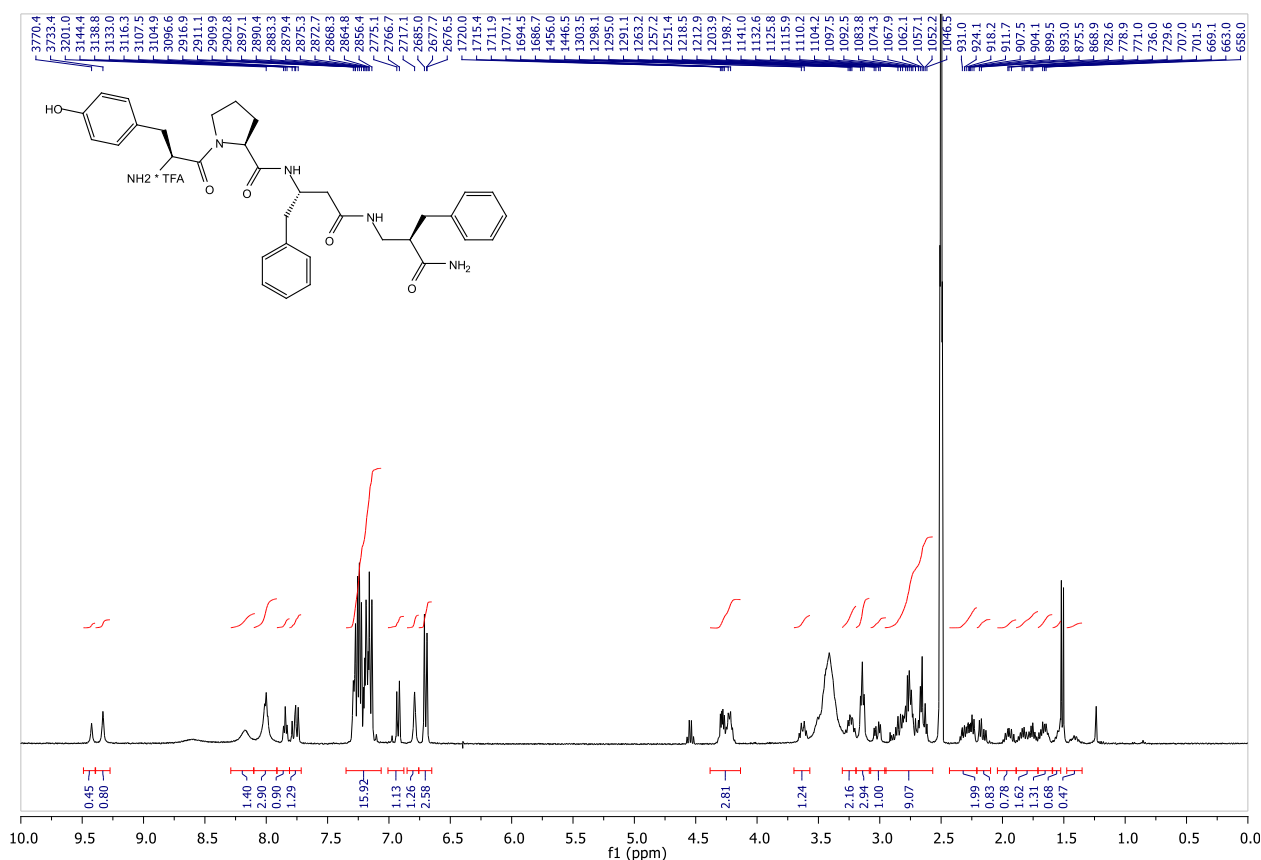H-Tyr-Pro-(S)-β²hPhe-(S)-β³hPhe-NH₂ (**49b**)

The following data has been collected on a complex conformer mixture.

¹H NMR (400 MHz, DMSO) δ 8.23 (bs, 1H), 8.14 – 7.82 (m, 2H), 7.74 (d, 1H, J = 8.4 Hz), 7.56 – 6.93 (m, 12H), 6.93 – 6.81 (m, 4H), 6.72 (d, 4H, J = 8.5 Hz), 4.34 (dd, 1H, J = 8.1, 5.5 Hz), 4.25 (m, 3H), 3.96 – 3.77 (bs, 1H), 3.72 – 3.58 (m, 3H), 3.33 - 3.23 (m, 3H), 3.22 – 3.00 (m, 7H), 2.94 (dd, 1H, J = 13.4, 5.3 Hz), 2.89 – 2.76 (m, 2H), 2.76 – 2.56 (m, 7H), 2.28 – 1.99 (m, 6H), 1.99 – 1.86 (m, 1H), 1.86 – 1.74 (m, 3H), 1.68 – 1.54 (m, 2H). HRMS (ESI) calcd. for $[C_{34}H_{41}N_5O_5]^+$: 599.3108, found 600.3134. (MH⁺)

¹H NMR of compound **49b**

Compound 50a:

H-Tyr-Pro-(S)-β^3hPhe-(R)-β^2hTbac-NH$_2$ (**50a**)

The following data has been collected on a complex conformer mixture.

^{1}H NMR (400 MHz, DMSO) δ 9.24 – 9.10 (m, 2H), 7.80 (dd, 1H, J = 15.5, 8.6 Hz), 7.60 (d, 1H, J = 7.9 Hz), 7.48 – 7.34 (m, 2H), 7.30 – 6.95 (m, 16H), 6.90 (dd, 4H, J = 11.5, 8.5 Hz), 6.71 – 6.59 (m, 4H), 4.81 (dd, 1H, J = 14.5, 5.5 Hz), 4.66 (d, 1H, J = 16.0 Hz), 4.55 – 4.41 (m, 2H), 4.35 – 4.10 (m, 3H), 3.91 (t, 1H, J = 10.6 Hz), 3.62 – 3.54 (m, 4H,), 3.48 – 3.34 (m, 1H), 3.27 – 2.97 (m, 5H), 2.97 – 2.71 (m, 5H), 2.71 – 2.58 (m, 4H), 2.48 – 2.06 (m, 5H), 1.96 – 1.33 (m, 8H). HRMS (ESI) calcd. for [C$_{35}$H$_{41}$N$_5$O$_5$]$^+$: 611.3108, found 612.3154. (MH$^+$)
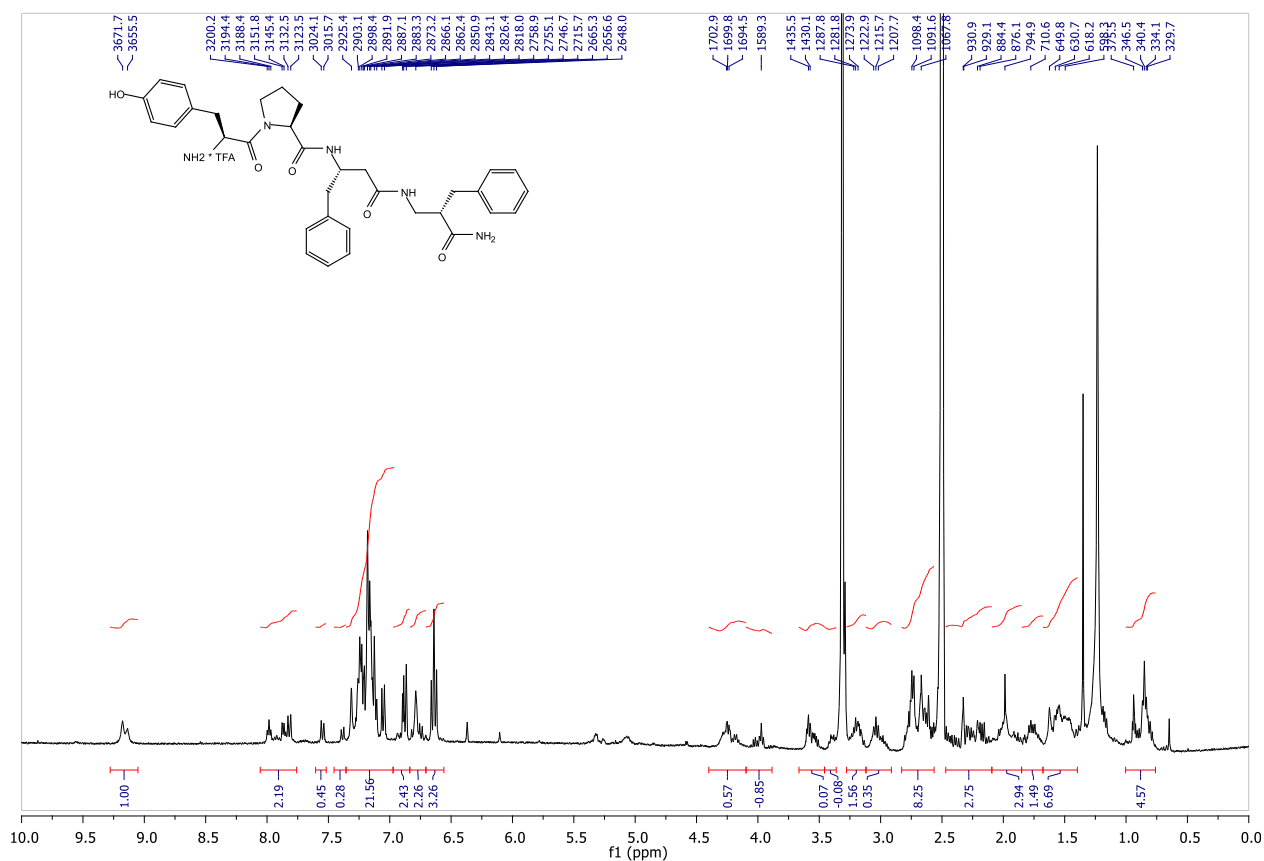
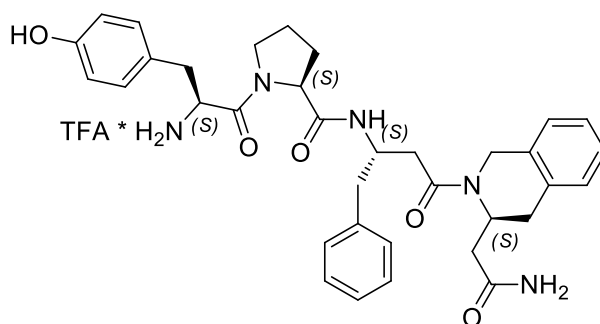^{1}H NMR of compound **50a**

Compound 50b:
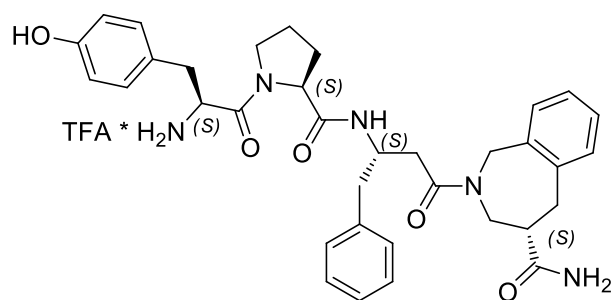
H-Tyr-Pro-(S)-β³hPhe-(S)-β²hTbac-NH₂ (**50b**)

The following data has been collected on a complex conformer mixture.

¹H NMR (400 MHz, DMSO) δ 9.18 (bs, 2H), 7.80 (dd, 1H, J = 13.8, 8.4 Hz), 7.60 (dd, 1H, J = 13.2, 8.2 Hz), 7.52 – 7.34 (m, 2H), 7.31 – 6.97 (m, 16H), 6.97 – 6.80 (m, 4H), 6.73 – 6.59 (m, 4H), 4.90 – 4.70 (m, 1H), 4.66 (d, 1H, J = 15.9 Hz), 4.57 – 4.33 (m, 3H), 4.33 – 4.09 (m, 3H), 3.94 (t, 1H, J = 13.3 Hz), 3.67 – 3.49 (m, 3H), 3.49 – 3.28 (m, 2H), 3.28 – 2.97 (m, 4H), 2.97 – 2.83 (m, 2H), 2.83 – 2.71 (m, 4H), 2.71 – 2.55 (m, 5H), 2.49 – 2.08 (m, 4H), 1.95 – 1.67 (m, 2H), 1.67 – 1.28 (m, 7H). HRMS (ESI) calcd. for $[C_{35}H_{41}N_5O_5]^+$: 611.3108, found 612.3149. (MH⁺)

¹H NMR of compound **50b**
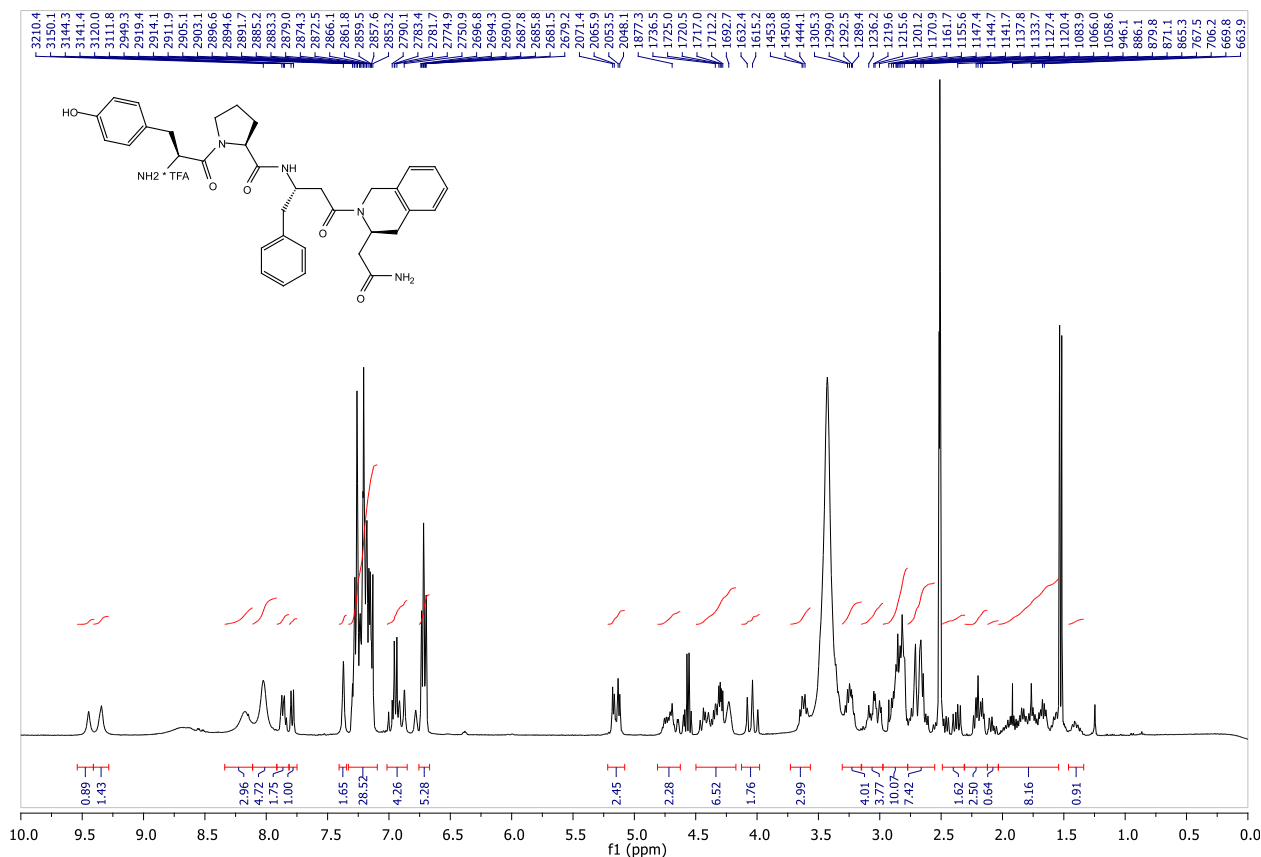
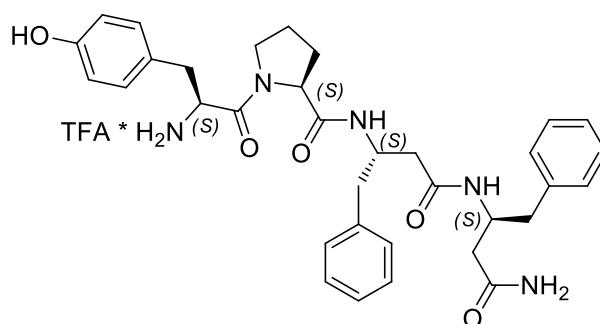## Compound 51a:

H-Tyr-Pro-(S)-β³hPhe-(R)-β²hPhe-NH₂ (**51a**)

The following data has been collected on a complex conformer mixture.

¹H NMR (400 MHz, DMSO) δ 9.42 (bs, 1H), 9.33 (bs, 1H), 8.17 (bs, 1H), 8.00 (bs, 3H), 7.84 (t, 2H, *J* = 5.7 Hz), 7.76 (dd, 1H, *J* = 11.2, 8.6 Hz), 7.35 – 7.06 (m, 22H), 6.93 (d, 1H, *J* = 8.4 Hz), 6.79 (bs, 1H), 6.76 – 6.65 (m, 4H), 4.38 – 4.14 (m, 3H), 3.70 – 3.57 (m, 1H, *J* = 9.5 Hz), 3.31 – 3.19 (m, 2H), 3.14 (t, 4H, *J* = 5.9 Hz), 3.02 (dd, 1H, *J* = 14.5, 5.4 Hz), 2.96 – 2.57 (m, 9H), 2.43 – 2.21 (m, 2H), 2.16 (dd, 1H, *J* = 14.6, 6.6 Hz), 2.04 – 1.89 (m, 3H), 1.89 – 1.71 (m, 3H), 1.71 – 1.59 (m, 3H), 1.53 (m, 2H), 1.48 – 1.35 (m, 2H). HRMS (ESI) calcd. for [$C_{34}H_{41}N_5O_5$]⁺: 599.3108, found 600.3128. (MH⁺)

¹H NMR of compound **51a**

Compound 51b:
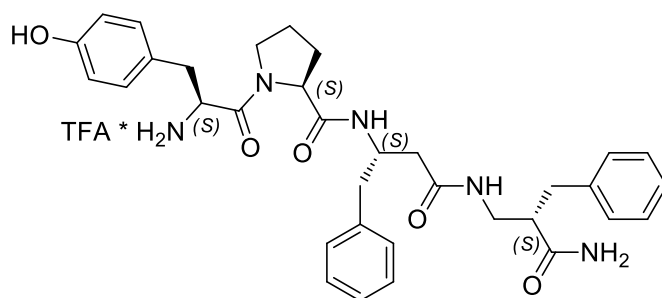
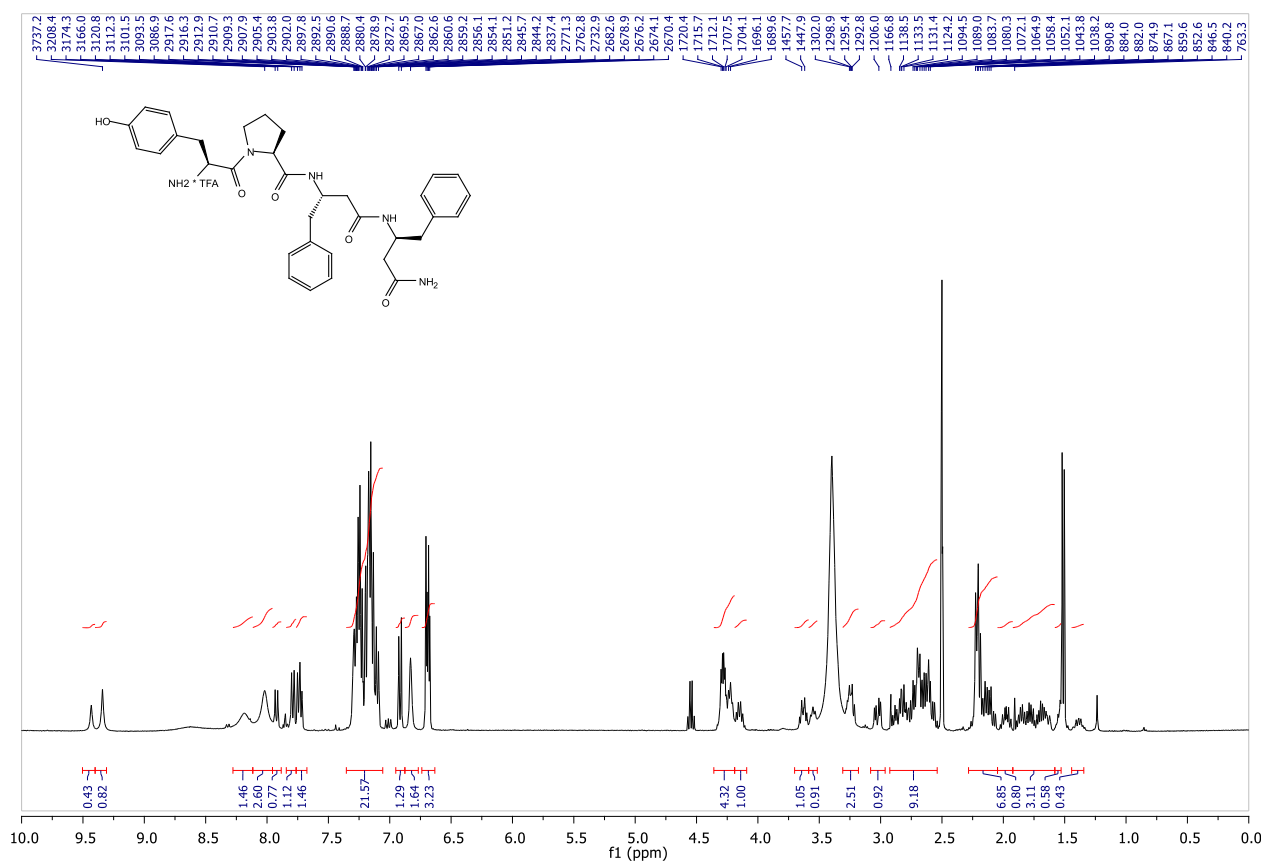H-Tyr-Pro-(*S*)-β³hPhe-(*S*)-β²hPhe-NH₂ (**51b**)

The following data has been collected on a complex conformer mixture.

¹H NMR (400 MHz, DMSO) δ 9.28 – 9.05 (m, 2H), 8.06 – 7.76 (m, 3H), 7.55 (d, 1H, *J* = 8.4 Hz), 7.38 (d, 1H, *J* = 8.5 Hz), 7.36 – 6.97 (m, 19H), 6.97 – 6.84 (m, 2H), 6.79 (bs, 2H), 6.64 (t, 4H, *J* = 8.6 Hz), 4.40 – 4.10 (m, 2H), 4.10 – 3.89 (m, 1H), 3.67 – 3.46 (m, 1H), 3.46 – 3.36 (m, 1H), 3.28 – 3.12 (m, 2H), 3.12 – 2.91 (m, 1H), 2.83 – 2.56 (m, 8H), 2.47 – 2.09 (m, 3H), 2.09 – 1.85 (m, 3H), 1.85 – 1.68 (m, 2H), 1.68 – 1.40 (m, 7H), 1.00 – 0.76 (m, 4H). HRMS (ESI) calcd. for [C₃₄H₄₁N₅O₅]⁺: 599.3108, found 600.3163. (MH⁺)

¹H NMR of compound **51b**

Compound 52:
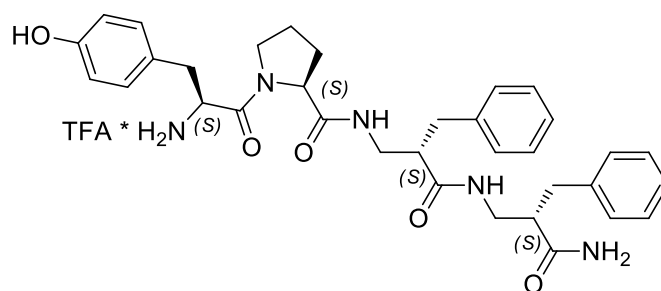

H-Tyr-Pro-(S)-β³hPhe-(S)-β³hTic-NH₂ (**52**)

The following data has been collected on a complex conformer mixture.

¹H NMR (400 MHz, DMSO) δ 9.45 (bs, 1H), 9.34 (bs, 1H), 8.34 – 8.11 (m, 2H), 8.02 (bs, 1H), 7.91 – 7.81 (m, 1H), 7.79 (d, 6H, J = 8.2 Hz), 7.37 (bs, 1H), 7.33 – 7.09 (m, 17H), 6.94 (m, 4H), 6.76 – 6.67 (m, 4H), 5.15 (dd, 2H, J = 17.9, 5.4 Hz), 4.81 – 4.63 (m, 2H), 4.50 – 4.17 (m, 4H), 4.04 (t, 2H, J = 17.1 Hz), 3.73 – 3.57 (m, 2H), 3.31 – 3.15 (m, 3H), 3.15 – 2.97 (m, 3H), 2.97 – 2.77 (m, 7H), 2.77 – 2.55 (m, 6H), 2.37 (dd, 1H, J = 14.9, 8.5 Hz), 2.31 – 2.12 (m, 2H), 2.12 – 2.03 (m, 1H), 2.03 – 1.54 (m, 8H), 1.46 – 1.34 (m, 1H). HRMS (ESI) calcd. for [$C_{35}H_{41}N_5O_5$]⁺: 611.3108, found 612.3121. (MH⁺)

¹H NMR of compound **52**
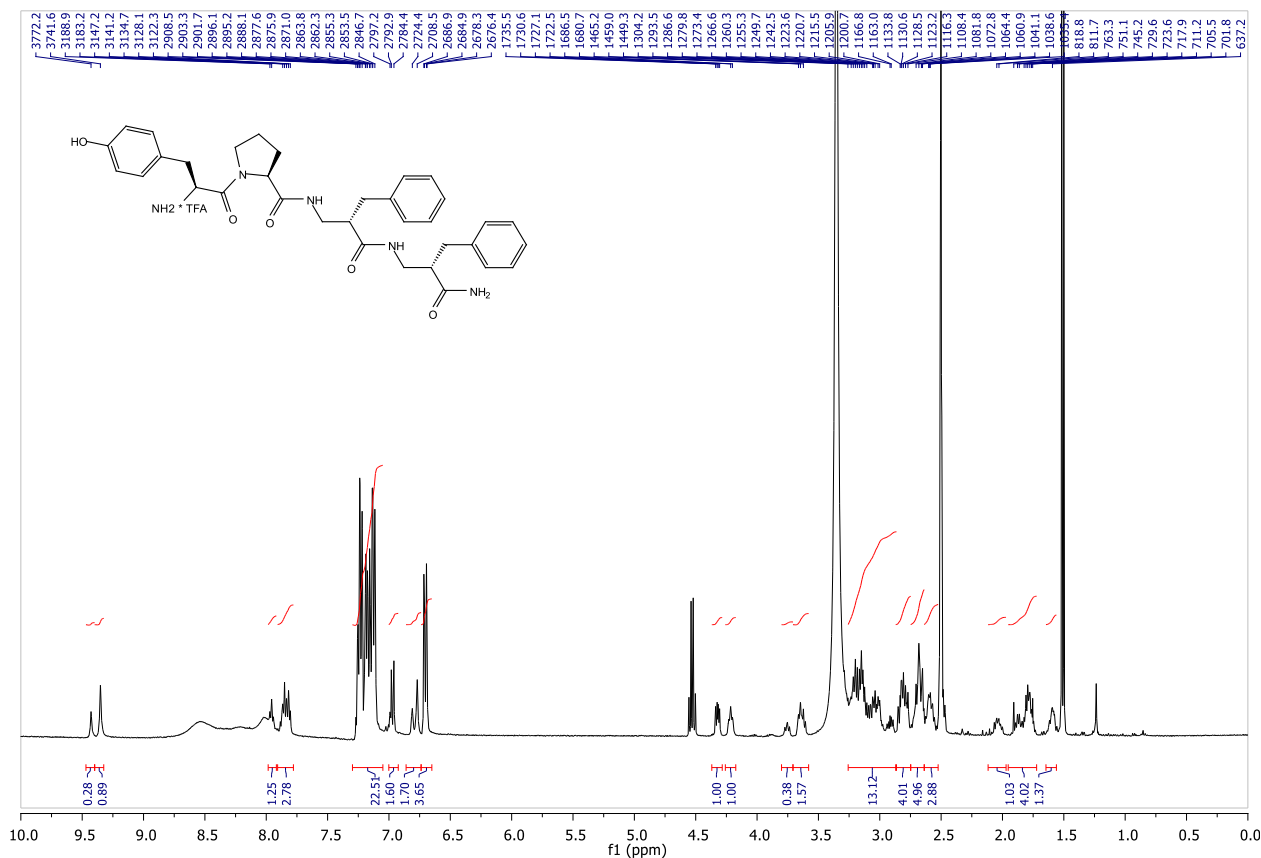
Compound 53:

H-Tyr-Pro-(S)-β³hPhe-(S)-β³hPhe-NH₂ (**53**)

The following data has been collected on a complex conformer mixture.

¹H NMR (400 MHz, DMSO) δ 9.43 (bs, 1H), 9.34 (bs, 1H), 8.19 (bs, 2H), 8.02 (bs, 2H), 7.92 (d, 1H, J = 8.4 Hz), 7.79 (d, 1H, J = 8.4 Hz), 7.76 – 7.68 (m, 2H), 7.35 – 7.06 (m, 20H), 6.92 (d, 2H, J = 8.5 Hz), 6.83 (bs, 2H), 6.74 – 6.63 (m, 4H), 4.36 – 4.19 (m, 3H), 4.19 – 4.09 (m, 1H), 3.62 (dd, 1H, J = 11.7, 4.9 Hz), 3.59 – 3.52 (m, 1H), 3.31 – 3.18 (m, 3H), 3.03 (dd, 1H, J = 14.4, 5.4 Hz), 2.93 – 2.54 (m, 10H), 2.28 – 2.05 (m, 8H), 2.05 – 1.92 (m, 1H), 1.92 – 1.58 (m, 4H), 1.58 – 1.53 (m, 2H), 1.39 (dd, 1H, J = 8.3, 6.9 Hz). HRMS (ESI) calcd. for [$C_{34}H_{41}N_5O_5$]⁺: 599.3108, found 600.3118. (MH⁺)

¹H NMR of compound **53**

Compound 54:

H-Tyr-Pro-(S)-β^{2}hPhe-(S)-β^{2}hPhe-NH$_2$ (**54**)

The following data has been collected on a complex conformer mixture.

^{1}H NMR (400 MHz, DMSO) δ 9.43 (s, 1H), 9.35 (s, 1H), 7.98 – 7.92 (m, 2H), 7.91 – 7.78 (m, 2H), 7.30 – 7.05 (m, 20H), 7.00 – 6.92 (m, 2H), 6.79 (d, 2H, J = 15.9 Hz), 6.70 (dd, 4H, J = 8.5, 2.0 Hz), 4.32 (dd, 1H, J = 8.2, 4.8 Hz), 4.21 (t, 1H, J = 5.9 Hz), 3.74 (t, 1H, J = 6.8 Hz), 3.68 – 3.61 (m, 2H), 3.26 – 2.86 (m, 12H), 2.87 – 2.75 (m, 4H), 2.75 – 2.64 (m, 6H), 2.64 – 2.52 (m, 3H), 2.12 – 1.97 (m, 1H), 1.95 – 1.72 (m, 4H), 1.65 – 1.56 (m, 1H). HRMS (ESI) calcd. for [C$_{34}$H$_{41}$N$_5$O$_5$]$^+$: 599.3108, found 600.3160. (MH$^+$)

^{1}H NMR of compound **54**

CHAPTER III: THBC-DKP SCAFFOLDS

3.1 *β-Carbolines*

Carbolines are benzofused tricyclic structures and they are a common motif in natural compounds. They consist of a pyridine ring fused to an indole skeleton. Their structure is similar to that of tryptamine, with a methylene connection on the indole position 2.
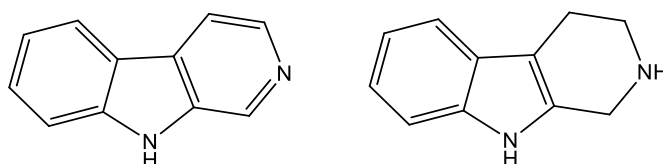

Figure 35. β-Carboline and tetrahydro-β-carboline.

The β-carboline core is usually built from a suitable functionalized indole, such as a tryptamine derivative, onto which the fused pyridine ring is introduced. Indoles are activated substrates that efficiently undergo intramolecular Friedel–Crafts reactions such as the Pictet–Spengler (PS) and the Bischler–Napieralski (BN) reactions. Other methodologies based on organometallic catalyzed cyclizations or the synthesis of the pyrrole ring have also emerged in recent times. However, once the β-carboline system is on hand, many syntheses still need further transformations en route to natural products or synthetic drug candidates. In addition, transformation of the β-carboline system into other heterocycles or synthetically useful compounds (i.e., the use of the β-carboline as a synthetic intermediate) has been growing in importance in recent years.

Carbolines can be easily transformed into fused tetracyclic derivatives like imidazolidin-2-ones (carbonyl bridge), imidazolidines (methylene bridge) and piperazin-2-ones.[91] The functionalization of the β-carboline system and its use as a synthetic intermediate for the synthesis of more complex heterocycles have reached a mature state with the use of various reactions such as carbon-carbon coupling, RCM, diverse cycloadditions and stereoselective organocatalytic functionalizations.[92]

From a long time, the alkaloids containing the 1,2,3,4-tetrahydro-β-carboline (THBC) skeleton represent important lead structures in view of their wide range of biological activities.[93] Due to their unique rigid heterocyclic skeleton, such cyclic tryptophan analogues are known to bind with high affinity to various receptor sites, such as the

[91] Pulka K., Feytens D., Misicka A., Tourwé D. "New tetracyclic tetrahydro-β-carbolines as tryptophan-derived peptidomimetics" *Mol. Divers.* **2010**, *14*, 97-108

[92] Dominguez G., Perez-Castells J. "Chemistry of β-Carbolines as Synthetic Intermediates" *Eur. J. Org. Chem.* **2011**, 7243-7253

[93] Cordell G.A. "*The Alkaloids, Chemistry and Pharmacology*" Academic Press: New York, **1993**, Vol. 43

benzodiazepine (BzR),[94] serotonin,[95] and dopamine[96] ones and to inhibit monoamine oxidase A.[97] Moreover, in the recent years, some tetracyclic β-carbolines have been described to act as selective inhibitors in the anticancer field,[98] or to be endowed with antimalarial properties.[99]

[94] Oakley N.R., Jones B.J. "The proconvulsant and diazepam-reversing effects of ethyl-beta-carboline-3-carboxylate" Eur. J. *Pharmacol.* **1980**, *68*, 381-382

[95] (a) Khorana N., Smith C., Herrick-Davis K., Purohit A., Teitler M., Grella B., Dukat M., Glennon R.A. "Binding of tetrahydrocarboline derivatives at human 5-HT5A receptors" *J. Med. Chem.* **2003**, *46*, 3930-3937 (b) Audia J.E., Evrard D.A., Murdoch G.R., Droste J.J., Nissen J.S., Schenk K.W., Fludzinski P., Lucaites V.L., Nelson D.L., Cohen M.L. "Potent, selective tetrahydro-beta-carboline antagonists of the serotonin 2B (5HT2B) contractile receptor in the rat stomach fundus" *J. Med. Chem.* **1996**, *39*, 2773-2780

[96] Abou-Gharbia M., Patel R.U., Webb M.B., Moyer J.A., Andree T.H., Muth T.A. "Antipsychotic activity of substituted gamma-carbolines" *J. Med. Chem.* **1987**, *30*, 1818-1823

[97] (a) Callaway J.C., Gynther J., Poso A., Vepsäläinen J., Airksinen M.M. " The Pictet-Spengler reaction and biogenic tryptamines: formation of tetrahydro-β-carbolines at physiological pH" *J. Heterocyclic Chem.* **1994**, *31*, 431-435 (b) Ho B.T. "Monoamine oxidase inhibitors" *J. Pharm. Sci.* **1972**, *61*, 821-837

[98] (a) Jenkins P.R., Wilson J., Emmerson D., Garcia M.D., Smith M.R., Gray S.J., Britton R.G., Mahale S., Chaudhuri B. "Design, synthesis and biological evaluation of new tryptamine and tetrahydro-beta-carboline-based selective inhibitors of CDK4" *Bioorg. Med. Chem.* **2008**, *16*, 7728-7739 (b) Sunder-Plassmann N., Sarli V., Gartner M., Utz M., Seiler J., Huemmer S., Mayer T.U., Surrey T., Giannis A. "Synthesis and biological evaluation of new tetrahydro-beta-carbolines as inhibitors of the mitotic kinesin Eg5" *Bioorg. Med. Chem.* **2005**, *13*, 6094-6111

[99] Gupta L., Srivastava K., Singh S., Puri S.K., Chauhan P.M.S. "Synthesis of 2-[3-(7-Chloro-quinolin-4-ylamino)-alkyl]-1-(substituted phenyl)-2,3,4,9-tetrahydro-1H-beta-carbolines as a new class of antimalarial agents" *Bioorg. Med. Chem. Lett.* **2008**, *18*, 3306-3309

3.2 *Diketopiperazines*

2,5-Diketopiperazine (DKP)-based compounds are heterocyclic scaffolds structurally similar to peptides. They have attracted attention in recent years because of their broad biological activities[100] and therapeutic applications, ranging from antibiotics[101] to anticancer agents.[102]

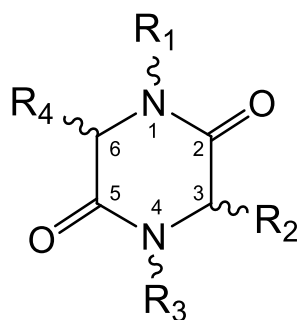**Figure 36.** 2,5-Diketopiperazine ring.

DKPs are a six member heterocycles possessing four points of functionalization. Two amidic positions and two stereocenters which belong to Amino acid constituting the DKP core. They are indeed the smallest cyclic peptide, commonly biosynthesized from amino acids by different organisms, including mammals, and are considered to be secondary functional metabolites or side products of terminal peptide cleavage.

A 2,5-diketopiperazine has two s-cis secondary amide groups that can hydrogen bond horizontally within the ring plane. As a result of their rigid cyclic structures, bearing amide groups, DKPs are usually poorly soluble in organic solvents. In the solid state, the vast majority of *N*-unsubstituted DKPs adopt a linear tape orientation, whereas the presence of one *N*-substituent leads either to the formation of one-dimensional hydrogen-bonded tapes through the establishment of nonreciprocal hydrogen-bond networks, or to hydrogen-bonded dimers.

[100] (a) Wang S., Golec J., Miller W., Milutinovic S., Folkes A., Williams S., Brooks T., Hardman K., Charlton P., Wren S., Spencer J. "Novel inhibitors of plasminogen activator inhibitor-1: development of new templates from diketopiperazines" *Bioorg. Med. Chem. Lett.* **2002**, *12*, 2367–2370 (b) Houston D.R., Synstad B., Eijsink V.G., Stark M.J., Eggleston I.M., Van Aalten D.M. "Structure-based exploration of cyclic dipeptide chitinase inhibitors" *J. Med. Chem.* **2004**, *47*, 5713–5720

[101] Fdhila F., Vazquez V., Sanchez J.L., Riguera R. "dd-diketopiperazines: antibiotics active against Vibrio anguillarum isolated from marine bacteria associated with cultures of Pecten maximus" *J. Nat. Prod.* **2003**, *66*, 1299–1301

[102] Nicholson B., Lloyd G.K., Miller B.R., Palladino M.A., Kiso Y., Hayashi Y., Neuteboom S.T. "NPI-2358 is a tubulin-depolymerizing agent: in-vitro evidence for activity as a tumor vascular-disrupting agent" *Anti-Cancer Drugs* **2006**, *17*, 25–31

Some of the chemical properties of 2,5-diketopiperazines are very interesting for medicinal chemistry, such as resistance to proteolysis, mimicking of peptidic pharmacophoric groups, substituent group stereochemistry (defined and controlled in up to four combinations), conformational rigidity, and donor and acceptor groups for hydrogen bonding (favouring interactions with biological targets). In addition, the compounds show a common scaffold, easily obtained by conventional procedures, that favours structural diversity as a function of substituent side chains particularly orientated. Favorable pharmacodynamic and pharmacokinetic characteristics are acquired by the compounds through these properties, leading to promising agents for the development of new drugs. Diketopiperazines are privileged structures for the discovery of new lead compounds by combinatorial chemistry and are considered ideal for the rational development of new therapeutic agents.

3.3 THBC-DKP Scaffold

Structural unification of THBC and DKP pharmacophores has led to new classes of biologically active tetracyclic compounds, either occurring in nature and synthetically made.[103] Highly complex natural products displaying the fused, tetracyclic THBC-DKP ring system were recently isolated from the fermentation broth of the marine-derived fungus *Aspergillus fumigatus*, already known as a valuable source of bioactive secondary metabolites.[104] Some of these compounds exhibited significant cell growth-inhibitory activities against various cell lines.[105] Specifically designed THBC-DKP-based compounds have received considerable attention over the last years for their valuable biological activities, ranging from inhibition of the cyclic guanosine monophosphate type 5 specific phosphodiesterase (PDE 5) for treatment of erectile dysfunction (Tadalafil),[106] inhibition of plasmodial PDE activity for antimalarial drugs,[107] topoisomerase II inhibition,[108] to oral anti-thrombotic properties.[109] (**Figure 37**)

[103] Chanda K., Chou C.-T., Lai J.J., Lin S.F., Yellol G.S., Sun C.M. "Traceless synthesis of diketopiperazine fused tetrahydro-β-carbolines on soluble polymer support" *Mol Divers*, **2011**, *15*, 569-581

[104] Wang Y., Li Z.L., Bai J., Zhang L.M., Wu X., Zhang L., Pei Y.H., Jing Y.K., Hua H.M. "2,5-Diketopiperazines from the Marine-Derived Fungus Aspergillus fumigatus YK-7" *Chem. & Biodiv.* **2012**, *9*, 385-393

[105] Deveau A.M., Costa N.E., Joshi E.M., Macdonald T.L. "Synthesis of diketopiperazine-based carboline homodimers and in vitro growth inhibition of human carcinomas" *Bioorg. Med. Chem. Lett.* **2008**, *18*, 3522-3525

[106] Daugan A., Grondin P., Ruault C., Gouville A.C., Le M., Coste H., Linget J.M., Kirilovsky J., Hyafil F., Labaudiniere R. "The discovery of tadalafil: a novel and highly selective PDE5 inhibitor. 2: 2,3,6,7,12,12a-hexahydropyrazino[1',2':1,6]pyrido[3,4-b]indole-1,4-dione analogues" *J. Med. Chem.* **2003**, *46*, 4533-4542

[107] (a) Beghyn T.B., Charton J., Leroux F., Henninot A., Reboule I., Cos P., Maes L., Deprez B. "Drug-to-genome-to-drug, step 2: reversing selectivity in a series of antiplasmodial compounds" *J. Med. Chem.* **2012**, *55*, 1274-1286 (b) Beghyn T.B., Charton J., Leroux F., Laconde G., Bourin A., Cos P., Maes L. Deprez B. "Drug to genome to drug: discovery of new antiplasmodial compounds" *J. Med. Chem.* **2011**, *54*, 3222-3240

[108] Deveau A.M., Labroli M.A., Dieckhaus C.M., Barthen M.T., Smith K.S., Macdonald T.L. "The synthesis of amino-acid functionalized beta-carbolines as topoisomerase II inhibitors" *Bioorg. Med. Chem. Lett.* **2001**, *11*, 1251-1255

[109] Liu J., Wu G., Cui G., Wang W.X., Zhao M., Wang C., Zhang Z., Peng S. "A new class of anti-thrombosis hexahydropyrazino-[1',2':1,6]pyrido-[3,4-b]-indole-1,4-dions: design, synthesis, logK determination, and QSAR analysis" *Bioorg. Med. Chem.* **2007**, *15*, 5672–5693
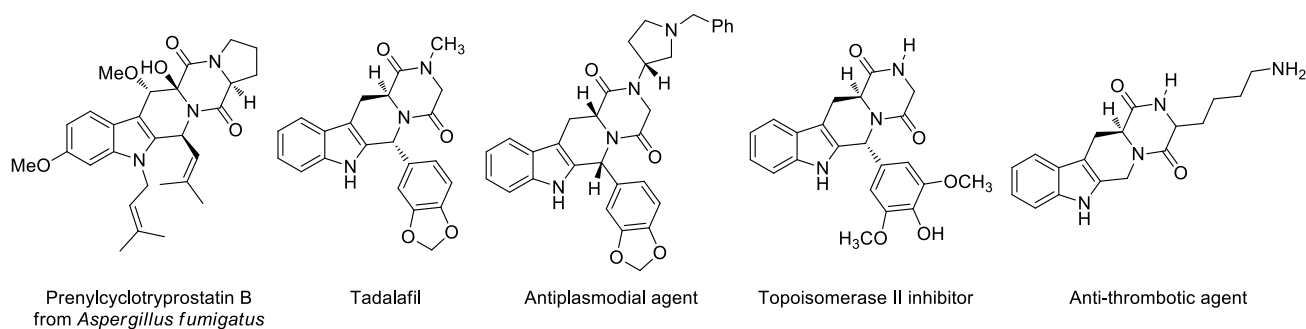
Figure 37. THBC-DKP-based natural and synthetically made compounds.

In our ongoing program of design of pharmacophore-based combinatorial libraries[110] and identification of new peptidomimetic scaffolds of potential interest in drug discovery,[111] we evaluated the THBC-DKP-based scaffold as a potential suitable motif for creation of unusual reverse turn nucleators.

In addition to mostly occurring β- and γ-turns, stabilized by ten- and seven-membered intramolecular H bonds respectively, reversal of the polypeptide chain direction in globular proteins can also occur thanks to less common substructures, for instance involving five amino acids residues, such as the case of the α-turns.

In many cases the α-turn occurs at the ends of extended strands, and whenever it occurs at the loop regions connecting two extended strands, it brings about a hairpin bend. Even if a very large majority of α-turns segments form part of regular α-helices, isolated α-turns have been reported,[112] which are stabilized by a 5→1 hydrogen bond between carbonyl oxygen at position *i* and amide at position *i+4*. The minor recurrence in proteins of this secondary structure is probably due to the necessity of particular combination of residues in the α-turn as well as those immediately preceding and succeeding this turn, able to hamper the propagation of the motif to α-helices.

However, quite recently the presence of *α*-turns in constrained peptides has been associated to some relevant biological activity. For instance, sugar amino acid based macrocyclic cationic peptides have been reported to show good bacteriolytic activity

[110] Danieli B., Giovanelli P., Lesma G., Passarella D., Sacchetti A., Silvani A. "Combinatorial solid-phase synthesis of 6-hydroxy-1,2,3,4-tetrahydro-beta-carbolines from l-5-hydroxytryptophan" *J. Comb. Chem.* **2005,** *7*, 458-462

[111] Lesma G., Landoni N., Sacchetti A., Silvani, A. "The spiropiperidine-3,3'-oxindole scaffold: a type II B-turn peptide isostere" *Tetrahedron* **2010**, *66*, 4474–4478 (b) Lesma G., Landoni N., Pilati T., Sacchetti A., Silvani A. "Tetrahydroisoquinoline-based spirocyclic lactam as a type II' beta-turn inducing peptide mimetic" *J. Org. Chem*. **2009**, *74*, 8098–8105 (c) Lesma, G.; Landoni, N.; Sacchetti, A.; Silvani A. "Pyrroloisoquinoline-based tetrapeptide analogues mimicking reverse-turn secondary structures" *J. Org. Chem.* **2007**, *72*, 9765–9768

[112] Nataraj D.V., Srinivasan N., Sowdhamini R., Ramakrishnan C. "α-Turns in protein structures" *Current Science* **1995**, *69*, 434-446

against the Gr^{+ve} and Gr^{-ve} bacteria while exhibiting low hemolytic activity.[113] In another work, a peptide was constrained in an α-helical conformation by means of cyclic α-turn mimetics, resulting in good activity in both a recombinant fusion assay and in a RSV antiviral assay.[114] Recently the antibody F425-B4e8, isolated from human (HIV-1) infected individuals, was showed to bind in complex with a V3 peptide through a five-residue α-turn, thus opening the way for HIV-neutralization.[115] Other examples of α-turns are observed in synthetic peptidomimetics.[113,116]

Despite the growing interest in this kind of reverse turn and the need for all kinds of conformationally constrained mimics as tools for medicinal chemistry, the development of constrained α-turn mimetics has received poor attention until now.

So I planned the synthesis of the THBC-DKP-based peptidomimetic **1a** (**Figure 38**) and performed the conformational evaluation for which molecular modeling let envisage a thirteen-membered hydrogen bond stabilized α-turn conformation.
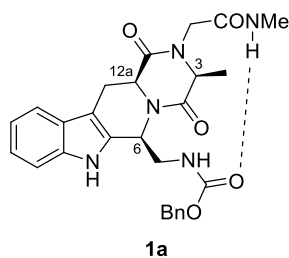
Figure 38. THBC-DKP-based peptidomimetic **1a**.

[113] Chakraborty T.K., Koley D., Ravi R., Krishnakumari V., Nagaraj R., Kunwar A.C. "Synthesis, conformational analysis and biological studies of cyclic cationic antimicrobial peptides containing sugar amino acids" *J. Org. Chem.* **2008**, *73*, 8731–8744

[114] Shepherd N.E., Hoang H.N., Desai V.S., Letouze E., Young P.R., Fairlie D.P. "Modular alpha-helical mimetics with antiviral activity against respiratory syncitial virus" *J. Am. Chem. Soc.* **2006**, *128*, 13284–13289

[115] Bell C.H., Pantophlet R., Schiefner A., Cavacini L.A., Stanfield R.L., Burton D.R., Wilson I.A. "Structure of antibody F425-B4e8 in complex with a V3 peptide reveals a new binding mode for HIV-1 neutralization" *J. Mol. Biol.* **2008**, *375*, 969–978

[116] (a) Hoang H.N., Driver R.W., Beyer R.L., Malde A.K., Le G.T., Abbenante G., Mark A.E., Fairlie D.P. "Protein α-turns recreated in structurally stable small molecules" *Angew. Chem. Int. Ed.* **2011**, *50*, 11107–11111 (b) Kelso M.J., Beyer R.L., Hoang H.N., Lakdawala A.S., Snyder J.P., Oliver W.V., Robertson T.A., Appleton T.G., Fairlie D.P. "Alpha-turn mimetics: short peptide alpha-helices composed of cyclic metallopentapeptide modules" *J. Am. Chem. Soc.* **2004**, *126*, 4828-4842

3.4 *Computational Design*

In order to investigate the presence of a preferred conformation able to mimic an ordered protein secondary structure, a computer aided conformational analysis was performed on **1a** (6*S*, 12a*S* stereochemistry, IUPAC atom numbering as in **Figure 37**) and diastereoisomeric **1b** (6*R*, 12a*S*). Compounds **1a** and **1b** were submitted to an unconstrained Monte Carlo (MC) conformational search combined with Molecular Mechanics (MM) minimization. For each compound 972 conformers were generated and after removal of duplicated minima, only conformations within 6 kcal/mol of the global minimum were considered. 35 and 33 conformers were kept for compound **1a** and **1b**, respectively. As a main indication of a stable secondary structure, the presence of intramolecular hydrogen bonds was first evaluated.

Two H-bond have been identified, a 7-membered ring H-bond (H-bond *A*, **Figure 39**) between the N_5H hydrogen and the C_3 carbonyl and a 13 membered ring H-bond (H-bond *B*) between the N_5H hydrogen and the C_1 carbonyl, here represented by the Cbz carbonyl. To assess the presence of turn conformations we also measured the interatomic distance $d\alpha$ between the terminal $C_{\alpha 5}$ atom and the benzyl oxygen of the Cbz (which emulates the $C_{\alpha 1}$ atom), assuming a value $d\alpha < 7$Å as a probe of a generic reverse turn. Results are reported as number of conformers which meet the geometrical features.

1a * = 6*S*, 12a*S*
1b * = 6*R*, 12a*S*
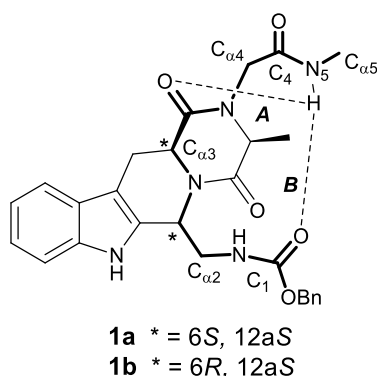
Figure 39. Hydrogen bond pattern for scaffolds **1a** and **1b**.

Table 6. MC/MM Conformational Analysis for peptidomimetics **1a** and **1b**.
The + symbol indicates the presence in the global minimum.

	Conf. within 6 kcal/mol	H-bond *A* (7-membered)	H-bond *B* (13-membered)	$d\alpha < 7$Å
1a	35	17	4 +	4 +
1b	33	22 +	1	1

The most frequently observed is the 5→3 H-bond (H-bond *A*) which is related to a classical γ-turn around these residues, and a 5→1 H-bond (H-bond *B*) which can be identified as an *α*-turn (this conformation is present in four conformers for compound **1a**). Inspection of the global minimum showed the *α*-turn conformation only for compound **1a**. For this diastereoisomer, the first four low energy conformers all adopt the *α*-turn conformation (presence of the 5→1 H-bond and average $d\alpha$ = 5.1 Å): according to a Boltzmann distribution analysis, these conformers take into account for the 94.5% of all the conformers obtained by the MC/MM analysis. On the other hand, for compound **1b**, the lowest energy conformers all have the 5→3 H-bond (classical γ-turn), with the only *α*-turn conformation lying 5.9 kcal/mol above the global minimum. Inspection of the virtual torsion angles of the amide backbone revealed the preference for an inverse γ-turn of the low energy conformers of **1b** (φ = -80.1°, ψ = 79.6° average based on the conformers accounting for the 93% of all the conformers from a Boltzmann distribution analysis). For compound **1a** the averages of torsion angles value were φ ($C_{\alpha 2}$) = -81.5°, ψ ($C_{\alpha 2}$) = 64.5°, φ ($C_{\alpha 3}$) = 146.3°, ψ ($C_{\alpha 3}$) = 36.9°, φ ($C_{\alpha 4}$) = 120.5°, ψ ($C_{\alpha 4}$) = -29.3°. According to the classification of *α*-turns in protein structures,[112] compound **1a** is an *α*-turn mimetic with a B-α_L-X designation. In **Figure 40** the low energy conformers of **1a** and **1b** are represented. These pictures well highlight the crucial role of the C6 configuration in favoring either an *α*-turn conformation (**1a**) or a γ-turn conformation (**1b**).
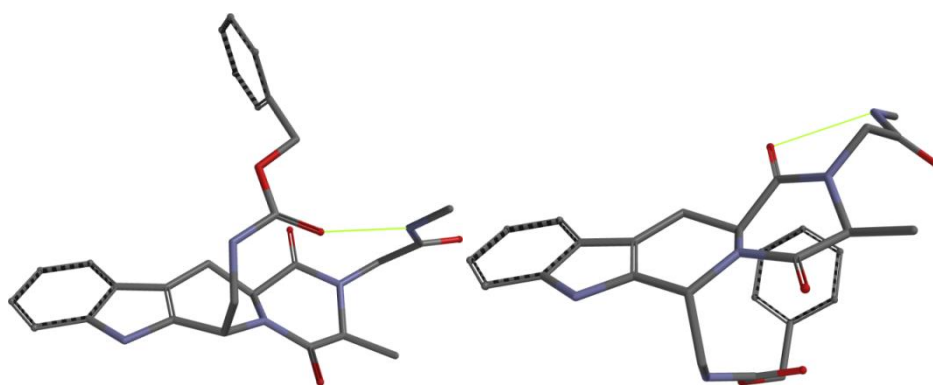
Figure 40. Perspective view of the low energy conformers of **1a** and **1b**.
Hydrogen atoms are omitted for clarity.

Finally, having ascertained by means of further calculations the irrelevance of the C3 configuration on the expected secondary structure, we fixed it as 3*S*. Being interested in unusual reverse turns, we then pursued the synthesis of peptidomimetic **1a**.

3.5 *Synthesis*

Starting from L-tryptophan methyl ester and *N*-Cbz-aminoacetaldehyde dimethyl acetal, tetrahydro-β-carboline **2** was obtained in good yield and high diastereoselectivity (d.r. 6:1 from ^{1}H NMR) by means of Pictet-Spengler reaction[117] and subsequent chromatographic separation.
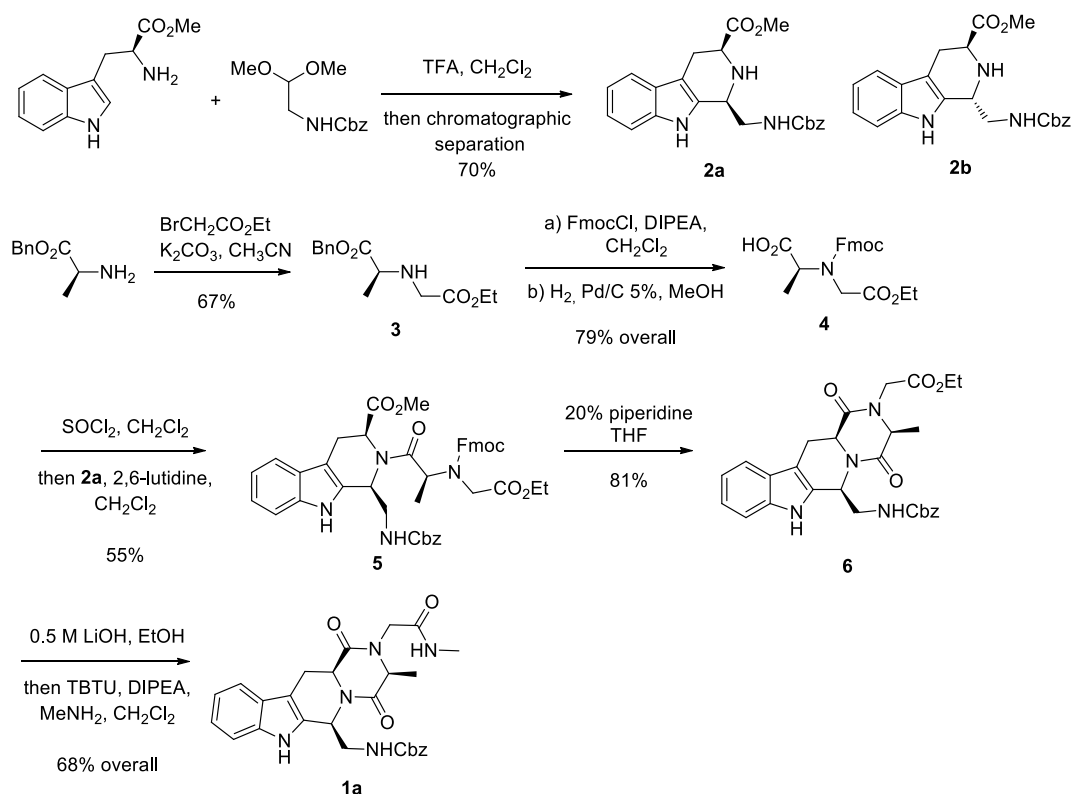
Scheme 14. Synthesis of **1a**.

The 6*S*, 12a*S* stereochemistry of the prevailing diastereoisomer was easily ascertained by application of the protocol of Ungemach et al.[118] on the ^{13}C NMR spectrum of compound **2** and, conclusively, by the observation of an intense NOE contact between H-6 and H-12a in the 2D NOESY spectrum. Alkylation of L-alanine benzyl ester with ethyl bromoacetate afforded amine **3**,[119] on which *N*-Fmoc protection and subsequent

[117] Pulka K., Tymecka D., Frankiewicz L., Wilczek M., Kozminski W., Misicka A. "Diastereoselective Pictet–Spengler condensation of tryptophan with *α*-amino aldehydes as chiral carbonyl components" *Tetrahedron*, **2008**, *64*, 1506-1514

[118] Ungemach F., Soerens D., Weber R., Di Pierro M., Campos O., Mokry P., Cook J.M., Silverton J.V. "General method for the assignment of stereochemistry of 1,3-disubstituted 1,2,3,4-tetrahydro-beta-carbolines by carbon-13 spectroscopy" *J. Am. Chem. Soc.* **1980**, *102*, 6976-6984

[119] Coppola G.M., Iwaki Y., Karki R.G., Kawanami T., Ksander G.M., Mogi M. PCT Int. Appl. (**2010**), WO 2010136493 A1 20101202

carefully conducted hydrogenolysis of the benzyl ester were performed,[120] to give acid **4** in acceptable overall yield.

Condensation of acid **4** with secondary amine **2** proved to be troublesome in a wide range of conditions, probably due to the severe steric hindrance of both the amine and acid coupling partners. At the end, acceptable yields could be obtained via formation of the chloride intermediate,[121] by reaction of acid **4** with thionyl chloride, and subsequent coupling with **2** in CH_2Cl_2 and 2,6-lutidine to give **5**. The formation of the fused, tetracyclic THBC-DKP ring system was then easily achieved by removal of the *N*-Fmoc protecting group[122]and spontaneous lactamization to give the diketopiperazine ring of **6**. The obtained compound **6** represents a valuable peptidomimetic, whose potential is also related to the possibility of further derivatization with desired pharmacophoric groups, on both the terminal acid and amine functional groups, for the development of conformationally constrained tryptophan-containing peptide ligands.

To investigate the actual secondary structure of the THBC-DKP scaffold also in solution, compound **6** was converted into the N-methyl carboxyamide derivative **1a**, by a two step procedure (0.5 M LiOH, 0 °C, then $MeNH_2$, TBTU, DIPEA), which was carefully conducted in order to avoid the easy epimerization of the C3 and C12a stereocenters. Direct transesterification performed with a methyl amine solution in ethanol showed such tendency to epimerize for the DKP constituting stereocenters.

 The study of conformational behavior was conducted in $CDCl_3$, to identify possible intramolecular hydrogen bonding.

[120] Shoulders M.D., Kotch F.W., Choudhary A., Guzei I.A., Raines R.T. "The aberrance of the 4S diastereomer of 4-hydroxyproline" *J. Am. Chem. Soc.* **2010**, *132*, 10857-10865

[121] Tantry S.T., Venkataramanarao R., Chennakrishnareddy G., Sureshbabu V.V. "Total synthesis of cyclosporin O by convergent approach employing Fmoc-amino acid chlorides mediated by zinc dust" *J. Org. Chem.* **2007**, *72*, 9360-9363

[122] Wang H., Ganesan A. "Concise synthesis of the cell cycle inhibitor demethoxyfumitremorgin C" *Tetrahedron Letters*, **1997**, *38*, 4327-4328

3.6 *Conformational Analysis*

The involvement of the NH amide protons in such bonding was first estimated from evaluation of their chemical shift value (δ) and of the temperature coefficients Δδ/ΔT (between 263 and 328 K). All data were measured at 2.0 mM concentration, that is in the absence of any noticeable intermolecular aggregation. While both NHMe and NHCbz chemical shift values are low (6.78 ppm for NHMe and 5.53 ppm for NHCbz), a significant difference could be appreciated between their temperature coefficients, ranging from 7.0 ppb K^{-1} (in absolute value) for the NHMe signal to 2.3 ppb K^{-1} (in absolute value) for the NHCbz signal. According to the literature,[123] these data could be attributed to a situation of equilibrium between hydrogen-bonded and non-hydrogen-bonded states for the NHMe amide proton and a completely non-hydrogen-bonded state for the NHCbz amide proton. In addition, a supplementary indication of the different hydrogen-bonding state for the two NH protons was obtained from DMSO titration studies in CDCl$_3$,[124] indicating that the chemical shift of the NHMe has a minor variation (0.24 ppm) upon addition up to 30% of the competitive solvent DMSO, with respect to the chemical shift of NHCbz, varying of 0.82 ppm.
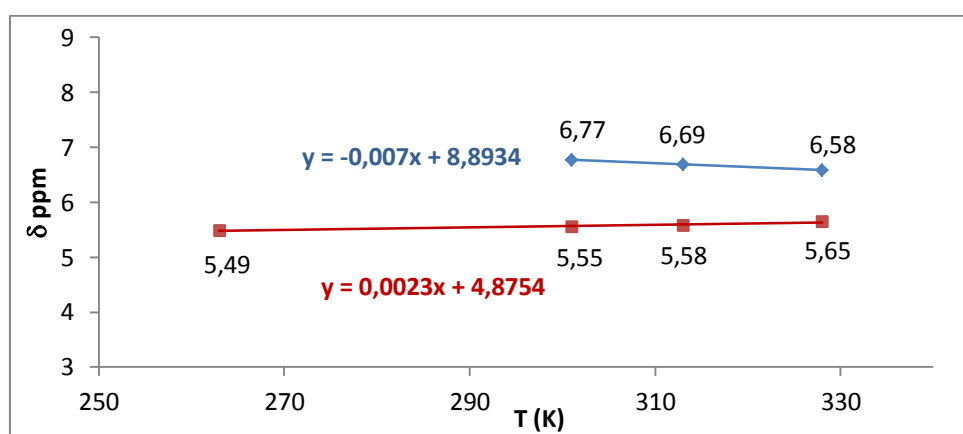
Figure 41. VT-NMR for N**H**-Me and N**H**-Cbz (CDCl$_3$, 2 mM, **1a**).

Taking into account the suggestions from the molecular modeling and these experimental results, for **1a** we can presume the presence in solution of conformers bearing a thirteen-membered intramolecular hydrogen bond involving the NHMe proton and the Cbz carbonyl group, as visualized in the perspective view of the low energy conformer of **1a**.

[123] Belvisi L., Gennari C., Mielgo A., Potenza D., Scolastico C. "Conformational Preferences of Peptides Containing Reverse-Turn Mimetic Bicyclic Lactams: Inverse γ-Turns versus Type-II' β-Turns – Insights into β-Hairpin Stability" *Eur. J. Org. Chem.* **1999**, 389-400

[124] For DMSO-d_6/CDCl$_3$ solutions, chemical shifts were standardized by reference to residual proton resonance for CHD$_2$CD$_3$SO (2.49 ppm).

3.7 *Underline* Conclusion

We realized the synthesis of a new constrained THBC-DKP based scaffold able to mimic an α-turn. It was designed with the aid of computational tools, which highlight the relative *cis* arrangement of the substituents on the THBC piperidine ring as a crucial requirement in order to obtain the correct geometry for mimicry.

Following these studies, the desired isomer **1a** of the THBC-DKP based peptidomimetic was synthesized. ^{1}H NMR conformational studies confirmed the presence of the intramolecular thirteen-membered hydrogen bond which characterizes the α-turn conformation, even if a situation of equilibrium between hydrogen-bonded and non-hydrogen-bonded states can be observed. Nevertheless, this scaffold represents one of the rare examples of a designed constrained α-turn mimic.[125]

---

[125] Airaghi F., Fiorati A., Lesma G., Musolino M., Sacchetti A., Silvani A. "The Diketopiperazine fused Tetrahydro-β-Carboline Scaffold as a Model Peptidomimetic with an Unusual α-Turn Secondary Structure" *submitted*

3.8 Experimental Details

Chemistry

All solvents were distilled and properly dried, when necessary, prior to use. All chemicals were purchased from commercial sources and used directly, unless otherwise indicated. All reactions were run under nitrogen atmosphere, unless otherwise indicated. All reactions were monitored by thin layer chromatography (TLC) on precoated silica gel 60 F_{254}; spots were visualized with UV light (254 nm) and by treatment with 1% aqueous $KMnO_4$ solution, Ninhydrin solution in ethanol or Cerium-ammonium-molybdate (CAM) reactive. Products were purified by flash chromatography on silica gel 60 (230-400 mesh). ^1H and ^{13}C NMR spectra were recorded with 300 and 400 Mhz spectrometers using chloroform-d (CDCl$_3$), dimethylsulfoxide-d_6 (DMSO-d_6), acetonitrile-d_3 (CD$_3$CN) or methanol-d_4 (CD$_3$OD). Chemical shifts (δ) are expressed in ppm relative to TMS at $\delta = 0$ ppm for ^1H NMR and relative to CDCl$_3$ at $\delta =$ 77.16 ppm for ^{13}C NMR. High-resolution MS spectra were recorded with a FT-ICR (Fourier Transform Ion Ciclotron Resonance) instrument, equipped with an ESI source, or a standard MS instrument, equipped with an EI source. Specific rotations were measured by a polarimeter "P-1030 Jasco" with 10 cm Optical path cells and 1 ml capacity.

Computational details

Conformational analysis was performed with the software Spartan '08 using a MC/MM protocol. The obtained conformers were then optimized with the semiempirical method AM1. The structures were then analyzed and clustered according to their secondary structure motifs.

Synthesis of 1a:
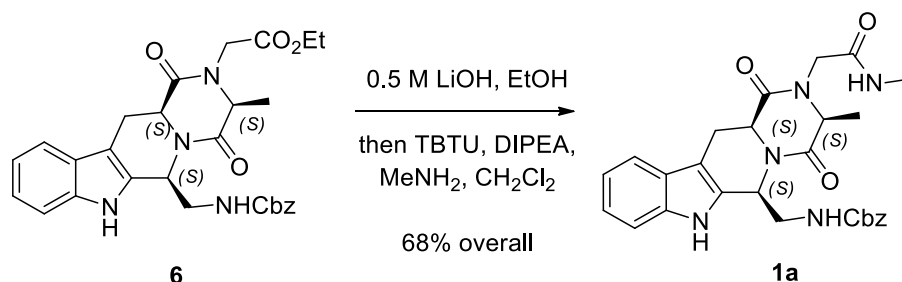
Benzyl (((3S,6S,12aS)-3-methyl-2-(2-(methylamino)-2-oxoethyl)-1,4-dioxo-1,2,3,4,6,7,12,12a-octahydropyrazino[1',2':1,6]pyrido[3,4-b]indol-6-yl)methyl)carbamate (1a)

Compound **6** (165 mg, 0.32 mmol, 518 g/mol) was dissolved in EtOH (3 ml). Aqueous LiOH (0.5 M, 2.54 mmol, 4.6 ml) was added and the reaction was stirred at 0 °C for 1 h. After then, the solution was acidified with HCl 1N (8 ml), extracted with AcOEt (3x20 ml), dried, filtered and concentrated. The crude was suspended in DCM (10 ml) under N$_2$, DIPEA (208 µl, 1.20 mmol) and TBTU (384 mg, 1.20 mmol) were added. After stirring for 30 minutes, MeNH$_2$ (2.0 M THF solution, 1.20 mmol, 601 µl) was added. The reaction was stirred for 24 h under N$_2$, then it was poured into water (20 ml) and extracted with AcOEt (3 x 20 ml), dried, filtered and concentrated. Purification by flash chromatography (AcOEt) afforded product **1a** (110 mg, 68% overall yield) as an oil.

The following data has been collected on a complex mixture of rotamers plus a 5% of **1b**.

$[\alpha]_D^{25}$ = -98.3 (*c* 0.75, MeOH). ^{1}H NMR (500 MHz, CD$_3$CN, major rotamer) δ 9.41 (bs, 1H) 7.55 (d, 1H, *J* = 7.6 Hz) 7.38 (d, 1H, *J* = 7.8 Hz) 7.34-7.23 (m, 5H) 7.13 (ddd, 1H, *J* = 7.8, 7.6, 0.9 Hz) 7.06 (dt, 1H, *J* = 7.6, 0.9 Hz), 6.95 (q, 1H, *J* = 4.7 Hz) 5.83 (q, 1H, *J* = 8.2, 5.1 Hz) 5.43 (t, 1H, *J* = 3.4 Hz) 4.90 (d, 1H, *J* = 12.3 Hz) 4.87 (d, 1H, *J* = 12.3 Hz) 4.26 (d, 1H, *J* = 17.0 Hz) 4.16 (q, 1H, *J* = 7.0 Hz) 4.14 (dd, 1H, *J* = 11.4, 5.5 Hz) 3.98 (ddd, 1H, *J* = 14.2, 8.2, 3.8 Hz) 3.94 (d, 1H, *J* = 17.0 Hz) 3.43 (dd, 1H, *J* = 15.6, 5.5 Hz) 3.26 (ddd, 1H, *J* = 14.2, 5.1, 3.2 Hz) 3.00 (dd, 1H, *J* = 15.6, 11.4 Hz) 2.69 (d, 3H, *J* = 4.7 Hz) 1.48 (d, 3H, *J* = 7.0 Hz). ^{13}C NMR (125.8 MHz, CD$_3$CN) δ 170.4, 170.0, 169.8, 157.8, 137.5, 135.2, 132.0, 129.0 (2C), 128.5, 128.3 (2C), 126.9, 122.2, 119.8, 118.7, 112.0, 108.1, 66.7, 55.4, 55.3, 53.5, 46.7, 44.7, 25.9, 22.7, 14.5. HRMS (EI) calcd. for [C$_{27}$H$_{29}$N$_5$O$_5$]$^+$: 503.2169, found 503.2186. (M$^+$)

¹H and ¹³C NMR of compound **1a**
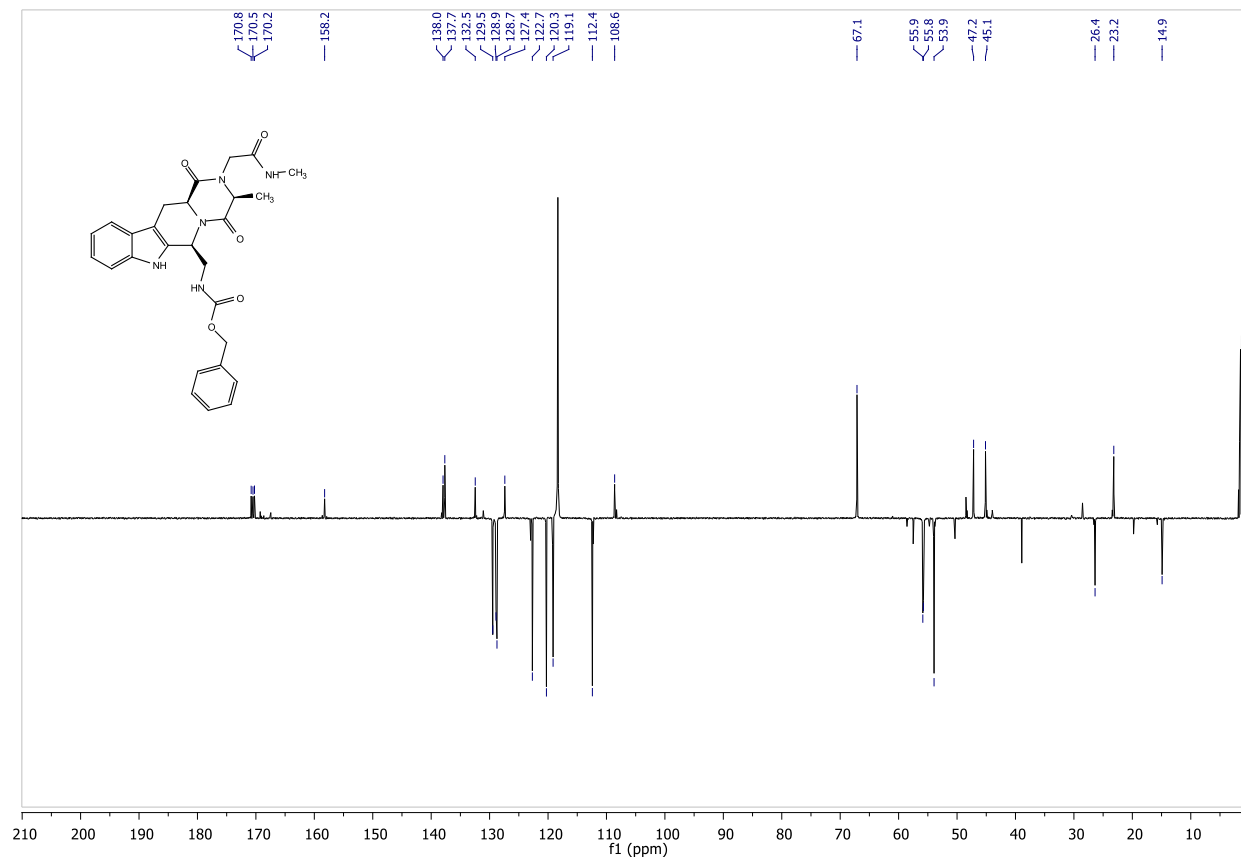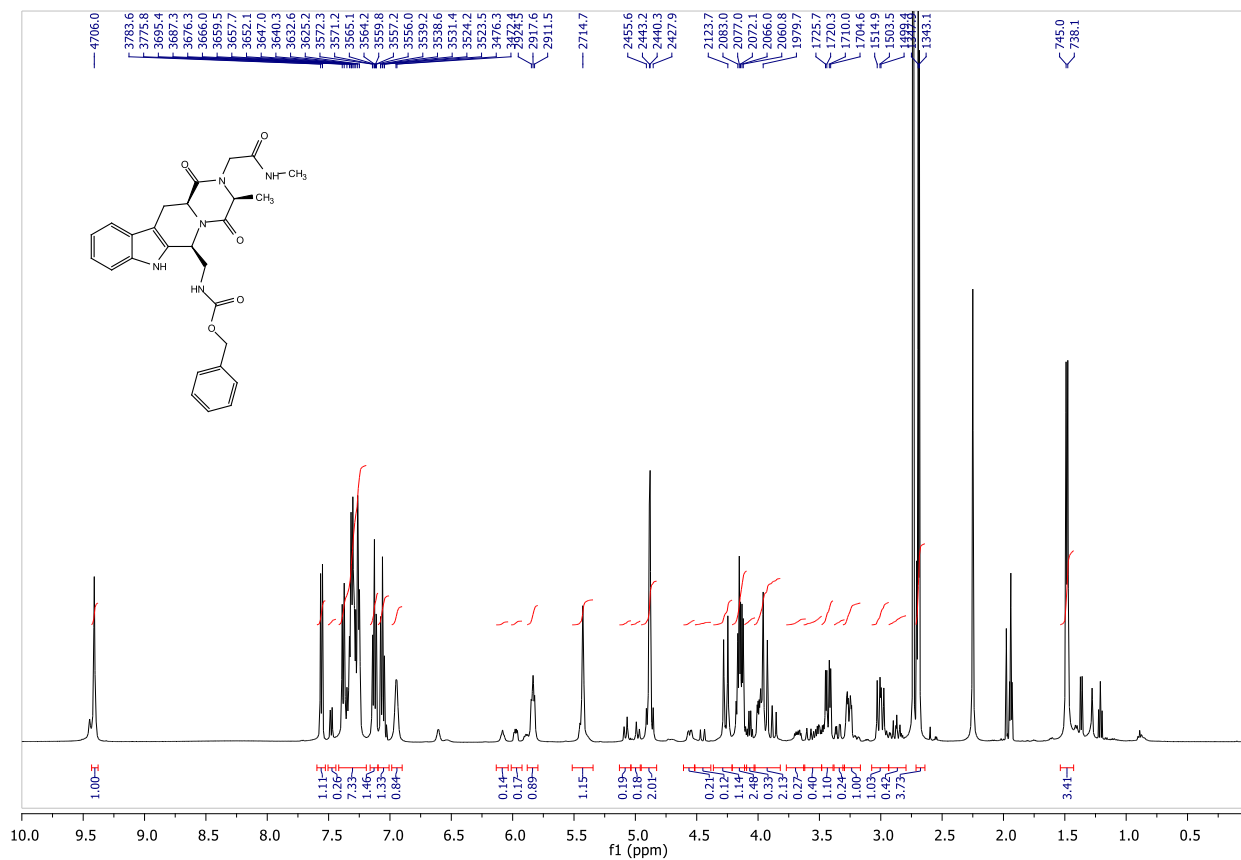
Synthesis of 2:
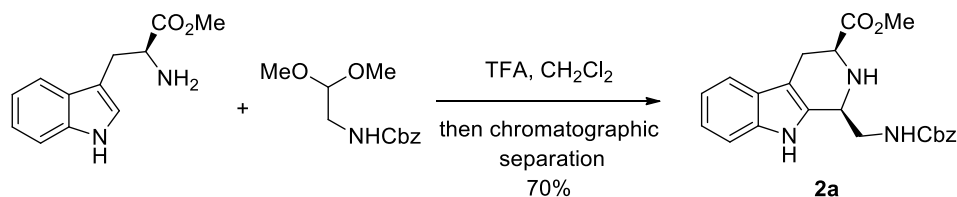
(1S,3S)-methyl 1-((benzyloxycarbonylamino)methyl)-2,3,4,9-tetrahydro-1H-pyrido[3,4-b]indole-3-carboxylate (2)

Under nitrogen atmosphere, L-tryptophan methyl ester (755 mg, 3.46 mmol, 1.0 eq) was dissolved in CH_2Cl_2 (30 ml, 0.12 M), then *N*-Cbz-aminoacetaldehyde dimethyl acetal (912 mg, 3.81 mmol, 1.1 eq) was added. The solution was cooled to -30 °C, then TFA was added (1.97 mg, 1.3 ml, 17.3 mmol, 5 eq). The mixture was kept for 2 hours at this temperature then reacted overnight at room temperature. The solution was diluted with AcOEt and washed three times with a saturated solution of $NaHCO_3$ (3x15 ml), dried over Na_2SO_4, filtered and evaporated under reduced pressure.

The crude mixture was purified by flash chromatography (Hex/AcOEt 6:4), 808 mg of (1S,3S)-**2** and 143 mg of the (1R,3S)-diastereoisomer were obtained (70% overall yield, 6:1 d.r.) as colourless oil.

$[\alpha]_D^{25}$ = -44.4 (*c* 1.0, CHCl₃). ¹H NMR (CDCl₃, 400 MHz) δ 8.96 (bs, 1H) 7.55-7.10 (m, 9H) 6.02 (dd, 1H) 5.03 (s, 2H) 4.40 (bs, 1H) 3.90-3.60 (m, 6H) 3.18 (dd, 1H, *J* = 15.0, 1.6 Hz) 2.88 (dd, 1H, *J* = 15.0, 11.2 Hz) 2.77 (bs, 1H). ¹³C NMR (CDCl₃, 101 MHz) δ 173.5, 157.3, 136.5, 136.3, 132.3,128.5-127.8 (5C), 127.0, 122.0, 119.5, 118.0, 111.3, 109.2, 66.9, 56.3, 53.6, 52.3, 44.3, 25.5. IR (cm⁻¹) 3018, 1709, 1514, 1362, 1267, 1228. HRMS (EI) calcd. for $[C_{22}H_{23}N_3O_4]^+$: 393.1689, found 393.1702. (M⁺)

^{1}H and ^{13}C NMR of compound **2**
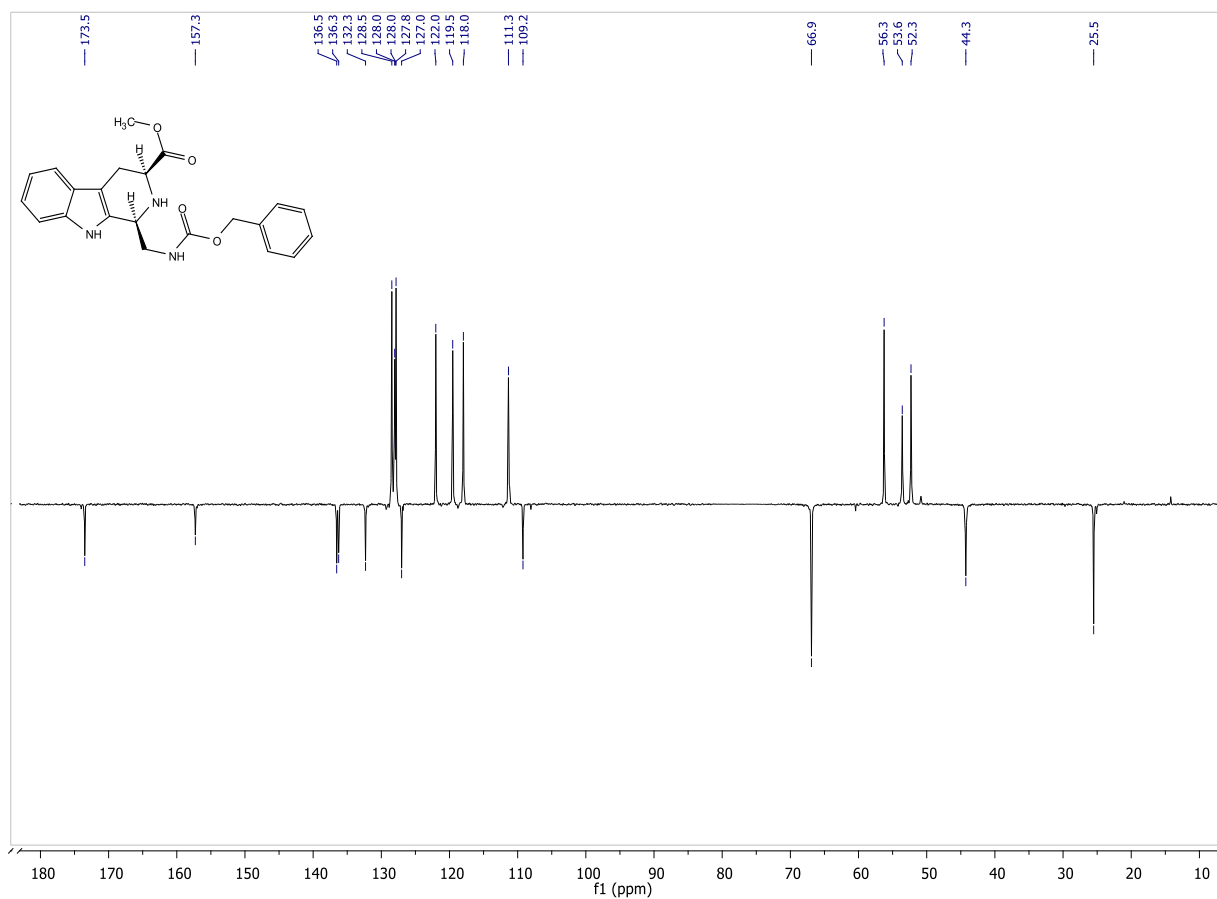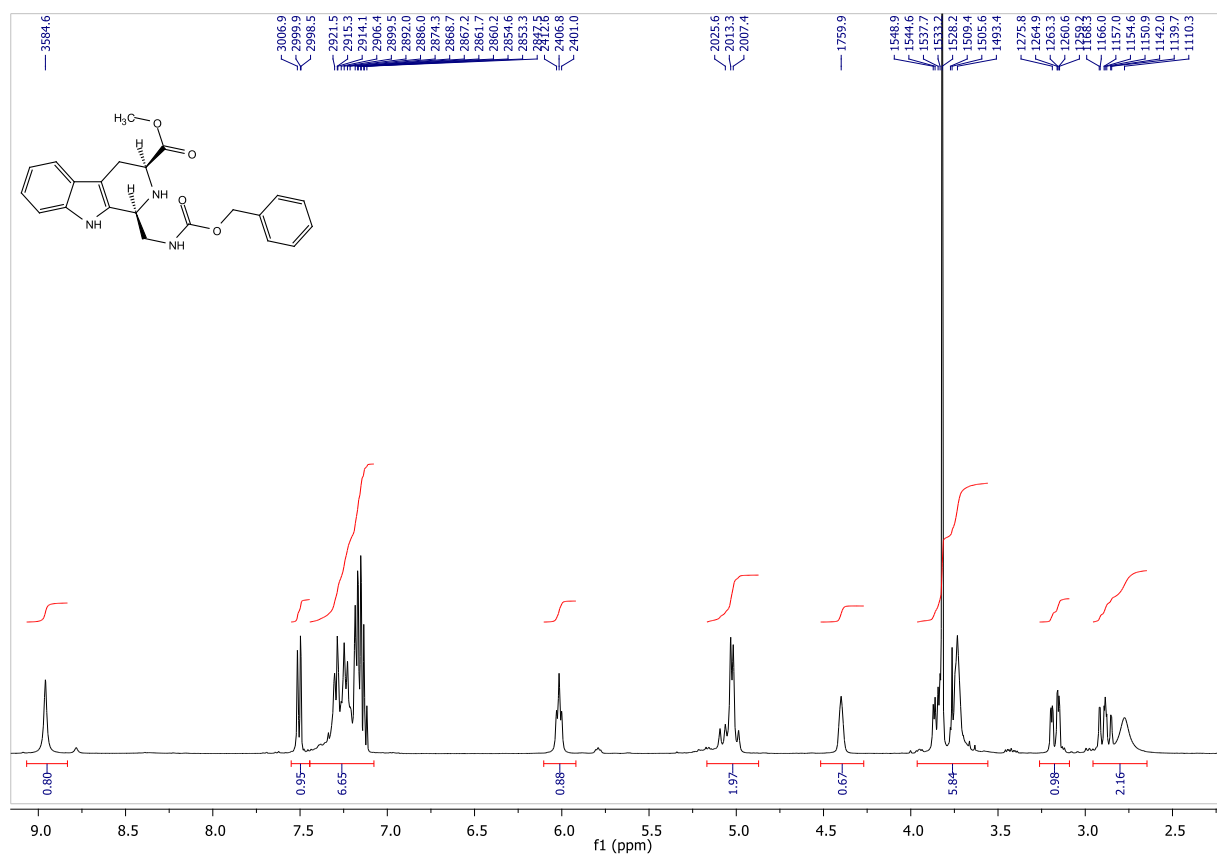
Synthesis of 3:
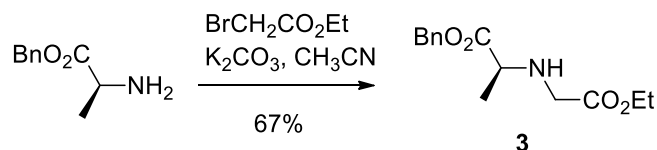
(*S*)-benzyl 2-((2-ethoxy-2-oxoethyl)amino) propanoate (3)

Under nitrogen atmosphere L-alanine-benzyl ester (500 mg, 2.79 mmol, 1 eq) was dissolved in CH_3CN (6 ml, 0.47 M), then K_2CO_3 (3.85 g, 27.90 mmol, 10 eq) was added. Ethyl bromoacetate (466 mg, 2.79 mmol, 310 μl, 1 eq) was added to the suspension, then mixture was reacted overnight at room temperature. The solvent was evaporated under reduced pressure, then the crude was dissolved in AcOEt (20 ml). The solution was extracted with an aqueous solution of H_3PO_4 5% (3x25 ml), the reunited aqueous layers were basified with Na_2CO_3 until pH 9 and extracted repeatedly with AcOEt. The reunited organic phases were dried with Na_2SO_4, filtered and evaporated under reduced pressure, to give compound 3 (503 mg, 67% yield), as a colourless oil.

$[\alpha]_D^{25}$ = -17.1 (*c* 1.0, CHCl$_3$). ^{1}H NMR (CDCl$_3$, 300 MHz) δ 7.4-7.28 (m, 5H) 5.2-5.1 (m, 2H) 4.15 (q, 2H, *J* = 8.6 Hz) 3.53 (q, 1H, *J* = 9.6 Hz) 3.49 (d, 1H, *J* = 17.3 Hz) 3.39 (d, 1H, *J* = 17.3 Hz) 2.37 (bs, 1H) 1.38 (d, 3H, *J* = 9.6 Hz) 1.25 (t, 3H, *J* = 8.6 Hz). ^{13}C NMR (CDCl$_3$, 75.4 MHz) δ 174.3, 171.4, 135.6, 128.6 (2C), 128.4, 128.2 (2C), 66.7, 61.0, 55.9, 48.7, 18.5, 14.2. HRMS (EI) calcd. for [$C_{14}H_{19}NO_4$]$^+$: 265.1314, found 265.1328. (M$^+$)

¹H and ¹³C NMR of compound **3**
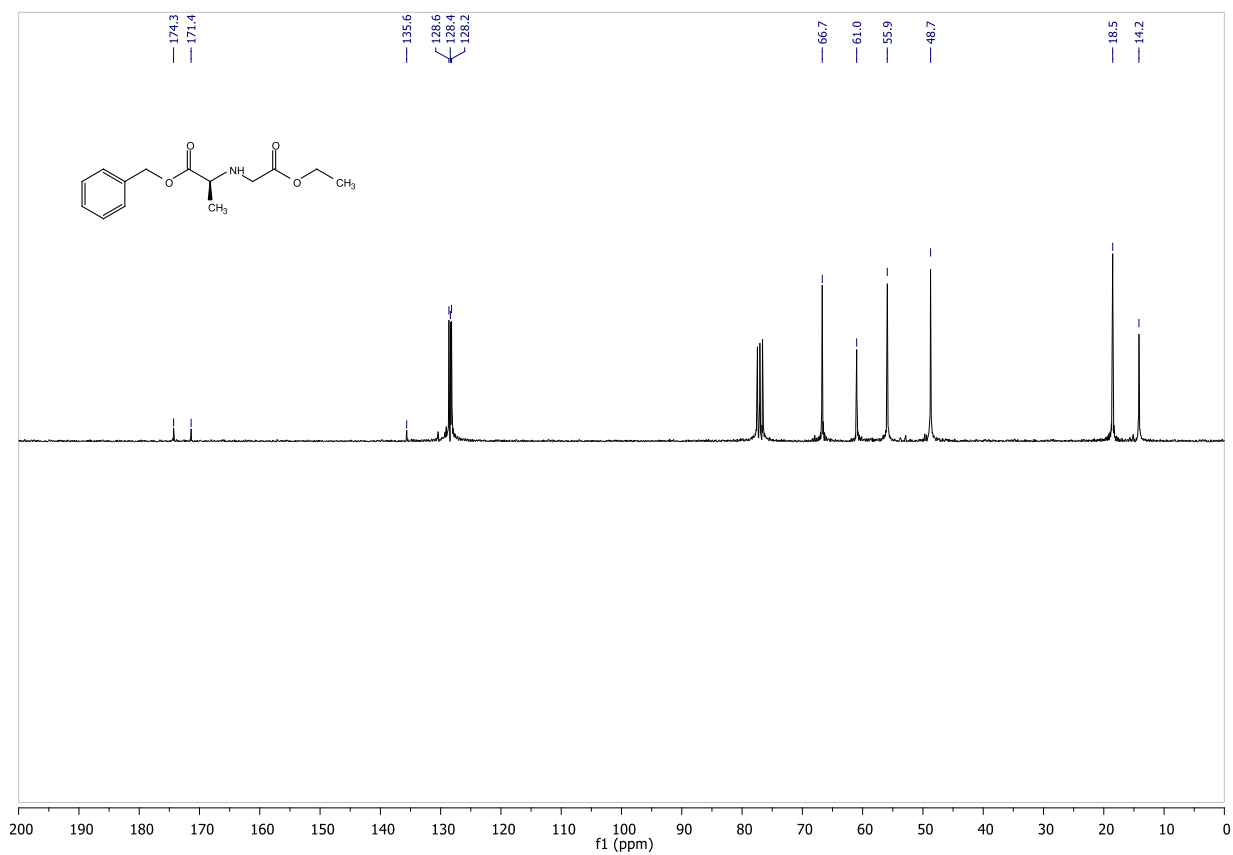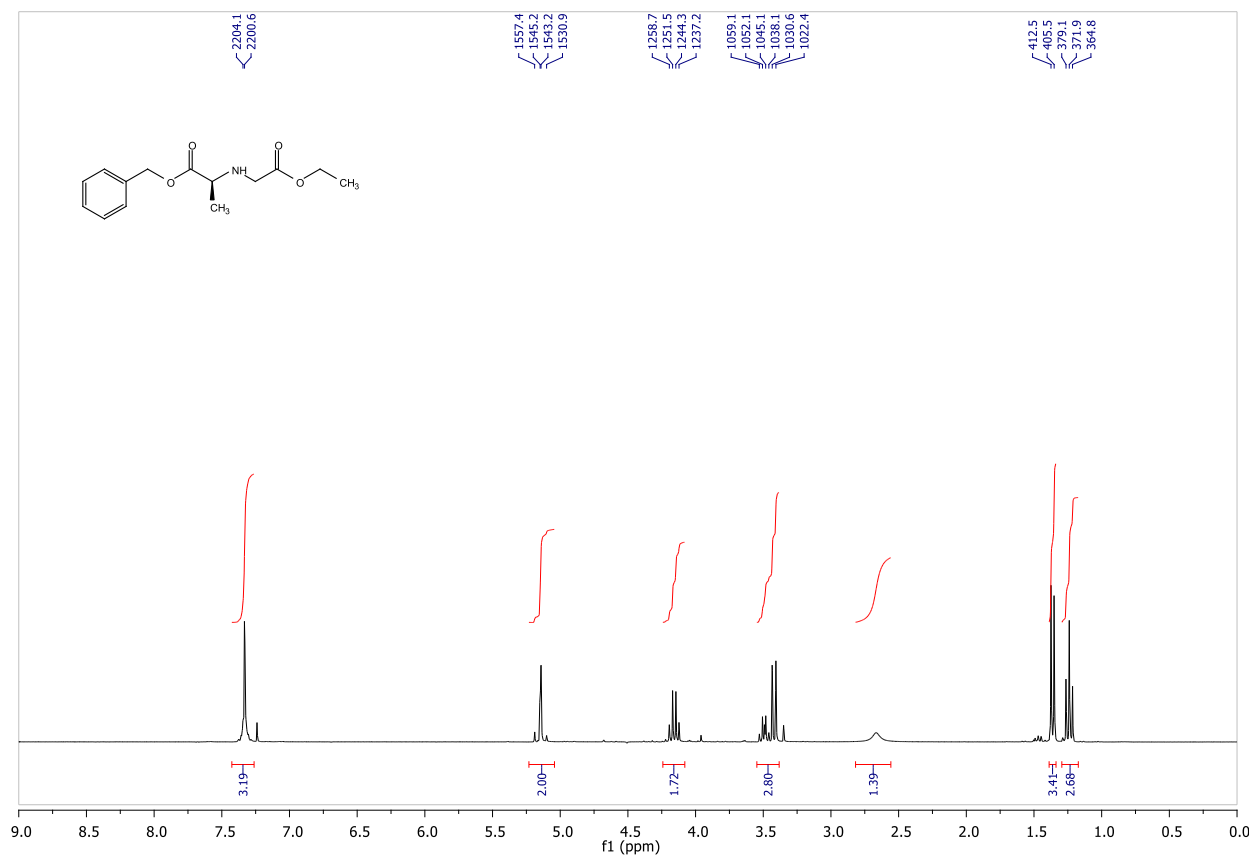
Synthesis of 4:
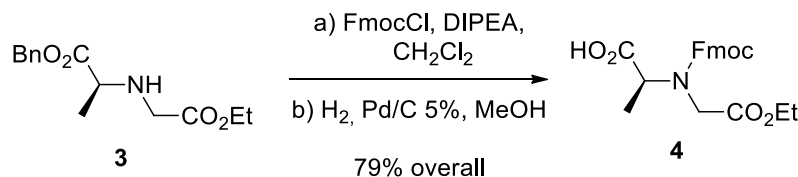
(S)-2-((((9H-fluoren-9-yl)methoxy)carbonyl)(2-ethoxy-2-oxoethyl)amino)propanoic acid (4)

Under nitrogen atmosphere, compound **3** (1.49 g, 5.62 mmol, 1 eq) and DIPEA (871 mg, 6.74 mmol, 1.17 ml, 1.2 eq) were dissolved in CH_2Cl_2 (40 ml, 0.14 M), then Fmoc-Cl (1.48 g, 5.73 mmol, 1.02 eq) was added. The mixture was stirred at room temperature overnight. Then CH_2Cl_2 (10 ml) was added, and the solution was washed with HCl 0.5 M (3x30 ml), the organic layer was dried with Na_2SO_4, filtered and evaporated under reduced pressure. The crude was dissolved in MeOH (100 ml, 0.045 M), then under nitrogen atmosphere Pd/C 5 % w/w (150 mg) was added. The resulting suspension was stirred for 3 hours under hydrogen atmosphere at room temperature. Reaction was accurately monitored by TLC in order to prevent hydrogenolysis of the Fmoc group. The suspension was filtered on a layer of celite, the solution was evaporated under reduced pressure, the crude was dissolved in AcOEt and then was extract three times with a saturated solution of $NaHCO_3$. The reunited aqueous phases were acidified with HCl 0.5 M and extracted with AcOEt (3x35 ml), dried with Na_2SO_4, filtered and evaporated under reduced pressure, to give pure **4** (1.76 g, 79% overall yield) as an oil.

$[\alpha]_D^{25}$ = -9.42 (*c* 1.0, MeOH). ^{1}H NMR (DMSO at 95°C, 300 MHz) δ 7.88 (d, 2H, *J* = 7.5 Hz) 7.64 (d, 2H, *J* = 7.4 Hz) 7.43 (t, 2H, *J* = 7.3 Hz) 7.34 (t, 2H, *J* = 7.3) 4.58 (q, 1H, *J* = 7.3 Hz) 4.38 (d, 2H, *J* = 6.3 Hz) 4.26 (t, 1H, *J* = 6.3 Hz) 4.12 (q, 2H, *J* = 7.1 Hz) 3.98 (d, 2H, *J* = 18.0 Hz) 1.37 (d, 3H, *J* = 7.3 Hz), 1.21 (t, 3H, *J* = 7.1 Hz). ^{13}C NMR (CDCl$_3$, 75.4 MHz, mixture of two rotamers) δ 175.4 and 174.5, 171.8 and 170.7, 155.7 and 155.6, 143.7, 143.6, 141.2 (2C), 127.7 (2C), 127.1 (2C), 124.9 (2C), 120.0 (2C), 68.6 and 68.2, 62.2 and 61.8, 55.7 and 55.5, 47.6 and 47.1, 47.0, 15.5 and 14.9, 14.1. IR (cm^{-1}) 2954, 1750, 1709, 1467, 1451, 1325, 1204. HRMS (EI) calcd. for $[C_{22}H_{23}NO_6]^+$: 397.1525, found 397.1541. (M$^+$)

¹H and ¹³C NMR of compound **4**
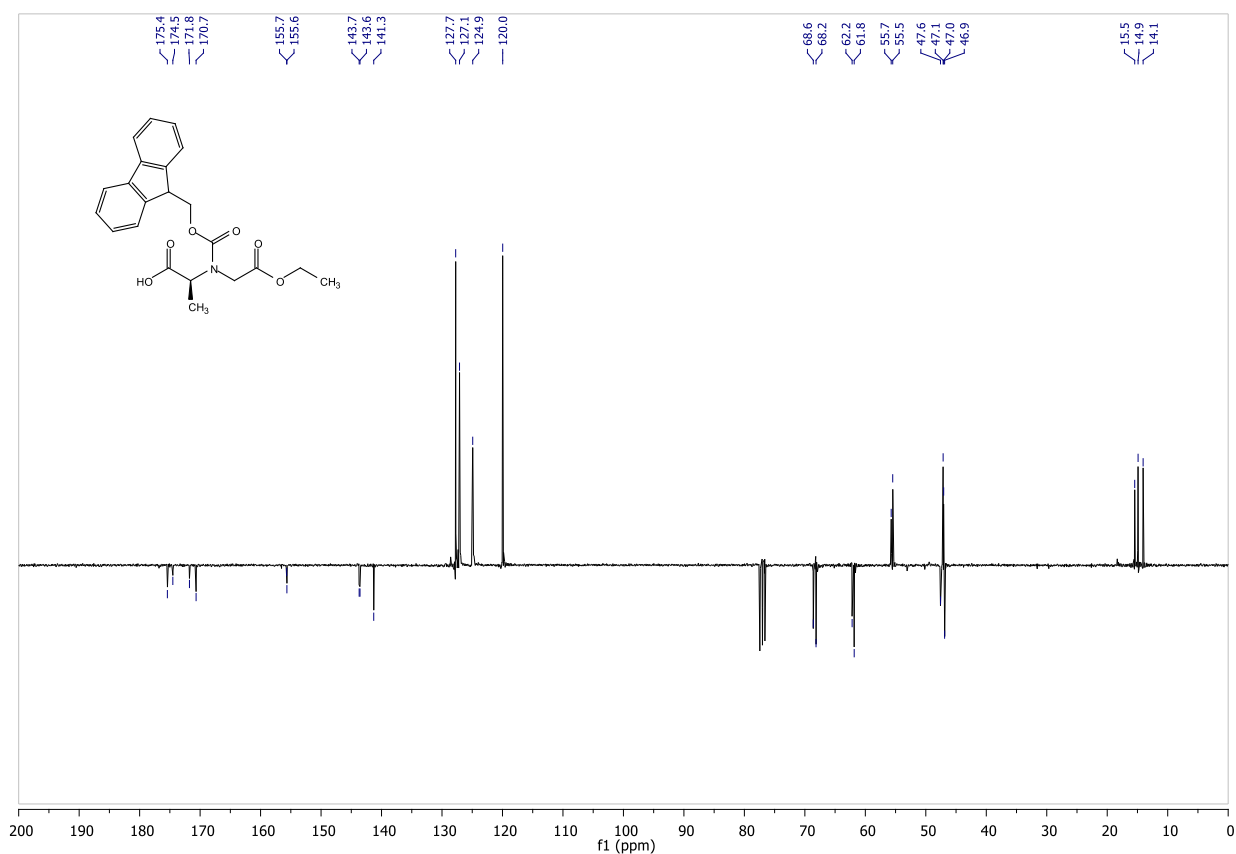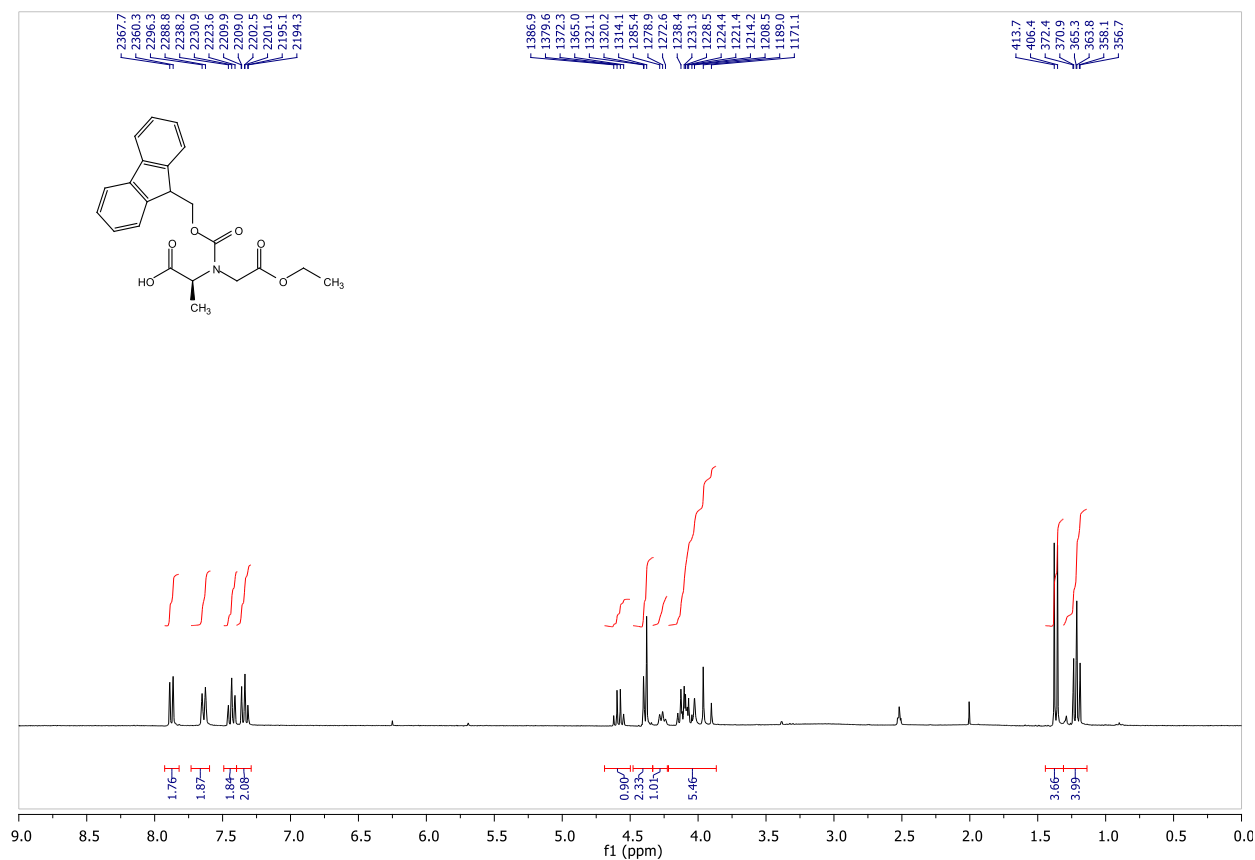
Synthesis of 5:
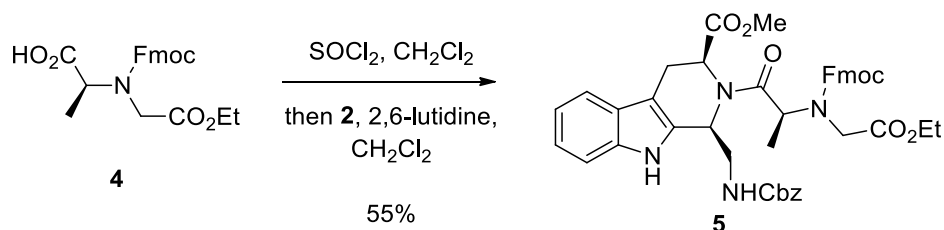
**(1S,3S)-methyl 2-((S)-2-((((9H-fluoren-9-yl)methoxy)carbonyl)(2-ethoxy-2-oxoethyl)amino)propanoyl)-1-((((benzyloxy)carbonyl)amino)methyl)-2,3,4,9-tetrahydro-1H-pyrido[3,4-b]indole-3-carboxylate (5)**

Under nitrogen atmosphere, compound **4** (302 mg, 0.76 mmol, 1 eq) was dissolved in CH_2Cl_2 (4 ml, 0.19 M), the solution was cooled at 0°C, then $SOCl_2$ (904 mg, 7.60 mmol, 550 μl, 10 eq) was added. The mixture was stirred at room temperature for 5 hours, then evaporated under reduced pressure. The obtained crude was dissolved in CH_2Cl_2 (3 ml) and slowly added to a solution of **2** (299 mg, 0.76 mmol, 1 eq) and 2,6 lutidine (110 mg, 1.03 mmol, 120 μl, 1.35 eq) in CH_2Cl_2 (5 ml), cooled at 0° C under nitrogen atmosphere. The mixture was stirred at room temperature overnight, then CH_2Cl_2 (10 ml) was added, the organic layer was washed with HCl 0.5 M (5 ml), saturated aq. $NaHCO_3$ (5 ml) and brine (5 ml). The organic phase was dried with Na_2SO_4, filtered and evaporated under reduced pressure. The crude was purified by chromatographic column (Hex/AcOEt, 6:4), affording **5** (321 mg, 55% yield) as an oil.

$[\alpha]_D^{25}$ = +17.87 (*c* 1.0, CHCl₃). ¹H NMR (CDCl₃, 300 MHz, major rotamer) δ 9.87 (bs, 1H) 7.88-7.00 (m, 17H) 6.07 (bs, 1H) 5.45 (br, q, 1H) 5.32 (bs, 1H) 5.23 (bs, 2H) 4.71-4.32 (m, 2H) 4.20-4.10 (m, 5H) 4.08-3.74 (m, 3H) 3.74-3.08 (m, 5H) 1.48 (d, 3H, *J* = 7.5 Hz) 1.25 (d, 3H, *J* = 7.3 Hz). ¹³C NMR (CDCl₃, 100 MHz, major rotamer) δ 171.1, 169.3, 169.1, 155.9, 154.2, 143.9, 141.2, 136.4, 130.6, 128.5-111.5 (22C), 68.8, 67.1, 61.4, 56.3, 54.8, 52.1, 51.0, 47.1, 47.0, 46.6, 24.4, 15.3, 14.2. HRMS (EI) calcd. for $[C_{44}H_{44}N_4O_9]^+$: 772.3108, found 772.3095. (M⁺)
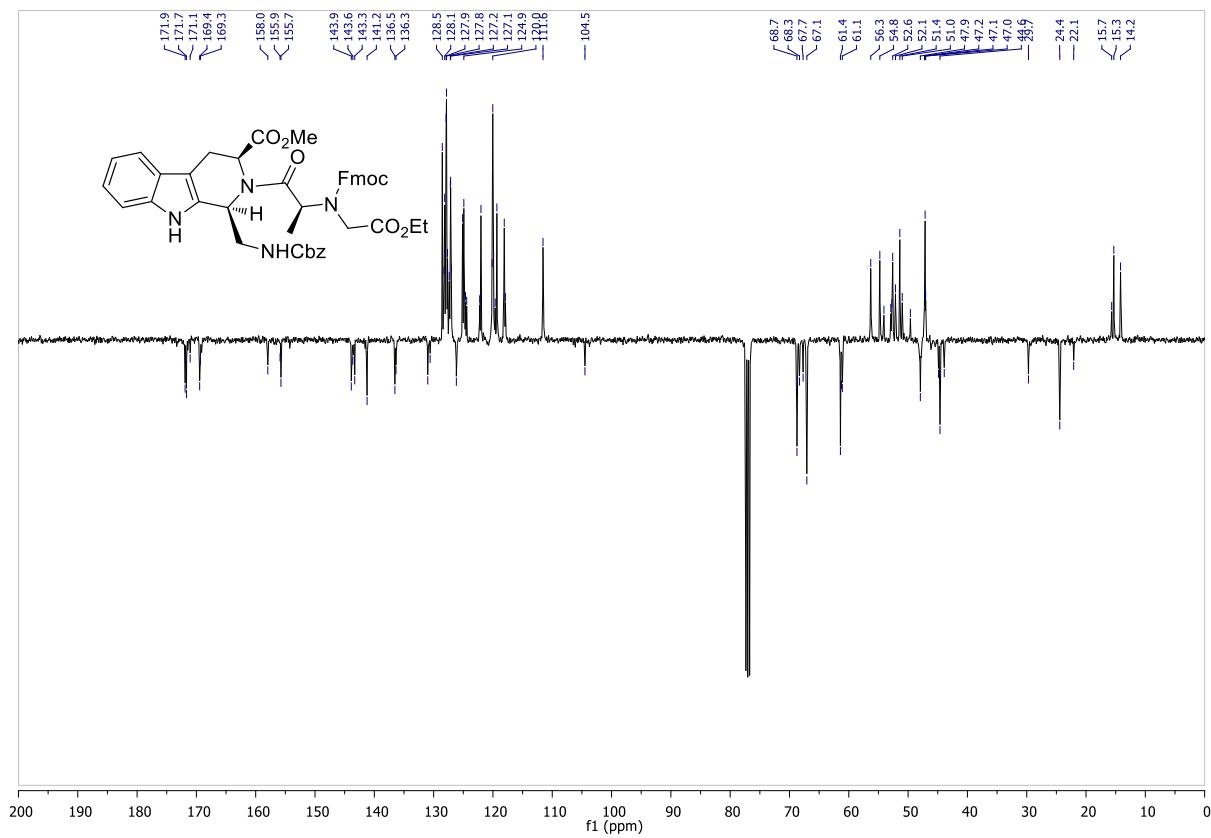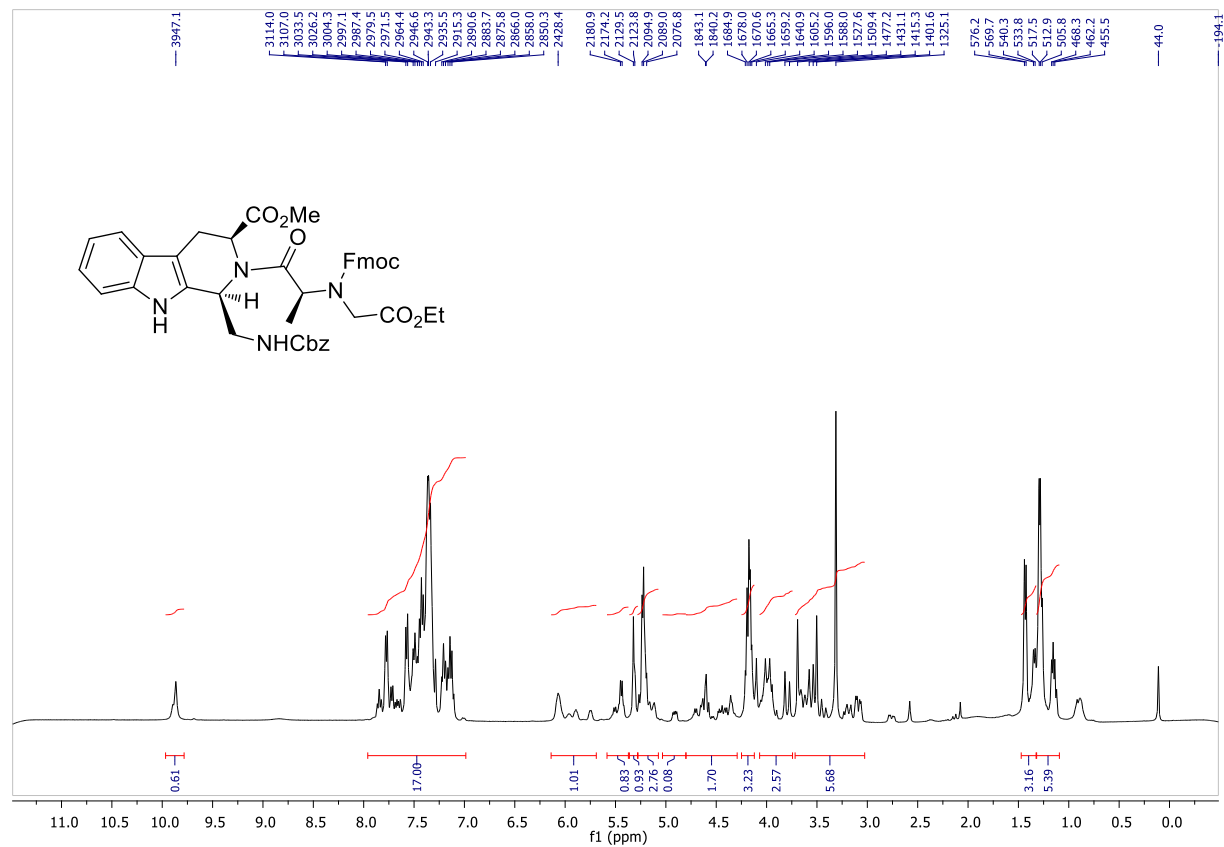
Synthesis of 6:
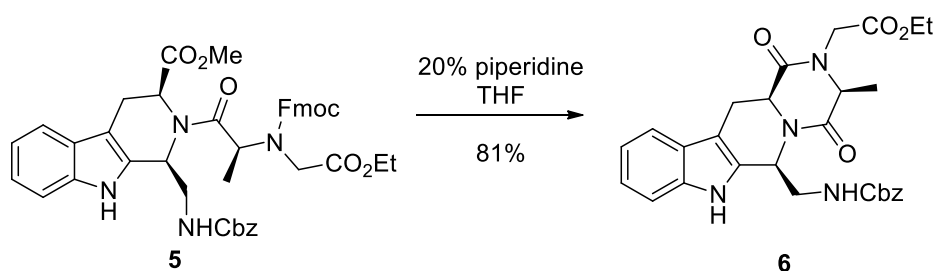
Ethyl 2-((3S,6S,12aS)-6-((benzyloxycarbonylamino)methyl)-3-methyl-1,4-dioxo-3,4,12,12a-tetrahydropyrazino[1',2':1,6]pyrido[3,4-b]indol-2(1H,6H,7H)-yl) acetate (6)

Compound **5** (300 mg, 0.39 mmol) was dissolved in THF (13 ml, 0.03 M), then piperidine was added (2.6 ml). The solution was reacted overnight, then HCl 0.5 M was added and the mixture was extracted with AcOEt (3x30 ml). The reunited organic layers were dried with Na_2SO_4, filtered and evaporated under reduced pressure. The crude was purified by chromatographic column (Hex/AcOEt from 6:4 to 4:6), to give **6** (165 mg, 81% yield) as an oil.

$[\alpha]_D^{25}$ = -59.5 (*c* 1.0, CHCl$_3$). ^{1}H NMR (CDCl$_3$, 400 MHz, major rotamer) δ 9.27 (bs, 1H) 7.55-7.10 (m, 9H) 5.91 (bs, 1H) 5.15-5.09 (m, 3H) 4.50 (d, 1H, *J* = 17.2 Hz) 4.26 (m, 4H) 4.05 (m, 1H) 3.97 (d, 1H, *J* = 17.5 Hz) 3.68 (m, 1H) 3.57 (d, 1H, *J* = 15.6 Hz) 3.07 (dd, 1H, *J* = 15.6, 11.8 Hz) 1.58 (d, 3H, *J* = 12.8 Hz) 1.31 (t, 3H, *J* = 7.2 Hz). ^{13}C NMR (CDCl$_3$, 75.4 MHz) δ 168.9, 168.5, 167.3, 157.6, 136.5, 136.3, 130.7, 128.6, 128.2, 128.0, 126.2, 122.5, 119.9, 119.8, 118.3, 111.7, 107.7, 67.1, 61.8, 57.6, 57.2, 56.3, 45.0, 44.7, 31.6, 25.2, 17.9, 14.2. IR (cm^{-1}) 3016, 1742, 1667, 1506, 1455, 1326, 1222. HRMS (EI) calcd. for [C$_{28}$H$_{30}$N$_4$O$_6$]$^+$: 518.2165, found 518.2178. (M$^+$)
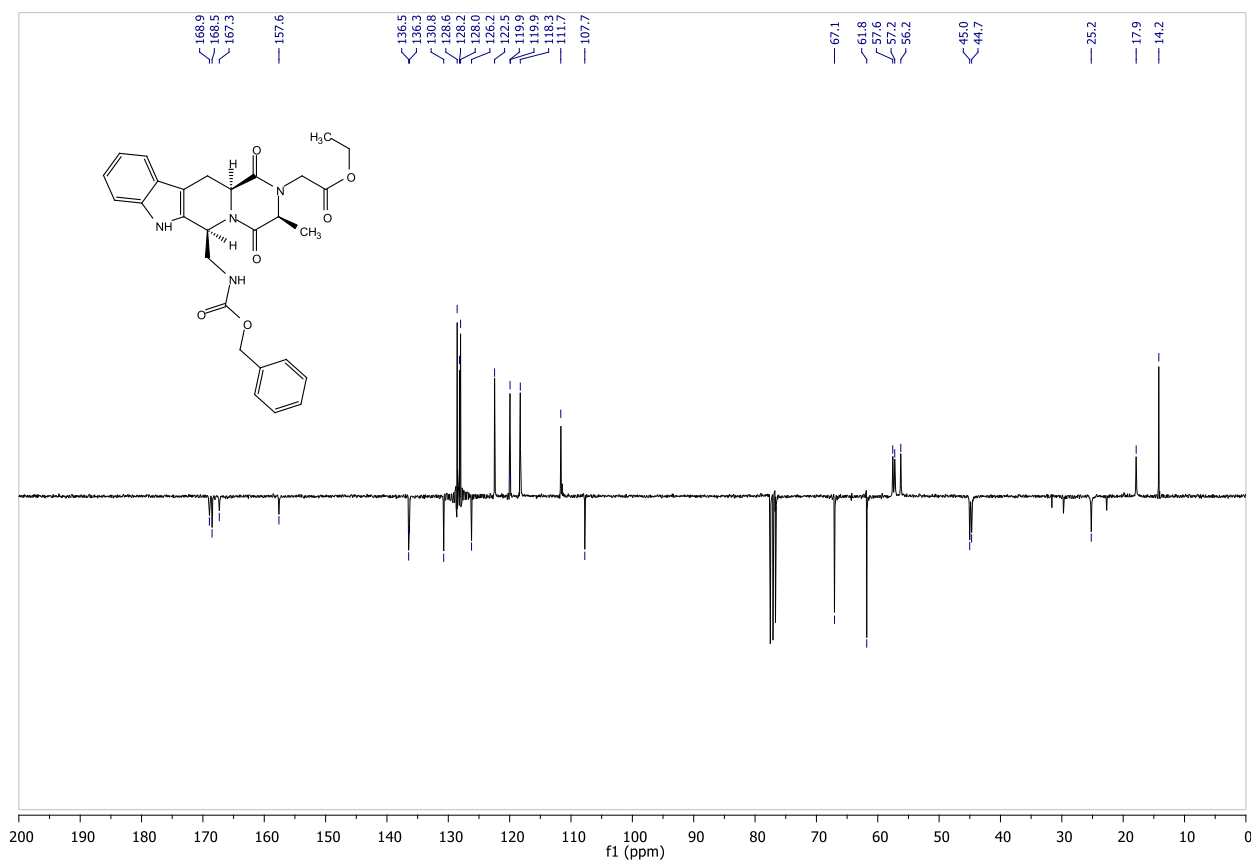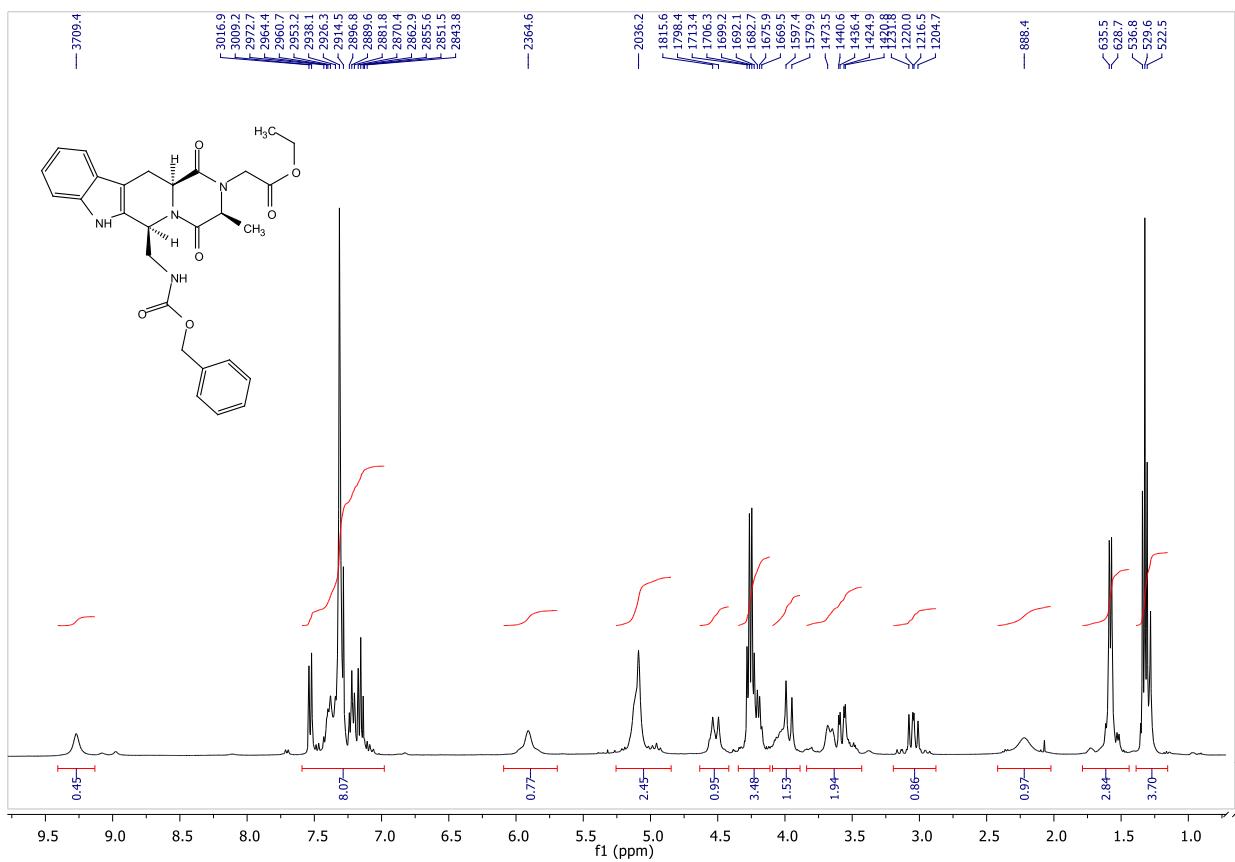
CHAPTER IV: POP INHIBITORS

The research presented in the following chapter has been exclusively carried out at McGill University (Montreal, QC – Canada) under the supervision of Prof. N. Moitessier.

4.1 *Prolyl OligoPeptidase*

Prolyl Oligopeptidase family represents a relatively new class of serine peptidases. It was first described in 1991, based on the amino acid sequence homology of prolyl oligopeptidase, dipeptidyl peptidase IV and acyl-aminoacyl peptidase.[126] The fourth major member of the group was added when the amino acid sequence of oligopeptidase B was determined.[127] Several complementary DNAs (cDNAs) related to the proteins of the prolyl oligopeptidase family have also been cloned from various sources. Some of them lacking the catalytic serine residue were inactive. The prolyl Oligopeptidase group called family S9 has been grouped with other families into the SC clan of serine peptidases.[128] Based on the structural relationship between these enzymes and lipases, and on secondary structural studies,[129] these enzymes have been considered as members of the α/β hydrolase fold enzymes. The amino acid sequence homology of the four basic peptidases is rather low, but they apparently share a similar three-dimensional structure. They display distinct specificities and represent different types of peptidases. Thus, prolyl oligopeptidase and oligopeptidase B are endopeptidases and are found in the cytosol. Acyl-aminoacyl peptidase and dipeptidyl peptidase IV are exopeptidases, acyl-aminoacyl peptidase is a cytoplasmic omega peptidase, whereas dipeptidyl-peptidase IV is a membrane bound enzyme that cleaves a dipeptide from the amino terminus of oligopeptides. The catalytically competent residues, the so-called catalytic triad (Ser, Asp and His), are concentrated in the carboxyl terminal region within about 130 residues.

The exopeptidases, can only cleave a few amino acids off the C-terminal or N-terminal ends of proteins, while others, the endopeptidases, can hydrolyze internal peptide bonds. Most proteases are highly specific and can only process a limited number of substrates with defined amino acid sequences. Similarly, some substrates are only processed by a very small number of proteases.

[126] Rawlings N.D., Polgár L., Barrett A.J. "A new family of serine-type peptidases related to prolyl oligopeptidase" *J. Biochem.* **1991**, *279*, 907–908

[127] Kanatani A., Masuda T., Shimoda T., Misoka F., Lin X.S., Yoshimoto T., Tsuru D. "Protease II from *Escherichia coli*: sequencing and expression of the enzyme gene and characterization of the expressed enzyme" *J. Biochem.* **1991**, *110*, 315–320

[128] Rawlings N.D., Barrett A.J. "Families of serine peptidases" *Methods Enzymol.* **1994**, *244*, 19–61

[129] Goossens F., De Meester I., Vanhoof G., Hendricks D., Vriend G., Scharpé S. "The purification, characterization and analysis of primary and secondary-structure of prolyl oligopeptidase from human lymphocytes. Evidence that the enzyme belongs to the α/β hydrolase fold family" *Eur. J. Biochem.* **1995**, *233*, 432–441

Prolyl oligopeptidase was discovered in the human uterus as an oxytocin-degrading enzyme.[130] The peptidase was originally named post-proline cleaving enzyme since it preferentially hydrolyzed the peptide bond on the carboxyl side of proline residues. Several enzymes with similar specificity, like tyrotropin releasing hormone deaminase, endo-oligopeptidase B, brain kinase B and others were then described, which later proved to be identical with prolyl oligopeptidase. The selectivity of the enzyme for oligopeptides was discovered in the 1970s.[131] The name prolyl endopeptidases was first recommended by the Enzyme Nomenclature, but later it was changed to prolyl oligopeptidase, emphasizing the special characteristics of the enzyme.
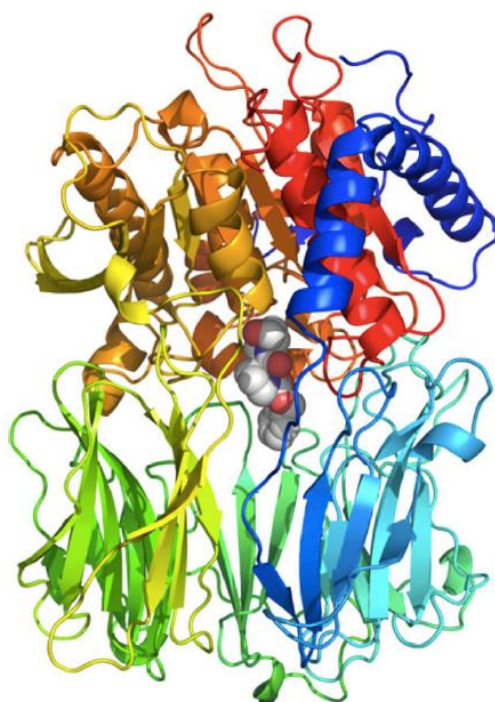
Figure 42. Crystal Structure of Prolyl OligoPeptidase.

POP cleaves short peptides, up to 30 amino acids long, and specific assays have been developed to screen for its occurrence in complex samples. These include digestion assays of model substrates and/or sensitivity to Cbz-Pro-Prolinal or analogues. Accordingly, in most of the studies, the cleavage of these putative POP-specific substrates has previously been taken to indicate the presence of the enzyme. According to all genetic or structural information in higher eukaryotes, POP is considered to be a soluble cytoplasmic protein.

[130] Koida M., Walter R. "Post-proline cleaving enzyme. Purification of this endopeptidase by affinity chromatography" *J. Biol. Chem.* **1976**, *251*, 7593–7599

[131] Camargo A.C.M., Caldo H., Reis M.L. "Susceptibility of a peptide derived from bradykinin to hydrolysis by endooligopeptidases and pancreatic proteinases" *J. Biol. Chem.* **1979**, *254*, 5304–5307

The peptidase domain is formed by the N- and C-termini (residues 1–72 and 428–710) containing the catalytic triad (Ser554, Asp641 and His680), and is arranged in a classical α/β hydrolase-fold. The seven-bladed β-propeller domain (residues 73–427) is radially arranged around the central tunnel embedded within the cylinder, where the narrow active site is located.

POP cleaves peptides at the carboxyl side of an internal proline (-Pro-Xaa-; where Xaa ≠ Pro), and it will not cleave an *N*-blocked peptide where Pro is the second amino acid (**Figure 43**).[132] The enzyme interacts maximally with six amino acid residues of the substrate peptide: those in positions P4, P3 and P2 from the N-side, and those in positions P10 and P20 from the C side of the proline which occupies the P1 position.[133] The highest reaction rates are obtained when P10 is a hydrophobic residue.
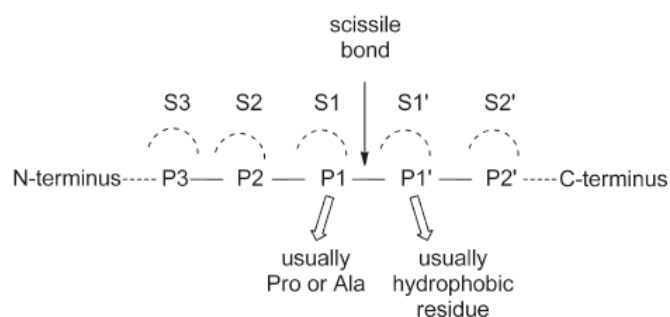
Figure 43. Interaction sites of POP active site.

It has been demonstrated that POP catalysis is controlled by a gating filter mechanism that only allows small peptides to gain access to the active site; in this way, larger structural peptides and proteins are protected from proteolysis.[134] The 3D structure of POP has helped to understand the mechanism for the specificity for small peptides and describe how the substrate-induced conformational change is the rate limiting step during catalysis.[135]

The enzyme active site is located in a large cavity at the interface of the two domains, and it has been proposed that there is a narrow hole at the centre of the β-propeller at the bottom of the enzyme, through which the substrate enters. This narrow entrance

[132] Rosenblum J.S., Kozarich J.W. "Prolyl peptidases: a serine protease subfamily with high potential for drug discovery" *Curr. Opin. Chem. Biol.* **2003**, *7*, 496–504.

[133] Fulop V., Szeltner Z., Renner V., Polgar L. "Structures of prolyl oligopeptidase substrate/inhibitor complexes. Use of inhibitor binding for titration of the catalytic histidine residue" *J. Biol. Chem.* **2001**, *276*, 1262–1266

[134] Fulop V., Szeltner Z., Polgar L. "Catalysis of serine oligopeptidases is controlled by a gating filter mechanism" *EMBO Rep. 1* **2000**, 277–281

[135] Szeltner Z., Rea D., Juhasz T., Renner V., Fulop V., Polgar, L. "Concerted structural changes in the peptidase and the propeller domains of prolyl oligopeptidase are required for substrate binding" *J. Mol. Biol.* **2004**, *340*, 627–637

could be widened by movements of residues with flexible bonds covering the central tunnel, thus this entrance would act as filter, permitting only small peptides to enter into the active site.[136]

The catalytic mechanism of POP conforms to the general serine protease reaction mechanism via base assisted catalysis by histidine, which occurs through a tetrahedral intermediate, generating a covalent acyl enzyme complex that is subsequently hydrolyzed. The hydrolysis involves a second tetrahedral intermediate which breaks down via acid-assisted catalysis by histidine.[137] The cycle has been confirmed by elegant X-ray and NMR experiments.[138]

Lithium is the standard treatment for bipolar depressions (manic depression/bipolar affective disorder) and is also effective in recurrent unipolar depression. It is used in conjunction with antidepressants or as a temporary mood stabilizer between treatments. The molecular basis of these disorders and their treatment by Li+ remains as yet unknown. A strongly supported theory is the inositol depletion theory (**Figure 44**). Li+ inhibits inositol monophosphatase and blocks the conversion of inositol monophosphate (IMP) to inositol. This causes a reduction of the free pool of inositol and ultimately lowers the cellular concentration of phosphatidyl(4,5)-biphosphate (PIP2). In addition, Li+ inhibits the enzyme inositol polyphosphatase which is required for the dephosphorylation of inositol(1,4)-biphosphate to IMP. In response to receptor stimulation, PIP2 is cleaved by phospholipase C to form the second messengers inositol(1,4,5)-triphosphate and diacylglycerol (DAG). These molecules cause the release of calcium from intracellular stores and activation of protein kinase C respectively. Li+ depletion of PIP2 therefore has the potential to cause a significant effect on signal transduction. The other primary target of Li+ in mammalian cells, next to the Inositol phosphate signaling is glycogen synthase kinase 3 (GSK-3), a multifunctional protein kinase.[139]

Investigating processes that counteract the effect of Li+, demonstrated an inverse relationship between POP activity and IP3 (Inositol triphosphate) concentration. Mutants of the cellular slime mould Dictyostelium discoideum, which lack all POP

[136] Fulop V., Bocskei Z., Polgar L. "Prolyl oligopeptidase: an unusual beta-propeller domain regulates proteolysis" *Cell* **1998**, *94*, 161– 170

[137] Leung D., Abbenante G., Fairlie D.P. "Protease inhibitors: current status and future prospects" *J. Med. Chem.* **2000**, *43*, 305–341

[138] Kahyaoglu A., Haghjoo K., Guo F., Jordan F., Kettner C., Felfoldi F., Polgar L. "Low barrier hydrogen bond is absent in the catalytic triads in the ground state but is present in a transition-state complex in the prolyl oligopeptidase family of serine proteases" *J. Biol. Chem.* **1997**, *272*, 25547–25554

[139] Williams R.S., Eames M,. Ryves W.J., Viggars J., Harwood A.J. "Loss of a prolyl oligopeptidase confers resistance to lithium by elevation of Inositol (1,4,5) trisphosphate" *EMBO J* **1999**, *18*, 2734–2745

activity, and wild-type cells treated with a selective POP inhibitor display an increase in basal concentrations of IP3. Other possible enzyme activities that generate or dephosphorylate IP3 were examined and found not to be present. The authors therefore concluded that loss of POP activity causes enhanced turnover of phosphoinositides which has the effect of increasing cellular concentration of IP3. Lithium had no direct effect on POP activity at up to 20 times the plasma concentrations used in therapeutic treatment of mood disorders, suggesting the enzyme may confer lithium resistance via an indirect mechanism. The authors state that if the pathway observed in Dictyostelium is conserved in the brain, it could explain the therapeutic effect of Li$^+$. Depression could result from a reduction in POP activity that leads to an elevated IP3 concentration, which in turn is reversed by Li$^+$ inhibition of inositol monophosphatase and inositol polyphosphatase.
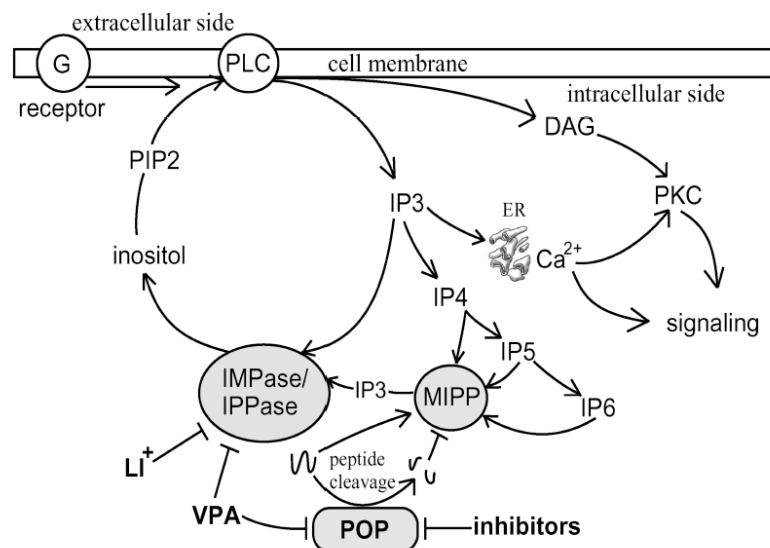
Figure 44. Mechanism of action for POP inhibition.

Researchers have shown that POP participates in several aspects and functions of the central nervous system (CNS), including learning, memory, mood, hypertension, and eating, and in some neurodegenerative diseases such as Alzheimer's and Parkinson's diseases. Subsequently, POP has been identified as a potential target in cognitive function, memory, and neurodegenerative disorders such as amnesia, Alzheimer's disease, and depression.

In the literature conflicting findings have been reported involving POP activity in brain tissue from control and AD cases. The most contradictory finding is the over expression compared to a lower POP concentration in patients. There have been reports

that POP activity is enhanced in AD brain. Aoyagi and collaborators[140] reported a significant increase in intra-cerebral POP activity in AD patients (n=7) when compared with the control group (n=6). An age-related increase in POP activity/expression in the brain has also been reported.[141] Other groups state that POP activity is decreased in specific regions of the brain of AD patients compared to controls.[142] A reduction of the POP activity in cortical tissue from AD cases (n=5) to 65% of the control activity (n=5) was also found.[143] However in authors' opinion the reduction in POP activity in AD tissue is not specific to this disorder, but a common factor in neurodegenerative disorders, since the activity was also reduced to 65–70% in comparison with control in tissue samples from Lewy body dementia (n=11), Parkinson's disease (n=13) and Huntington's disease (n=9). They suggested that loss of POP activity might be a marker of neuronal degeneration in the cerebral cortex in these disorders.

Hagihara and Nagatsu[144] measured POP in human cerebrospinal fluid (CSF) and although the enzyme activity in the CSF was extremely low, the activity measured in 37 control samples was significantly higher than in the CSF of 34 Parkinson patients. In contrast the enzyme activity in serum was not different between control patients (n=30) and Parkinson patients (n=13).

[140] Aoyagi T., Wada T., Nagai M., Kojima F., Harada S., Takeuchi T., Takahashi H., Hirokawa K., Tsumita T. "Deficiency of kallikrein-like enzyme activities in cerebral tissue of patients with Alzheimer's disease" *Experientia* **1990**, *46*, 94–97

[141] Rossner S., Schulz I., Zeitschel U., Schliebs R., Bigl V., Demuth H.U. "Brain prolyl endopeptidase expression in aging, APP transgenic mice and Alzheimer's disease" *Neurochem. Res.* **2005**, *30*, 695–702

[142] Laitinen K.S., van Groen T., Tanila H., Venäläinen J.I., Männistö P.T., Alafuzoff I. "Brain prolyl oligopeptidase activity is associated with neuronal damage rather than beta-amyloid accumulation" *Neuroreport* **2001**, *12*, 3309–3312

[143] Mantle D., Falkous G., Ishiura S., Blanchard P.J., Perry E.K. "Comparison of proline endopeptidase activity in brain tissue from normal cases and cases with Alzheimer's disease, Lewy body dementia, Parkinson's disease and Huntington's disease" *Clin. Chim. Acta* **1996**, *249*, 129-139

[144] Hagihara M., Nagatsu T. "Post-proline cleaving enzyme in human cerebrospinal fluid from control patients and parkinsonian patients" *Biochem. Med. Metab. Biol.* **1987**, *38*, 387–391

4.2 POP Inhibitors: State of the art

Researchers have reported many synthetic POP inhibitors, of which most are substrate-like short pseudopeptides that have little potential of crossing the BBB, a very unfavorable pharmacokinetics characteristic. The lead compound in development of POP inhibitors is Cbz-Pro-Prolinal (**1**) which is a covalent binder because of the highly reactive aldehydic moiety.[145] There are peptidic like inhibitors, analogues of **1**, and non peptidic ligands which display complementary properties. For instance, S-17092 (**3**) reached the phase 1 clinical trial[146], and some of them were found to improve memory and learning in animal models of brain disorders (**2**).[147]
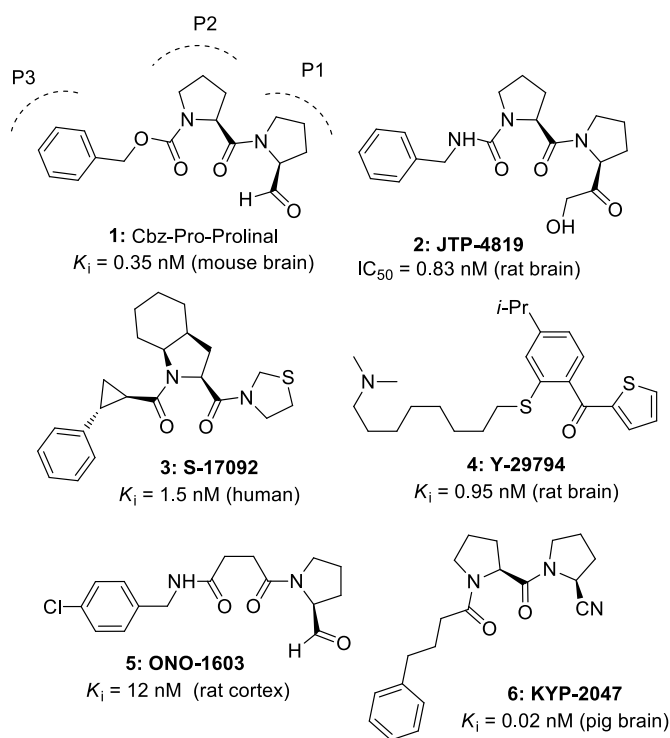
Scheme 15. Selected active POP inhibitors.

[145] Yoshimoto T., Kawahara K., Matsubara F., Kado K., Tsuru D. "Comparison of inhibitory effects of prolinal-containing peptide derivatives on prolyl endopeptidases from bovine brain and Flavobacterium" *J. Biochem.* **1985**, *98*, 975–979

[146] Morain P., Robin J.L., De Nanteuil G., Jochemsen R., Heidet V., Guez D. "Pharmacodynamic and pharmacokinetic profile of S 17092, a new orally active prolyl endopeptidase inhibitor, in elderly healthy volunteers. A phase I study" *Br. J. Clin. Pharmacol.* **2000**, *50*, 350–359

[147] Toide K., Shinoda M., Fujiwara T., Iwamoto Y. "Effect of a novel prolyl endopeptidase inhibitor, JTP-4819, on spatial memory and central cholinergic neurons in aged rats" *Pharmacol., Biochem. Behav.* **1997**, *56*, 427–434.

Compound **4** is an example of a very effective non peptidic POP inhibitor that abolished the formation of β-amyloid protein.[148] Amyloid beta (Aβ or Abeta) is a peptide of 36–43 amino acids that is processed from the Amyloid precursor protein. While best known as a component of amyloid plaques in association with Alzheimer's disease, evidence has been found that Aβ is a highly multifunctional peptide with significant non-pathological activity. Aβ is the main component of deposits found in the brains of patients with Alzheimer's disease and it's an indicator of generic proteases inhibition. However others demonstrated that POP inhibitors had no effect on β-amyloid levels in certain cell types, indicating that other proteases are involved or that the enzymes producing the β-amyloid peptides, as well as the β-amyloid precursor, were located in

different cell compartments than the β-amyloid peptides.[149]

ONO-1603 (**5**)[150] and KYP-2047 (**6**)[151] are probably the most studied and led to hundreds of natural or synthetic derivatives tested. Both effectively delay age-induced apoptosis of cerebral neurons. They display a neuroprotective action and, at the same time, a lower neurotoxicity compared to already known anti-dementia drugs like tetrahydroaminoacridine (THA), a benzofused α-tetrahydroquinoline ring.

A systematic analysis of POP inhibitors and different substitution is obtainable in a recent review here reported.[152] Summarizing, longer alkyl chains lead not only to poor solubility but also probably to steric clashes in the S3 pocket and large entropy penalties upon binding, resulting in less potent inhibitors.[153] Although most of the reported investigations on P3 inhibitor-enzyme interaction recommend flexible linkers to properly fill the S3 site of POP and to avoid any detrimental clashes with the protein, long and rigid moieties have also been successfully introduced. The carbonyl group between the two pyrrolidine rings of **1** has been shown to interact with the protein binding site (PDB code 1h2y). In fact, removal of this oxygen led to a complete loss of

[148] Kato A., Fukunari A., Sakai Y., Nakajima T. "Prevention of amyloid-like deposition by a selective prolyl endopeptidase inhibitor, Y-29794, in senescence-accelerated mouse" *J. Pharmacol. Exp. Ther.* **1997**, *283*, 328–335

[149] Petit A., Barelli H., Morain P., Checler F. "Novel proline endopeptidase inhibitors do not modify Aβ40/42 formation and degradation by human cells expressing wild-type and Swedish mutated β-amyloid precursor protein" *Br. J. Pharmacol.* **2000**, *130*, 1613–1617

[150] Katsube N., Sunaga K., Aishita H., Chuang D.M., Ishitani R. "ONO-1603, a potential antidementia drug, delays ageinduced apoptosis and suppresses overexpression of glyceraldehyde-3-phosphate dehydrogenase in cultured central nervous system neurons" *J. Pharmacol. Exp. Ther.* **1999**, *288*, 6–13

[151] Jalkanen A.J., Puttonen K.A., Venäläinen J.I., Sinervä V., Mannila A., Ruotsalainen S., Jarho E.M., Wallén E.A., Männistö P.T. "Beneficial effect of prolyl oligopeptidase inhibition on spatial memory in young but not in old scopolamine-treated rats" *Basic Clin. Pharmacol. Toxicol.* **2007**, *100*, 132–138

[152] Lawandi J., Gerber-Lemaire S., Juillerat-Jeanneret L., Moitessier N. "Inhibitors of Prolyl Oligopeptidases for the Therapy of Human Diseases: Defining Diseases and Inhibitors" *J. Med. Chem.* **2010**, *53*, 3423–3438

[153] Karoly K., Sandor E., Edit S., Miklos F., Judit S., Benjamin P., Andrea S., Istvan H. "Prolyl endopeptidase inhibitors: N-acyl derivatives of L-thioproline-pyrrolidine" *Bioorg. Med. Chem. Lett.* **1997**, *7*, 1701–1704

potency.[154] Once more, the structural modifications at P1 reported to date focused on proline mimics. However, as we can see from the structures of the substrates, POP is very selective for proline residues (alanine residues are tolerated but with a significant decrease in protease activity) and drastic changes at P1 are expected to correlate with a loss of inhibitory potency.[155]

Key interactions between inhibitors and POP are summarized in **Figure 45**. A lipophilic interaction between Phe173 and an aromatic residue occurs in a pocket at a defined distance from the carbonyl group. For this reason Cbz or longer side chain, terminating with an aromatic ring, have been exploited. Like **1**, peptidic and non peptidic inhibitors posses two carbonyl groups able to accept hydrogen bonding from Trp595 and Arg643.

While the most important interaction is located on the right side of the ligands. Covalent inhibitors are more potent than the noncovalent inhibitors developed thus far, although subnanomolar noncovalent inhibitors have been discovered.[156] The most exploited reactive group are aldehydes and nitriles which can interact with the nucleophilic Ser554. Still, correct stereochemistry of the reactive electrophilic specie is mandatory for high affinity, that is *S* configuration related to natural Pro properly functionalized at the carboxy group.
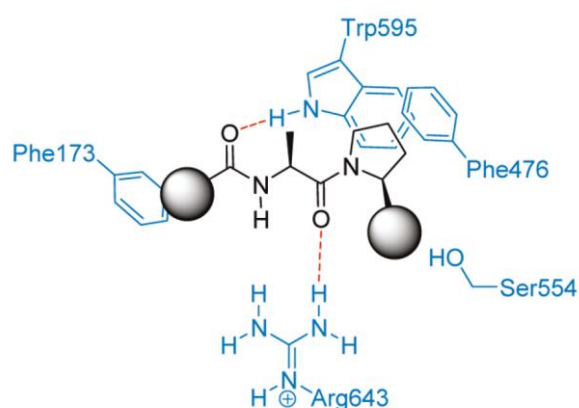
Figure 45. Key interactions between inhibitors and POP.

[154] Yoshimoto T., Tsuru D., Yamamoto N., Ikezawa R., Furukawa S. "Structure activity relationship of inhibitors specific for prolyl endopeptidase" *Agric. Biol. Chem.* **1991**, *55*, 37–43

[155] Arai H., Nishioka H., Niwa S., Yamanaka T., Tanaka Y., Yoshinaga K., Kobayashi N., Miura N., Ikeda Y. "Synthesis of prolyl endopeptidase inhibitors and evaluation of their structure-activity relationships: in vitro inhibition of prolyl endopeptidase from canine brain" *Chem. Pharm. Bull.* **1993**, *41*, 1583–1588

[156] Kanai K., Aranyi P., Bocskei Z., Ferenczy G., Harmat V., Simon K., Batori S., Naray-Szabo G., Hermecz I. "Prolyl oligopeptidase inhibition by *N*-acyl-pro-pyrrolidine-type molecules" *J. Med. Chem.* **2008**, *51*, 7514–7522

4.3 *Structural Study: Docking*

A structure of POP from porcine brain (PDB code: 2XDW) was downloaded from the Protein Data Bank and prepared as reported previously.[157] It was next prepared for docking using PROCESS, a module of the docking program FITTED.[158] The ligands were prepared using Maestro and SMART, a third module of FITTED. They were subsequently docked using the FITTED docking engine and defaults parameters. For the covalent docking to be used, the Ser554 has been selected as a reactive residue. To the best of our knowledge, MacDOCK[159] and FITTED are the only two programs considering covalent binding in a fully automated fashion.

We have combined and applied X-ray crystallography data, docking predictions, higher level computations (e.g., density functional theory, DFT), and chemical tools, also evaluating the inhibition of enzymatic activity, to reveal insight into binding and inhibition modes that each of them alone cannot predict. Using this strategy, we have designed a series of pseudopeptidic and peptidomimetic inhibitors, built around bicyclic scaffolds. These scaffolds closely mimic the known prolyl oligopeptidase inhibitor Cbz-Pro-Prolinal (**1**, Scheme 15).

Previous research was focused on the conformational restriction of lead compounds **1** and **2**. Recently, the research group were I spent part of the Ph.D. project, synthesized and tested different compounds library which are related to bicyclic scaffolds **7** and **8**. Molecule **7**, despite a low activity, showed a promising pharmacokinetic profile crossing the BBB and is characterized by a conformational restriction on the right side of the lead (green).[160] On the other hand, molecule **8** represents a candidate characterized by a cyclization on the left side of the lead compound (blue).[161] Both series, are composed by peptidic like Cbz-Pro-Prolinal analogues which display all the key interaction with the binding site. (Scheme 16)

[157] Corbeil C.R., Englebienne P., Moitessier N. "Docking Ligands into Flexible and Solvated Macromolecules. 1. Development and Validation of FITTED 1.0" *J. Chem. Inf. Model.* **2007**, *47*, 435–449

[158] Corbeil C.R., Englebienne P., Moitessier N., Therrien E. "FITTED Docking Program" www.fitted.ca **2009**

[159] Fradera X., Kaur J., Mestres J. "Unsupervised guided docking of covalently bound ligands" *J. Comput.-Aided Mol. Des.* **2004**, *18*, 635–650

[160] Lawandi J., Toumieux S., Seyer V., Campbell P., Thielges S., Juillerat-Jeanneret L., Moitessier N. "Constrained Peptidomimetics Reveal Detailed Geometric Requirements of Covalent Prolyl Oligopeptidase Inhibitors" *J. Med. Chem.* **2009**, *52*, 6672–6684

[161] De Cesco S., Deslandes S., Therrien E., Levan D., Cueto M., Schmidt R., Cantin L.D., Mittermaier A., Juillerat-Jeanneret L., Moitessier N. "Virtual Screening and Computational Optimization for the Discovery of Covalent Prolyl Oligopeptidase Inhibitors with Activity in Human Cells" *J. Med. Chem.* **2012**, *55*, 6306–6315

Because of these interesting results, we developed a methodology for the synthesis of new conformationally constrained POP inhibitors, placing the bicyclic scaffold alternatively on the right (**9**) or the left side (**10**,**11**) of the lead compound.

The difference between compounds **10** and **11** relies on the aromatic distance from the structure core

1: K_i = 0.35 nM (mouse brain)

6: K_i = 0.02 nM (pig brain)

7
IC_{50} = 200-700 nM (human brain)

8
IC_{50} = 45 nM (human brain)

9

10

11
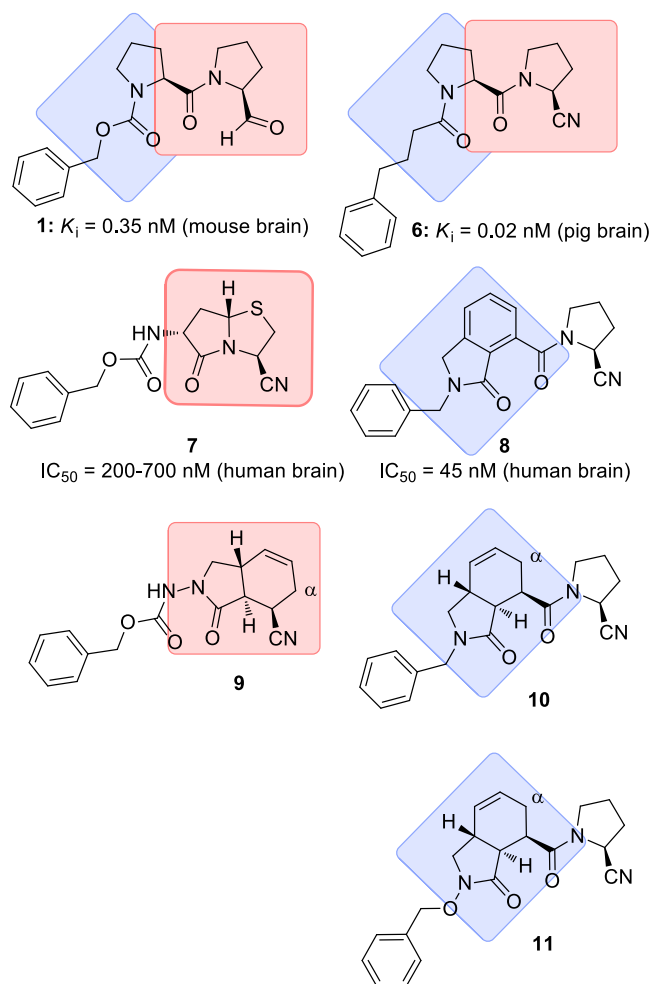
Scheme 16. Cyclization Strategies.

In **Figure 46** is depicted the superimposition of Cbz-Pro-Prolinal (**1**) with compound **9** in the POP binding site. Reference compound is not obtained by docking but it's the crystallized structure bound to the enzyme. It is possible to recognize a good aromatic side chain positioning and a good overlap of the covalent binder moiety compared to reference.

According to the docking and previous results, several key parameters have been drawn. These new bicyclic scaffolds should have the cyano-pyrrolidine ring with *S* configuration, as stated in previous works. Moreover, any substitution at position α, relative to amide and nitrile, should be avoided because of clashing with POP binding site. The relative configuration of the junction ring stereocenters has to be *anti* favoring

the proper spatial orientation of the aromatic and the proline residue. Whereas the absolute configuration seems to poorly influence the correct ligand positioning.
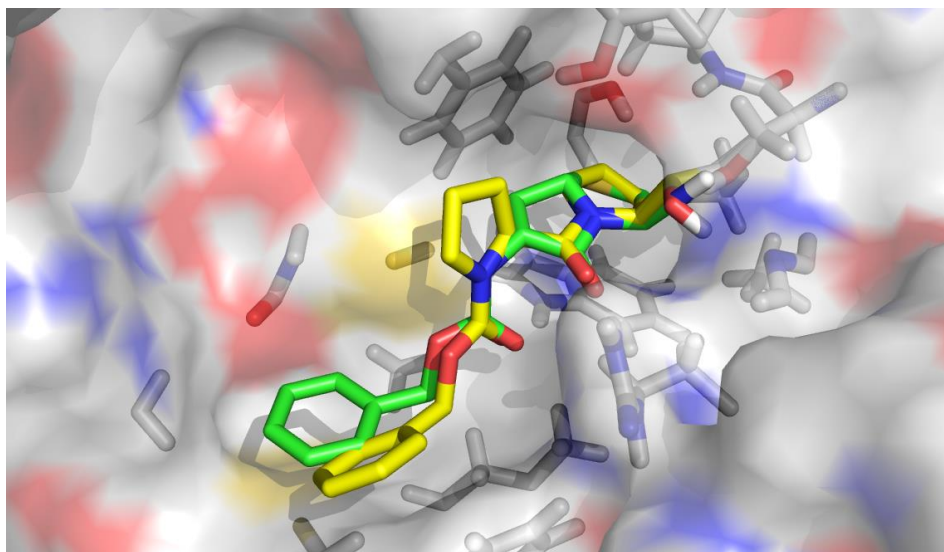
Figure 46. Binding mode towards the POP model of **1** (yellow) and **9** (green).

Furthermore, docking was performed on derivatives **10** and **11** corresponding to **Figure 47** and **48** respectively. In this pictures is very clear the key factor related to α- position which requires no steric hindrance. Moreover, the scaffolds seems to fit and overlap pretty well with reference **1**.

Compound **11** shows a one atom longer spacer which drives deeper in the hydrophobic cavity the aromatic residue.
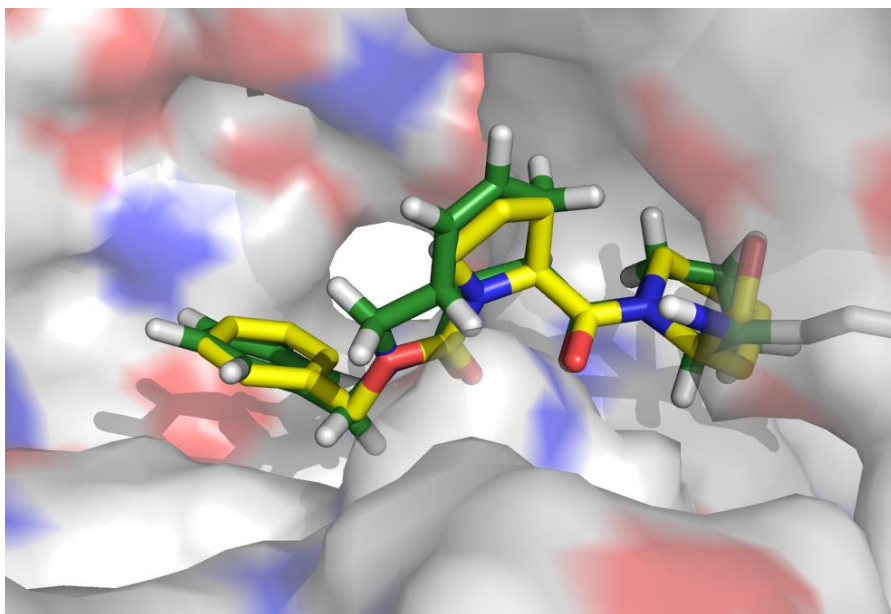
Figure 47. Binding mode towards the POP model of **1** (yellow) and **10** (green).
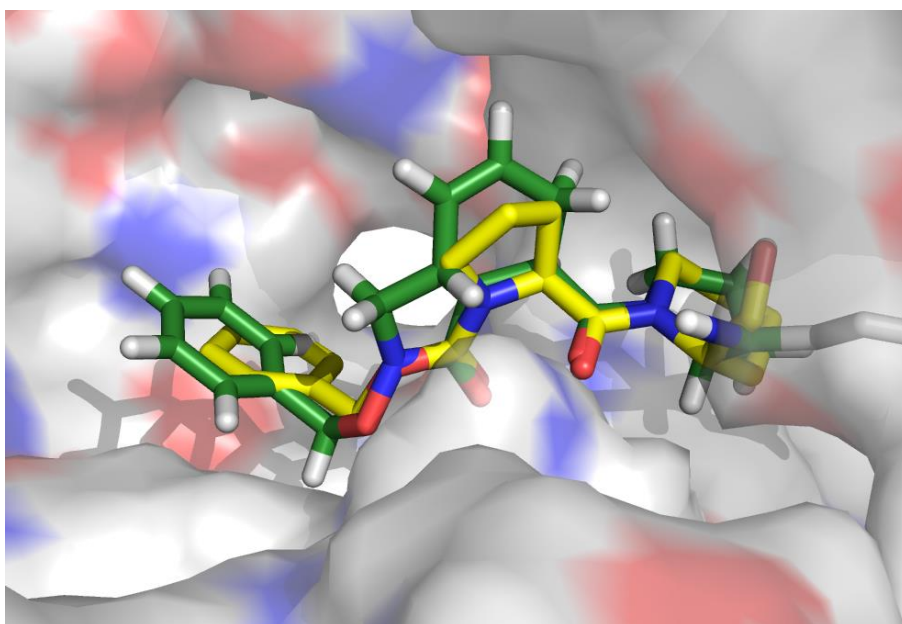
Figure 48. Binding mode towards the POP model of **1** (yellow) and **11** (green).

4.4 *Synthesis*

Few years ago, the group where I recently worked with, reported preliminary results leading to a rigid Ala-Val dipeptide mimic.[162] As shown in **Figure 49**, conformational analysis revealed that the designed *trans-cis-trans* isomer adopts a conformation similar to the mimicked dipeptide. More specifically, the *trans* configuration of the methyl and amide groups resembles the staggered conformation of the Val side chain while a *cis* configuration would be closer to the eclipsed conformation. The successful preparation of these structures prompted us to look at other analogues and optimized synthesis.

Ala-Val dipeptide

Bicyclic mimetics
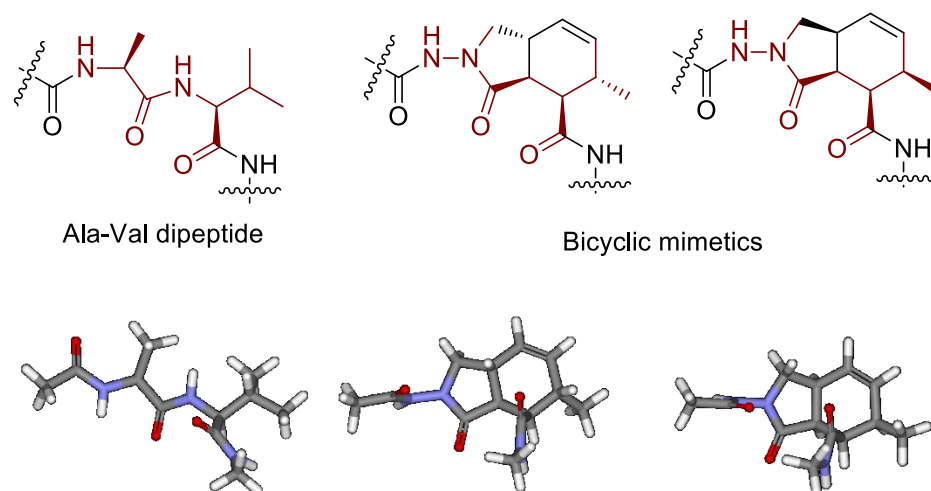
Figure 49. Ala-Val mimetics: chemical structures (top panel)
and their corresponding 3D conformations optimized with ACE.[163]

At the outset of this research program we set criteria including atom economy and expediency for the synthesis of bicyclic scaffolds that could be used in medicinal chemistry. In order to devise an expedient synthesis, we focused on telescoping the steps and relied on tandem or one-pot reactions. These reactions would build complexity using Diels Alder cycloadditions from very simple building blocks.

[162] Huot M., Moitessier N. "Expedient synthesis of novel bicyclic peptidomimetic scaffolds" *Tetrahedron Lett.* **2010**, *51*, 2820-2823

[163] Weill N., Corbeil C.R., De Schutter J.W., Moitessier N. "Toward a computational tool predicting the stereochemical outcome of asymmetric reactions: Development of the molecular mechanics-based program ACE and application to asymmetric epoxidation reactions" *J. Comp. Chem.* **2011**, *32*, 2878-2889
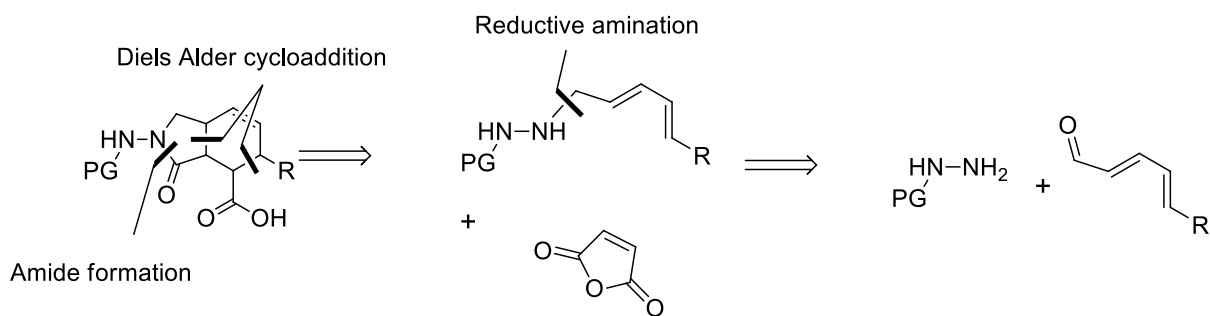
Figure 50. Synthesis of Ala-Xaa mimetics.

The following methodology has been extended to different unsaturated aldehyde which are then related to several amino acidic side chains. With the aim of preparing potential POP inhibitors, R = H became my point of investigation.

With this designed strategy, three bonds and four stereogenic centers were formed in a single step. Reaching this high level of complexity within a few steps was in fact the major challenge. Through the key step, the major diastereomer formed was the Diels-Alder *exo* adduct resembling the natural dipeptide conformation as discussed above. In order to reduce or eliminate the need for environmentally harmful reagents and protecting groups, we selected maleic anhydride. Due to the specific cyclic form of this chemical, the protecting group is the chemical itself. Through cleavage of the anhydride group and ring opening, the carboxylic acid is released. Thus, most of the low-toxicity chemicals used in the entire strategy would be incorporated into the final molecule. The only remaining issue is the stereocontrol of the reactions as *exo* and *endo* adducts are obtained. Furthermore, the modular nature of this synthesis should allow for the introduction of not only amino acid like structures but permit the incorporation of many functional groups to enable the synthesis of "drug-like" molecules that can interact with the hydrophobic and hydrophilic regions of enzymes and proteins.

Based on our conformational analysis, the stereochemical outcome of the Diels-Alder (DA) reaction is critical as the trans configuration of the fused ring must be obtained. Considering this information, it was integral for us to find a set of conditions that would selectively lead to the trans fused ring. Cayzer et al. have previously reported a similar strategy using alcohols in place of hydrazide.[164] In particular a complete intramolecular Diels-Alder reaction (IMDA) preferentially affords *exo* adduct whereas an inter molecular reaction is more *endo* oriented.[165] A DFT computational study revealed a highly asynchronous transition state and indicated that the *exo* selectivity is most likely induced by the strain of the forming five-membered ring.

[164] Cayzer T.N., Paddon-Row M.N., Moran D., Payne A.D., Sherburn M.S., Turner P. "Intramolecular Diels-Alder reactions of ester-linked 1,3,8-nonatrienes" *J. Org. Chem.* **2005**, *70*, 5561-5570

[165] Cayzer T.N., Lilly M.J., Williamson R.M., Paddon-Row M.N., Sherburn M.S. "On the Diels–Alder reactions of pentadienyl maleates and citraconates" *Org. Biomol. Chem.* **2005**, *3*, 1302-1307

In order to achieve the desired bicyclic scaffolds I synthesized the required conjugated aldehyde **12** following a described procedure. This approach involves a malonic addition to acrolein followed by decarboxylation and a reductive-oxidative protocol to afford the volatile aldehyde.[166] Then I subjected **12** to reductive amination with Boc-hydrazide. Subsequent DA reaction afforded with low diastereoselectivity the two *exo* and *endo* adduct as racemic mixture. An extensive study to improve diastereoselectivity have been performed on different scaffolds by varying environment lipophilicity.

However, the diastereoselectivity and the difficult separation of the diastereomers remain a hurdle for the use of these scaffolds in medicinal chemistry. To tackle this problem, the use of various auxiliaries, Brønsted acids, reaction conditions were investigated but proved unsuccessful until we found that substituting the Boc group by a Cbz group and the use of dichloromethane for the tandem reaction led to selective precipitation of the major *exo* adduct. Not only does this optimized strategy provide a single isolated diastereomer but it also removed the need for chromatographic purification of the polar bicyclic scaffolds.[167]
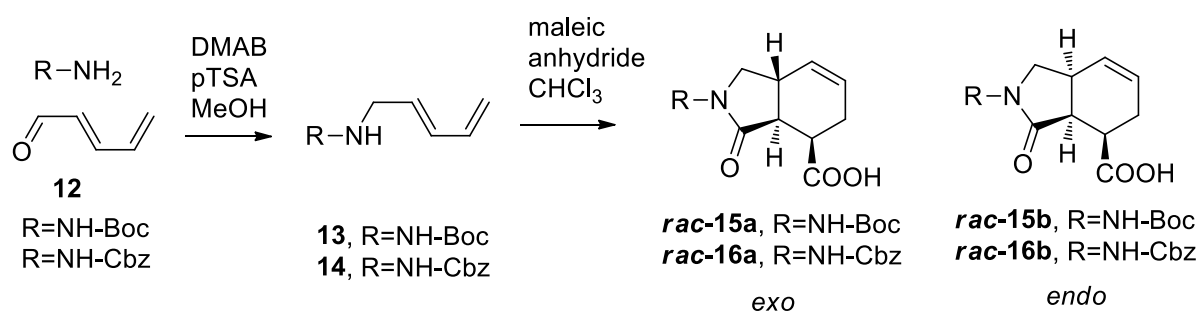
Scheme 17. IMDA reaction for bicyclic scaffolds.

With this methodology available, I pursued the synthesis of *rac*-**9** by coupling with a source of ammonia (NH$_4$ HCO$_3$) and then dehydration of the corresponding amide with TFAA.

The synthesis of scaffolds **19** and **20** required the preparation of dienes **17** and **18** which was performed using standard reducing agent like NaBH$_4$. The following DA reaction gave an unexpected result because if the diene **17** afforded a bicyclic compound in a 7:1

[166] Mitton-Fry M.J., Cullen A.J., Sammakia T. "The Total Synthesis of the Oxopolyene Macrolide RK-397" *Angew. Chem. Int. Ed.* **2007**, *46*, 1066-1070

[167] Airaghi F., De Cesco S., Huot M., Moitessier N. "Chiral Rigid Dipeptide Mimics – Design and Expedient Synthesis" *submitted*

exo/endo ratio, showing a clear intramolecular cyclization preceded by the coupling,[168] diene **18** afforded the bicyclic scaffold **20** in a 1:1 ratio, with no diastereoselectivity at all.

Indeed, reaction took 72 hours to afford a reasonable yield. We think that such slow reactivity might promote first the DA reaction and then the coupling to form the five membered ring.
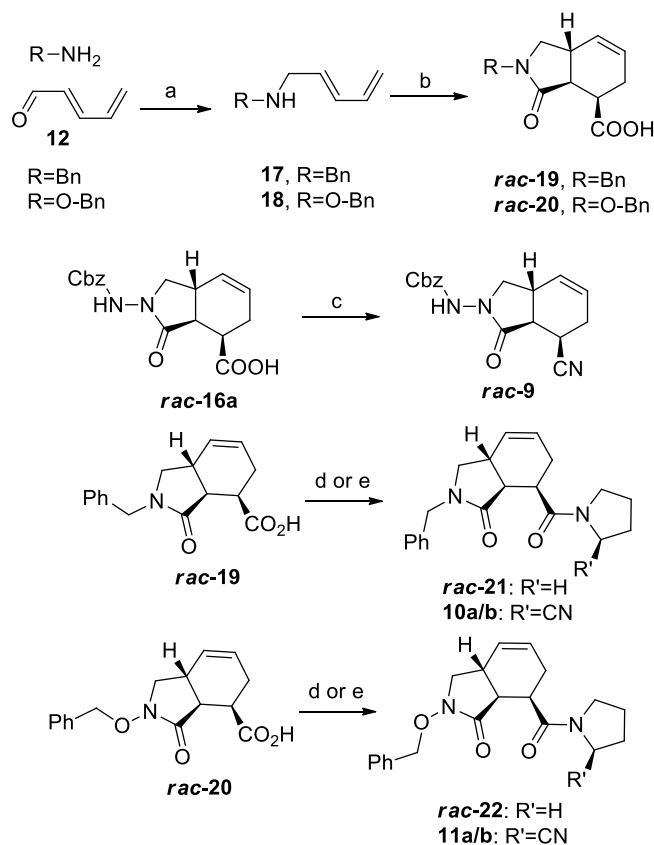
Scheme 18. Synthesis of POP inhibitors.

a) NaBH₄, MeOH, 31% (**17**); DMAB, pTSA, MeOH, 28% (**18**); b) maleic anhydride, DCM, 98% (**19**), 74% (**20**); c) PivCl, NH₄ HCO₃, Pyridine, CH₃CN then TFAA, pyridine, THF, 26% (**9**) (over two steps); d) Pyrrolidine, PivCl, TEA, DMF, 34% (**21**), 17% (**22**); e) *S*-Cyanopyrrolidine, BOP, TEA, DMF, 31%, (**10**), 27% (**11**).

Table 7. IMDA stereochemical outcome.

R	products	yield (%)	*exo/endo*
Boc	**15**	65	1.5
Cbz	**16**	66	1.5
Bn	**19**	98	7
Bn-O	**20**	74	1

[168] Mellor J.M., Wagland A.M. "Synthesis of hydroisoindoles via intramolecular Diels–Alder reactions of functionalised amido trienes" *J. Chem. Soc. Perkin Trans. 1*, **1989**, 997-1005

The racemic acid **16** has been coupled to a source of ammonia and then dehydrated with TFAA to afford the corresponding nitrile. The more obvious two steps conversion to methyl ester, followed by transesterification with an ammonia solution in methanol revealed to be unreactive, even under refluxing conditions.

The two racemic acid **19** and **20** have been coupled with pyrrolidine and *S*-CN-Pro in order to give covalent and non covalent potential inhibitors. Coupling yields were low because of a lack of reactivity of the exocyclic carboxyl moiety to any coupling agent. We think that the shape of such small scaffold may exert a steric hindrance, shielding the activated acid from the nucleophile approach. Moreover, I observed an absence of reactivity for the *endo* DA adduct. For compound **19**, the high IMDA selectivity has obviated any purification procedure, while derivative **20**, in a 1:1 *exo/endo* ratio, led to a pure *anti* (*exo*) non covalent inhibitor **22** and a 5:1 *anti:syn* covalent inhibitor **11a/b**. The steric hindrance occurring for the tight *endo* adduct together with a general lack of reactivity allowed us to obtain pure *anti* diastereomers derivatives, as racemates, explaining also the coupling yield below 50%.
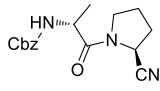
Once obtained the covalent and non-covalent ligands, they have been subjected to biological evaluation towards POP enzyme from cell extracts and living intact cells.[169]

4.5 _Biological Evaluation_

These various synthesized compounds were evaluated for their ability to inhibit POP. These assays were carried out on cell extracts and intact cells and on six different cell strains. All this data allowed us to measure the inhibitory potency and also to evaluate the selectivity for POP over DPP-IV, FAP-α-seprase, DPP8 and DPP9 as described in a previous report.[160] Preliminary results are presented in Table 8.

Table 8. Inhibition of POP activity in cell extracts.[a]

Compound	human astrocyte derived cells[b]	human brain-derived endothelial cells[c]
	+++	+++
1 (Cbz-Pro-Prolinal)	+++	+++
6 (KYP-2047)	+++	+++
7	+++	+++
8	+++	+++
rac-**9**	-	-
rac-**21**	+++	+++
10a/b	+++	+++
rac-**22**	++	++
11a/b	+++	+++

[a] -, No inhibition at 0.8 μM; +, 10-50% inhibition at 0.8 μM; ++, >50% inhibition at 0.8 μM; +++, >90% inhibition at 20 μM. [b] LN18, LN229, LNZ308: human glioblastoma cells. [c] HCEC, human brain-derived endothelial cells.

According to preliminary data, compound **9** is not active at all, thus demonstrating not to be a valid surrogate of the lead compound **17**, although the shape of the designed molecule was predicted to be optimal. On the other hand, the couples **21** and **10**, **22** and **11** are highly active with no distinction between covalent and non covalent binding in which the electrophilic nitrile can react with nucleophilic Ser554, key residue of the enzyme active site. The only exception is _rac_-**22** which is less potent compared to analogues **11a/b**. Apparently, the usage of this bicyclic scaffold for the rigidification on the right side of the lead compound **1** does not rise positive effects. Conformational restriction on the left side displayed a very good inhibition profile, in most cases above 90% at low concentration. Non covalent ligands display almost the same activity, but covalent ones (**10**, **11**) have higher potency.

4.6 *Conclusions*

We performed the synthesis of a novel family of rigid Ala-Ala dipeptide mimics by mean of few synthetic steps with an high degree of complexity, forming simultaneously 3 stereocenters. We were able to discriminate the two diastereomers through a selective precipitation for the IMDA derived hydrazide.

I synthesized other bicyclic scaffolds varying the *N-* substitution in order to tune the aromatic ring distance from the core. This new compounds family has been subjected to coupling with pyrrolidine and *S*-CN-pyrrolidine for the synthesis of potentially POP inhibitors.

They were designed with the aid of computational tools, which highlight the key requirements for valuable drug candidates: proper aromatic ring 3D positioning, no substitution on the bicyclic scaffold and the correct absolute and relative stereochemistry.

Following these studies, compounds identified have been tested for their biological activity in cell extracts and intact living cells. According to preliminary results in our hand, we observed a very good POP inhibition profile for compounds **10**, **11** and **21**.

We still observed inhibition for non covalent inhibitors (**21**, **22**), however covalent binders display an higher potency.

4.7 *Experimental Details*

Chemistry

All solvents were distilled and properly dried, when necessary, prior to use. All chemicals were purchased from commercial sources and used directly, unless otherwise indicated. All reactions were run under argon atmosphere, unless otherwise indicated. All reactions were monitored by thin layer chromatography (TLC) on precoated silica gel 60 F_{254}; spots were visualized with UV light (254 nm) and by treatment with 1% aqueous $KMnO_4$ solution, Ninhydrin solution in ethanol or Cerium-ammonium-molybdate (CAM) reactive. Products were purified by flash chromatography on silica gel 60 (230-400 mesh). ^1H and ^{13}C NMR spectra were recorded with 300, 400 and 500 Mhz spectrometers using chloroform-*d* ($CDCl_3$), dimethylsulfoxide-*d$_6$* (DMSO-*d$_6$*), acetonitrile-*d$_3$* (CD_3CN) or methanol-*d$_4$* (CD_3OD). Chemical shifts (δ) are expressed in ppm relative to TMS at δ = 0 ppm for ^1H NMR and relative to $CDCl_3$ at δ = 77.16 ppm for ^{13}C NMR. High-resolution MS spectra were recorded with a FT-ICR (Fourier Transform Ion Ciclotron Resonance) instrument, equipped with an ESI source.

Biology

Inhibitory Potency. The human glioblastoma-derived cell lines LN18, LN229, and LNZ308 were a kind gift of A.C. Diserens, Neurosurgery Department, Lausanne, Switzerland, the immortalized human brain-derived HCEC cells were kindly provided by D. Stanimirovic, Ottawa, Canada. Cells were grown in DMEM culture medium containing 4.5 g/l glucose, 10% fetal calf serum (FCS) (HCEC cells), or 5% FCS (LN18, LN229, and LNZ308 cells), and antibiotics (all from Gibco, Basel, Switzerland). One to two days before evaluation, cells were seeded in 48-well plates (Costar, Corning, NY) in complete medium in order to reach confluence on the day of experiment. On the day of experiment, the culture medium was removed, and either 200 μl of phosphate-buffered saline (PBS, pH 7.2–7.4) were added in half of the wells or 200 μl of PBS containing 0.1% Triton X-100 (Fluka, Buchs, Switzerland) were added in the other half of the wells for the evaluation of the inhibition of enzyme activities in intact cells or cell extracts, respectively. Experiments were performed in duplicate wells. The synthetic molecules were dissolved at 10 mg/ml in methanol and then diluted 1:10 in H_2O, and 1 or 5 μl of the water solution were added to duplicate PBS and PBS-Triton wells, followed after 5–10 min at room temperature by either 1 μl of Gly-Pro-AMC (DPPIV activity) or Z-Gly-Pro-AMC (POP activity) substrates (1 mg/ml DMSO, both from Bachem, Bubendorf, Switzerland), final concentration 10 μM. Increase in fluorescence at λex/λem = 360/460 nm was recorded for 30 min at 37 °C in a thermostatted multiwell

fluorescence reader (Cytofluor, PerSeptive BioSystems, Switzerland). For the determination of IC_{50}, cells in PBS or in PBS-Triton X-100 were exposed to decreasing concentrations of the inhibitors, and then determination of residual activity was measured and plotted against inhibitor concentration. IC_{50} values were determined graphically.

Recombinant human prolyl oligopeptidase/PREP (rhPOP/PREP, 0.5 mg/ml, catalogue no. 4308-SE) and fibroblast activation protein α (rhFAPα, 0.5 mg/mL, catalogue no. 3715-SE) were obtained from R&D Systems (Abingdon, UK). The stock solutions were diluted in PBS containing 1 mg/ml bovine serum albumin (BSA, Sigma), a protein concentration comparable to the protein concentration of cell extracts. For comparison of inhibitory potencies, IC_{50} and K_M in cell extracts with rhPOP/PREP and rhFAPα, cells were grown in 6 cm Petri dishes (Falcon, BD, Erembodegem, Belgium) and extracted in 3 ml of PBS-Triton (resulting in solutions of ~0.5 mg protein/ml). For the evaluation of the inhibition of the recombinant human enzymes, the experimental design was similar to the experimental design of cell extracts. For K_M determinations, increasing substrate concentrations were added to the cell extracts in PBS-Triton or to the recombinant enzymes in PBS-BSA, and the K_M values were determined graphically using a double-reciprocal Michaelis–Menten plot.

Docking Simulations

The protein structure (PDB code: 2XDW) was downloaded from the Protein Data Bank and prepared as reported previously. It was next prepared for docking using PROCESS, a module of our docking program FITTED. The ligands were prepared using Maestro and SMART, a third module of FITTED. They were subsequently docked using the FITTED docking engine and defaults parameters. For the covalent docking to be used, the Ser554 has been selected as a reactive residue.

Synthesis of *rac*-9:
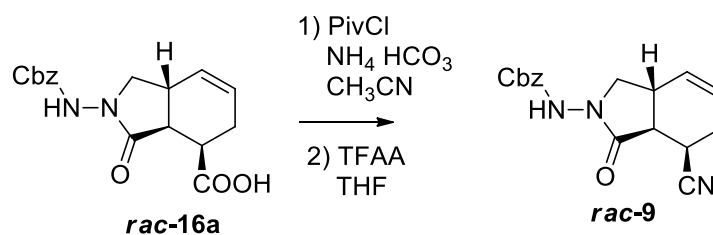
Benzyl ((3a*R*,7*R*,7a*S*)-7-cyano-1-oxo-3,3a,7,7a-tetrahydro-1H-isoindol-2(6H)-yl) carbamate (*rac*-9).

The acid **16a** (38 mg, 0.11 mmol) was dissolved, under argon atmosphere, in CH_3CN (1 ml), then PivCl (21 µl, 0.17 mmol) was added. After 30 minutes NH_4HCO_3 (14 mg, 0.17 mmol) was added followed by Pyridine (6 µl, 0.08 mmol) and the mixture was reacted for 3 days. The reaction was quenched with water, then extracted 3 times with DCM. The organic phases were washed with saturated $NaHCO_3$, HCl 1M, brine, dried over Na_2SO_4 and concentrated under reduced pressure. The crude was directly used in the next reaction step.

To a cooled solution of the amide (16 mg, 0.05 mmol) in THF (1 ml) was added Pyridine (33 µl, 0.41 mmol) then TFAA (18 µl, 0.13 mmol). After 4 hours the reaction was quenched with saturated $NaHCO_3$ and extracted with AcOEt. The organic phases were washed with saturated $NaHCO_3$, HCl 1M, brine, dried over Na_2SO_4 and concentrated under reduced pressure. The crude was purified by flash chromatography (Hex/AcOEt 4:6) to afford nitrile **9** as a white solid (8 mg, 26% over two steps).

R_f = 0.35 (1:1 Hex/AcOEt). IR (film) ν_{max}: 3278, 2923, 2241, 1754, 1738, 1711. ^{1}H NMR (300 MHz, $CDCl_3$) δ 7.45 – 7.29 (m, 5H), 6.94 (bs, 1H), 5.92 (d, 1H, J = 9.8 Hz), 5.74 – 5.65 (m, 1H), 5.26 – 5.06 (m, 2H), 3.70 – 3.42 (m, 3H), 3.21 – 2.99 (m, 1H), 2.63 – 2.54 (m, 2H), 2.46 (bd, J = 9.4 Hz, 1H). ^{13}C NMR (75 MHz, $CDCl_3$) δ 154.9, 135.3, 128.6 (2C), 128.5 (2C), 128.2, 126.0, 125.6, 119.4, 68.0, 51.9, 44.7, 33.5, 29.8, 23.6. HRMS (ESI) calcd. for $[C_{17}H_{17}N_3O_3]^+$: 311.1270, found 334.1160 (MNa$^+$)
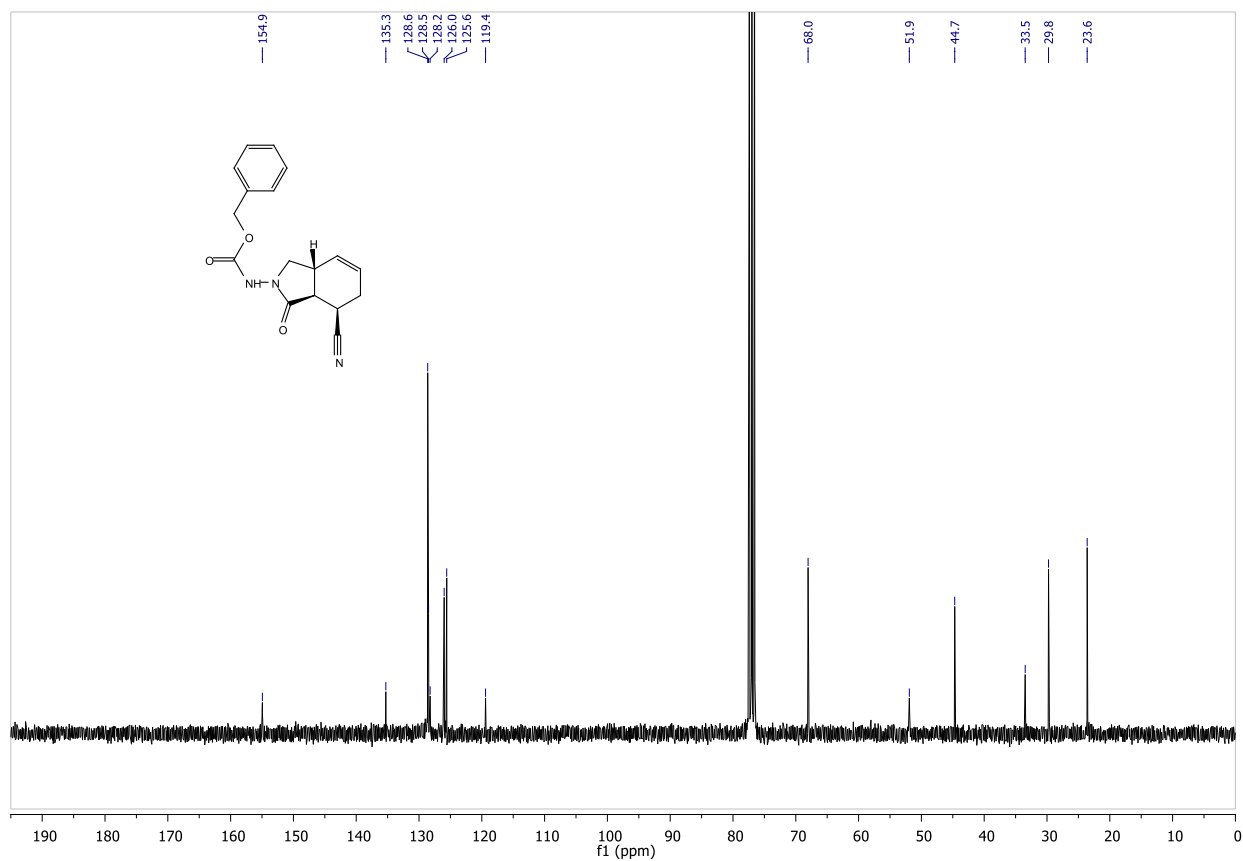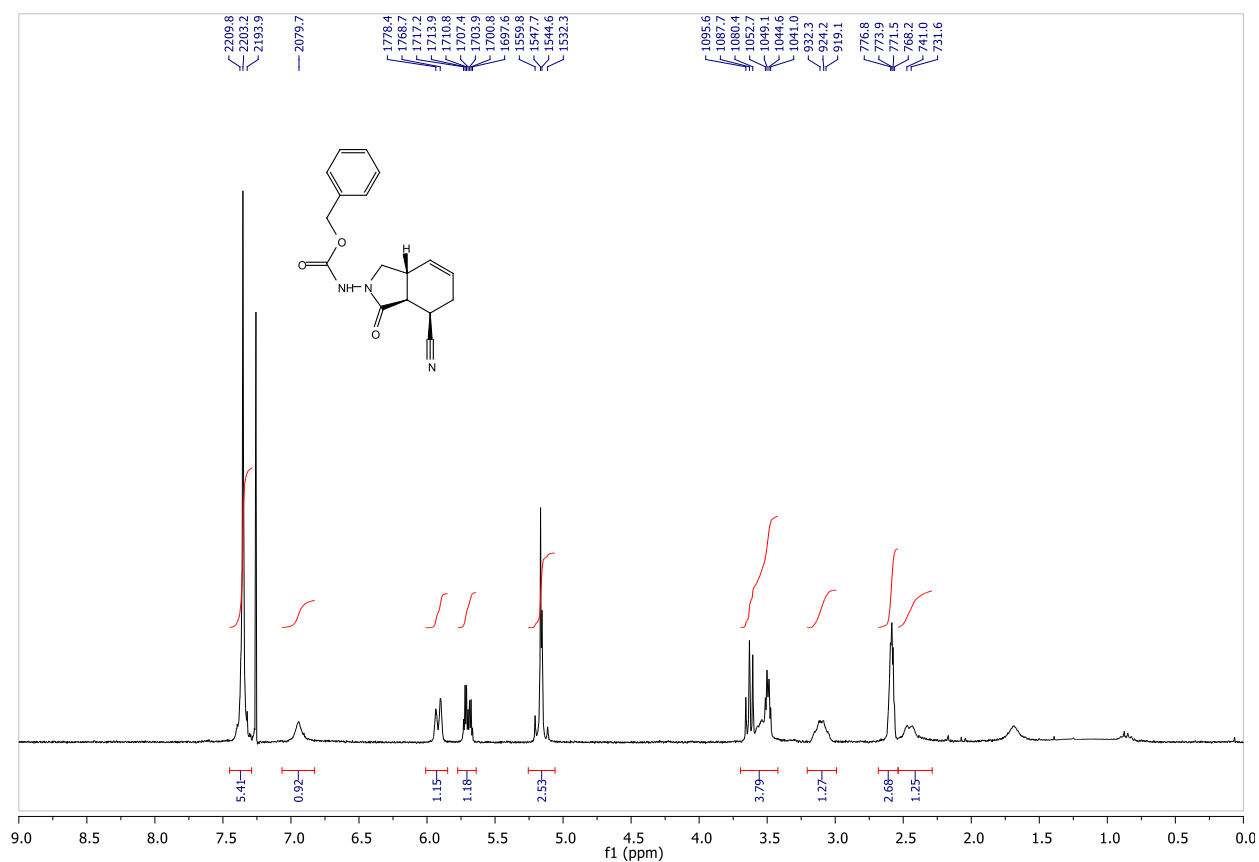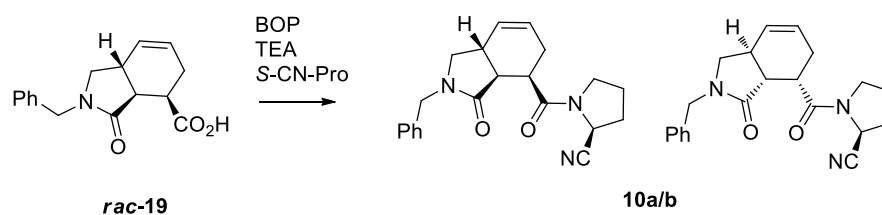
Synthesis of 10a/b:

(S)-1-((3aS,4R,7aR)-2-benzyl-3-oxo-2,3,3a,4,5,7a-hexahydro-1H-isoindole-4-carbonyl)pyrrolidine-2-carbonitrile (10a/b).

The acid **rac-19** (23 mg, 0.08 mmol) was dissolved, under argon atmosphere, in DMF (1 ml). The solution was cooled to 0° and BOP (58 mg, 0.11 mmol) was added, followed by S-CN-Proline•pTSA salt (34 mg, 0.13 mmol) and TEA (60 μl, 0.34 mmol). The mixture was reacted for 18h at rt. The reaction was quenched with H_2O, extracted with DCM and the organic phases washed with HCl 1M, saturated $NaHCO_3$, brine, dried over Na_2SO_4 and concentrated under reduced pressure. The crude was purified by flash chromatography (gradient Hex/AcOEt from 3:7 to 1:9) to afford the product **10** as a white solid (26 mg, 31%). The following data has been collected on a 1:1 diastereomeric mixture.

R_f = 0.32 (2:8 Hex/AcOEt). IR (film) ν_{max}: 3476, 2968, 2043, 1689, 1632. ^{1}H NMR (300 MHz, CDCl$_3$) δ 7.38 – 7.27 (m, 6H), 7.21 – 7.13 (m, 4H), 5.89 – 5.80 (m, 2H), 5.76 – 5.62 (m, 2H), 4.75 (dd, 2H, J = 6.3, 3.7 Hz), 4.58 (d, 2H, J = 14.8 Hz), 4.27 (d, 2H, J = 14.8 Hz), 3.74 – 3.56 (m, 2H), 3.47 – 3.21 (m, 6H), 3.05 – 2.79 (m, 4H), 2.60 – 2.32 (m, 6H), 2.32 – 2.00 (m, 8H). ^{13}C NMR (75 MHz, CDCl$_3$) δ 173.5, 173.0, 172.8, 172.7, 136.3, 136.2, 128.8, 128.8, 128.8, 128.2, 127.9, 127.8, 127.8, 127.7, 127.5, 127.4, 126.9, 125.9, 125.3, 124.8, 119.5, 118.5, 49.7, 49.3, 48.5, 48.4, 47.1, 47.0, 46.6, 46.5, 36.6, 34.9, 34.6, 34.3, 34.1, 34.0, 32.2, 30.1, 29.0, 28.8, 25.4, 23.1. HRMS (ESI+) calcd. for $[C_{21}H_{23}N_3O_2]^+$: 349.1790, found 372.1863. (MNa$^+$)

¹H and ¹³C NMR of compound **10a/b**
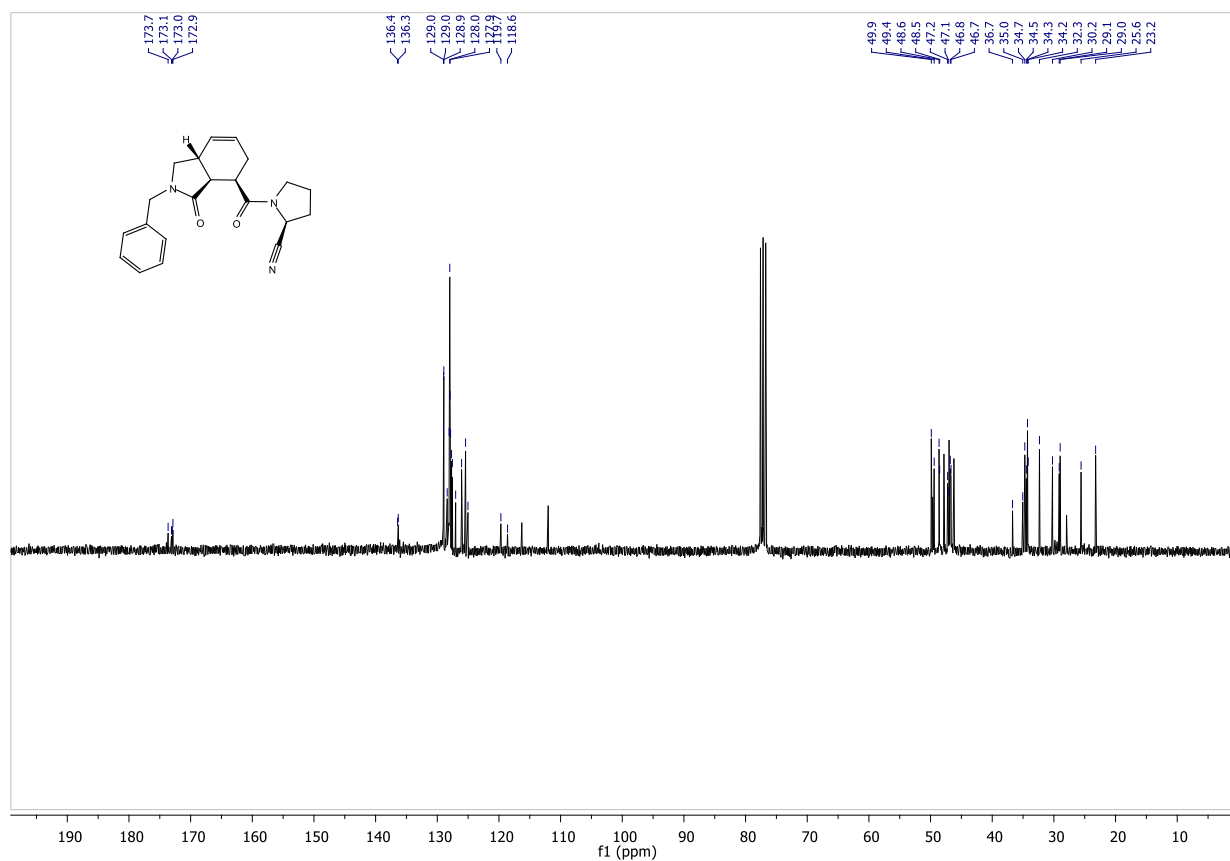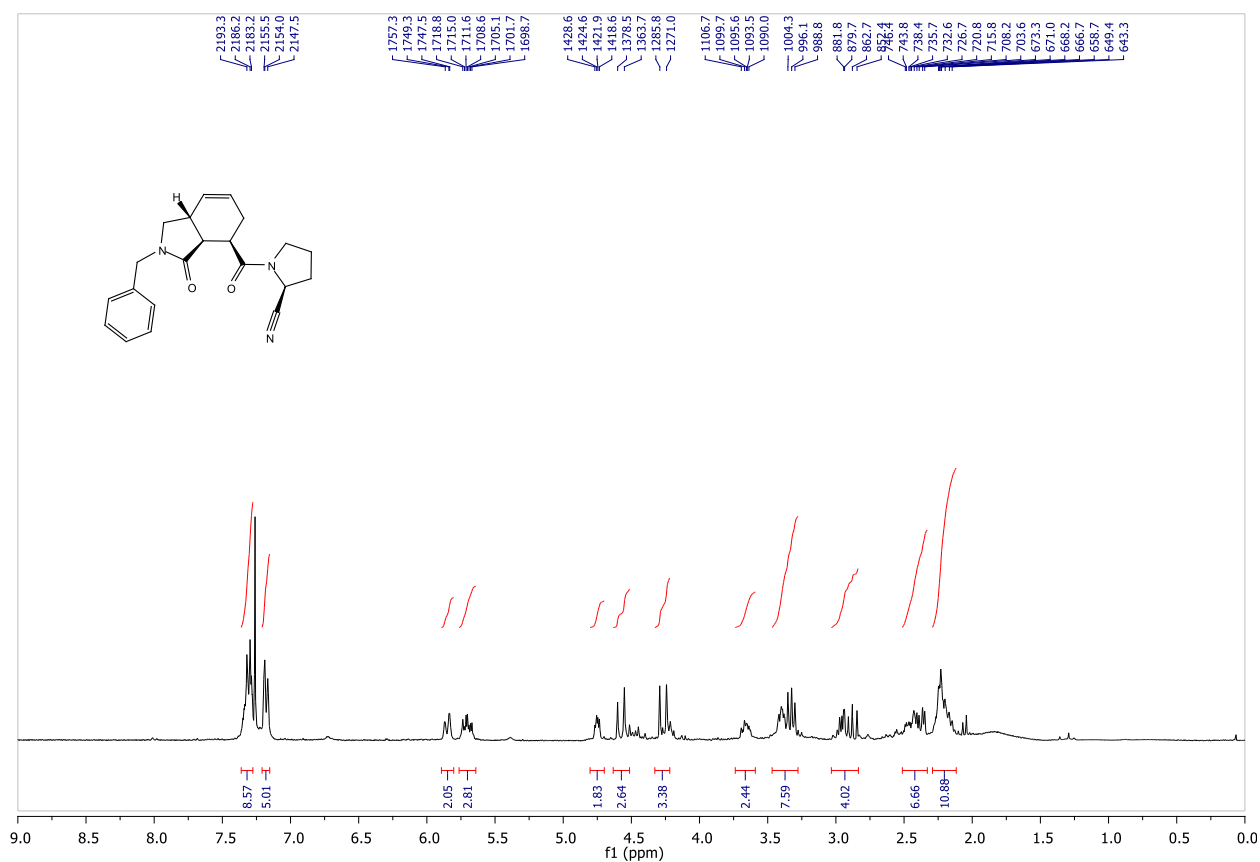
Synthesis of 11a/b:
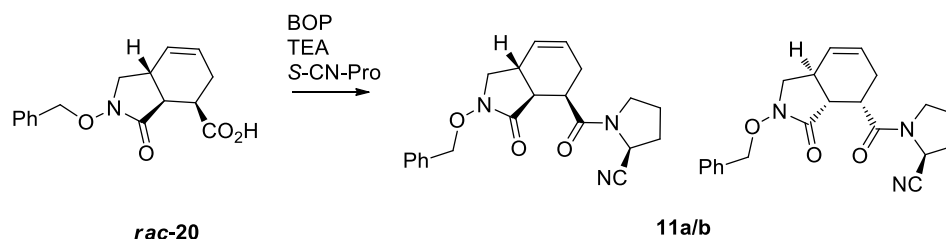
(*S*)-1-((3a*S*,4*R*,7a*R*)-2-benzyloxy-3-oxo-2,3,3a,4,5,7a-hexahydro-1H-isoindole-4-carbonyl)pyrrolidine-2-carbonitrile (11a/b).

The acid *rac*-**20** (45 mg, 0.16 mmol) was dissolved, under argon atmosphere, in DMF (1 ml). The solution was cooled to 0°C and BOP (83 mg, 0.34 mmol) was added, followed by *S*-CN-Proline•pTSA salt (42 mg, 0.16 mmol) and TEA (48 μl, 0.34 mmol). The mixture was reacted for 18h at RT. The reaction was quenched with H_2O, extracted with DCM and the organic phases washed with HCl 1M, saturated $NaHCO_3$, brine, dried over Na_2SO_4 and concentrated under reduced pressure. The crude was purified by flash chromatography (gradient Hex/AcOEt from 2:8 to 1:9) to afford the product **11** as a white solid (16 mg, 27%). The following data has been collected on a 1:1 diastereomeric mixture.

R_f = 0.35 (1:9 Hex/AcOEt). IR (film) ν_{max}: 2926, 2880, 2238, 1708, 1648. ^{1}H NMR (300 MHz, CDCl$_3$) δ 7.48 – 7.30 (m, 5H), 5.92 – 5.84 (m, 0.5H), 5.77 – 5.63 (m, 1.5H), 5.03 – 4.82 (m, 2H), 4.79 – 4.67 (m, 0.5H), 4.67 – 4.53 (m, 0.5H), 3.72 – 3.59 (m, 0.5H), 3.52 – 3.29 (m, 3H), 3.18 – 3.13 (m, 0.5H), 3.05 – 2.95 (m, 2H), 2.53 – 1.97 (m, 7H). ^{13}C NMR (75 MHz, CDCl$_3$) δ 172.6, 172.3, 169.7, 169.6, 135.4, 135.1, 129.9 (2C), 129.7 (2C), 129.1, 129.0, 128.8 (2C), 128.7 (2C), 128.0, 127.5, 125.4, 124.7, 119.6, 118.6, 77.9, 76.9, 51.4, 51.1, 47.7, 47.2, 46.7, 46.5, 46.3, 46.2, 34.3, 34.1, 32.3, 31.8, 31.1, 30.2, 28.6 (2C), 25.6, 23.1. HRMS (ESI+) calcd. for $[C_{21}H_{23}N_3O_3]^+$ 365.1739, found 366.1814. (MH$^+$)

¹H and ¹³C NMR of compound **11a/b**
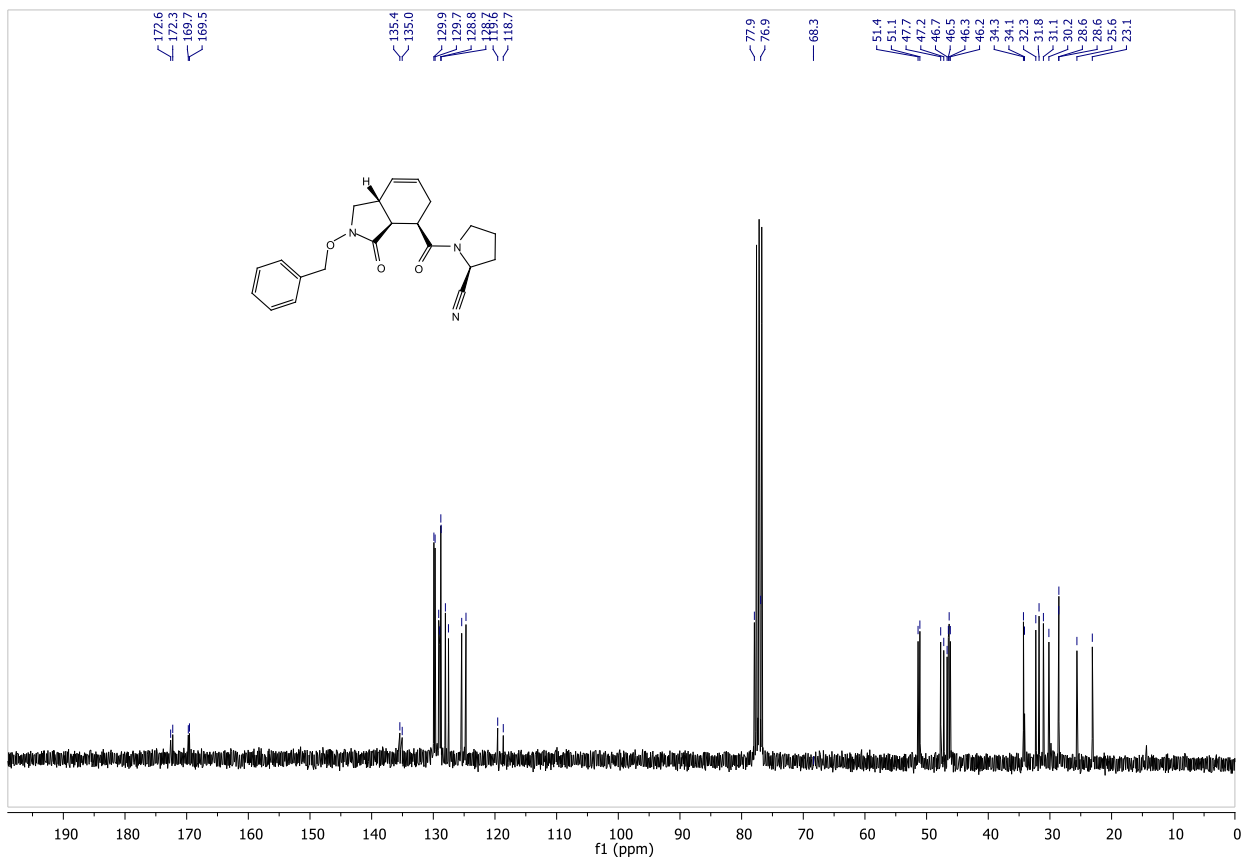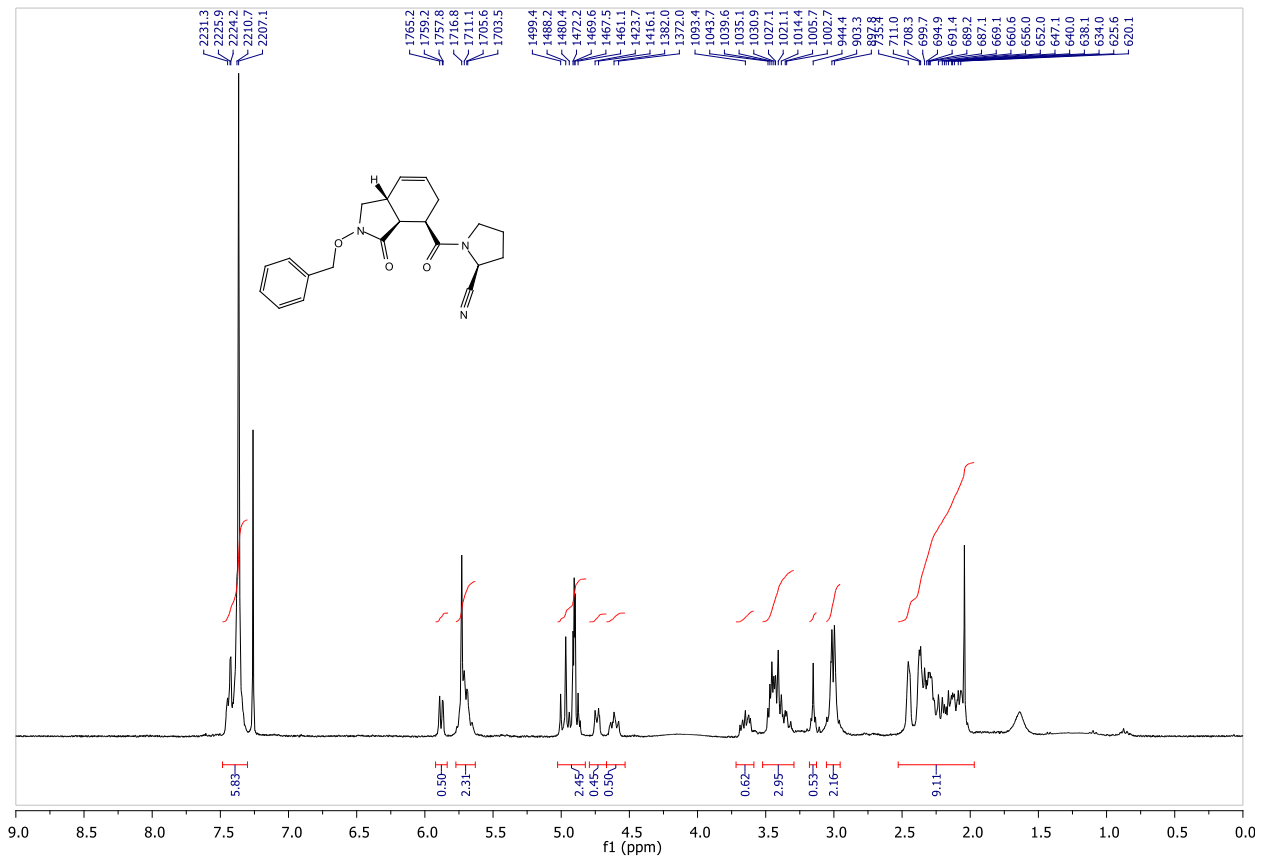
Synthesis of 13:
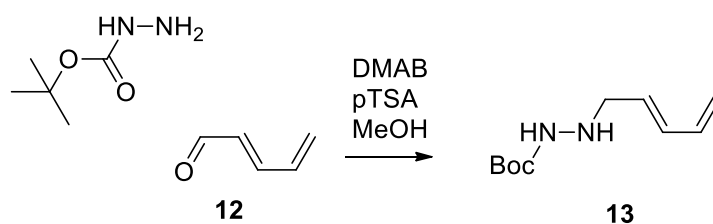
tert-Butyl 2-((3E)-penta-2,4-dienyl)hydrazinecarboxylate (13).

To a solution of dienal **12** (100 mg, 1.2 mmol) in DCM/MeOH (5 ml, 5:1) was added Boc-hydrazide (158 mg, 1.2 mmol). The mixture was stirred for 30 minutes. The resulting solid was dissolved in MeOH (5 ml) and $Me_2NH\cdot BH_3$ (110 mg, 1.9 mmol) was added slowly at 0°C followed by a solution of pTSA (1.37 g, 7.2 mmol) in MeOH (10 ml). After stirring for another 2h, a solution of Na_2CO_3 (aq) (20 ml, 10% w/v) was added and the mixture stirred for 2h then concentrated under reduced pressure, extracted with CH_2Cl_2, dried over Na_2SO_4 and concentrated under reduced pressure to afford the product as a yellow oil (159 mg, 67%).

IR (film) ν_{max}: 3308.95, 2977.22, 2931.35, 1706.19. ^{1}H NMR (300 MHz, CDCl3) δ 6.52 - 6.03 (m, 2H), 5.78 – 5.59 (m, 1H), 5.17 (d, 1H, J = 15.8 Hz), 5.06 (d, 1H, J = 9.0 Hz), 3.48 (d, 2H, J = 6.6 Hz), 1.44 (s, 9H). ^{13}C NMR (75 MHz, CDCl3) δ 156.6, 136.4, 134.2, 129.6, 117.2, 80.5, 53.6, 28.3. HRMS (ESI) calcd. for $[C_{13}H_{16}N_2O_2]^+$: 198.13683, found 221.12605. (MNa^+)

¹H and ¹³C NMR of compound **13**
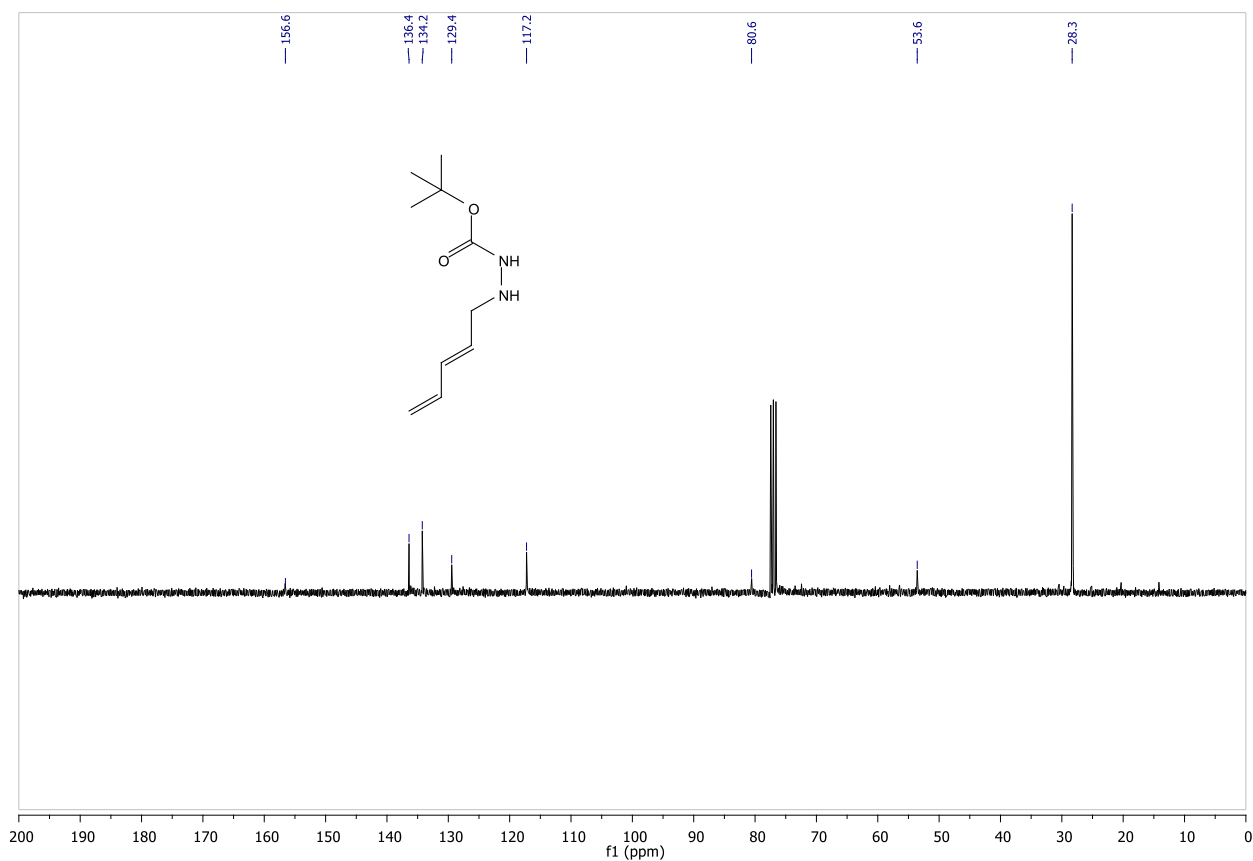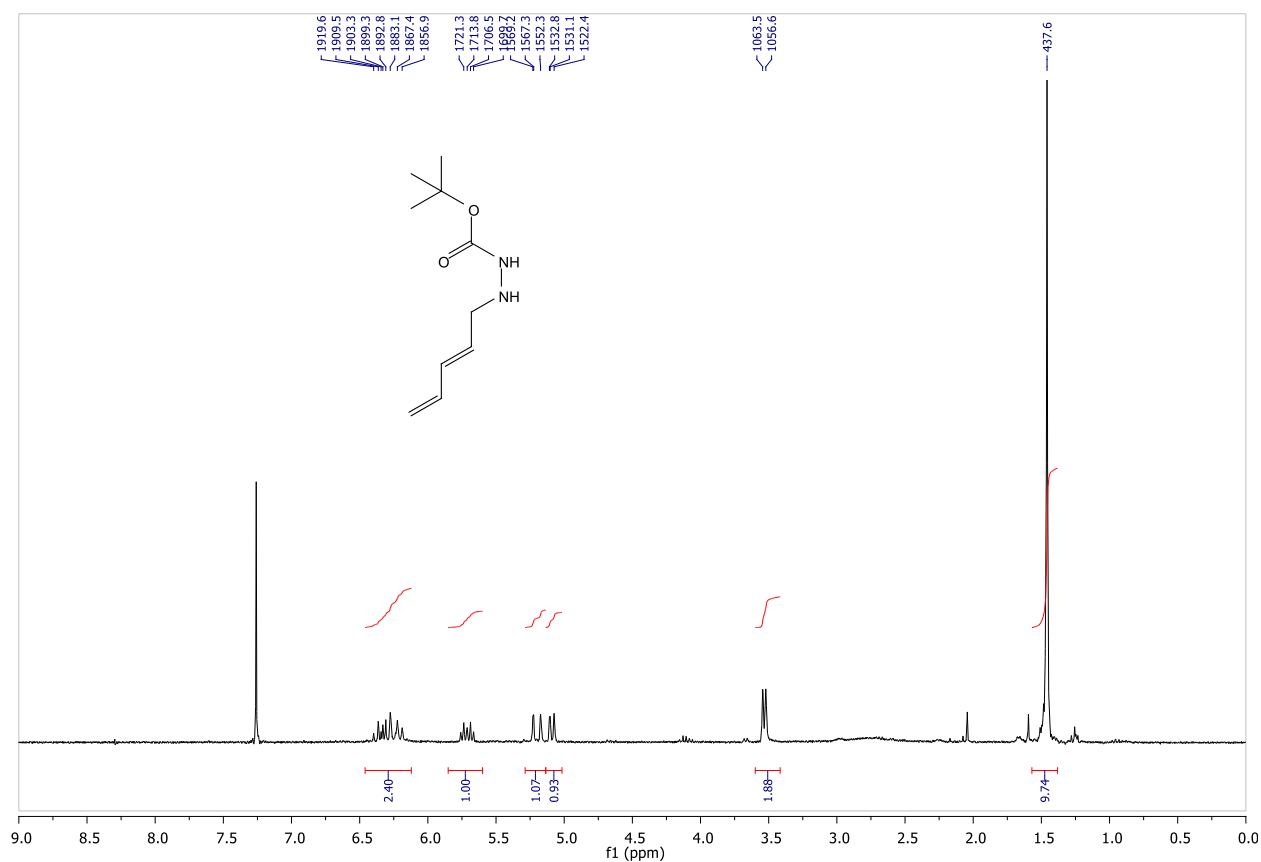
Synthesis of 14:
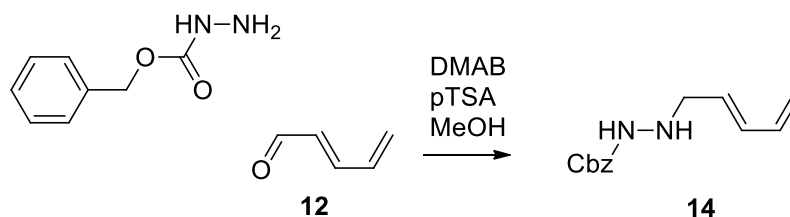
Benzyl 2-((2E)-penta-2,4-dienyl)hydrazinecarboxylate (14).

To a solution of dienal **12** (121 mg, 1.5 mmol) in DCM/MeOH (5 ml, 5:1) was added Cbz-hydrazide (245 mg, 1.5 mmol). The mixture was stirred for 30 minutes. The resulting solid was dissolved in MeOH (5 ml) and $Me_2NH \cdot BH_3$ (132 mg, 2.25 mmol) was added slowly at 0°C followed by a solution of pTSA (1.7 g, 9.0 mmol) in MeOH (10 ml). After stirring for another 2h, a solution of Na_2CO_3 (aq) (20 ml, 10% w/v) was added and the mixture stirred for 2h then concentrated under reduced pressure, extracted with CH_2Cl_2, dried over Na_2SO_4 and concentrated under reduced pressure to afford the product as a white solid (250 mg, 73%).

IR (film) ν_{max}: 3314.85, 2972.36, 2891.14, 1686.76. ^{1}H NMR (300 MHz, CDCl3) δ 7.45-7.30 (m, 5H), 6.32 (dt, 1H, J = 16.7, 10.2 Hz), 6.25 – 6.15 (m, 1H), 5.76 – 5.62 (m, 1H), 5.20 (d, 1H, J = 16.5 Hz), 5.14 (s, 2H), 5.11 – 5.02 (m, 1H), 3.58 – 3.48 (m, 2H). ^{13}C NMR (75 MHz, CDCl3) δ 157.2, 136.3, 136.0, 134.5, 129.2, 128.6 (2C), 128.3 (2C), 128.2, 117.5, 67.1, 53.5. HRMS (ESI) calcd. for $[C_{13}H_{16}N_2O_2]^+$: 232.12118, found 233.12845. (MH$^+$)

¹H and ¹³C NMR of compound **14**
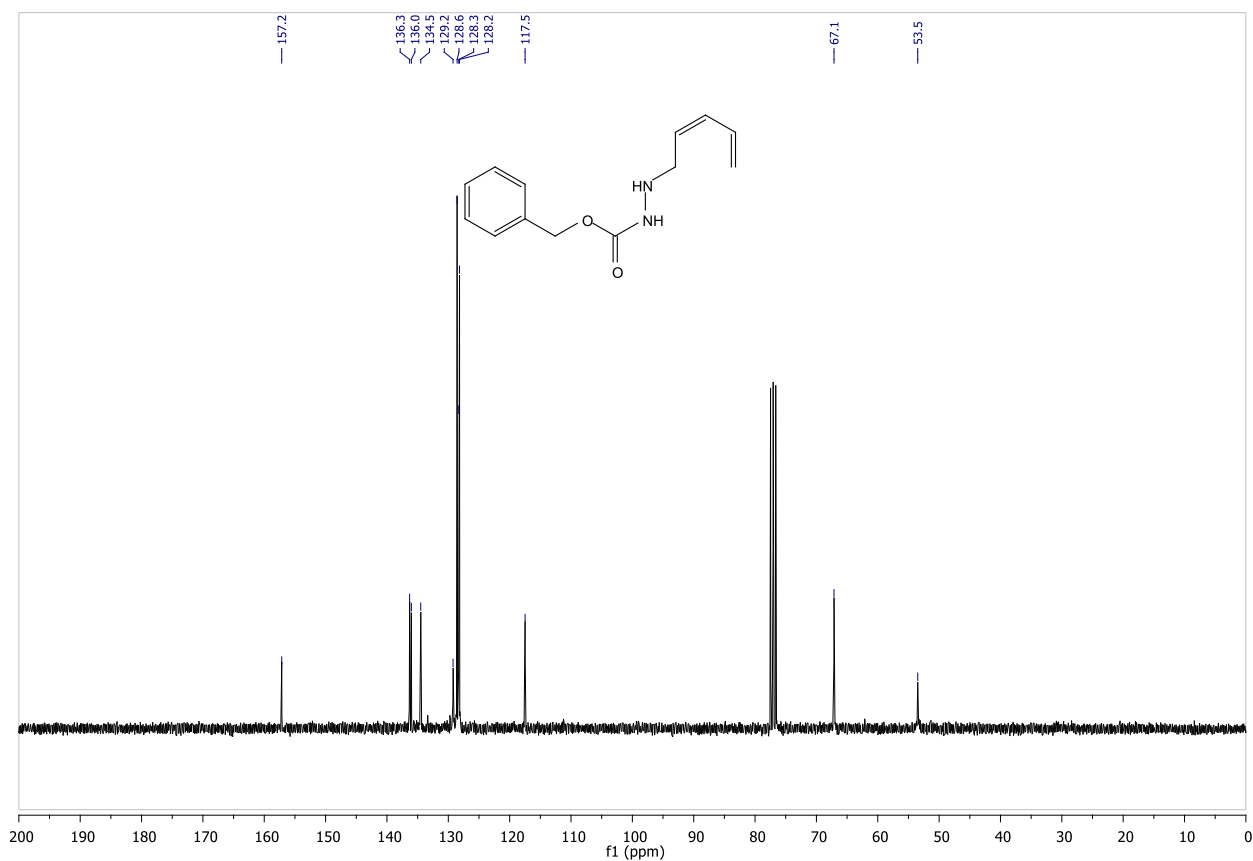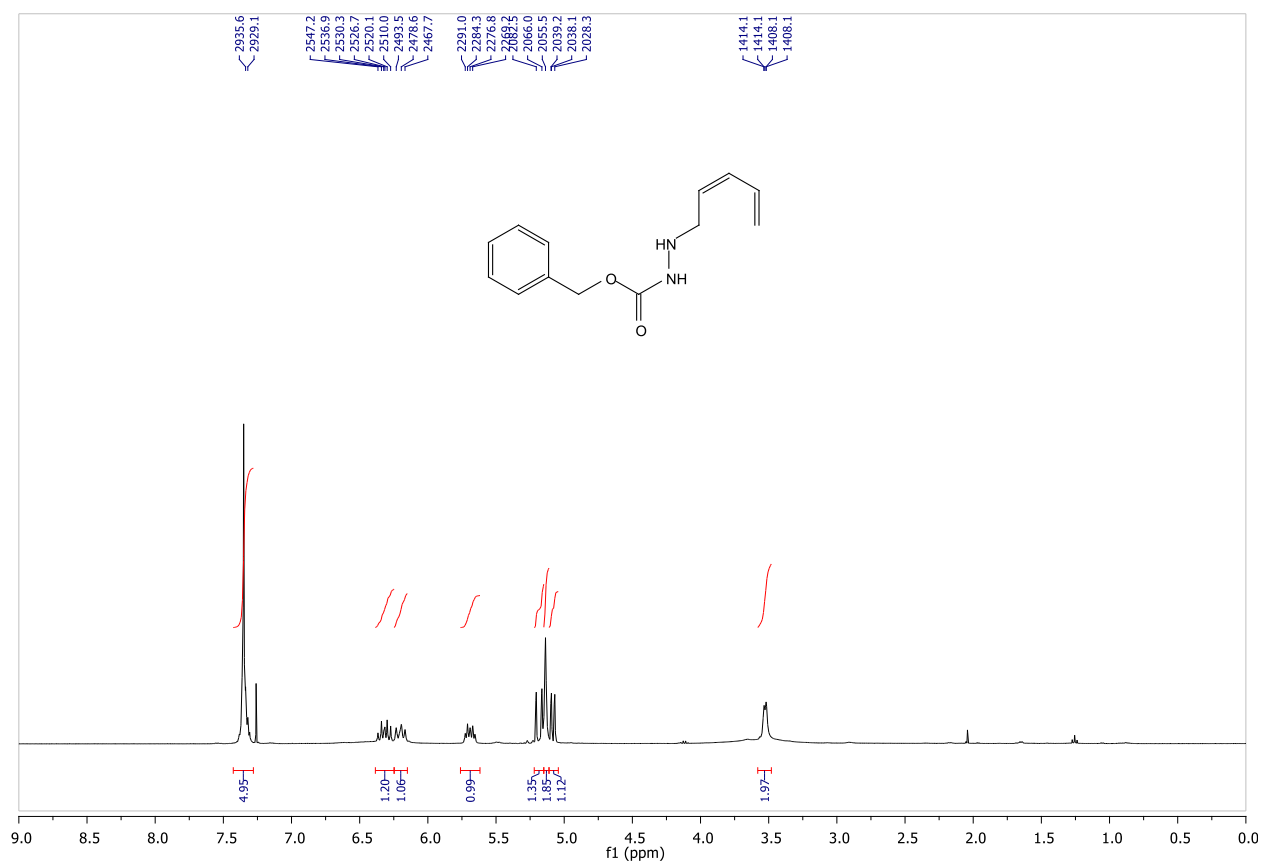
Synthesis of 15:
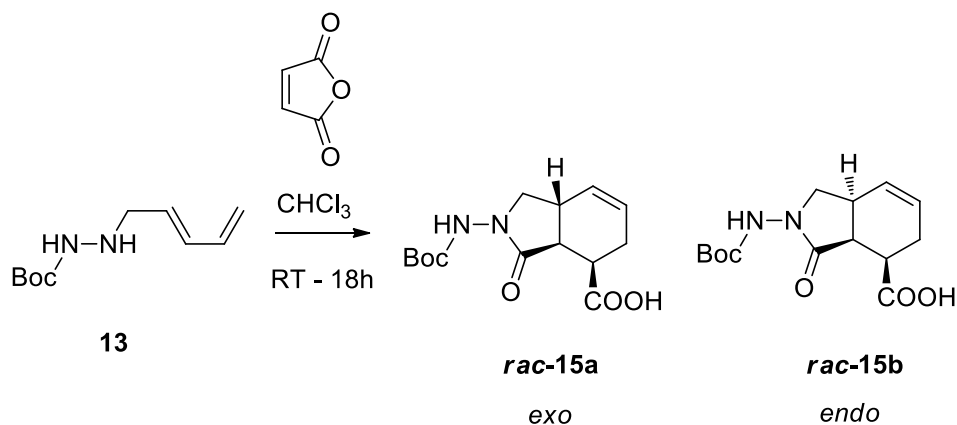
Rac-(3aS,4R,7aR)-2-(tert-butoxycarbonylamino)-3-oxo-2,3,3a,4,5,7a-hexahydro-1H-isoindole-4-carboxylic acid (15a) and *Rac*-(3aS,4R,7aS)-2-(tert-butoxycarbonylamino)-3-oxo-2,3,3a,4,5,7a-hexahydro-1H-isoindole-4-carboxylic acid (15b).

To a solution of **13** (99 mg, 0.5 mmol) in CHCl$_3$ (2 ml) was added maleic anhydride (49 mg, 0.5 mmol) and stirred at rt for 18h. The solution was concentrated under reduced pressure and the residue purified by flash chromatography (Hex/AcOEt 3:1) to afford the product as a white solid (96 mg, 65%). The following data has been collected on a 1.5:1 mixture.

IR (film) ν_{max}: 3275, 3063, 2924, 2886, 1659, 1651, 1645. ^{1}H NMR (400 MHz, CDCl3) δ 6.60 (s, 0.7H), 6.48 (s, 0.3H), 5.97-5.92 (s, 0.3H), 5.84 - 5.79 (m, 0.7H), 5.75 – 5.67 (m, 0.7H), 5.59 (d, 0.3H, *J* = 10.0 Hz), 3.99 – 3.88 (m, 0.3H), 3.58 (t, 0.7H, *J* = 7.5 Hz), 3.48 – 3.40 (m, 0.7H), 3.38 – 3.31 (m, 1H), 3.25 (d, 0.7H, *J* = 9.1 Hz), 3.07 – 3.01 (m, 0.3H), 3.01 - 2.9 (m, 0.3H), 2.91 – 2.81 (m, 0.3H), 2.75 (d, 0.7H, *J* = 19.4 Hz), 2.5 - 2.4 (m, 1H), 2.40 – 2.27 (m, 1H), 1.46 (s, 9H). ^{13}C NMR (75 MHz, CDCl3) δ 175.8 , 174.0, 157.6, 154.5, 128.6, 127.8, 126.8, 125.2, 82.4, 82.0, 54.0, 52.5, 45.2, 40.4, 39.1, 35.9, 32.6, 32.3, 29.7, 28.1 (2C), 23.6. HRMS (ESI) calcd. for [C$_{14}$H$_{20}$N$_2$O$_5$]$^+$: 296.13722, found 295.12994. (M$^-$)
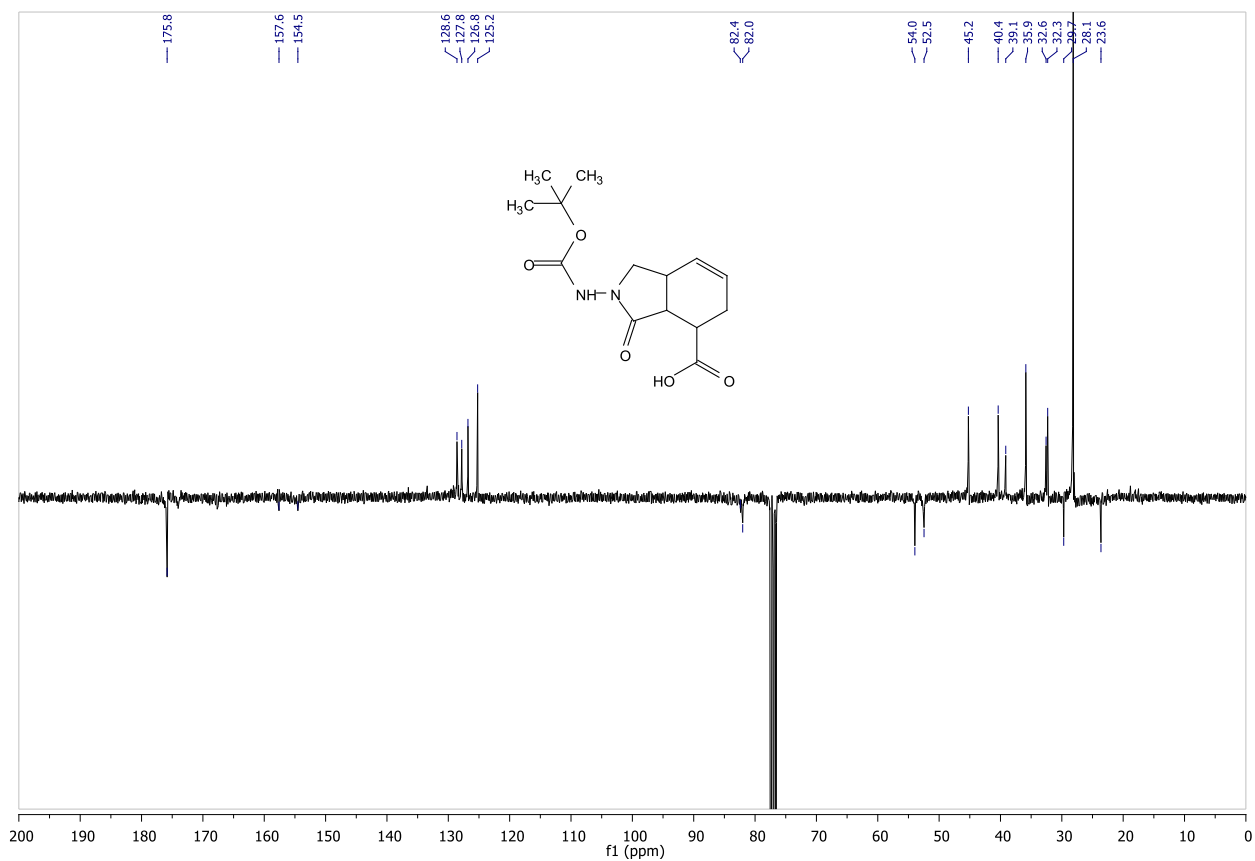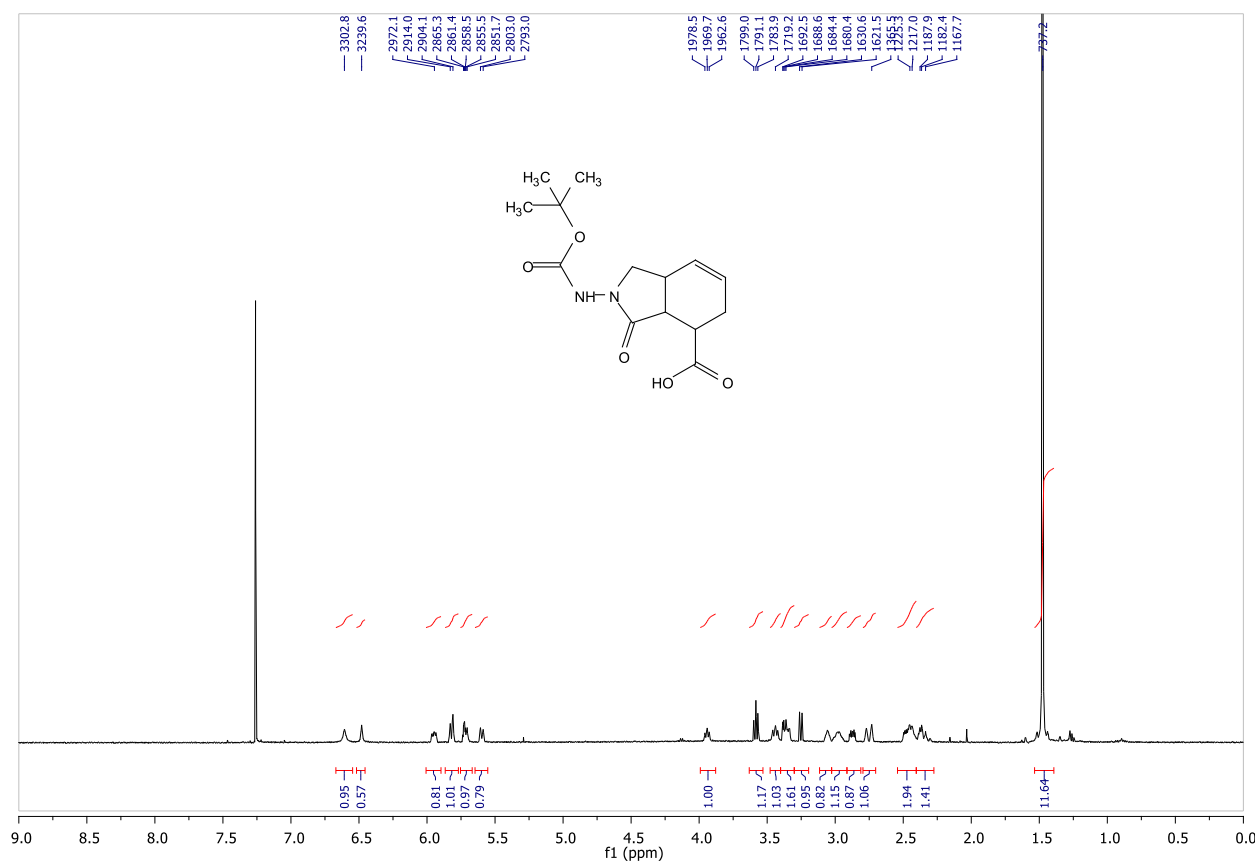
Synthesis of 16:
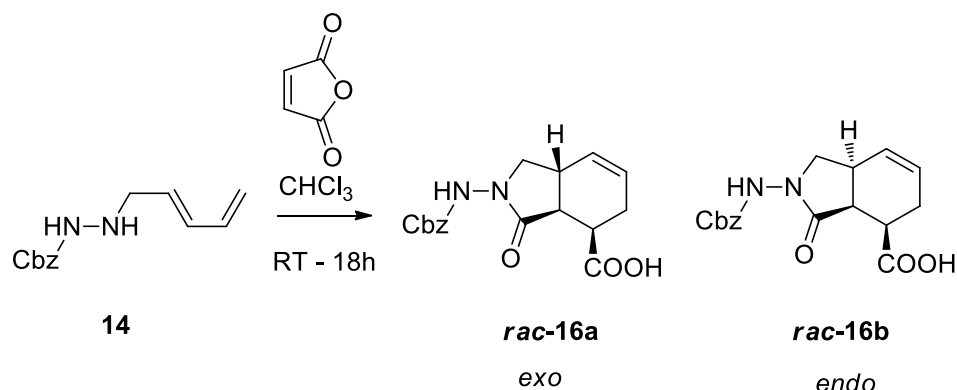
Rac-(3aS,4R,7aR)-2-(benzyloxycarbonylamino)-3-oxo-2,3,3a,4,5,7a-hexahydro-1H-isoindole-4-carboxylic acid (16a).

To a solution of **14** (116 mg, 0.5 mmol) in CHCl$_3$ (2 ml) was added maleic anhydride (49 mg, 0.5 mmol) and stirred at rt for 18h. The solution was concentrated under reduced pressure and the residue purified by flash chromatography (Hex/AcOEt 3:1) to afford the product as a white solid (165 mg, 99%). The *exo* compound was selectively precipitated using CH$_2$Cl$_2$ and afforded the pure compound as a white solid (105 mg, 66%).

IR (film) ν_{max}: 3030, 2941, 2922, 2853, 1739, 1720, 1709. ^{1}H NMR (400 MHz, CDCl$_3$) δ 7.4 – 7.2 (m, 5H), 5.77 (bd, 1H, *J* = 10.0 Hz), 5.67 (bd, 1H, *J* = 6.9 Hz), 5.14 (s, 2H), 3.58 (dd, 1H, *J* = 7.5, 7.4 Hz), 3.5 - 3.41 (m, 1H), 3.4 - 3.31 (m, 1H), 3.1 - 3.0 (m, 1H), 2.68 (bd, 1H, *J* = 20.0 Hz), 2.45 – 2.4 (m, 1H). ^{13}C NMR (125 MHz, CDCl$_3$) δ 175.4 (2C), 155.3, 135.5, 128.6 (2C), 128.5, 128.5, 128.3, 128.3, 127.8, 125.1, 67.8, 45.1, 40.3, 35.8, 32.7, 28.1. HRMS (ESI) calcd. for [C$_{17}$H$_{18}$N$_2$O$_5$]$^+$: 330.12157, found 329.11429. (M$^-$)

¹H and ¹³C NMR of compound *rac*-**16**
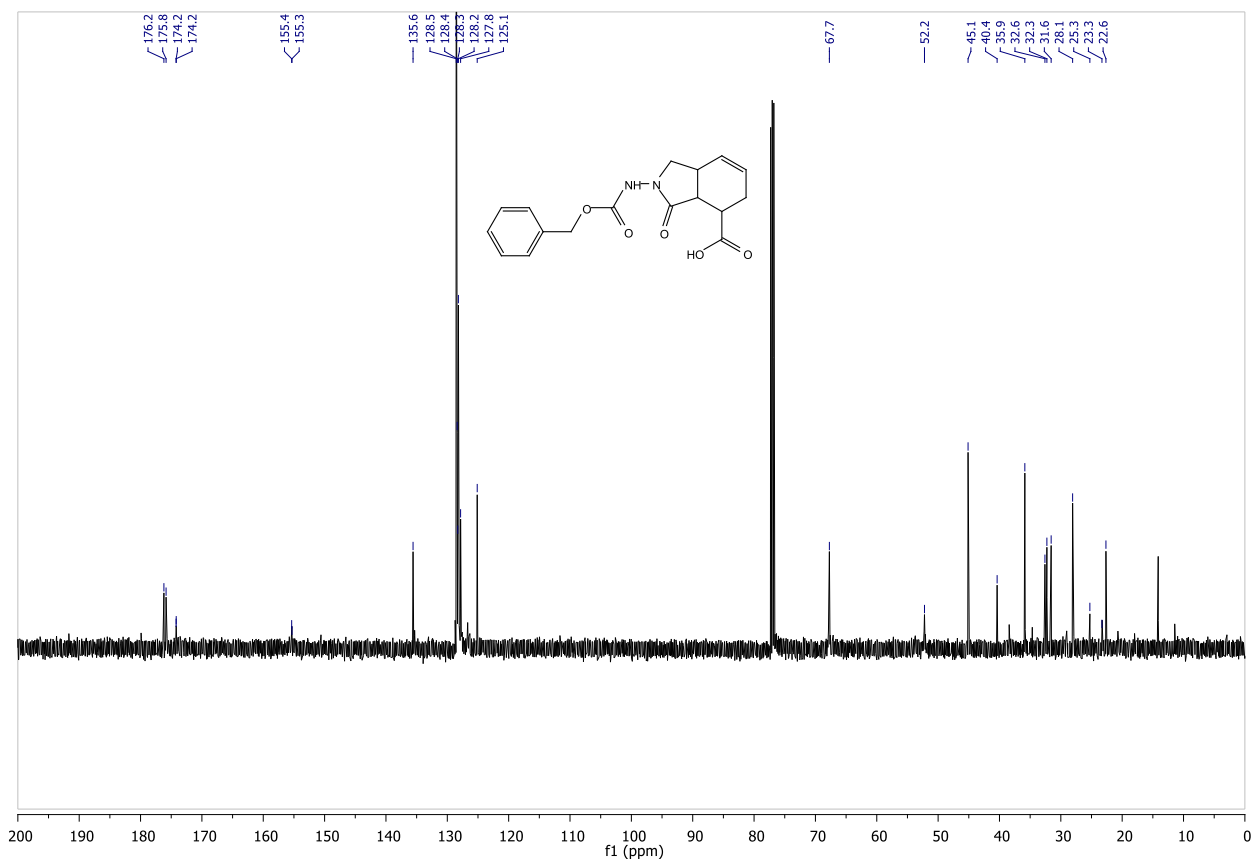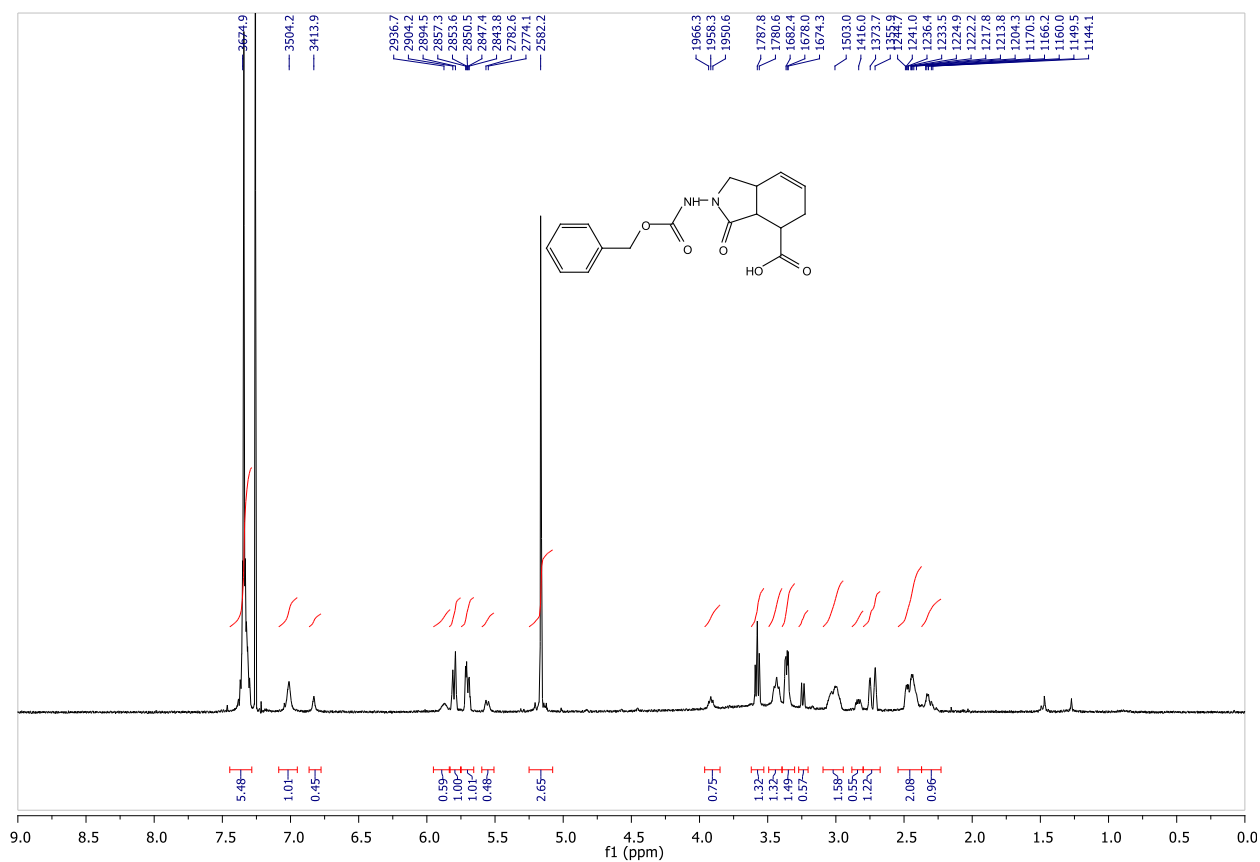
^{1}H and ^{13}C NMR of compound *rac*-16a
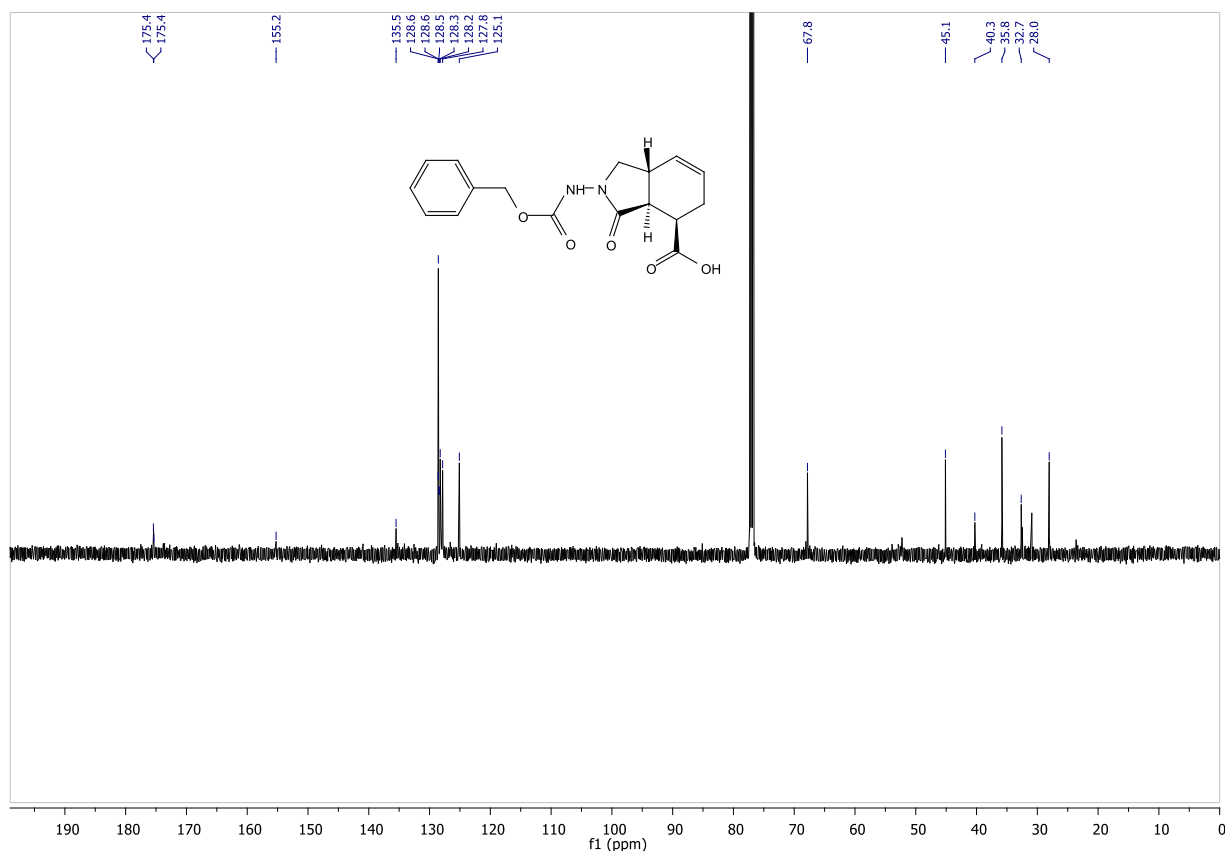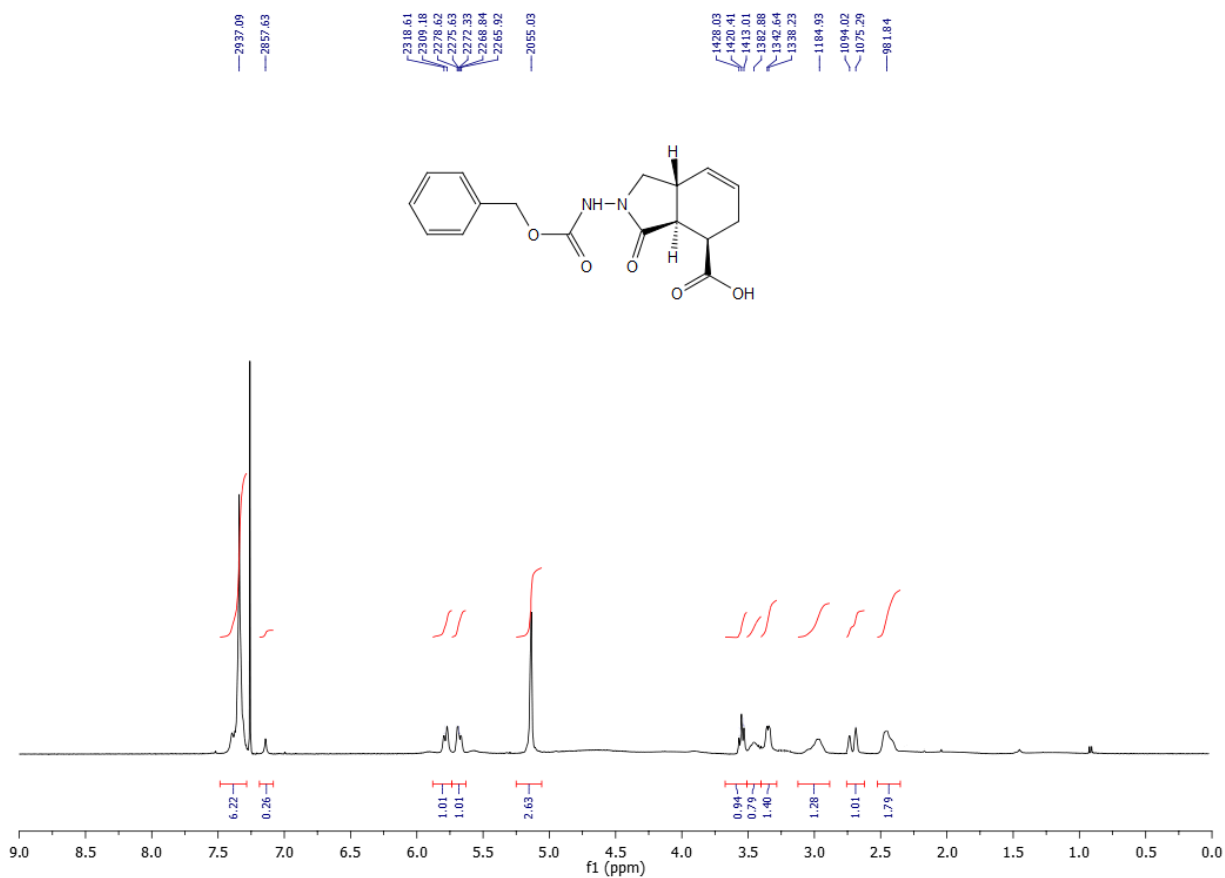
Synthesis of 18:
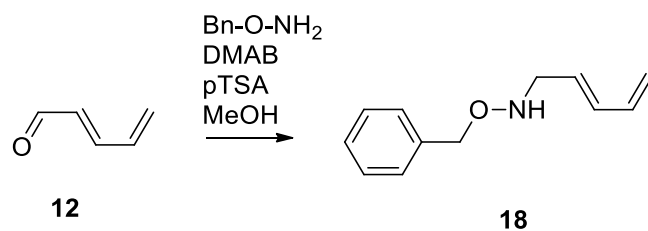
(E)-O-benzyl-*N*-(penta-2,4-dien-1-yl)hydroxylamine (18).

To a solution of O-benzylhydroxylamine (142 mg, 1.16 mmol) in MeOH (1 ml), was added a solution of dienal (95 mg, 1.16 mmol) in DCM dropwise. The mixture was stirred for 30 minutes at rt. The solution was cooled to 0°C and Me$_2$NH·BH$_3$ (109 mg 1.86 mmol) was added slowly, followed by a solution of pTSA (1.3 g, 6.9 mmol) in MeOH (10 ml). After stirring for another 2 h, a solution of Na$_2$CO$_3$(aq) (20 ml, 10% w/v) was added and the mixture reacted for 2 h then concentrated under reduced pressure, extracted with CH$_2$Cl$_2$, washed with brine, dried over Na$_2$SO$_4$ and concentrated under reduced pressure. The crude was purified by flash chromatography (Hex/AcOEt 95:5) to afford the product as a colorless oil (61 mg, 28%).

R_f = 0.36 (9:1 Hex/AcOEt). IR (film) ν_{max} 3265, 3087, 1603 cm^{-1}. ^{1}H NMR (300 MHz, CDCl$_3$) δ 7.42 – 7.27 (m, 5H), 6.43 – 6.14 (m, 2H), 5.77 (dt, 1H, *J* = 14.6, 6.7 Hz), 5.26 – 5.14 (m, 1H), 5.14 – 5.03 (m, 1H), 4.76 (s, 2H), 3.66 – 3.55 (m, 2H). ^{13}C NMR (75 MHz, CDCl$_3$) δ 136.4, 134.5, 129.0, 128.5 (2C), 128.4 (2C), 128.3, 128.0, 117.4, 76.3, 53.7. HRMS (ESI) calcd. for [C$_{12}$H$_{15}$NO]$^+$: 189.1154, found 190.1151. (MH$^+$)

¹H and ¹³C NMR of compound 18
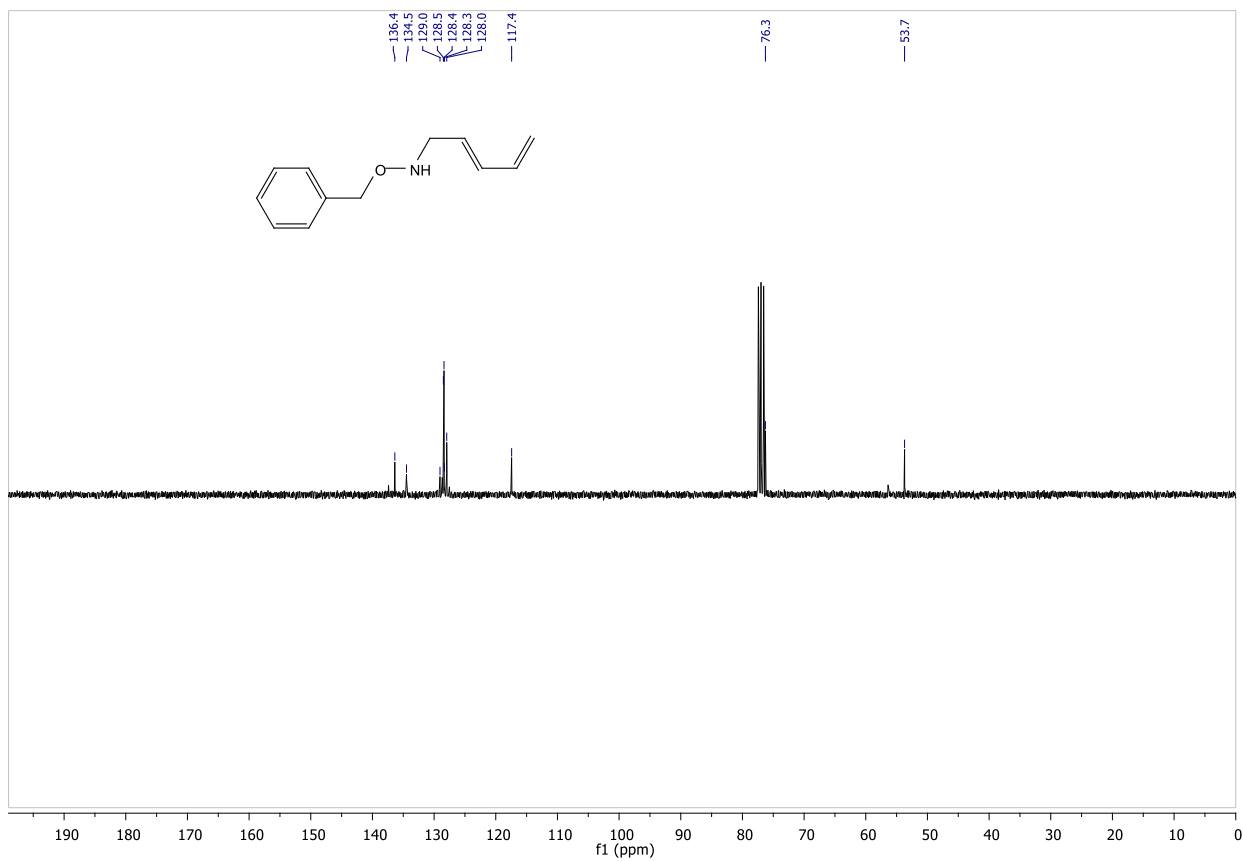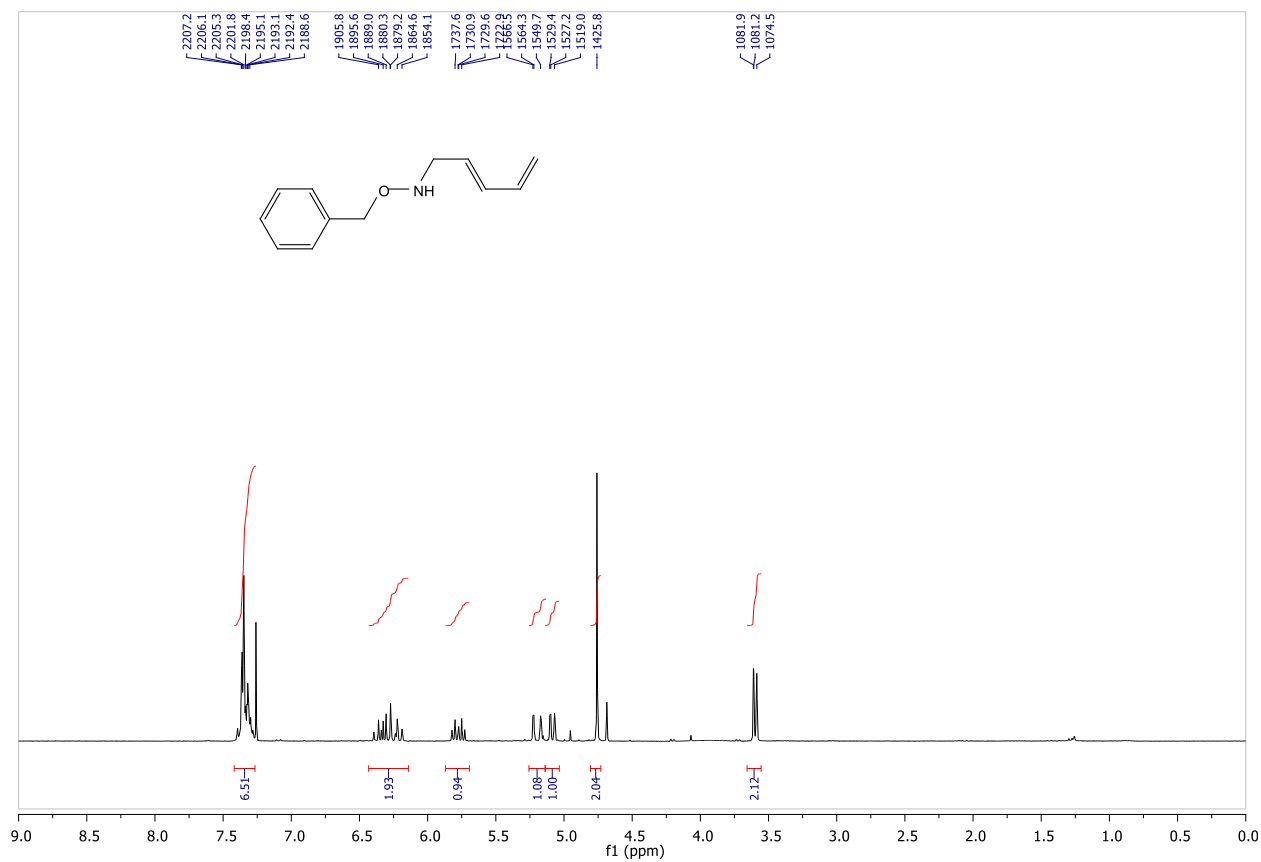
Synthesis of 19:
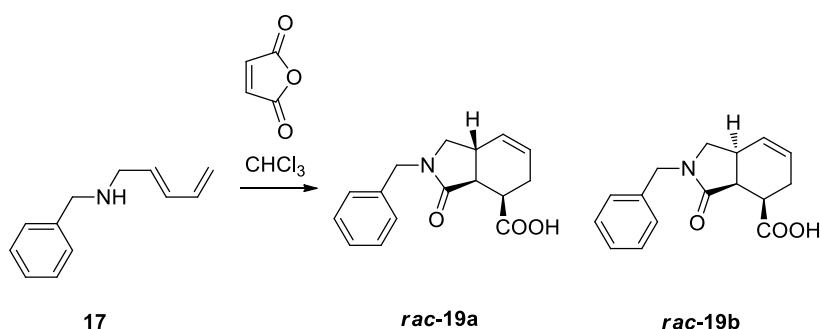
**rac-(3aS,4R,7aR)-2-benzyl-3-oxo-2,3,3a,4,5,7a-hexahydro-1H-isoindole-4-carboxylic acid (rac-42).**

Diene **17** (41 mg, 0.23 mmol) was dissolved in CHCl₃ (2 ml). To the solution was added maleic anhydride (23 mg, 0.23 mmol) After stirring for 18 h, the solution was concentrated under reduced pressure and the residue purified by flash chromatography (Hex/AcOEt 4:6) to afford the product as a white solid (55 mg, 98%). The following data has been collected on a 7:1 diastereomeric mixture.

R_f = 0.29 (4:6 Hex/AcOEt). IR (film) ν_{max}: 3028, 1722, 1697, 1650. ^{1}H NMR (400 MHz, CDCl₃) δ 7.44 – 7.06 (m, 5H), 5.96 – 5.89 (m, 0.2H), 5.76 (bd, 0.8H, J = 10.1 Hz), 5.73 – 5.58 (m, 0.8H), 5.43 (d, 0.2H, J = 10.1 Hz), 4.49 (s, 2H), 3.53 (dd, 0.2H, J = 10.0, 6.4 Hz), 3.42 (dd, 0.8H, J = 8.0, 3.9 Hz), 3.35 – 3.28 (m, 1H), 3.09 – 2.84 (m, 2.2H), 2.75 (bd, 0.8H, J = 19.1 Hz), 2.56 – 2.34 (m, 2H). ^{13}C NMR (75 MHz, CDCl₃) δ 175.7, 174.5, 136.2, 128.8 (2C), 128.0 (3C), 127.7, 125.31, 49.4, 46.9, 46.8, 36.3, 34.4, 28.2. HRMS (ESI) calcd. for [C₁₆H₁₇NO₃]⁺: 271.1208, found 294.1096. (MNa⁺)

¹H and ¹³C NMR of compound *rac*-19
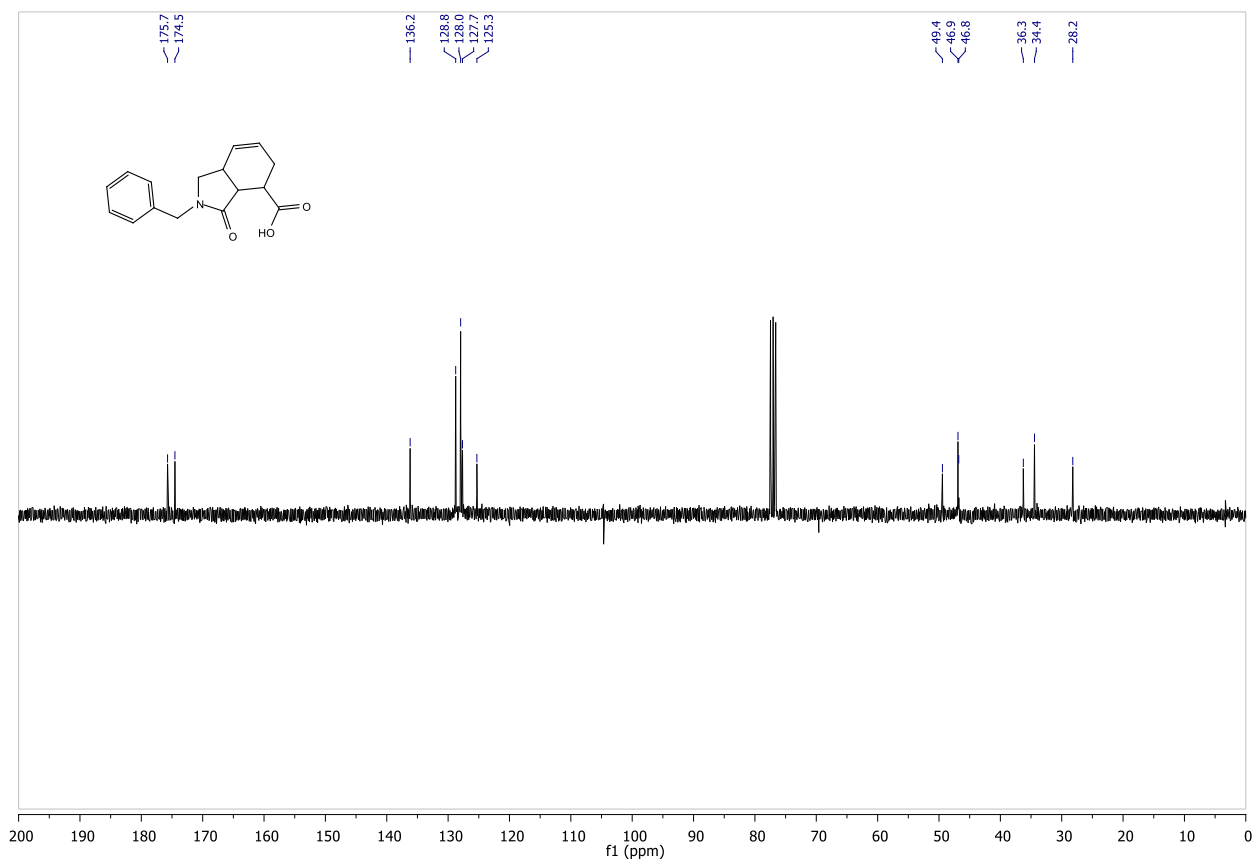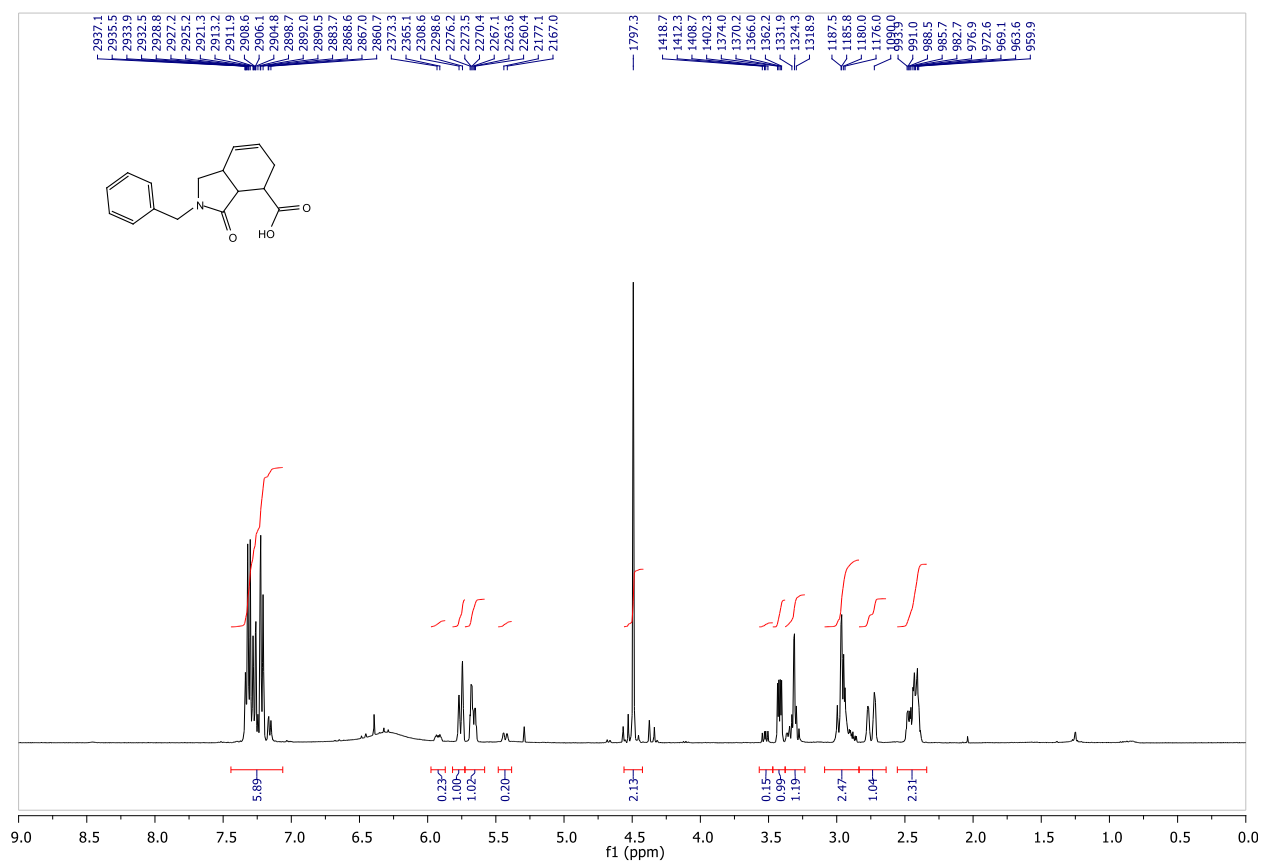
Synthesis of 20:
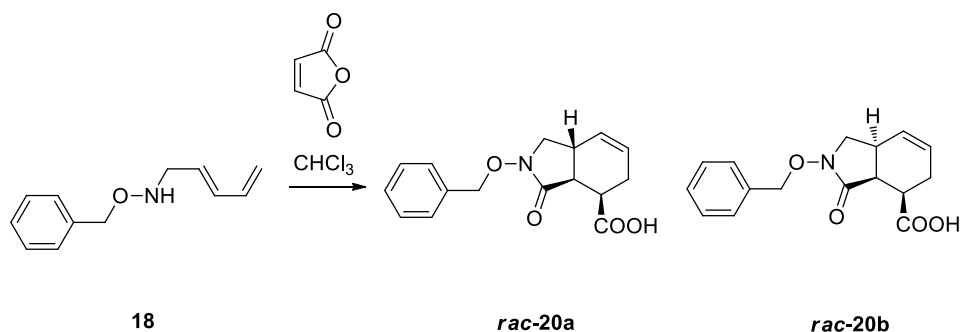
rac-(3aS,4R,7aR)-2-benzyl-3-oxo-2,3,3a,4,5,7a-hexahydro-1H-isoindole-4-carboxylic acid (*rac*-20).

Diene **18** (60 mg, 0.31 mmol) was dissolved in CHCl$_3$ (2 ml). To the solution was added maleic anhydride (31 mg, 0.31 mmol) After stirring for 3 days, the solution was concentrated under reduced pressure and the residue purified by flash chromatography (Hex/AcOEt 4:6) to afford the product as a white solid (66 mg, 74%). The following data has been collected on a 1:1 diastereomeric mixture.

R_f = 0.24 (7:3 Hex/AcOEt). IR (film) ν_{max}: 3030, 1734, 1709. ^{1}H NMR (300 MHz, CDCl$_3$) δ 7.47 – 7.30 (m, 5H), 5.92 – 5.81 (m, 0.5H), 5.73 – 5.60 (m, 1H), 5.37 (d, 0.5H, *J* = 10.2 Hz), 5.05 – 4.94 (m, 2H), 3.55 (dd, 0.5H, *J* = 8.7, 6.7 Hz), 3.39 (dd, 0.5H, *J* = 8.0, 3.6 Hz), 3.30 – 3.15 (m, 1H), 3.07 – 2.95 (m, 1H), 2.91 (bs, 0.5H), 2.86 – 2.66 (m, 1.5H), 2.52 – 2.38 (m, 0.5H) 2.37 – 2.20 (m, 1.5H). ^{13}C NMR (75 MHz, CDCl$_3$) δ 174.9 (2C), 170.3 (2C), 135.0, 134.3, 129.8, 129.8, 129.3, 129.1, 129.0, 128.6, 128.6, 127.8, 126.4, 124.8, 77.1 (2C), 52.7, 51.3, 44.8, 41.0, 39.4, 35.8, 32.0, 31.8, 27.8, 24.3. HRMS (ESI) calcd. for [C$_{16}$H$_{17}$NO$_4$]$^+$: 287.1158, found 310.1049. (MNa$^+$)

^{1}H and ^{13}C NMR of compound *rac*-20

Synthesis of 21:

rac-**19** → rac-**21**

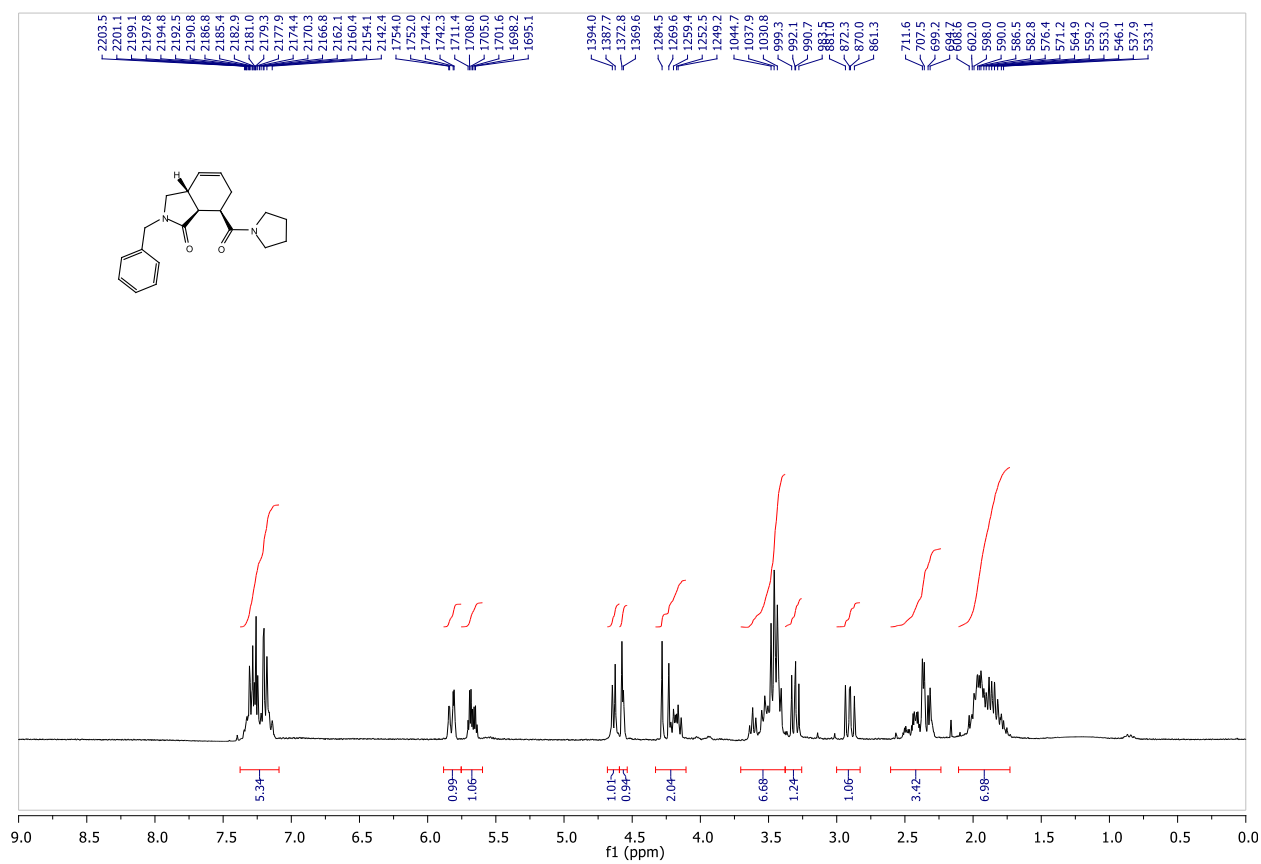(PivCl, TEA, Pyrrolidine)
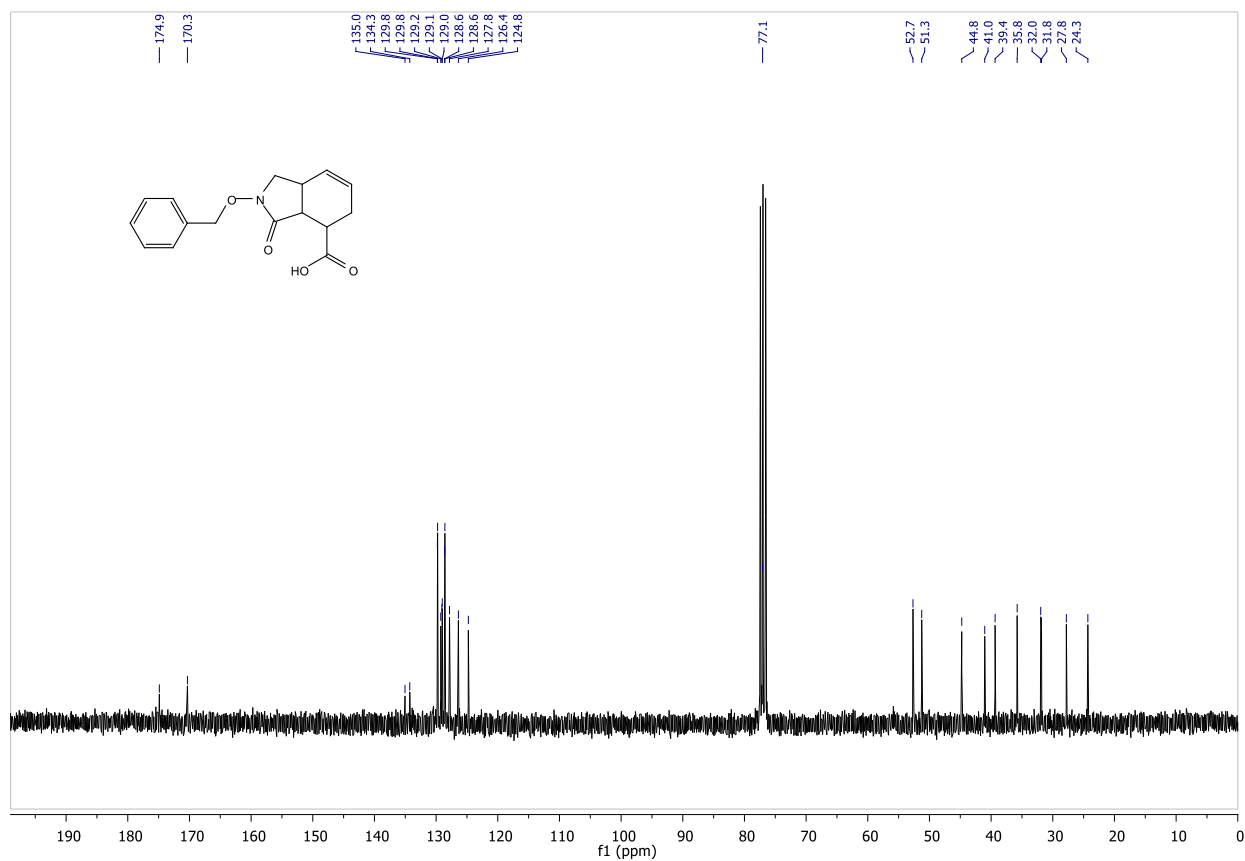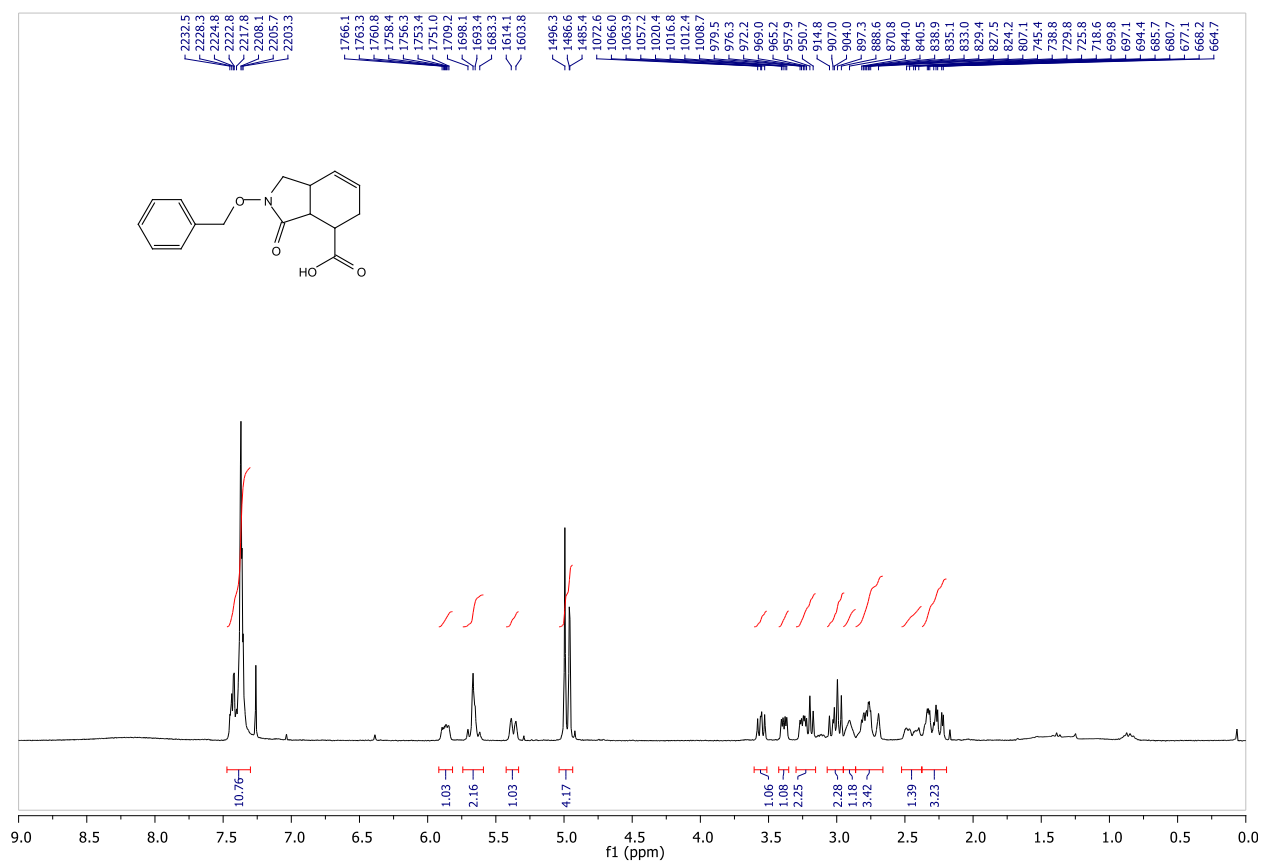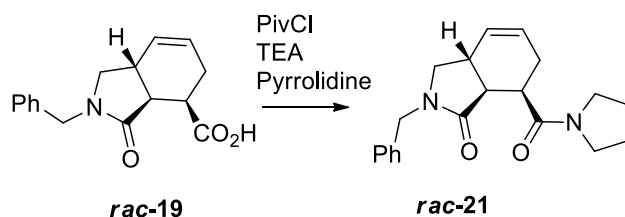
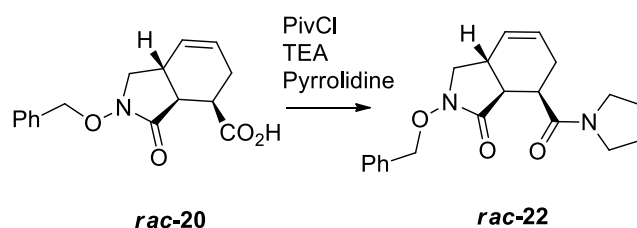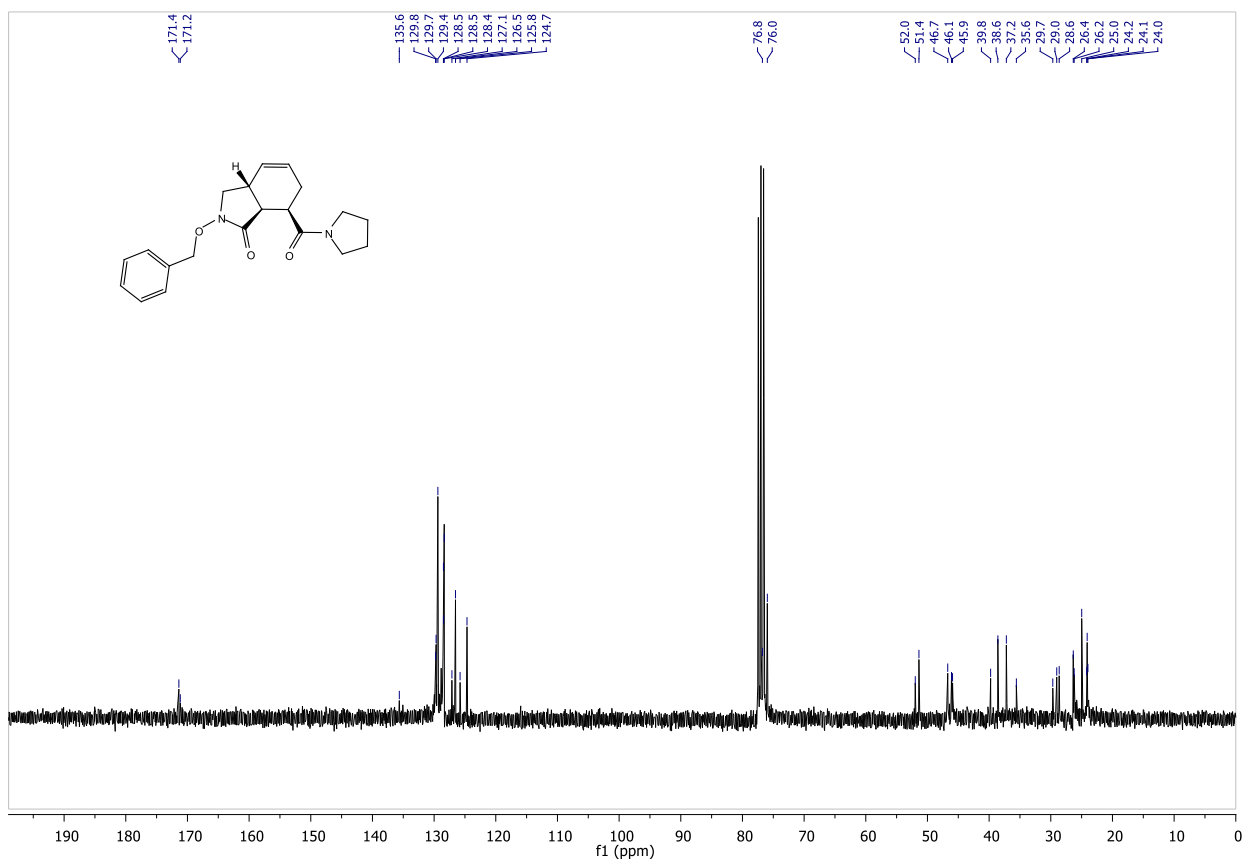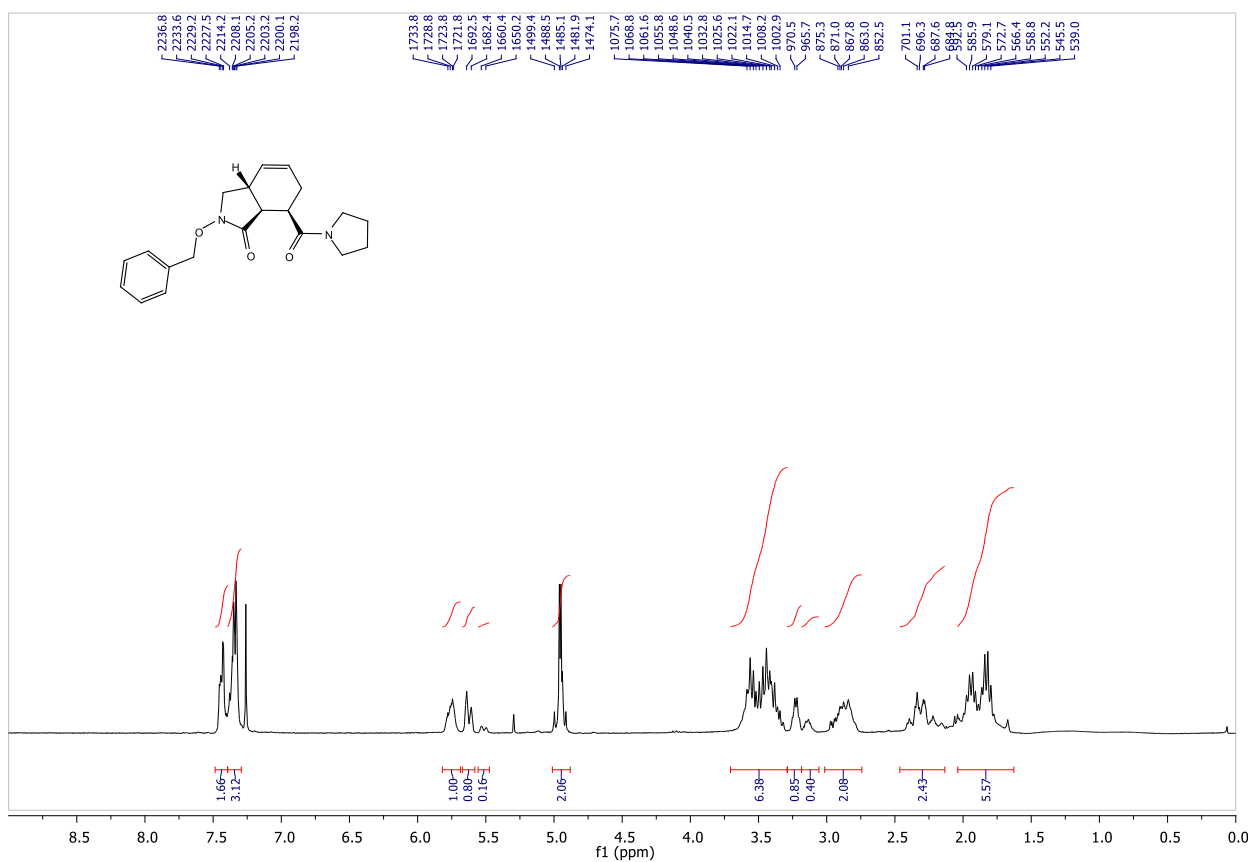**rac-(3a*R*,7*R*,7a*S*)-2-benzyl-7-(pyrrolidine-1-carbonyl)-2,3,3a,6,7,7a-hexahydro-1H-isoindol-1-one (*rac*-21).**

The acid **19** (34 mg, 0.125 mmol) was dissolved, under argon atmosphere, in DMF (1.2 ml). The solution was cooled to 0°C and TEA (87 µl, 0.625 mmol) was added followed by PivCl (23 µl, 0.18 mmol). After 1 h Pyrrolidine (52 µl, 0.625 mmol) was added and the mixture was reacted for 18h. The reaction was quenched with H_2O, extracted with AcOEt and the organic phases washed with HCl 1M, saturated $NaHCO_3$, brine, dried over Na_2SO_4 and concentrated under reduced pressure. The crude was purified by flash chromatography (Hex/AcOEt 2:8) to afford the product **21** as a white solid (14 mg, 34%).

R_f = 0.36 (2:8 Hex/AcOEt). IR (film) ν_{max}: 3480, 1689, 1638, 1623. ^{1}H NMR (300 MHz, CDCl$_3$) δ 7.38 – 7.09 (m, 5H), 5.83 (dd, 1H, *J* = 9.8, 1.9 Hz), 5.68 (dt, 1H, *J* = 9.8, 3.2 Hz), 4.64 (d, 1H, *J* = 6.3 Hz), 4.6 – 4.54 (m, 1H) 4.33 – 4.11 (m, 2H), 3.70 – 3.38 (m, 5H), 3.30 (dd, 1H, *J* = 8.6, 7.2 Hz), 2.90 (dd, 1H, *J* = 11.0, 8.7 Hz), 2.51 – 2.28 (m, 2H), 2.11 – 1.73 (m, 4H). ^{13}C NMR (75 MHz, CDCl$_3$) δ 173.6, 172.4, 136.7, 128.7 (2C), 128.0 (2C), 127.4, 127.4, 126.2, 49.6, 48.4, 46.9, 46.7, 45.8, 33.9, 33.6, 28.9, 26.2, 24.3. HRMS (ESI+) calcd. for $[C_{20}H_{24}N_2O_2]^+$ 324.1838, found 347.1732. (MNa$^+$)

^{1}H and ^{13}C NMR of compound *rac*-21
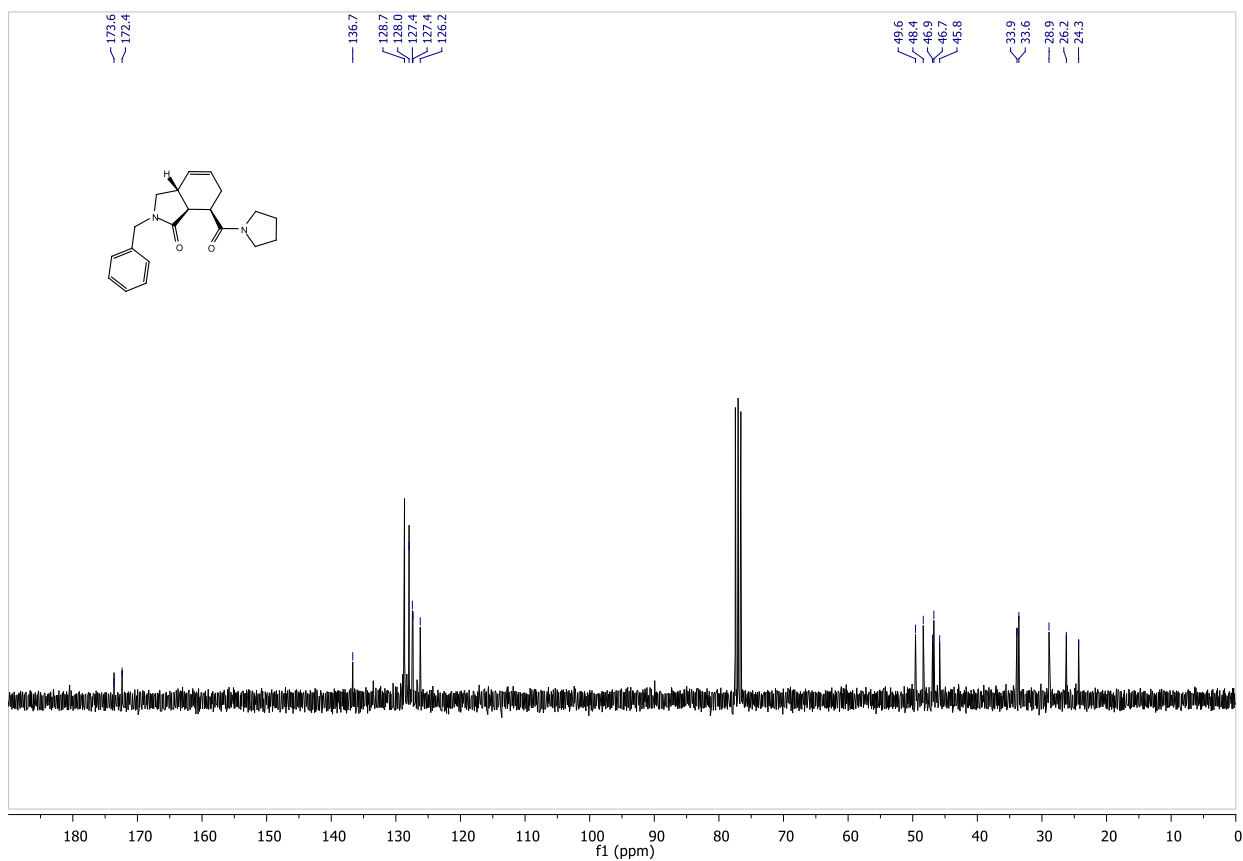
Synthesis of 22:

rac-20 → rac-22

rac-(3aR,7R,7aS)-2-benzyloxy-7-(pyrrolidine-1-carbonyl)-2,3,3a,6,7,7a-hexahydro-1H-isoindol-1-one (rac-22).

The acid **20** (34 mg, 0.12 mmol) was dissolved, under argon atmosphere, in DMF (1 ml). The solution was cooled to 0°C and TEA (50 µl, 0.29 mmol) was added followed by PivCl (23 µl, 0.18 mmol). After 1 h Pyrrolidine (25 µl, 0.29 mmol) was added and the mixture was reacted for 18h. The reaction was quenched with H_2O, extracted with AcOEt and the organic phases washed with HCl 1M, saturated $NaHCO_3$, brine, dried over Na_2SO_4 and concentrated under reduced pressure. The crude was purified by flash chromatography (Hex/AcOEt 2:8) to afford the product **22** as a white solid (7 mg, 17%). The following data has been collected on a 5:1 diastereomeric mixture.

R_f = 0.27 (2:8 Hex/AcOEt). IR (film) ν_{max}: 3480, 2951, 1705, 1634. ^{1}H NMR (300 MHz, CDCl$_3$) δ 7.49 – 7.39 (m, 2H), 7.39 – 7.29 (m, 3H), 5.82 – 5.69 (m, 1H), 5.62 (bd, 0.8H, J = 10.2 Hz), 5.52 (bd, J = 10.2 Hz, 0.2H), 5.01 – 4.88 (m, 2H), 3.71 – 3.29 (m, 6H), 3.29 – 3.18 (m, 0.8H), 3.18 – 3.06 (m, 0.2H), 3.01 – 2.74 (m, 2H), 2.46 – 2.13 (m, 2H), 2.13 – 1.63 (m, 4H). ^{13}C NMR (75 MHz, CDCl$_3$) δ 171.4, 171.2, 135.6 (2C), 129.8, 129.7, 129.4 (2C), 128.6, 128.5, 128.4 (2C), 127.1, 126.5, 125.8, 124.7, 76.8, 76.0, 52.0, 51.4, 46.7, 46.1, 45.9, 39.8, 38.6, 37.2, 35.6, 29.7, 29.0, 28.64, 26.4, 26.2, 25.0, 24.2, 24.1, 24.0. HRMS (ESI+) calcd. for $[C_{20}H_{24}N_2O_3]^+$: 340.1769, found 363.1686. (MNa$^+$)

¹H and ¹³C NMR of compound *rac*-22

ACKNOWLEDGEMENTS